

Intrinsic and Extrinsic Factors Affecting Proteasome Inhibitor Resistance in Multiple Myeloma

A thesis submitted for the degree of PhD

Catriona Ann Hayes (CAH), MB BCh.

School of Biotechnology

Dublin City University

January 2015

The experiment work described in this thesis was carried out under the supervision of Prof. Martin Clynes and Dr. Paul Dowling, School of Biotechnology; and Dr. Peter O' Gorman, Mater Misericordiea University Hospital, Dublin.

*I hereby certify that this material, which I now submit for assessment on the programme of study leading to the award of Ph.D. is entirely my own work, and that I have exercised reasonable care to ensure that the work is original, and does not to t
he best of my knowledge breach any law of copyright, and has not been taken from the work of others save and to the extent that such work has been cited and acknowledged within the text of my work.*

Signed:

Candidate ID No.: 12210012

Date:

The experimental work outlined in this thesis was undertaken at two institutions, the National Institute for Cellular Biotechnology at Dublin City University, and at the Jerome Lipper Centre for Multiple Myeloma and Harvard Institutes for Medicine at the Dana-Farber Cancer Institute in Boston, USA over a period of 3 years.

Work completed at the National Institute for Cellular Biotechnology was done so under the supervision of Prof. Martin Clynes, Dr Paul Dowling, and Dr. Peter O'Gorman, in collaboration with the Mater Misericordiae University Hospital.

At the Dana-Farber Cancer Institute work completed was supervised by Dr Constantine Mitsiades and Dr. Kenneth Anderson.

Acknowledgements

While working under the supervision of Dr. Peter O' Gorman at the Mater Misericordiae University Hospital in Dublin as a Medical Senior House Officer I developed a keen interest in haematology, particularly in multiple myeloma (MM). The clinical diversity of this disease, in addition to on-going efforts to decipher mechanisms of its pathogenesis, given the inevitable emergence of bortezomib resistance in these patients, prompted my initial interest in this field. Following encouraging discussions with Dr O' Gorman, Prof. Martin Clynes and Dr Paul Dowling, I subsequently undertook a PhD program in Biotechnology at the National Institute for Cellular Biotechnology (NICB), Dublin City University (DCU), in collaboration with the Dana-Farber Cancer Institute (DFCI) in Boston, USA, in the field of multiple myeloma research.

In Dublin, I received outstanding mentorship and guidance from all the staff at the NICB, to whom I am truly indebted, given the anticipated anxiety of transferring directly from a hospital-based setting to bench work that I had not completed since my undergraduate degree in medicine. The kindness and helpfulness of the staff there during this challenging transition cannot be quantified. In particular I would like to thank Justine Meiller, Michael Henry, Kay Reen Ting and Colm Cosgrove.

In Boston, I was fortunate enough to be trained in on basic laboratory skills by my predecessor, Dr Melissa Ooi, a physician who was completing her PhD when I was beginning, who provided me with the skills necessary to undertake basic experiments independently. Dr. Constantine Mitsiades and Dr Ken Anderson with years of experience in multiple myeloma research were a constant source of innovative ideas for my PhD project and provided me with constant supervision to ensure timely and effective completion of my research during my time in Boston. In addition I was so grateful to be allowed shadow in the Multiple Myeloma out-patients clinic at Dana-Farber under the supervision of Dr Paul Richardson who gave me a wonderful insight into the current and most up-to-date clinical management of patients with multiple myeloma, where I learned the conduction and management of patients on clinical trials.

For the constant support provided to me by my three Dublin-based supervisors, Prof Martin Clynes, Dr Peter O' Gorman and Dr Paul Dowling, I will be forever indebted for their time and dedication committed to my PhD project, and for their constant encouragement regardless of which side of the Atlantic I was based at any particular time, and irrespective of Greenwich Mean Time, they were always available for a word of advice, how to tweak an experiment to ensure its successful completion and continued encouragement throughout this programme.

Finally I thank my fiancé Paul Rubin, and my family, especially my parents Michael and Isobel, and my siblings Paula, Patrick, James and Michael, who were a constant source of support and encouragement to me throughout the PhD process.

Table of Contents

CHAPTER 1. INTRODUCTION	6
1.1 OVERVIEW OF MULTIPLE MYELOMA IN THE CLINICAL SETTING.....	6
1.1.1 Introduction.....	6
1.1.2 Overview of monoclonal gammopathies	6
1.1.3 Epidemiology of multiple myeloma.....	8
1.1.4 Clinical Presentation	8
1.1.5 Definition of multiple myeloma	9
1.1.6 Staging of MM.....	9
1.1.7 Management of Multiple Myeloma	10
1.1.8 Novel/ Investigational Therapies for MM.....	13
1.2 RELAPSED AND REFRACTORY MULTIPLE MYELOMA	14
1.2.1 Definition of relapsed and refractory MM	14
1.2.2 Poor prognosis associated with relapsed and refractory MM	16
1.2.3 Treatment options in relapsed and refractory multiple myeloma..	18
1.3 PROTEASOME INHIBITION IN MULTIPLE MYELOMA	18
1.3.1 The role of the 20S proteasome	18
1.3.2 Rationale for use of bortezomib in multiple myeloma.....	19
1.3.3 Second generation proteasome inhibitors.....	20
1.3.4 The Immunoproteasome	22
1.3.5 Novel immunoproteasome inhibitors	24
1.3.6 <i>In Vitro</i> Models of Bortezomib Resistance.....	24
1.3.7 Functional significance of PSMB5 mutations <i>in vitro</i>	25
1.4 GENETICS OF MULTIPLE MYELOMA.....	26
1.4.1 Cytogenetics.....	26
1.4.2 Whole genome mapping in MM	26
1.4.3 Role of PSMB5 mutations in MM in the clinical setting	27
1.5 EXTRINSIC RESISTANCE MECHANISMS: ROLE OF THE BONE MARROW MICROENVIRONMENT.....	27
1.5.1 The role of the bone marrow accessory cells in MM pathogenesis.	27
1.5.2 The role of osteoblasts in multiple myeloma.....	28
1.5.3 Role of the microenvironment in drug resistance in multiple myeloma	31
1.6 SUMMARY	32
1.7 AIMS OF THE THESIS.....	35
CHAPTER 2. MATERIALS AND METHODS	37
2.1 Ultrapure H2O, glassware and sterilisation procedures	37
2.2 Preparation of cell culture media.....	37
2.3 Cells / cell culture/ subculturing / freezing / thawing / co-culture studies	37

2.4	STR analysis of cell lines.....	39
2.5	Reagents.....	40
2.6	Generation of a bortezomib resistant cell line.....	42
2.7	<i>In vitro</i> toxicity assays measuring cell viability.....	42
2.8	<i>In vivo</i> mouse model treatment with bortezomib or carfilzomib.....	43
2.9	Immunoblot.....	44
2.10	Whole exome sequencing.....	45
2.11	Validation of mutPSMB5 in VDR cell line.....	46
2.12	Gene expression profiling.....	46
2.13	shRNA knockdown studies.....	46
2.14	Lentiviral infection of mutPSMB5 in bortezomib-sensitive cell lines	48
2.15	Label-free mass spectrometry	49
2.16	Transwell co-cultures of hFob 1.19 and MM.1S cells.....	49
2.17	Characteristics of bortezomib-refractory patients selected from Multiple Myeloma BioBank.....	50
2.18	Immunohistochemistry	54
2.19	Statistical Analysis.....	54
CHAPTER 3. RESULTS.....		57
3.1	CHARACTERISATION OF AN ISOGENIC CELL LINE MODEL OF BORTEZOMIB RESISTANCE <i>IN VITRO</i> AND <i>IN VIVO</i>	57
3.1.1	Introduction.....	57
3.1.2	Generation of a cell line model of bortezomib resistance.....	57
3.1.3	Response profile of VDR cells to conventional and novel therapies	60
3.1.4	Sensitivity of VDR to novel proteasome inhibitors	69
3.1.5	The role of p-glycoprotein in bortezomib resistance in VDR.	72
3.1.6	Baseline proliferation rate of MM.1R and VDR cell lines	75
3.1.7	Sensitivity of isogenic cell lines MM.1R and VDR to bortezomib and carfilzomib <i>in vivo</i>	77
3.1.8	Summary of <i>in vitro</i> and <i>in vivo</i> studies.....	82
3.2	WHOLE EXOME SEQUENCING OF MM.1R AND VDR CELL LINES.....	83
3.2.1	Introduction.....	83
3.2.2	Frequency of single nucleotide variants observed between isogenic cell lines MM.1R and VDR	83
3.2.3	Insertions and deletions identified in VDR vs. MM.1R.....	87
3.2.4	Identification of PSMB5 mutation in VDR cell line	89
3.2.5	Sensitivity of KMS11 cell line to bortezomib following lentiviral infection with mutPSMB5	90
3.2.6	Summary of whole exome sequencing study.....	92

3.3	GENE EXPRESSION PROFILING OF MM.1R AND VDR	94
3.3.1	Introduction	94
3.3.2	Transcripts over-expressed in VDR compared to MM.1R	95
3.3.3	Transcripts downregulated in VDR compared to MM.1R.....	111
3.3.4	Identification of transcripts of interest for shRNA knockdown screening	117
3.3.5	Results of shRNA knockdown screen	119
3.3.6	Validation of shRNA knockdown of PSMB5	124
3.3.7	Conclusion of gene expression profiling studies	128
3.4	PROTEOMIC PROFILE OF MM.1R AND VDR BY LABEL-FREE MASS SPECTROMETRY.....	130
3.4.1	Introduction.....	130
3.4.2	Proteins over-expressed in VDR vs. MM.1R	132
3.4.3	Proteins down-regulated in VDR compared to MM.1R.....	141
3.4.4	Individual biomarkers down-regulated in MM.1R or VDR following bortezomib treatment.....	149
3.4.5	Proteins over-expressed in bortezomib treated VDR compared to bortezomib treated MM.1R	163
3.4.6	PSMB5 protein expression in MM.1R and VDR with and without bortezomib treatment.....	173
3.4.7	Immunoblot validation of proteins differentially expressed in VDR compared to MM.1R.....	175
3.4.8	Summary of proteomic profiling studies.....	177
3.5	FUNCTIONAL STUDIES AND POTENTIAL ROLE OF THE BONE MARROW MICROENVIRONMENT IN THE PATHOGENESIS OF BORTEZOMIB RESISTANCE IN VDR	180
3.5.1	Introduction.....	180
3.5.2	Effect of HS-5 stromal cells on sensitivity of MM1R and VDR to bortezomib and carfilzomib.....	181
3.5.3	Investigation of the role for combination therapies to overcome bortezomib resistance in VDR cells in co-culture with HS-5 stromal cells.	184
3.5.4	Effect of osteoblasts on proliferation rate and sensitivity of MM.1S, MM.1R and VDR to therapies <i>in vitro</i>	187
3.5.5	Role of direct cell-to-cell contact in osteoblast-like cell-induced drug resistance in MM.1S.....	191
3.5.6	Role of cell-to-accessory cell ratio and protein content in observed osteoblast-like cell-induced resistance.....	193
3.5.7	Upregulation of PSMB8 by interferon-gamma increases the sensitivity of VDR cell lines to bortezomib	196
3.5.8	PSMB5 and PSMB8 expression <i>in vivo</i>	200
3.5.9	Summary of functional studies	206
	CHAPTER 4. DISCUSSION.....	209
4.1	CHARACTERISATION OF AN ISOGENIC CELL LINE MODEL OF BORTEZOMIB RESISTANCE IN VITRO AND IN VIVO.	209
4.1.1	Introduction.....	209
4.1.2	The use of cell line models to examine bortezomib resistance <i>in vitro</i> and <i>in vivo</i>	210

4.1.3	Variations in the sensitivity of bortezomib-resistant cells to other therapies <i>in vitro</i>	211
4.1.4	Potential FDA-approved compounds that overcome bortezomib resistance in VDR	212
4.1.5	The efficacy of novel proteasome inhibitors in the setting of bortezomib resistance <i>in vitro</i>	215
4.1.6	P-glycoprotein does not mediate bortezomib resistance in VDR..	215
4.1.7	The <i>in vivo</i> efficacy of bortezomib and carfilzomib in bortezomib-resistant VDR cell line.....	216
4.2	MUTATIONAL ALTERATIONS IN MM.1R AND VDR AS IDENTIFIED BY WHOLE EXOME SEQUENCING	219
4.2.1	Introduction to whole exome sequencing.....	219
4.2.2	Single nucleotide variants identified in bortezomib-resistant VDR but not MM.1R.....	220
4.2.3	Deletion in ABCA7 gene identified in VDR cell line	224
4.2.4	<i>In vitro</i> and <i>in vivo</i> significance of mutPSMB5 identified in VDR..	226
4.3	TRANSCRIPTIONAL PROFILE OF ISOGENIC CELL LINE MODEL OF BORTEZOMIB RESISTANCE	227
4.3.1	Introduction to gene expression profiling	227
4.3.2	Pathways associated with genes over-expressed in VDR compared to MM.1R.....	227
4.3.3	Pathways associated with genes down-regulated in VDR compared to MM.1R.....	228
4.3.4	shRNA knockdown studies of genes up-regulated in VDR.....	229
4.4	PROTEOMIC PROFILING OF ISOGENIC CELL LINE MODEL OF BORTEZOMIB RESISTANCE	232
4.4.1	Introduction to proteomic profiling in MM.1R and VDR.....	232
4.4.2	Protein expression in VDR compared to MM.1R.....	232
4.4.3	Protein expression in bortezomib-treated VDR and bortezomib-treated MM.1R.....	234
4.4.4	Potential significance of PSMB5 in bortezomib resistance	236
4.5	THE ROLE OF THE BONE MARROW MICROENVIRONMENT AND ITS FURTHER CONTRIBUTION TO DRUG RESISTANCE	239
4.5.1	Introduction.....	239
4.5.2	VDR is subject to HS-5 stromal cell-induced drug resistance.....	239
4.5.3	Osteoblasts promote myeloma cell proliferation and contribute to drug resistance.....	240
4.5.4	Role of the immunoproteasome and interferon-gamma in bortezomib resistance <i>in vitro</i>	243
4.5.5	Role of the immunoproteasome in the <i>in vivo</i> setting in bortezomib-refractory myeloma.....	245
CHAPTER 5. SUMMARY, CONCLUSION AND FUTURE WORK.....		250
5.1	SUMMARY AND CONCLUSION	250
5.1.1	Characterisation of an isogenic cell line model of bortezomib resistance <i>in vitro</i> and <i>in vivo</i>	250

5.1.2	Whole exome sequencing of MM.1R and VDR.....	251
5.1.3	Gene expression profiles of MM.1R and VDR	252
5.1.4	Proteomic profiling of MM.1R and VDR by label-free mass spectrometry.....	253
5.1.5	Functional studies and potential role of the bone marrow microenvironment in the pathogenesis of bortezomib resistance in VDR.	254
5.1.6	CONCLUSION	255
5.2	FUTURE WORK.....	259
5.2.1	Characterisation of an isogenic cell line model of bortezomib resistance <i>in vitro</i> and <i>in vivo</i>	259
5.2.2	Whole exome sequencing of MM.1R and VDR.....	259
5.2.3	Gene expression profiles of MM.1R and VDR	259
5.2.4	Proteomic profiling of MM.1R and VDR by label-free mass spectrometry.....	259
5.2.5	Role of the bone marrow microenvironment in the pathogenesis of bortezomib resistance in VDR.....	260
6.	SCIENTIFIC WORK PUBLISHED OR PRESENTED.....	261
	REFERENCES	263

ABBREVIATIONS

ALL	Acute lymphoblastic leukaemia
AML	Acute myeloid leukaemia
ASCT	Autologous Stem Cell Transplant
BJP	Bence-Jones Proteins
BMSC	Bone marrow stromal cell
BR	Bortezomib Resistance
c	Monoculture
C-L	Caspase-like
cc	Co-culture
CFZ	Carfilzomib
CI	Confidence interval
CRAB	Hypercalcaemia, Renal Impairment, Anaemia, Lytic Bone Lesions
CSBLI	Compartment-specific bioluminescence imaging
CT-L	Chymotrypsin-like
CTG	Cell Titre Glo
DAVID	Database for Annotation, Visualization and Integrated Discovery
DCU	Dublin City University
Del	Deletion
DFCI	Dana-Farber Cancer Institute
EFS	Event free survival
FDA	Federal Drug Association
GEP	Gene expression profiling
GFP	Green-fluorescent protein
GO	Gene Ontology
HDAC	Histone deacetylase
hFob	Human Foetal Osteoblast-like

HS-5	Human Stromal Cell line-5
HSP	Heat shock protein
IFN	Interferon
IHC	Immunohistochemistry
IL-6	Interleukin-6
IMiD	Immunomodulator (e.g. lenalidomide/ pomalidomide/ thalidomide)
IMWG	International Myeloma Working Group
IV	Intravenously
Luc	Luciferase
M-protein	Monoclonal Protein
Mcl	M-Cherry-luc
MGUS	Monoclonal Gammopathy Of Uncertain Significance
MM	Multiple Myeloma
MRI	Magnetic Resonance Imaging
MSC	Mesenchymal stem cell
MTT	3-(4,5-dimethylthiazol-2-yl)-2,5-diphenyltetrazolium bromide
Mut	Mutant
NEDD8	Neural precursor cell expressed, developmentally down-regulated 8
NF- κ B	Nuclear factor-kappaB
NICB	National Institute for Cellular Biotechnology
nM	Nanomolar
OB	Osteoblast
OC	Osteoclast
OS	Overall survival
P-gp	P-glycoprotein
PET-CT	Positron Emission Tomography-Computerised Tomography
PI	Proteasome inhibitor
PO	Per oral

PSMB5	Proteasome subunit beta-5
PSMB8	Proteasome subunit beta-8
Rpm	Rounds per minute
RT-PCR	Reverse transcriptase polymerase chain reaction
RVD	Revlimid (Lenalidomide), Velcade (Bortezomib), Dexamethasone
SD	Standard Deviation
sFLCs	Serum Free Light Chains
shRNA	Small hairpin ribonucleic acid
SMM	Smouldering Multiple Myeloma
SNV	Single nucleotide variants
SPC	Solitary Plasmacytoma
SPEP	Serum Protein Electrophoresis
STR	Short Tandem Repeat
T-L	Trypsin-like
TOP	Topoisomerase
uL	Microlitre
uM	Micromolar
VDR	Velcade (Bortezomib) And Dexamethasone Resistant (also termed MM.1VDR)
Vel/Bort	Velcade/ bortezomib
VGPR	Very good partial response
WES	Whole exome sequencing
Wt	Wild type
β-5	Beta-5 constitutive subunit
β-5i	Beta-5 immunoproteasome subunit

Abstract

Intrinsic and Extrinsic Factors Affecting Proteasome Inhibitor Resistance in Multiple Myeloma

Dr. Catriona Ann Hayes

The proteasome inhibitor bortezomib remains a key component of high potency combination regimens for multiple myeloma (MM), whose primary site of inhibition includes proteasome subunit beta-5 (PSMB5). However, all MM patients inevitably develop resistance. We therefore investigated intrinsic and extrinsic mechanisms underlying resistance to bortezomib *in vitro* and *in vivo*.

We investigated a bortezomib-resistant human cell line termed MM1.VDR-gfp-luc (VDR) with a 12-fold increase in IC₅₀ for bortezomib, compared to its isogenic parental cell line MM1.R-gfp-luc (termed MM.1R), that is resistant to dexamethasone. VDR also retained its resistance to dexamethasone, similar to parental MM.1R. In an *in vivo* SCID-beige mouse model, VDR also retained its decreased responsiveness to bortezomib.

By whole exome sequencing we identified a previously documented mutation in the PSMB5 gene in VDR, in addition to a number of other mutations of interest. We subsequently examined both the genomic and proteomic profiles of MM.1R and VDR cell lines, and further explored target genes or proteins of interest. We examined the role the bone marrow microenvironment in bortezomib resistance *in vitro*. Finally we analysed bone marrow trephine samples from bortezomib-refractory multiple myeloma patients for their expression of proteasome-related subunits.

In summary, we identified a number of known and potential novel biomarkers of bortezomib resistance in multiple myeloma, which firstly validated our model of bortezomib resistance, and secondly revealed a number of novel targets, some for which small molecule inhibitors are currently available. In addition we emphasized the pertinent role of the bone marrow microenvironment in the pathogenesis of drug resistance in multiple myeloma. Finally we measured the expression levels of PSMB5 and PSMB8 in clinical samples of patients with bortezomib-refractory myeloma, and suggested a role for the use of interferon-gamma and PSMB8 inhibitors concomitantly in the clinical setting for bortezomib-refractory multiple myeloma.

(Word count=293)

Chapter 1

Introduction

CHAPTER 1. INTRODUCTION

1.1 OVERVIEW OF MULTIPLE MYELOMA IN THE CLINICAL SETTING

1.1.1 Introduction

Multiple myeloma (MM) is characterised by unrestrained proliferation of terminally differentiated B-lymphocytes (i.e. plasma cells). It remains an incurable disease. Myeloma is the second most common lymphoid malignancy after non-Hodgkin's lymphoma, and third most common haematological malignancy in Europe.^[1] In the past decade, MM overall survival rates have dramatically improved in an era of proteasome inhibitors by the first-in-class agent, bortezomib. The APEX (Assessment of Proteasome Inhibition for Extending Remissions) Phase III clinical trial demonstrated a 6-month overall survival advantage with bortezomib monotherapy compared to high dose dexamethasone alone for relapsed MM.^[2] Presently bortezomib is currently used in combination schedules as up-front treatment for newly diagnosed MM, in addition to forming a core component of treatment regimens for relapsed and refractory disease.^[3] However a dismal 9-month overall survival associated with relapsed and refractory MM provokes an urgent need to decipher fundamental mechanisms involved in bortezomib resistance (BR).^[4] By delineating bortezomib-specific resistance pathways that can be overcome by targeted therapy, we aim to further improve the prognosis of patients with relapsed and refractory multiple myeloma.

1.1.2 Overview of monoclonal gammopathies

Multiple myeloma develops from an earlier indolent form of monoclonal plasma cell proliferation, called monoclonal gammopathy of undetermined significance (MGUS), whereby a monoclonal protein is detected in the patient's blood. Approximately 1% of MGUS patients will progress to multiple myeloma each year.^[5] In MGUS or MM, uncontrolled plasma cell proliferation results in the secretion of a monoclonal protein of a specific isotype, resulting in abnormal heavy chain (IgG/ IgA/ IgD) and/or light chain (kappa, lambda) immunoglobulin production. This results in varying isotypes of multiple myeloma, such as IgG

kappa myeloma (by far the most common), IgA kappa myeloma, IgA lambda myeloma, or light chain myeloma (characterised by the detection of free light chains only in the serum or urine), or much less frequently, IgD myeloma. The monoclonal protein (or M-protein) is quantified by immunofixation and serum protein electrophoresis, and is one of the criteria used to monitor response to treatment. The distinction between MGUS and multiple myeloma depends on the percentage of monoclonal plasma cells in the patients bone marrow (<10% in MGUS, versus ≥10% in myeloma), and the presence of “CRAB” criteria: hyperCalcaemia, Renal impairment, Anaemia and lytic Bone lesions. An intermediate form known as smouldering myeloma (SMM) is characterised by a high monoclonal protein in the serum or urine, ≥10% monoclonal plasma cells in the bone marrow, but the absence of CRAB criteria. Approximately 10% of patients with SMM progress to symptomatic multiple myeloma each year. Finally, solitary plasmacytoma (SPC) is a further entity of the malignant monoclonal plasma cell spectrum, whereby one bone lesion has proven monoclonal plasma cell proliferation, but in the presence of a low M-protein in the serum or urine, and the absence of both CRAB criteria and absence of monoclonal plasma cells in the bone marrow,^[6] (see table 1.1.2 for summary).

	MGUS	SMM	MM	SPC
Presence of M-protein	Present (<3g/dL)	Present (≥3g/dL)	Present (≥3g/dL)	Present (<3g/dL)
Percentage monoclonal plasma cells in bone marrow	<10%	≥10%	≥10%	<10%
CRAB criteria	Not present	Not present	Present	Not present

Table 1.1.2: Spectrum of monoclonal gammopathies. To fulfil diagnostic criteria for multiple myeloma (highlighted in red), an M-protein of ≥3g/dL needs to be present in the serum or urine, ≥10% monoclonal plasma cells in the bone marrow trephine and exhibit at least one of the four CRAB criteria.

1.1.3 Epidemiology of multiple myeloma

A large retrospective study examining the survival of patients with haematological malignancies recently published in the Lancet journal outlines the frequency of haematological malignancies in Europe and associated survival scores for each subtype. As previously mentioned, multiple myeloma is the second most common lymphoid malignancy after non-Hodgkin's lymphoma, and third most common haematological malignancy in Europe. Of all the lymphoid malignancies, multiple myeloma was the most frequently occurring, compared to Hodgkin's lymphoma and individual non-Hodgkin's lymphoma subtypes. Between 1996 and 2007, 81,562 cases of multiple myeloma or plasmacytoma have been documented. In 1997-1999, the 5-year relative survival for myeloma was 29.8% which dramatically increased to 39.6% by 2006-2008, and this stark increase has been attributed to novel therapies for myeloma such as the immunomodulators thalidomide and lenalidomide, and the proteasome inhibitor bortezomib.^[1]

1.1.4 Clinical Presentation

Multiple myeloma exhibits varying degrees of clinical presentation. Patients with known MGUS or smouldering myeloma have routine monitoring of monoclonal-protein (M-protein) by serum protein electrophoresis (SPEP), serum free light chains (sFLCs), Bence-Jones proteins (BJP), creatinine, calcium, and haemoglobin. A rise in M-protein/sFLC/BJP or the development of CRAB criteria warrant restaging and this is a common means of detecting symptomatic myeloma in the clinic. CRAB criteria manifest clinically as bone pain (secondary to lytic lesions), fatigue, perioral paraesthesia (secondary to hypercalcaemia), anuria or oliguria (secondary to renal impairment), or autonomic neuropathy (a paraneoplastic phenomenon associated with myeloma). Suppression of normal immunoglobulins by the predominating monoclonal protein can cause impaired immune function and increased frequency of infections.

Other patients are diagnosed following investigation of unexplained hypercalcaemia or renal impairment. Some patients will have an incidental finding of a raised total serum protein on routine liver profile testing, with a

large globulin-to-total-protein ratio. Finally, a number of patients will present with multiple myeloma without preceding MGUS or SMM, and will exhibit a monoclonal protein in the serum or urine, 10% or more monoclonal plasma cells in the bone marrow, and end-organ damage such as debilitating vertebral body collapse manifesting with severe back pain or even paralysis. Finally, if the tumour burden in the bone marrow is over-whelming, patients may even present with a secondary plasma cell leukaemia, whereby circulating malignant plasma cells can be seen on blood film by light microscopy.

1.1.5 Definition of multiple myeloma

To recap, diagnosis of multiple myeloma is based on the International Myeloma Working Groups diagnostic criteria as defined by the following parameters: $\geq 10\%$ monoclonal plasma cells present in the bone marrow, the detection of an M (monoclonal)-protein in the serum and/or urine, whilst also fulfilling at least one of the four “CRAB” criteria, that cannot be explained by another concomitant pathological process.^[6]

1.1.6 Staging of MM

The Durie-Salmon staging system was historically used to determine stage of multiple myeloma, and is based on total M-protein in serum or urine, haemoglobin level, serum calcium level and the number of lytic lesions identified on skeletal survey. This staging system was first published in 1975, however with more advanced means of determining the extent of lytic bone disease and with increased availability of PET-CT and MRI to identify lytic bone lesions, this staging system is less frequently used nowadays.^[7]

Currently the cornerstone of staging of multiple myeloma is determined by the International Staging System, which incorporates the patients’ serum albumin and beta-2-microglobulin levels. Patients with a serum albumin measurement greater than or equal to 3.5g/dL and a serum beta-2-microglobulin lower than 3.5mg/L are by definition stage 1 disease. Stage 3 disease is defined as having a serum beta-2-microglobulin greater than 5.5mg/L. Stage 2 disease is defined as a

serum albumin or beta-2-microglobulin level not fulfilling either stage 1 or stage 3 disease (see table 1.1.6). A higher disease stage correlates with shorter overall survival.^[8]

Newer staging systems have been designed to take the patients co-morbidities into account, such as the Freiburg Comorbidity Index, which takes into account the patients renal function, respiratory status and Karnofsky Performance score.^[9]

ISS Staging of MM	Stage I	Stage II	Stage III
Serum albumin	>3.5g/dL	<3.5 g/dL (and B2M<3.5mg/L)	N/A
Serum B2M	<3.5mg/L	3.5-5.5mg/L (with any albumin level)	>5.5mg/L

Table 1.1.6: International Staging System (ISS) of Multiple Myeloma. Stage of myeloma is determined by serum albumin and serum beta-2-microglobulin (B2M) levels.

1.1.7 Management of Multiple Myeloma

MM is increasingly becoming a disease that requires individualised patient therapy, depending on the stage of their disease and characteristic features at presentation. The European Myeloma Network published a new set of guidelines in relation to management of patients with newly diagnosed multiple myeloma in February 2014. Patients are first risk stratified based on ISS stage and cytogenetic abnormalities that are present in the malignant plasma cell clone. Induction therapy with a triple regimen to include bortezomib and dexamethasone with the addition of adriamycin/thalidomide/cyclophosphamide is recommended as first line for induction therapy. In patients who are medically

fit, induction therapy should be followed by autologous stem cell transplant (ASCT), with subsequent thalidomide or lenalidomide-based maintenance therapy. Bortezomib consolidation should also be considered following ASCT should the patient fail to achieve an excellent response to ASCT. In patients who are non-transplant eligible, a combination of melphalan and prednisolone with either bortezomib or thalidomide is recommended, with the possibility of lenalidomide monotherapy or lenalidomide plus reduced-dose dexamethasone maintenance,^[10] (see figure 1.1.7 for summary).

Locally in our tertiary referral centre at the Mater Misericordiae University Hospital, patients initially undergo induction therapy with a bortezomib-based regimen for example RVD (lenalidomide (i.e. Revlimid), bortezomib (i.e. Velcade), dexamethasone).^[11] Patients also receive monthly bisphosphonate infusions, mainly zoledronic acid, which has been shown to reduce skeletal-related events (i.e. bone fractures) in MM patients and also appears to increase overall survival in MM.^[12] For transplant eligible candidates, if an appropriate response is achieved with induction therapy, autologous stem cell transplant (ASCT) will be considered depending on the individual's risk for progression. Following ASCT, or achievement of clinical response in the absence of ASCT, patients are assigned maintenance therapy, often in the form of lenalidomide which has been shown to prolong time to progression and overall survival, and are maintained on same until progression occurs.^[13]

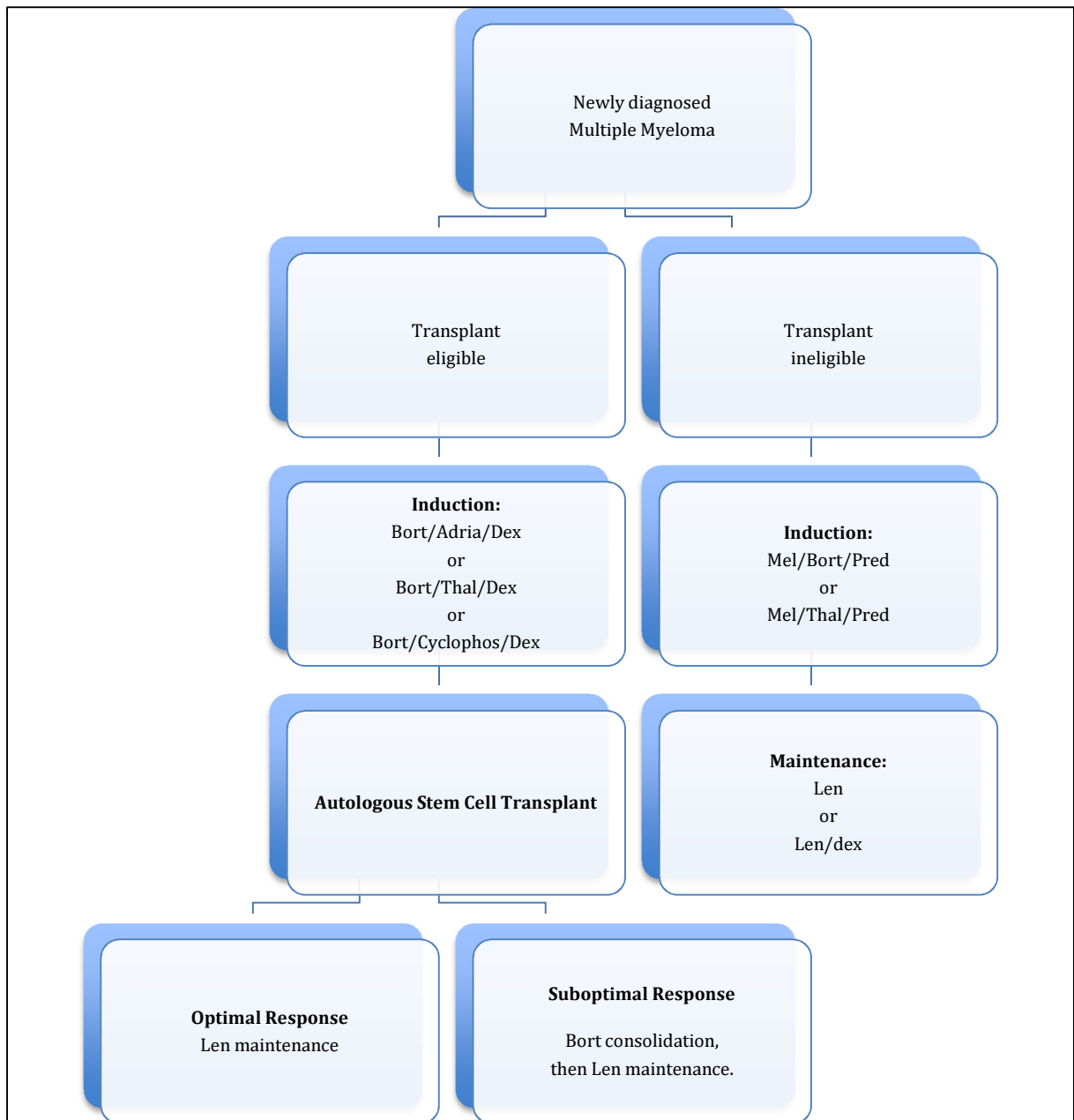


Figure 1.1.7: European Myeloma Network 2014 Guidelines on Management of Newly diagnosed Multiple Myeloma. Overview of recent guidelines for the management of newly diagnosed MM. Note: Bort= bortezomib; Adria= adriamycin; Dex= high dose dexamethasone; Thal= thalidomide; Cyclophos= cyclophosphamide; Len= lenalidomide; Mel= melphalan; Pred= prednisolone; dex= low dose dexamethasone.

1.1.8 Novel/ Investigational Therapies for MM

A variety of promising novel agents are currently under investigation for the management of MM. These include novel histone deacetylase inhibitors (e.g. panobinostat), second generation proteasome inhibitors (carfilzomib, ixazomib), novel immunomodulators (such as pomalidomide), a novel PI3K-Akt (phosphatidylinositol 3-kinase-Akt) inhibitor (perifosine), a NEDD8-activating enzyme inhibitor (MLN4924) and an mTOR inhibitor (BEZ235).

Histone deacetylase (HDAC) inhibitors such as vorinostat have successfully undergone Phase I clinical trials in 2008 demonstrating tolerability in relapsed and refractory MM as a single agent,^[14] and furthermore efficacy when used in combination with bortezomib in another clinical trial in 2012.^[15] Panobinostat, a class I, II and IV HDAC inhibitor is considered the most efficacious HDAC inhibitor and allows dual inhibition of the proteasome and aggresome when combined with bortezomib.^[16] A number of phase 1 and 2 clinical trials, including PANORAMA 2 at our collaborating centre at Dana-Farber Cancer Institute, have proven its efficacy for use in relapsed and refractory multiple myeloma in the clinical setting.^[17-19] Panobinostat is also undergoing clinical trials for its use in newly diagnosed transplant-eligible multiple myeloma in combination with lenalidomide-bortezomib-dexamethasone, and in the relapsed and refractory setting in combination with carfilzomib (www.clinicaltrials.gov).

With the success of bortezomib, second generation proteasome inhibitors (PIs) are now at the forefront of investigation for MM treatment. In particular carfilzomib, a proteasome inhibitor which binds irreversibly to the proteasome, received FDA approval in July 2012 for use in relapsed and refractory multiple myeloma, in patients who have received at least 2 previous treatment regimens containing bortezomib and an immunomodulator such as lenalidomide or thalidomide.^[20] A number of further studies have proven the efficacy of carfilzomib in both newly diagnosed and relapsed and refractory multiple myeloma.^[21-24] Furthermore, oral proteasome inhibitors are also under investigation such as marizomib, a broad spectrum proteasome inhibitor that is

at the pre-clinical phase of investigation and targets multiple sites of proteolytic activity within the proteasome,^[25] and ixazomib, a twice weekly oral proteasome inhibitor which has just completed phase 1 clinical trial with promising results for its use in refractory myeloma.^[26]

In an era of novel proteasome inhibitors, we also see novel immunomodulatory drugs at the forefront of multiple myeloma research. In particular pomalidomide in February 2013 was granted accelerated FDA-approval for its use in refractory multiple myeloma in the United States, and subsequently achieved approval in Europe in August 2013.^[27-31] At our local haematology department at the Mater Misericordiae Hospital in Dublin we have enrolled a number of patients in the STRATUS study that is examining the use of pomalidomide in combination with low dose dexamethasone in relapsed and refractory myeloma.

Finally, perifosine, the Akt inhibitor that targets phosphatidylinositol 3-kinase-Akt signalling, has successfully completed Phase I clinical trials in relapsed myeloma with encouraging results.^[32, 33] Down the pipeline additional agents that are currently under investigation include those targeting two pathways strongly implicated in multiple myeloma pathogenesis including (a) the ubiquitination pathway, in particular NEDD-8-activating enzyme inhibition via MLN4924 (of which phase 1 clinical trial has been completed, results pending),^[34] and (b) inhibitors of the phosphatidylinositol 3-kinase (PI3K)-Akt-mammalian target of rapamycin (mTOR) pathway via BEZ235 (which is currently in clinical trials for solid tumour malignancies).^[35]

1.2 RELAPSED AND REFRACTORY MULTIPLE MYELOMA

1.2.1 Definition of relapsed and refractory MM

The International Myeloma Working Group, in addition to providing us with diagnostic criteria for myeloma, have also provided us with response criteria in multiple myeloma.^[6] Response is broken down into a number of categories that include complete response (CR), very good partial response (VGPR), partial response (PR), stable disease (SD), minimal response (MR) and progressive

disease (PD). These responses are based mainly on the degree of reduction in serum or urine M-protein, reduction in number of clonal plasma cells in the bone marrow, disappearance of soft tissue plasmacytomas, and if clinically indicated, reduction in free light chain assays.

Progressive disease is based on an increase of 25% from initially documented value in any of the following: serum M-protein, urine M-protein, serum free light chains (if serum or urine M-protein not detectable at baseline). In addition an increase in the percentage plasma cells in the bone marrow must be $\geq 10\%$. The development of new lytic lesions or new hypercalcaemia that can solely be attributed to the myeloma also correlate with progressive disease.

“Relapsed myeloma” is defined based on criteria indicating increased disease burden, or new/ worsening CRAB criteria. “Clinical relapse” is used in the clinical setting to document the recurrence of disease following completion of therapy, however it is not used to calculate time to progression or progression free survival. Specifically, the development of new bone lesions or new soft tissue plasmacytomas, increasing size of known plasmacytomas by 50% (that are at least 1cm larger than before), elevated serum calcium levels $>2.65\text{mmol/L}$, a reduction in haemoglobin $\geq 2\text{g/dL}$, or an increase in serum creatinine $>177\text{umol/L}$ all correlate with relapsed myeloma.

“Refractory myeloma” is defined as a lack of any measurable response in a patient to current treatment, or progression of disease within 60 days of their last treatment. There are two main groups of refractory myeloma, primary refractory myeloma whereby patients do not respond to induction chemotherapy; and secondary refractory myeloma, whereby patients respond to induction therapy but do not respond to salvage therapy after relapse following induction therapy.

Finally, *“relapsed and refractory myeloma”* is defined clinically as someone who obtained at least a minimal response to therapy, then develops progressive disease, undergoes salvage chemotherapy, and either does not respond to salvage treatment at all or experiences progressive disease within sixty days of their last treatment.^[36]

1.2.2 Poor prognosis associated with relapsed and refractory MM

Despite an era of novel therapies including the proteasome inhibitor bortezomib and the immunomodulators (IMiD) thalidomide and lenalidomide, patients inevitably develop a state of relapsed and refractory disease. The prognosis at this disease stage was vividly outlined by Kumar et al. in a large multicentre study in 2012. In total, 286 patients were studied. The inclusion criteria included patients who were refractory to bortezomib, and/or were resistant to an immunomodulator (thalidomide or lenalidomide) or intolerant of /ineligible for treatment with an IMiD. Time zero (or T₀) was defined as the time in which the patients fulfilled the aforementioned criteria. The average age of the patients included in the study was 58 years at time zero. The average EFS (event free survival) from time zero for the entire group was 5 months (95% CI; 4, 6), and the average overall survival was 9 months (95% CI; 7, 11). The total overall survival for the group from time of diagnosis was 4.7 years (or 56 months; 95% CI; 44, 72). For patients specifically refractory to bortezomib, their median overall survival was found to be just 9 months ((95% CI; 7,11), and for those refractory to or intolerant of an IMiD overall survival was also 9 months (95% CI; 7,13). Figure 1.2.2.1 represents the survival outcomes for both bortezomib refractory and IMiD refractory/intolerant patients.

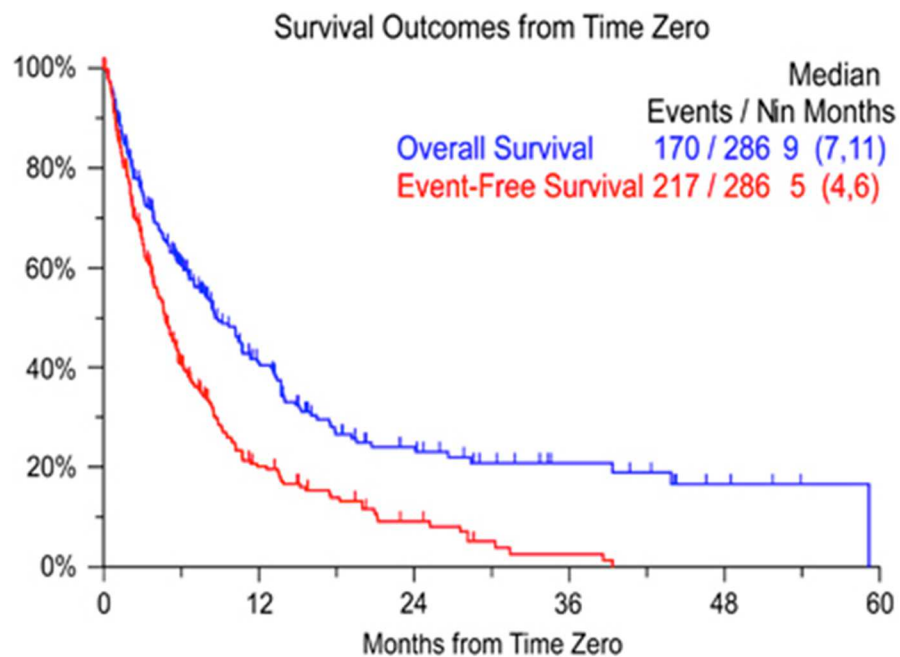


Figure 1.2.2.1: Survival outcomes of patients with bortezomib and immunomodulator refractoriness. The mean overall survival of patients found to be refractory to an immunomodulator or bortezomib was found to be 9 months. (Figure extracted from Leukaemia Journal, January 2012; 26(1):149-57. *“Risk of progression and survival in multiple myeloma relapsing after therapy with IMiDs and bortezomib: a multicenter international myeloma working group study.”* Kumar et al.)

1.2.3 Treatment options in relapsed and refractory multiple myeloma

As the majority of patients will eventually relapse, salvage therapies with both conventional and novel agents are deployed.^[36] For a first and indolent relapse, salvage therapy with bortezomib or an immunomodulator (lenalidomide, thalidomide) in combination with dexamethasone may be considered, depending on the patient's prior response to these agents. For aggressive relapse or relapse late in the disease a combination regimen including a novel agent as part of a clinical trial should be considered, for example encompassing a novel Akt inhibitor such as perifosine with lenalidomide and dexamethasone,^[33] or using monoclonal antibody therapy for example bortezomib/elotuzumab regimen^[37]. Alternatively a chemotherapy-based regimen such as DCEP (Dexamethasone, cyclophosphamide, etoposide, cisplatin) or DT-PACE (Dexamethasone, thalidomide- cisplatin, doxorubicin, cyclophosphamide, and etoposide) may be used.^[36] Autologous stem cell transplant can be considered at this stage also, however the disease-free survival in relapsed and refractory myeloma versus newly diagnosed patients under-going ASCT may be somewhat shorter.

In summary, bortezomib now forms the cornerstone of combination regimens for MM patients at diagnosis and at time of relapse, therefore examining resistance to bortezomib is of utmost importance in the clinical setting.

1.3 PROTEASOME INHIBITION IN MULTIPLE MYELOMA

1.3.1 The role of the 20S proteasome

The proteasome has been studied in great detail since the emergence of first and more recently second generation proteasome inhibitors. It is an intracellular structure located in both the nucleus and cytoplasm and functions in recycling ubiquitinated proteins that have been tagged for degradation. The proteasome consists of a 20S core particle and two 19S regulatory caps on either end. The 20S core contains two outer rings of α subunits, and 2 inner rings of β (beta) subunits. The catalytic sites for proteolysis lie within the β subunits. Three catalytic activities occur in protein degradation: chymotrypsin-like (CT-L),

caspase-like (C-L) and trypsin-like (T-L) activities, and these predominate in the $\beta 5$, $\beta 1$ and $\beta 2$ subunits respectively.^[38]

1.3.2 Rationale for use of bortezomib in multiple myeloma

Bortezomib preferentially binds and reversibly inhibits the chymotrypsin (CT)-like active site by binding to threonine residues within the $\beta 5$ subunit, and to a lesser degree inhibits caspase-like and trypsin-like activity.^[39] This results in subsequent endoplasmic reticulum stress, accumulation of misfolded proteins within the cell, and resultant cellular apoptosis.^[40]

The original rationale for use of bortezomib as an anti-MM agent was to suppress anti-apoptotic nuclear factor-kappaB (NF- κ B) activity by preventing recycling of its inhibitor, IkappaB, as outlined by Hideshima et al in 2002.^[41] A vast body of further pre-clinical and clinical evidence for the many roles of bortezomib in MM has since emerged. Bortezomib re-sensitises drug resistant LR5 and RPMI-8226-Dox40 myeloma cells *in vitro* (that are resistant to melphalan and doxorubicin respectively) to their respective resistance-related agents when treated in combination with bortezomib.^[42] Bortezomib when used in combination with a human homologue of Mdm2-(Hdm2)/p53 inhibitor (i.e. nutlin-3) demonstrates synergistic cell death in MM cells co-cultured in the presence of bone marrow stromal cells, which is not efficacious when the Mdm2 inhibitor is used in isolation.^[43] In addition to the anti-myeloma effect of bortezomib, a positive impact on bone remodelling has been attributed to bortezomib by its stimulatory effects at the transcript level on genes promoting osteoblast differentiation such as alkaline phosphatase and osteocalcin, and at the molecular level by up-regulating Runx2, as seen in C2C12 mouse myeloblast cells.^[44] In an *in vivo* mouse model (engrafted with plasma cells from 16 MM patients), bortezomib has been shown to counteract the secondary effects of myelomatous bone disease by stimulating osteocalcin secretion by osteoblasts, (thus promoting osteoblastogenesis), in addition to suppressing osteoclastogenesis.^[45] Finally a prospective trial examining patients under-going single agent bortezomib treatment confirmed the pro-osteogenic effects of bortezomib *in vivo* by micro-

CT demonstrating increased osteoid deposition in bortezomib-responsive patients.^[46]

1.3.3 Second generation proteasome inhibitors

Proteasome inhibitors can be divided into three subgroups: peptide boronates (bortezomib, ixazomib, delanzomib), peptide epoxyketones (carfilzomib, oprozomib), and beta-lactones (marizomib), see table 1.3.3 for a summary of their properties.

Following the success of bortezomib the aforementioned second generation proteasome inhibitors have been developed, the most notable of these includes the epoxyketone carfilzomib, which has also achieved FDA approval for use in multiple myeloma. Carfilzomib selectively inhibits CT-like activity, but does so irreversibly.^[47, 48] In addition it inhibits trypsin-like and caspase-like proteolytic activity but to a lesser degree in comparison to bortezomib. Carfilzomib has been shown to overcome bortezomib resistance in both bortezomib-resistant cell lines and in clinical samples of bortezomib-refractory multiple myeloma patients in the *in vitro* setting.^[48] In addition in the *in vivo* setting, the frequency of peripheral neuropathy associated with bortezomib treatment, which can frequently warrant dose reduction or drug discontinuation, is markedly reduced with carfilzomib treatment.^[49] This adverse side effect has been attributed to the off-target inhibition of HtrA2/Omi (which correlates with survival of neurons) and reduction in neurite length by bortezomib *in vitro*, however these off-target effects do not occur with carfilzomib treatment.^[50] Oprozomib is an orally bioavailable epoxyketone that maintains the same efficacy of carfilzomib in inhibiting the chymotrypsin-like catalytic site within the proteasome, however gastrointestinal side effects have been frequently reported in *in vivo* pre-clinical studies.^[51]

The novel boronates including ixazomib and delanzomib inhibit the proteasome reversibly, like bortezomib, and mainly act via inhibition of the beta-5 proteasome subunit. They potently inhibit nuclear-factor-kappa-B activation,

exert an anti-myeloma effect, an anti-angiogenic effect, and suppress osteoclasts. Both are under investigation for their efficacy in parenteral administration, however can also be used intravenously, like bortezomib. Ixazomib (or MLN9708) converts to its active form MLN2238 when exposed to water.^[51] This compound has successfully completed Phase 1 clinical trials in relapsed and refractory multiple myeloma as previously outlined.^[26]

Marizomib, an alternative novel proteasome inhibitor, is a naturally occurring substance extracted from *Salinospora tropica* marine bacteria. Marizomib has been shown to inhibit irreversibly all three proteolytic sites: chymotrypsin-like, trypsin-like and caspase-like activities in the proteasome. It has potential also for use as an oral therapy in cancer.^[51] In a phase 1 clinical trial involving 22 patients with non-small-cell lung cancer, melanoma or pancreatic cancer, marizomib in combination with the histone deacetylase inhibitor vorinostat was well tolerated by patients and resulted in disease stability in 61% and reduction in tumour burden in 39% of patients evaluated.^[52] These results encourage assessment of marizomib for other malignancies including multiple myeloma, in which proteasome inhibitors are now well established as a successful therapy.

Proteasome Inhibitor	Class	FDA-Approval	Proteolytic Activity	Inhibitory Effect	Mode of Delivery
Bortezomib	Boronate	Yes	CT-L	Reversible	IV/SC
Ixazomib	Boronate	-	CT-L	Reversible	IV/PO
Delanzomib	Boronate	-	CT-L	Reversible	IV/PO
Carfilzomib	Epoxyketone	Yes	CT-L	Irreversible	IV
Oprozomib	Epoxyketone	-	CT-L	Irreversible	IV/PO
Marizomib	Beta-lactone	-	CT-L, T-L	Irreversible	IV/PO

Table 1.3.3 Characteristics of proteasome inhibitors. Characteristics of first and second generation proteasome inhibitors, information courtesy of Lawasut et al, "New Proteasome Inhibitors in Myeloma", Curr Hematol Malig Rep 2012.^[51] (Note: CT-L= chymotrypsin-like; T-L= trypsin-like; IV= intravenous; PO= per oral).

1.3.4 The Immunoproteasome

In the majority of cells in the body, stress caused by oxidative forces and inflammatory cytokines results in an increase in production of what is known as the immunoproteasome. For this reason, cells of the immune system express greater levels of immunoproteasome rather than constitutive proteasome. Immunoproteasomes have historically been documented for their pertinent role in the process of major-histocompatibility class-1 antigen presentation within cells in response to infections.^[53]

The immunoproteasome itself contains catalytic active sites that correlate to the catalytic active sites found in constitutive proteasomes. So, the β -5 subunit in the constitutive proteasome corresponds to β -5i immunoproteasome, β -1 to β -1i, and β -2 to β -2i respectively (see table 1.3.4 for summary of proteasomal subunits and their associated protein targets).

Catalytic Activity	Constitutive Subunit	Uniprot Symbol	Immuno-proteasome Subunit	Uniprot Symbol
CT-L	β -5	PSMB5	β -5i	PSMB8/ LMP7
C-L	β -1	PSMB1	β -1i	PSMB9/ LMP2
T-L	β -2	PSMB2	β -2	PSMB10/MECL1

Table 1.3.4: Constitutive and Immunoproteasome Subunits. Constitutive and immunoproteasome subunits (with corresponding protein symbols) highlighted in red and blue respectively. (Note: CT-L= chymotrypsin-like; C-L= caspase-like; T-L= trypsin-like.)

Immunoproteasome subunit generation can be induced in cells by the presence of the inflammatory cytokine interferon-gamma. Once generated, immunoproteasome subunits are introduced into newly generated proteasome 20S cores instead of the constitutive subunits. Even though interferon- gamma abrogates incorporation of constitutive subunits into the proteasome structure, its presence does not appear to alter the overall content of β 5, β 1 or β 2 mRNA

within cells. In fact following interferon-gamma stimulation of cells, cells are found to contain proteasomes with a mixture of $\beta 5$, $\beta 1$ and $\beta 2$ subunits, or $\beta 5i$, $\beta 1i$ and $\beta 2i$ subunits.^[54]

In 2005, Altun et al demonstrated that myeloma cell lines contain both constitutive and immunoproteasome subunits. At baseline, MM cell lines contain more constitutive than immunoproteasome subunits, however the latter is up-regulated by interferon-gamma. By 2-dimensional gel electrophoresis the active catalytic subunits for $\beta 5$, $\beta 1$ and $\beta 2$, or $\beta 5i$, $\beta 1i$ and $\beta 2i$ were examined following their treatment with bortezomib, with and without interferon-gamma pre-treatment. They found that pre-treatment with interferon gamma up-regulated the $\beta 5i$ subunit and that bortezomib had the ability to inhibit its catalytic activity, in addition to its better known mode of action, i.e. inhibition of the constitutive $\beta 5$ active site.^[55]

Secondly, in 2008, another group suggested a role for use of interferon-gamma to ameliorate the effects of bortezomib in preclinical models of B cell neoplasms including Burkitt's lymphoma, mantle cell lymphoma and myeloma. They found that pre-treatment with interferon-gamma of the B cell lymphoma cell line KARPAS422, and in 5 out of 6 bortezomib-sensitive B cell neoplastic cell lines tested (including RPMI8226 myeloma cell line) induced a marked increase in the sensitivity of these cell lines to bortezomib. The plasmacytoma cell line U266 demonstrated the greatest increase in sensitivity to bortezomib when pre-treated with interferon-gamma. These findings may be mediated at least in part by increased immunoproteasome assembly as demonstrated by RT-PCR subunit expression levels following interferon-gamma pre-treatment.^[56] Interferon-gamma however is also known to alter transcription of a large number of genes including caspase-8 that promotes apoptosis,^[57] and Mitsiades et al have also demonstrated caspase-8 up-regulation by bortezomib.^[40] Therefore we cannot assume that the synergistic effects of interferon-gamma with bortezomib are solely mediated by immunoproteasome subunit up-regulation. However these data support a role for interferon-gamma pre-treatment with bortezomib to

augment its potency, and in particular support a role for interferon-gamma pre-treatment in the setting of bortezomib-refractory myeloma.

1.3.5 Novel immunoproteasome inhibitors

Following an era of first and second generation proteasome inhibitors, the immunoproteasome inhibitors are now coming to the forefront of research for their use in haematological malignancies. PR-924, a tri-peptide epoxyketone proteasome inhibitor has been shown to selectively inhibit PSMB8 (also known as LMP7). Singh et al have shown in particular how PR-924 suppress proliferation of and induce myeloma cell line apoptosis with subsequent upregulation of caspase-3, caspase-8 and caspase-9. The same group also demonstrated the efficacy of PR-924 in a human plasmacytoma mouse model *in vivo* with reduction in tumour burden and increase in overall survival of PR-924 treated-mice over vehicle mice.^[58] These findings pave the way for use of immunoproteasome inhibitors in multiple myeloma in the future.

1.3.6 *In Vitro* Models of Bortezomib Resistance

In order to investigate bortezomib resistance (BR) *in vitro*, a number of investigators have generated bortezomib resistant models of haematological and solid tumour cell lines. In 2008 Oerlemans et al initially produced an acute monocytic leukaemia BR-model (THP-1) exhibiting a 45-129 fold reduction in sensitivity to bortezomib.^[59] In the same year, Lu et al described a bortezomib resistant T cell acute lymphoblastic leukaemia cell line (Jurkat), which demonstrated an increase in IC₅₀ from parental to bortezomib-resistant-model of 10nM to 268nM respectively after 24-hour treatment.^[60] Both aforementioned models identified a common mutation (G322A substitution) in the PSMB5 subunit as a causative factor for bortezomib resistance. Ri et al next described the first model of BR in multiple myeloma in 2010, again demonstrating marked resistance to the proteasome inhibitor, and confirming the previously published PSMB5 mutation delineated by Oerlemans, in both KMS-11 and OPM-2 BR models.^[61] Perez-Galan et al in 2011 developed mantle cell lymphoma cell lines (JEKO, HBL-2) that acquired a 40-80 fold reduction in bortezomib sensitivity

secondary to undergoing plasmacytic differentiation, but the previously documented PSMB5 mutations were not detected in these models.^[62] Suzuki et al, again in 2011, chose a colon cancer model (HT-29) to study bortezomib resistance and demonstrated further unique PSMB5 mutations.^[63] Finally, Kuhn et al in 2012 demonstrated an additional model of BR in MM, which although it did not demonstrate PSMB5 mutations, underlined the efficacy of targeting the insulin-like growth factor receptor to overcome bortezomib resistance.

1.3.7 Functional significance of PSMB5 mutations *in vitro*

There remains limited clinical evidence for the role of PSMB5 mutations in bortezomib resistance *in vivo* to date. This can be perhaps explained by the limited number of samples obtainable from bortezomib refractory patients, as it is often not appropriate to repeat bone marrow biopsies late in the disease course, in particular at a stage when patients require only palliative and supportive care. An alternative explanation is perhaps the mechanisms of bortezomib resistance may differ between the *in vitro* and *in vivo* setting. Much functional evidence suggests that these mutations play a role in bortezomib resistance thus far *in vitro*. For example, Oerlemans, using a bortezomib-resistant AML cell line encoding the mutant G322A substitution in the PSMB5 gene, demonstrated that siRNA knockdown of the PSMB5 gene in the resistant clone re-sensitised the cells to bortezomib.^[59] Furthermore, Lu et al, who also described the same G322A substitution in the PSMB5 gene in a T cell ALL model of BR, demonstrated how retroviral insertion of the mutant-PSMB5 into parental Jurkat cells rendered them resistant to bortezomib and also interfered with chymotrypsin-like inhibition.^[60] In MM, similar findings were confirmed when this same PSMB5 mutation, found in a KMS-11 BR clone, was inserted into parental KMS-11 cells, which resulted in a marked reduction in bortezomib-associated apoptosis in the parental cells.^[61] Suzuki described a novel PSMB5 mutation of particular interest, a Cys63Phe mutation, whereby Cys63 is a residue with known critical drug binding affinity for bortezomib, and its substitution with phenylalanine resulted in a change in the angle of the bortezomib active site binding-helix, with resultant change in the orientation and conformation of bound bortezomib within the active site, and thus may explain reduced

inhibition of chymotrypsin-like activity in the resistant clone.^[63] Finally, Franke et al furthermore demonstrated, by 3D *in silico* modelling, a number of PSMB5 mutations that alter the structural conformation of the bortezomib-binding pocket within the $\beta 5$ subunit, and impair bortezomib binding *in vitro*.^[64] In conclusion a vast body of evidence has outlined the potential role PSMB5 mutations play in bortezomib resistance in the *in vitro* setting.^[65] However it remains to be fully elucidated whether or not these findings translate clinically in the *in vivo* setting.

1.4 GENETICS OF MULTIPLE MYELOMA

1.4.1 Cytogenetics

As part of their initial work-up, cytogenetic analysis of the CD138-positive monoclonal plasma cells of patients with multiple myeloma are examined as these anomalies can help assist in predicting outcome and this is examined by conventional cytogenetics or fluorescent in situ hybridisation. The malignant myeloma cells generally fall into one of two groups: hypodiploid or hyperdiploid. Hypodiploidy is associated with translocations t(4;14) or t(14;16) and hyperdiploidy associated with t(11;14), the former of which is associated with a poorer overall prognosis. Later on in the disease secondary aberrations develop and these generally involve deletions such as del17p, del13q, del1p, or amplification of 1q. Del17p is associated with a very poor prognosis.^[66]

1.4.2 Whole genome mapping in MM

A highly comprehensive sequencing analysis involving whole exome sequencing or whole genome sequencing of 38 MM patients in 2011, although did not focus on resistance to therapy, underlined the invaluable application of whole genome sequencing for determining pathogenesis mechanisms in MM. The previously established role of the NF- κ B pathway was further expanded by this study, by demonstrating 11 distinct mutations implicated in its activation. Furthermore, additional sequencing studies demonstrated mutations of BRAF kinase in 4% of subjects, which have not been previously recognized in MM patients.^[67] This

novel finding has high potential for rapid clinical translation as these patients may benefit from BRAF kinase targeting via BRAF inhibitors, which are now used in metastatic malignant melanoma.^[68]

1.4.3 Role of PSMB5 mutations in MM in the clinical setting

Despite vast evidence for the role of PSMB5 mutations in bortezomib resistance *in vitro*, no evidence of these mutations have yet been implicated in bortezomib resistance *in vivo*. A recent study was undertaken whereby whole exome sequencing of 76 MM patients was completed to include the following groups: 10 patients with reduced sensitivity to single agent bortezomib (where bortezomib insensitivity was defined as minimal response/ stable disease/ progressive disease) and 6 MM patients who relapsed on single agent bortezomib after having achieved a partial response. Alterations in the PSMB5 gene were not found to be associated with bortezomib refractoriness in these 16 patients. Also, the PSMB5 mutation previously described by Lu, Oerlemans and Ri was not identified in the *in vivo* analysis. However the sample size was somewhat limited (n=16). Therefore the question still remains unclear as to whether or not PSMB5 mutations are implicated in bortezomib resistance in multiple myeloma *in vivo*. Larger studies are needed to clarify this question.^[69]

1.5 EXTRINSIC RESISTANCE MECHANISMS: ROLE OF THE BONE MARROW MICROENVIRONMENT

1.5.1 The role of the bone marrow accessory cells in MM pathogenesis

The role of the bone marrow microenvironment in MM pathogenesis has been studied in great detail and the protective effect it confers to clonal plasma cells in multiple myeloma patients has been well documented. The “seed and soil” hypothesis was first introduced in the late 1800s by a British surgeon, Dr. Stephen Paget, who proposed a neoplastic growth (the seed i.e. the myeloma cell) will proliferate in an environment (the soil i.e. the bone marrow microenvironment) that supports its survival.^[70] Since then vast evidence has emerged demonstrating the role of the myeloma cells local environment in augmenting its survival, in particular in relation to the protective effects conferred to myeloma cells by bone marrow stromal cells and osteoclasts

(OCs).^[71-73] In normal bones, osteoclasts function in bone remodelling or breakdown, so that osteoblasts can replace damaged bone with new healthy bone. In multiple myeloma, osteoclasts are activated and are responsible for the lytic lesions seen at clinical presentation and throughout the disease course. In contrast, MM cells suppress osteoblast (OB) activity that would normally allow bone remodelling following its reabsorption by activated OCs, compounding the burden of lytic bone lesions in patients with multiple myeloma.

In relation to bone marrow stromal cells, direct interaction of these and clonal plasma cells via adhesion molecules on the cell surface of each has been shown to induce nuclear-factor-kappa-B activation and up-regulation of interleukin-6, both of which contribute to the survival of the malignant plasma cell clone.^[74]

In relation to osteoclasts, a vicious cycle of interactions between these accessory cells and myeloma cells allows co-operative survival of both entities. Firstly, myeloma cells attach to osteoclasts directly by numerous adhesion molecules such as vascular cell adhesion molecule-1 (VCAM-1), with resultant stimulation of osteoclastogenesis.^[75] It has also been shown that reduction of osteoprotegerin (which normally allows bone remodelling via osteoblasts) occurs when myeloma cells are co-cultured with bone marrow stromal cells, with resultant increase in myeloma cell survival and increased production of osteoclasts.^[76] A further study involving co-culture of osteoclasts with myeloma cells *in vitro* has demonstrated osteoclast-induced increase in myeloma cell viability, (compared to myeloma cells culture in isolation), in addition to reduction in myeloma cell apoptosis.^[77]

1.5.2 The role of osteoblasts in multiple myeloma

Osteoblasts are large mononuclear cells found abundantly in bone and function to secrete and mineralise bone matrix. They arise primarily from pluripotent mesenchymal stem cells (MSCs) and when these progenitors over-express RUNX2 (Runt-related transcription factor 2) they become committed to the osteoblastic lineage of differentiation. The most immature form of osteoblast secretes low levels of osteopontin and very high levels of collagen type 1, and these are termed “pre-osteoblasts”. As they mature, they secrete additional

factors involved in bone formation in particular osteocalcin, osteopontin and alkaline phosphatase, (ALP) and can now produce osteogenic matrix, but at this stage RUNX2 expression is reduced compared to pre-osteoblasts. As they mature further their osteocalcin expression increases further allowing for bone mineralization.^[78]

The effects of MM cells on attenuation of osteoblastic activity can be explained partly by inhibition of pre-osteoblastic differentiation into mature OBs. The main pathway involved in inhibition of osteoblastogenesis is by direct cell-to-cell contact between the mesenchymal stem cells (MSCs) and MM cells. Adhesion of these two entities via VCAM-1 and very late antigen-4 (VLA-4) results in a reduction in RUNX2 expression, a critical factor involved in osteoblast maturation.^[79] Secondly, MM cells secrete factors that inhibit differentiation of osteoblasts, such as Dickkopf 1 (DKK-1), soluble frizzled related protein-2 (SFRP-2), tumour necrosis factor alpha (TNF- α) and Activin A. DKK-1 and SFRP-2 act by inhibiting the Wnt pathway, a pathway that plays a significant role in osteoblastic maturation.^[80, 81] More recently p38 mitogen-activated protein kinase (MAPK) has been identified as a major regulator of Wnt inhibition via DKK-1 by up-regulating DKK-1 secretion in MM cells.^[82] TNF- α inhibits differentiation of MSCs into mature osteoblasts and also induces apoptosis of mature osteoblasts and this appears to be RUNX2-dependent, mediated by a RUNX2 transcriptional inhibitor, Gfi1.^[83] Activin A (which is expressed at high levels in patients with lytic bone disease) has also been shown to attenuate osteoblastic differentiation, in addition to increasing osteoclastic activity, via the Activin type-2A receptor, and thus concurrently worsens myelomatous bone disease.^[84] A pro-inflammatory chemokine, CCL3 (i.e. MIP-1 α) that has known stimulatory effects on osteoclasts has also recently been implicated in inhibition of mature osteoblasts by suppressing osteocalcin secretion and thus abrogating bone mineralisation.^[85] Thus not only do myeloma cells deter differentiation of immature osteoblasts into osteogenic cells, but also inhibit the essential function of bone mineralisation in mature osteoblasts.

Research efforts to stimulate osteoblastogenesis and hence improve myelomatous bone disease have been at the forefront of myeloma research in

recent times, in an attempt to counteract the suppressive effect of myeloma cells on mature osteoblasts. It had not previously been anticipated that osteoblasts could in contrast confer a protective effect to myeloma cells until 2000, when Karadag et al demonstrated that co-culture of myeloma cell lines and hFob 1.19 (a human foetal osteoblast-like cell line) resulted in a significant increase in MM cell viability. The protection conferred to MM cells by hFob 1.19 was found to be IL-6 mediated, mainly by direct cell-to-cell contact between the two entities.^[86] More recently in 2009, Fu et al documented the role of TRAIL (tumour necrosis factor (TNF)-related apoptosis-inducing ligand)-induced apoptosis in MM pathogenesis and the interplay between OBs and myeloma cells in this setting. It had been previously documented that myeloma cells in monoculture are sensitive to TRAIL-induced apoptosis. hFob 1.19 and osteoblasts derived from normal donors in monoculture were not sensitive to TRAIL-induced apoptosis in this study. However when osteoblasts were in co-culture with MM cells, this resulted in TRAIL-induced apoptosis of the osteoblasts. Furthermore they demonstrated that while MM cells in monoculture are sensitive to TRAIL-induced apoptosis, their co-culture with osteoblasts interestingly allows them to escape TRAIL-induced apoptosis and subsequently proliferate. This data demonstrates how osteoblasts have the potential to support myeloma cell growth by allowing MM cell escape of TRAIL-induced apoptosis, and also could explain why osteoblasts are reduced in number in MM patients,^[87] (see table 1.5.2 for summary).

TRAIL-effect	Myeloma cell monoculture	Osteoblast monoculture	Co-culture of MM cells and OBs
MM cell apoptosis	Yes	-	No
OB apoptosis	-	No	Yes

Table 1.5.2: Effect of TRAIL on myeloma cells or osteoblasts in monoculture or co-culture. In monoculture, myeloma cells are sensitive to TRAIL-induced apoptosis, where as osteoblasts are not. However, when myeloma cells are in co-culture with osteoblasts, myeloma cells appear to escape and osteoblasts become subject to TRAIL-induced apoptosis. (Note: MM= multiple myeloma; OB= osteoblast).

In summary, while the majority of previously published literature demonstrates MM cell suppression of osteoblast differentiation and function, some data exists to support the hypothesis that osteoblasts themselves may confer survival advantage to malignant plasma cells.

1.5.3 Role of the microenvironment in drug resistance in multiple myeloma

In general two forms of microenvironment-mediated drug resistance occur: (i) cytokine-mediated resistance and (ii) adhesion-mediated resistance.

Cytokine-mediated drug resistance is mainly secondary to interleukin-6, which alone also contributes to myeloma cell survival even before treatment is commenced.^[88] When myeloma cells and bone marrow stromal cells adhere to one another, interleukin-6 production is up-regulated and has been shown to contribute to bortezomib resistance, and subsequent blockade of IL-6 using a monoclonal antibody for IL-6 (CNTO 328) results in resensitisation of the cells to bortezomib.^[89]

Insulin-like growth factor-1 (IGF-1) has also been found to contribute to drug resistance in myeloma. In particular IGF-1 cytokine production (that is up-regulated secondary to adhesion of bone marrow accessory cells and myeloma cells) has been shown to contribute to bortezomib resistance in both a bortezomib resistant cell line and myeloma cells taken from patients with bortezomib-resistant disease. Inhibition of IGF-1 or IGF-1R, (insulin-like growth factor-1 receptor) resulted in resensitisation of resistant cells to bortezomib.^[65]

Nuclear-factor-kappa-B has been found to be over-expressed in the bone marrow stromal cells of patients with multiple myeloma, in association with over-expression of interleukin-8, and contributes to drug resistance in multiple myeloma including resistance to bortezomib.^[90]

Finally adhesion-mediated resistance in multiple myeloma is mainly as a result of myeloma cells adhering to bone marrow stromal cells by beta-1 integrins. Noborio-Hatano et al in 2009 revealed VLA-4 as a pivotal adhesion molecule contributing to drug resistance to vincristine, doxorubicin and dexamethasone,

and bortezomib treatment appeared to down-regulated CD49d (or alpha4-integrin, a subunit of VLA-4) and overcome adhesion-mediated resistance.^[91]

1.6 SUMMARY

In summary, multiple myeloma is an incurable malignancy of terminally differentiated B-lymphocytes or plasma cells. Increased survival has been observed with the introduction of bortezomib. Patients present with hypercalcaemia, lytic bone lesions, renal failure or anaemia, and a monoclonal protein detected in the serum or urine. Induction therapy with a bortezomib-containing regimen is recommended as first-line treatment, and bortezomib can also be used as part of consolidation or maintenance therapy. A number of other classes of novel therapies have also become available in recent years including panobinostat (HDAC inhibitor), carfilzomib (second generation proteasome inhibitor), and pomalidomide (immunomodulator).

Relapsed and refractory myeloma is defined as a patient who has achieved at least a minimal response to treatment, then develops progressive disease, undergoes salvage chemotherapy, and either does not respond or relapses within 60 days of salvage therapy. Patients with multiple myeloma refractory to bortezomib or an IMiD have a 5-month event free survival and a 9-month overall survival. Relapsed and refractory myeloma chemotherapy regimens also incorporate bortezomib with a number of additional therapies such as another novel approved therapy or one as part of a clinical trial. The reasoning behind this is because bortezomib attacks malignant plasma cells by a number of means: inhibiting NF- κ B which is pertinent to the survival of the cancerous clone, overcoming resistance to conventional therapies and improving myelomatous bone disease.

Second generation proteasome inhibitors are now being investigated for their use in myeloma, and following the success of bortezomib, carfilzomib has also been recently approved for use in myeloma. A number of oral therapies are also being investigated such as oprozomib and ixazomib. The immunoproteasome is also known to be subject to proteasomal inhibition by bortezomib and its subunits can be up-regulated by interferon-gamma. Immunoproteasome

inhibitors such as PR-924 are also being investigated in preclinical studies for their use in myeloma.

Resistance to bortezomib in the *in vitro* setting has been so far mainly attributed to mutations of the PSMB5 gene, through which bortezomib principally inhibits the proteasome. However mutations in PSMB5 have not yet been found to be clinically significant in the *in vivo* setting. Cytogenetic abnormalities such as hypodiploidy and translocations t(4;14) and t(14;16), in addition to del17p, del13q and del1p are associated with a poor prognosis in the *in vivo* setting. Genetic mutations of NF- κ B and BRAF-kinase have been shown to contribute to multiple myeloma pathogenesis in the *in vivo* setting also. To further complicate things, myeloma is now known to express not just one but multiple clones with varying genotypes at diagnosis, each which can further mutate as the disease progresses.

Extrinsic mechanisms of multiple myeloma pathogenesis induced by the bone marrow microenvironment include again NF- κ B, but also increased secretion of IL-6. Cell-to-cell adhesion of MM cells and BMSCs occurs by the adhesion molecule VCAM-1. Osteoclasts also contribute to MM pathogenesis by increasing the proliferation rate of MM cells, contributing to drug resistance, and conversely MM cells promote osteoclastogenesis. Historically, osteoblasts were not assumed to contribute to MM pathogenesis as it has been shown that mature osteoblasts are suppressed by clonal plasma cells, mediated by interactions between malignant plasma cells and bone marrow stromal cells that results in suppression of RUNX-2, which is a major determinant of osteoblast maturation. However the osteoblast-like cell line hFob 1.19 has been shown to promote myeloma cell survival and this is thought to be mediated by TRAIL-induced apoptosis, whereby reciprocal TRAIL-induced apoptosis of mature osteoblasts occurs instead of apoptosis of myeloma cells when the two entities are in co-culture. Drug resistance in the *in vitro* setting again has also been attributed to the over-expression of IL-6; in the case of bortezomib resistance specifically, IGF-1 has been implicated.

The aetiology of proteasome inhibitor resistance is clearly multifactorial and is secondary to both intrinsic and extrinsic mechanisms. Given the complexity of multi-clonal plasma cells and their interaction with the bone marrow milieu we chose to further examine the potential intrinsic mechanisms of specifically bortezomib resistance by examining the genomic, proteomic and mutational profile of a bortezomib resistant cell line (termed VDR) developed in the laboratory of Dr Mitsiades. We next examined the effect of HS-5 bone marrow stromal cells on the sensitivity of this bortezomib resistant cell line to proteasome inhibitors and other novel therapies. We also examined the osteoblast-induced changes in proliferation rate and drug sensitivity in a number of myeloma cell lines, to ascertain whether not osteoblasts can contribute to myeloma cell survival and drug resistance. Finally, we examined the proteasome subunit expression of β -5 (PSMB5) and β -5i (PSMB8) in bone marrow trephine samples of patients with bortezomib-refractory myeloma, to determine whether or not a PSMB8 inhibitor might be useful in this setting.

1.7 AIMS OF THE THESIS

To:

- Examine the sensitivity of bortezomib-resistant VDR and parental MM.1R to conventional, novel and investigational therapies *in vitro*.
- To determine if bortezomib sensitivity is restored in VDR by the combination of bortezomib with a p-glycoprotein inhibitor, elacridar.
- Determine if our *in vitro* model retains its resistance to bortezomib in an *in vivo* mouse model.
- By whole exome sequencing define mutations present in VDR compared to MM.1R.
- Examine the gene expression profile of VDR compared to MM.1R to determine which genes or sets of genes in a given pathway are over-expressed or suppressed in bortezomib-resistant VDR.
- Examine the proteomic profile of VDR compared to MM.1R to determine which individual proteins or groups of proteins in a given pathway are over-expressed or suppressed in bortezomib-resistant VDR.
- Determine the effect of HS-5 stromal cells and hFob 1.19 osteoblast-like cells on proliferation rate and drug sensitivity in VDR and other multiple myeloma cell lines.
- Examine the expression of proteasome subunits PSMB5 and PSMB8 in bone marrow trephine samples of patients with newly diagnosed and relapsed and refractory multiple myeloma.

Chapter 2

Materials and Methods

CHAPTER 2. MATERIALS AND METHODS

2.1 Ultrapure H₂O, glassware and sterilisation procedures

Ultrapure water was used when preparing media or any solutions or compounds requiring dilution. The water was purified to a standard of 12-18 M Ω /cm resistance by a reverse osmosis system (Millipore Milli-RO 10 Plus, Elgastat UHP), and the quality of the water was monitored continuously by a conductivity metre within the system.

Sterile glass bottles were used for storing cells or solutions during experiments. These bottles were submerged in a 2% solution of RBS-25 (AGB Scientific) for 1 hour, subsequently rinsed off with tap water, then further washed in an industrial dishwasher using Neodisher detergent and then twice rinsed with ultrapure water. Finally glass bottles were autoclaved at 121°C for 20 minutes, then allowed to dry completely.

2.2 Preparation of cell culture media

Roswell Park Memorial Institute medium (RPMI)-1640 purchased from Cellgro Mediatech, Manassas, VA, USA was used for culture of all myeloma cell lines. A 1:1 mixture of Ham's F12 Dulbecco's Modified Eagle's Medium (DMEM), with 2.5 mM L-glutamine (without phenol red) was used for culture of hFob 1.19 osteoblast-like cell line, which was purchased from Sigma-Aldrich. Foetal calf serum (FCS) 10% (purchased from GIBCO/BRL, Gaithersburg, MD, USA), in addition to 100U/L of penicillin and 100ug/ml streptomycin (Cellgro) were added to media containers as needed. Media prepared as outlined were stored at 4°C for up to a maximum of 2 weeks.

2.3 Cells / cell culture/ subculturing / freezing / thawing / co-culture studies

The cell lines used in our studies were as follows: MM1S-mcl (here termed MM.1S), MM1R-gfp-luc (here termed MM.1R), MM.1VDR-gfp-luc (here termed VDR), RPMI8226-Dox40-mcl (termed Dox40), KMS11-mcl, OPM2-mcl, OCI-my-5-mcl, KMS34-mcl, RPMI8226-mcl, luciferase-negative MM.1S, HS-5 and hFob1.19.

All multiple myeloma cell lines were stably transduced with lentiviral vectors that expressed M-Cherry (denoted “mc”) or green-fluorescent protein (denoted “gfp”), and a luciferase-containing vector (denoted “l” or “luc”), as previously described.^[92, 93] Thus cell lines above with suffix “mcl” contain an M-cherry and luciferase vector; cell lines with suffix “gfp-luc” contain a green fluorescent protein and luciferase vector. Stromal cells HS-5 and osteoblast-like hFob 1.19 were both negative for M-Cherry, GFP and luciferase.

All myeloma cell lines and HS-5 stromal cell line were cultured in RPMI 1640 media containing 10% foetal bovine serum, 100 U/mL penicillin and 100 µg/mL streptomycin at 37°C under sterile conditions. hFob 1.19 was cultured in Ham’s F12 DMEM containing 10% foetal bovine serum, 100 U/mL penicillin and 100 µg/mL streptomycin at 37°C under sterile conditions.

Cells were passaged twice weekly. For semi-adherent cell lines, cells were first scraped using a cell-scraper. Seventy-five percent of old media was removed and discarded, and replaced with an equal volume of fresh RPMI media, flasks were then placed back in the incubator.

For hFob 1.19 and HS-5, cells were detached from the tissue culture flask as follows: all media was removed by suctioning, then 10mL of Trypsin EDTA 1x (Cellgro) was added, the flask replaced in the incubator for 10 minutes to allow cells to detach, then 50% of old media was removed and fresh Ham’s F12 DMEM (for hFob 1.19) or RPMI media (for HS-5) was added. Flasks were then placed back in the incubator.

In order to preserve early passage numbers of cell lines, aliquots of cells were stored in liquid nitrogen for future use as follows: Cell lines were removed from tissue culture flasks as outlined above. Cells were next counted using a haemocytometer. Aliquots of 2 million cells were transferred to clean eppendorf tubes. Tubes were centrifuged and supernatant removed. Next, cells were washed with 20mL Phosphate-Buffered Saline 1X (PBS; from Cellgro), recentrifuged, and supernatant removed. This was repeated a second time. Then the cell pellet was re-solubilised in a solution of foetal calf serum containing 10% DMSO (Dimethyl sulfoxide, Sigma Aldrich) and transferred to a cryovial, which

was snap-frozen in liquid nitrogen. Then cells were transported to the liquid nitrogen tank on dry ice and stored in liquid nitrogen tanks up for up to 2 years.

On thawing, media was heated to 37°C in the water bath prior to removal of the cryovial tubes from the liquid nitrogen. Tissue culture flasks were labelled with cell line name, passage number, cell line source, and date of thawing. Cryovials containing frozen cells were removed carefully from the liquid nitrogen tank and placed on dry ice. Cells were then quickly brought to the water bath and thawed at 37°C. Once cells were completely thawed, they were added to 20mL of fresh warm media (as described above) and washed twice with PBS (as described above) before adding them to tissue culture flasks (in order to remove any DMSO). Tissue culture flasks containing thawed cells were then transferred to the incubator.

For *in vitro* tissue culture studies requiring subsequent drug treatment, aliquots of cells were removed from tissue culture flasks as described above. Cells were washed twice with fresh media, and then counted using a haemocytometer. Cells were diluted as necessary for plating on a 96-well or 384-well flat, clear-bottom tissue culture plate (Corning). For single cell line testing of sensitivity to compounds, cell lines were plated at all times at least 6 hours prior to drug treatment to allow the cells to re-adhere. In the case of co-culture with HS-5 or hFob 1.19, stromal cell to myeloma cell ratio used was 2:1 and 1:1 respectively (unless otherwise stated in results section). For all co-cultures, stromal cells were first plated at stated seeding densities, and allowed to adhere for at least 6 hours. Then myeloma cells were added, and the conditions allowed to co-culture for at least 24 hours prior to drug treatment (unless otherwise specified in results section). Cells were cultured in a total volume of 100uL (50uL each for myeloma cells and accessory cells if co-cultured) in 96-well plates, or 40uL total volume when 384-well plates were used (20uL each for myeloma cells and accessory cells when in co-culture).

2.4 STR analysis of cell lines

The identification of our stock of cell lines were frequently examined as per departmental protocol by analysing their short tandem repeats (STR). QIAamp

DNA Mini Kit (Quiagen) was used to extract DNA from cell pellets as per protocol provided, and 5ng/uL of DNA in 10uL of AE Buffer was transported to the Dana-Farber Cancer Institute Molecular Diagnostics core facility where routine STR testing as per departmental protocol was performed.

2.5 Reagents

Bortezomib was purchased from Millennium Pharmaceuticals; lenalidomide from Fisher-Scientific; dexamethasone, doxorubicin and elacridar from Sigma Aldrich; vorinostat from Merck; carfilzomib from Selleck; oprozomib from Onyx; pomalidomide from VWR; vorinostat and MLN2238 from Selleck; JQ1 was made available by the Bradner laboratory at DFCI; MLN4924 from Active-Biochem; and interferon-gamma from R&D Systems. FDA-approved datasets for high-throughput screening were obtained from the Developmental Therapeutics Program of the National Cancer Institute (NCI). All compounds were reconstituted as per protocol provided under sterile conditions and stored as recommended on product datasheet. See table 2.5 below for complete list of compounds tested in high-throughput screen.

In 96-well plates, compounds were added to plates containing cells in a total volume of 50uL at stated concentrations (or 25uL each when 2 compounds were added); or in 384-well plates compounds were added in a total volume of 10uL.

FDA Plate No. 4762			
Allopurinol	Cytarabine; Ara-C	Lapatinib Ditosylate	Quinacrine
Altretamine	Dacarbazine	Lenalidomide	Raloxifene HCl
Aminolevulinic Acid	Dasatinib	Letrozole	Romidepsin
Anastrozole	Daunorubicin HCl	Lomustine; CCNU	sorafenib
Arsenic Trioxide	Decitabine	Mechlorethamine HCl	Streptozocin
Axitinib	Dexrazoxane HCl	Megestrol acetate	Sunitinib Malate
Azacitidine	Doxorubicin HCl	Mercaptopurine	Tamoxifen Citrate
Bendamustine HCl	Etoposide	Methotrexate	Temozolomide
Bortezomib	Exemestane	Methoxsalen	Teniposide
Busulfan	Floxuridine	Mitomycin C	Thalidomide
Capecitabine	Fludarabine Phosphate	Mitotane; o,p'-DDD	Thioguanine
Carboplatin	Fluorouracil (5-FU)	Mitoxantrone HCl	Thiotepa
Carmustine	Fulvestrant	Nelarabine	Topotecan HCl
Celecoxib	Gefitinib	Oxaliplatin	Tretinoin
Chlorambucil	Gemcitabine HCl	Pazopanib HCl	Uracil mustard
Cisplatin	Hydroxyurea	Pemetrexed Disodium	valrubicin
Cladribine	Ifosfamide	Pentostatin	vandetanib
Clofarabine	Imatinib Mesylate	Pipobroman	Vemurafenib
Crizotinib	Irinotecan HCl	Pralatrexate	Vismodegib
Cyclophosphamide	Ixabepilone	Procarbazine HCl	Vorinostat
FDA Plate No. 4763			
Abiraterone	Docetaxel	Nilotinib	Vincristine Sulfate
Amifostine	Erlotinib HCl	Paclitaxel	Vinorelbine Tartrate
Bleomycin	Estramustine phosphate	Plicamycin	Zoledronic Acid
Cabazitaxel	Everolimus	Sirolimus (Rapamycin)	
Carfilzomib	Imiquimod	Triethylenemelamine	
Dactinomycin	Melphalan	Vinblastine Sulfate	

Table 2.5 Library of FDA-approved compounds tested in MM.1R and VDR.

List of all compounds tested in high-throughput CSBLI screen for their toxicity to MM.1R or VDR.

2.6 Generation of a bortezomib resistant cell line.

The bortezomib-resistant cell line was generated at the laboratory of Dr Mitsiades at the Dana-Farber Cancer Institute by Mr Joseph Negri as follows: MM.1R-gfp-luc cells were plated at a density of ~1 cell/well in 384-well-plates, and treated with Bortezomib 2.5nM. Resistant clones that survived in the presence of Bortezomib were collected and subsequently progressively exposed to increasing concentrations of bortezomib (5-40nM). Serial dose-response analyses confirmed the generation of several clones with variable reduction in bortezomib-sensitivity (IC_{50} range 80-100nM vs. <10nM for parental MM.1R). One of these clones termed VDR that displayed stable bortezomib resistance (IC_{50} 60nM) was used for this study.

2.7 *In vitro* toxicity assays measuring cell viability

In vitro cell viability assays used in these studies included CTG (Cell Titre Glo), CSBLI (Compartment-specific bioluminescence imaging), or MTT (3-(4,5-dimethylthiazol-2-yl)-2,5-diphenyltetrazolium bromide).

CTG (or Cell Titre Glo) purchased from Promega is a homogeneous method to determine the number of viable cells in culture based on quantitation of the ATP present, which signals the presence of metabolically active cells. At the end of drug treatment, CTG is added to each well in a ratio of 1:10. This results in cell lysis and the release of ATP that generates a luminescent signal proportional to the amount of ATP released. Luminescent signal is recorded by a luminometer.

CSBLI was used to determine percentage cell viability of myeloma cell lines when treated with reagents alone or following co-culture. CSBLI is particularly useful in co-culture experiments because myeloma cells have been transduced with a luciferase-containing vector, and our stromal or accessory cells do not contain luciferase vectors. Following drug treatment luciferin (2.5 mg/mL stock, Xenogen Corp) is added at a ratio of 1:10 to each well and incubated for 30 minutes at 37°C; then the bioluminescence signal is measured with a Luminoskan (Labsystems) or Envision (Perkin Elmer) luminometer. The degree of luminescence detected correlates to the relative number of viable cells in each

well, and this is reflective of luciferase-positive cells only; i.e. will detect relative viability of myeloma cells only despite their co-culture with accessory cells.^[92, 93]

MTT (3-(4,5-dimethylthiazol-2-yl)-2,5-diphenyltetrazolium bromide) assay is used to determine cell viability as a function of redox potential. Cells that are actively respiring convert water-soluble MTT to insoluble formazan, which is purple in colour. After drug treatment MTT is added at a ratio of 1:10 and plates are then incubated at 37°C for 4 hours. Then the plates are centrifuged for 10mins at maximum speed and supernatant removed. Then DMSO is quickly added to solubilise the formazan and its absorbance determined by optical density. The absorbance calculated directly correlates with relative cell viability.

2.8 *In vivo* mouse model treatment with bortezomib or carfilzomib

This *in vivo* study including analysis of results was kindly completed by Ms. Amanda Christie at the Lurie-Family Imaging Centre at Dana-Farber Cancer Institute, under the supervision of Dr. Nancy Kohl. Seventy-five mice were injected intravenously with either MM1R (n=38) or VDR cells (n=37). All mice were imaged at least once weekly until disease burden was established by Xenogen imaging, which detects the bioluminescent signal of the MM.1R or VDR cells due to the presence of their luciferase-containing vectors. At this point mice from each cell line were divided into four treatment groups (n=7 or 8 per group):

1. Velcade (bortezomib) 0.75mg/kg
2. Carfilzomib 1.5mg/kg
3. Carfilzomib 3mg/kg
4. Vehicle.

All treatments were administered intravenously (IV) twice weekly. The two weekly doses of Velcade/bortezomib were administered 72 hours apart, while doses for Carfilzomib and vehicle were administered 24 hours apart. Due to the declining condition of the tail veins that compromised IV dosing (especially noticeable in the carfilzomib-treated mice), starting with the 5th week of dosing for both cell lines Velcade/bortezomib was switched to subcutaneous dosing and

carfilzomib was switched to treatment with oprozomib (the oral analogue of carfilzomib). Oprozomib was dosed PO at 15mg/kg (for carfilzomib 1.5mg/kg mice) or 30mg/kg (for carfilzomib 3mg/kg mice) on the same dosing schedule. Mice were weighed and imaged weekly until all mice were sacrificed in the VDR group. At this point the few remaining mice in the MM1R group were imaged every 7-14 days until sacrifice. All mice were sacrificed when they became paralyzed or suffered from hydrocephalus, at which time whole mice were fixed in 10% formalin. Tukey's multiple comparison test was used to analyse for statistical significance between treatment groups for reduction in tumour burden and overall survival.

2.9 Immunoblot

Whole cell pellets of MM.1S, MM.1R and VDR were collected at 4°C, centrifuged and supernatant removed, and stored at -80°C. The following day, cell pellets were lysed using a mixture of proteinase and phosphatase inhibitors. Protein concentration was determined using the Bradford curve and 20ug of protein loaded into 4-12% gels (Invitrogen). Once gel run was completed, proteins were transferred to methanol-activated PVDF membrane. Protein transfer was confirmed by Ponceau stain. Membranes were blocked in 5% milk and probed with primary antibody overnight. The following day, membranes were washed with TBST (Tri-buffered saline with 0.1% Tween), probed with secondary antibody for 1 hour and re-washed. Membranes were exposed to Pico Chemiluminescent Substrate (Thermo Scientific, 1:1 ratio) and films developed in the dark room.

Immunoblot validation studies on proteins of interest were performed using the following antibodies:

Primary Antibody	Secondary	Source	Catalogue Number
GAPDH	HRP-conjugated (no secondary)	Abcam	9482
Anti-PSMB5	Rabbit	Abcam	3330

Primary Antibody	Secondary	Source	Catalogue Number
Anti-PSMB8	Mouse	Abcam	58094
Anti-NEDD8	Rabbit	Epitomics	1571-1
Anti-Poly-Ub	Mouse	Cell Signal	3936

2.10 Whole exome sequencing

Whole cell pellets of MM.1R and VDR were collected at 4°C and 600ng DNA extracted as previously described using QIAamp DNA Mini Kit (Quiagen). Whole exome sequencing on the 2 cell lines was performed at the Centre for Cancer Genome Discovery (CCGD) at DFCl as per departmental protocol. Prior to library preparation DNA was fragmented using Covaris sonication to 150 bp and further cleaned up to under 100 bp using Agencourt AMPure XP beads. 50ng of size selected DNA was then ligated to specific adaptors during library preparation (Illumina TruSeq). All the steps of library preparation were performed according to departmental standards and had sufficient yield to continue with hybrid capture. Each library was made with sample specific molecular barcodes and quantified by qPCR. Capture was performed with the Agilent Sure-Select all exon v2.0 hybrid capture kit using 500ng input DNA per capture. The minimum criterion for CCGD is that 80% of all targets are covered at least 30x times. This was reached for all samples. Point mutation analysis was performed using MuTect v1.0.27200 developed by the Cancer Biology group at the Broad Institute (<https://confluence.broadinstitute.org/display/CGATools/MuTect>). Functional annotation clustering tool (<http://david.abcc.ncifcrf.gov/tools.jsp>) from DAVID Bioinformatics Resources 6.7 was used to find statistically significant gene-clusters with in the gene list obtained from the SNV and Indel reports. Whole exome sequencing and resultant statistical analysis were completed by the team at CCGD, and results interpreted with their expertise and the expertise of Dr Mitsiades.

2.11 Validation of mutPSMB5 in VDR cell line

A PSMB5 (proteasome subunit, beta type, 5) mutation in exon 2 of the PSMB5 gene was detected by WES in VDR cell line, that was absent in parental cell line MM1R and was validated by Sanger sequencing. DNA was extracted from freshly collected cell pellets of MM1R and VDR, and exon 2 of the PSMB5 subunit was amplified by polymerase chain reaction (PCR) using melting temperature of 50°C with the following primers purchased from IDT, Integrated DNA Technologies: PSMβ5 forward: 5'-CCTCTGATCTTAACAGTTCC-3', PSMβ5 reverse: 5'-GTGGTTGCAGCTTAACTCAC-3'. The complete PCR product was separated in 2% agarose gel (with TAE buffer and ethidium bromide 0.5ug/mL), and the purified product extracted from the gel using Qiagen Gel Extraction kit (#28704). Sanger sequencing was then completed at the DF/HCC DNA Resource Core that confirmed the presence of mutPSMB5 that was originally identified by whole exome sequencing.

2.12 Gene expression profiling

Whole cell pellets containing 2x10⁶ MM.1R and VDR cells were collected at 4°C. RNA was extracted as per protocol using RNEasy Mini kit (Qiagen) and 500ng RNA sent to Beth Israel Deaconess Medical Centre Genomics Core facility for oligonucleotide microarray analysis using Human Gene 1.0 ST Gene Arrays, (catalogue # 901085). CEL files from Affymetrix Human Gene 1.0 ST Arrays (HuGene-1_0-st) were analysed by Gene Pattern using RMA method and collapsed probe set to maximum values, this analysis was kindly provided by Dr. Panisinee Lawasut. Expression values comparison (t-test) was made by d-Chip. Fold change of greater than 1.2 and p-values less than or equal to 0.05 were used as level of significance.

(Gene Pattern: <http://www.broadinstitute.org/cancer/software/genepattern>)

(dChip: <http://www.hsph.harvard.edu/cli/complab/dchip/>)

2.13 shRNA knockdown studies

27 genes were selected for shRNA knockdown studies to determine if their knockdown would resensitise VDR to bortezomib. 5 puromycin-resistant lentiviral hairpins were used for knockdown of each specific gene examined and

this study was undertaken at the DFCI RNA Interference (RNAi) Screening Facility under the supervision of Dr. Anna Shinzel. On day 1 cells were plated at a density of 400×10^3 cells/mL in 384-well-plates, in the presence of polybrene (8ug/mL), and allowed to adhere overnight. The following day small hairpins for each vector were added (5 hairpins for each gene analysed in triplicate in individual wells) and plates were then centrifuged at 2000rpm for 30 minutes at 37°C. Twenty-four hours following lentiviral infection plates were centrifuged for 10mins at 2000rpm and media containing virus removed and discarded as per departmental protocol. Then fresh media containing puromycin 2.5ug/mL was added to each condition and incubated for 48 hours so that only cells that had been successfully infected with puromycin-resistant lentivirus were further analysed. Plates were then treated with bortezomib 50nM (i.e. the IC₂₀ for MM1VDR), or vehicle (fresh media) for 24 hours and relative cell viability analysed by CTG. Empty vector and LacZ were used as control hairpins in this study.

Given that PSMB5 is known to play a pertinent role in bortezomib's mode of action, and that we also identified a mutation in the PSMB5 gene in VDR, we chose to validate the successful knockdown of PSMB5 gene and completed same as follows:

Day 1: MM.1R and VDR cells were seeded in 12-well plates at a concentration of 1 million cells/well in 2mL of fresh media. Polybrene (8ug/mL) was added to the media-containing cells prior to plating. Cells were allowed to adhere overnight. Two duplicate 12-well plates per cell line were set up as follows: one for treatment with bortezomib, and one for collection of cell pellets for validation of PSMB5 knockdown by immunoblot.

Day 2: 300uL lentivirus containing 5x PSMB5 hairpins or 2x control hairpins were added to each cell line. Plates were then centrifuged at 2000rpm for 30mins at 37°C.

Day 3: 24-hours after infection: plates were centrifuged for 10mins at 2000rpm, then media containing lentivirus was discarded and 2mL fresh media added with puromycin 2.5ug/mL to each condition.

Day 5: One plate for each cell line was used for drug treatment: all wells scraped with a fresh cell scraper; 1mL fresh media added to each well; transferred to 96 well plate for dose response curve using bortezomib 0-40nM for 24hours, and subsequently relative cell viability analysed using CTG. For duplicate plates: cells scraped using a fresh cell scraper for each well, cell pellets collected and prepared for immunoblot to determine PSMB5 expression in MM.1R or VDR for the following 7 conditions: 5x PSMB5 lentiviral hairpins and 2x control hairpins.

2.14 Lentiviral infection of mutPSMB5 in bortezomib-sensitive cell lines

We investigated whether or not mutant PSMB5 that was identified by the whole exome sequencing study, when introduced into bortezomib-sensitive cells, would render them resistant to bortezomib. On day 1, KMS11mcl cells were plated in a 12-well plate at a seeding density of 200,000 cells/mL in 400uL of RPMI media with polybrene 8ug/mL, with 3 biological replicates for each condition. The cells were subsequently allowed to adhere for 6 hours. Next 122uL of lentiviral construct as provided by the DFCI RNA Interference (RNAi) Screening Facility of BFP-control, wild-type PSMB5 or mutant PSMB5 blasticidin-resistant lentiviral vectors, were added. The solution within each well was mixed using a pipette briefly, then centrifuged at 2000rpm for 90 minutes each at 37°C, then placed back in the incubator. On day 3, the plates were again centrifuged at 2500rpm for 10 minutes, the supernatant was removed and quickly replaced with fresh RPMI media containing blasticidin 10ug/mL. The plates were returned to the incubator and subsequently reviewed daily by light microscopy. Every 3 days 1mL of old media was removed and 1mL media containing blasticidin (10ug/mL) was added to each condition, until each well was approximately 75% confluent, therefore allowing sufficient number of cells to perform a dose response curve. As previously described, a dose response curve for each condition was performed to assess the sensitivity of the cell line to bortezomib (0-40nM for 24 hours) in the setting of BFP-control, wtPSMB5 and mutPSMB5 and cell viability was analysed by CTG.

Lentiviral infection of MM.1S and MM.1R cell lines was also tried; however difficulty with lentiviral infection of above constructs proved technically

challenging most likely because MM.1S and MM.1R are semi-adherent cells, compared to KMS11 cells which are fully adherent, allowing a greater degree of lentiviral infection as the viral constructs and cells both rest at the bottom of the wells, thus allowing increased infection rate.

2.15 Label-free mass spectrometry

Triplicates of cell pellets containing 10×10^6 cells each for MM.1R and VDR were collected at 4°C and stored at -80°C until time of mass spectrometry. Mass spectrometry was completed at the National Institute for Cellular Biotechnology in Dublin, Ireland, under the supervision of Dr Paul Dowling. Protein extraction was achieved by the addition of lysis buffer (6M urea, 2M thiourea, 10mM Tris, pH 8) to each sample, with subsequent removal of ionic contaminants using 2D Clean-Up Kit (BioRad) and stored in acetone overnight. The following day all tubes were centrifuged, the supernatant discarded, and pellet re-suspended in the aforementioned lysis buffer. 10ug of protein per sample was determined by Bradford curve and each was transferred to a fresh tube. Each sample then underwent reduction (using dithiothreitol at 37°C for 20mins), alkylation (using iodoacetamide in ammonium bicarbonate for 20minutes), and protein digestion (via Lys-C for 4 hours, and then trypsin overnight). Peptide purification was achieved using Pep-Clean C-18 Spin Columns as per protocol (Thermo Scientific). Finally, protein quantification was determined based on measurements of ion intensity changes and on spectral counting of identified peptides after MS-MS analysis. Fold change, Mascot scores (a measure of confidence for the identity of a given protein) and ANOVA scores for differentially expressed proteins were determined using the Progenesis LC-MS software (<http://www.nonlinear.com>) as previously described.[94-98]

2.16 Transwell co-cultures of hFob 1.19 and MM.1S cells

Transwell plates purchased from Westnet (HTS Transwell®-96 Permeable Support with 0.4µm Pore Polycarbonate Membrane, catalogue number 3881) and used to determine whether or not drug resistance in MM.1S, which appeared to be induced by hFob 1.19, required direct cell-to-cell contact for same to occur. In the Transwell system two different cell types can be co-cultured but without direct contact by placing one cell line in the lower chamber and the other cell line

in the upper chamber. The upper chamber sits into the lower chamber during culture, so that cytokines secreted by either cell line are free to move across the membrane that separates the two cell lines, however the cells are never in direct contact.

On day 1, 2,000 MM.1S-mcl cells were added to the lower well in 200uL of media and 8,000 hFob 1.19 cells added to the upper chamber in 50uL of media, then upper chamber inserted into lower wells. Cells were allowed to culture without direct contact for 24hours. For comparison a duplicate experiment was performed where by MM.1S-mcl cells and hFob 1.19 cells were co-cultured in a single chamber 96-well plate system whereby the cells were in direct contact. Twenty-four hours later, doxorubicin 62ng/mL, vorinostat 0.5uM or lenalidomide 2uM, or fresh media as a control was added to each condition in both the direct co-culture plates and Transwell plates. When treatment was complete, plates were briefly centrifuged to ensure cells in the lower chambers of the Transwell had adhered. Then the upper chamber was removed from the Transwell plates and luciferase was added as previously outlined to determine viability of MM.1S-mcl cells by bioluminescence. Results of cell viability of MM.1S-mcl cells from Transwell versus non-Transwell co-cultures were then compared.

2.17 Characteristics of bortezomib-refractory patients selected from Multiple Myeloma BioBank

The clinical data pertaining to bone marrow trephine samples previously stored following patient consent and as per departmental protocol in the Mater Misericordiae University Hospital Multiple Myeloma biobank were kindly analysed by Dr. Kay Reen Ting and Dr. Colm Cosgrove. A number of samples were selected from patients for immunohistochemical analysis of PSMB5 and PSMB8 proteasomal subunits. Clinical response to treatment were as per IMWG response criteria (Introduction section 1.2.1). Samples were selected as follows:

- 7 diagnostic samples of patients who achieved at least a VGPR following one bortezomib-based regimen (called “Diagnostic: Responder”)

- 6 diagnostic samples of patients who received a bortezomib-based regimen and subsequently relapsed (called “Diagnostic: Non-responder”)
- 7 samples from patients who relapsed following a bortezomib-based regimen (6 of which correlate to aforementioned “Diagnostic: Non-responders”, (called “Relapsed: Non-responder”).

See tables 2.1.7.1 and 2.1.7.2 below that provides further clinical details for each sample tested.

Sample ID:	% Plasma cells pre-treatment	Chemotherapy	No of cycles of chemotherapy	IMWG Response	% plasma cells post-treatment
DNR 1	>10%	Nil	-	Dignostic	>10%
PTNR 1	100%	Bort/Thal/Dex	4	Relapse	100%
DNR 2	>90%	Nil	-	Dignostic	>90%
PTNR 2	>90%	Bort/Dex and Len/Dex	2 & 3 (respectively)	Relapse	>90%
DNR 3	Extensive	Nil	-	Dignostic	Extensive
PTNR 3	Multifocal	Bort/Dex	4	Relapse	Multifocal
DNR 4	70-80%	Nil		Dignostic	70-80%
PTNR 4	Diffuse	Bort/Dex	3	MR	Diffuse
DNR 5	80-90%	Nil	-	Dignostic	80-90%
PTNR 5	50%	Len/Bort/Dex	6	Relapse	50%
DNR 6	30%	Nil	-	SMM	30%
PTNR 6	60%	Bort	6	Relapse	60%
DNR not available	-	-		-	-
PTNR 7	80-90%	Bort	4	Relapse	80-90%

Table 2.1.7.1 Clinical details pertaining to bone marrow trephine samples of bortezomib non-responders at time of diagnosis and relapse.

DNR (blue)= Diagnostic Non-responder; PTNR (red)= Post-treatment non-responder (otherwise known as “Relapsed: Non-Responder”); Bort= bortezomib; Thal= thalidomide; Dex= dexamethasone; Len= lenalidomide; MR= minimal response; SMM=smouldering multiple myeloma.

Sample ID:	Plasma cells pre-treatment	Chemotherapy	No. of cycles	Plasma cells post-treatment	IMWG Response
RE 1	50-60%	Bort/Dex	2	<5%	VGPR
RE 2	20%	Bort/Dex	4	<5%	VGPR
RE 3	70%	Bort/Dex	6	10%	VGPR
RE 4	20-30%	Bort/Dex	4	<5%	VGPR
RE 5	90%	Bort/Dex	4	<5%	VGPR
RE 6	25%	Bort/Thal/Dex	4	<5%	CR
RE 7	60-70%	Bort/Thal/Dex	4	1%	VGPR

Table 2.1.7.2 Clinical details pertaining to bone marrow trephine samples of bortezomib responders at time of diagnosis.

RE= Bortezomib-Responder; (otherwise known as “Diagnostic: Responder”);
 Bort= bortezomib; Thal= thalidomide; Dex= dexamethasone; VGPR= very good partial response; CR= complete remission.

2.18 Immunohistochemistry

5-micrometre sections of formalin-fixed paraffin-embedded bone marrow trephine biopsies were kindly prepared by the pathology team at the Mater Misericordiae University hospital pathology laboratory, in preparation for immunohistochemistry.

The following reagents were utilised for the immunohistochemistry analysis: DAKO peroxidase blocking solution, DAB stain (containing 1mL of substrate buffer and 140mL chromogen), Real ENVision visualisation system (prepared according to manufacturer's instructions); haematoxylin; PSMB5 primary antibody (Abcam catalogue no. Ab3330, at a dilution of 1:350), PSMB8 primary antibody (Abcam catalogue no. Ab58094, at a dilution of 1:300); negative control (DAKO antibody diluent) and DAKO wash buffer (10x solution diluted in deionised water).

Slides were initially heat treated for antigen retrieval at 97°C in pH of 9 for 20 minutes. Dako REAL EnVision Detection System (Dako) was used for immunohistochemical analysis of the bone marrow trephines according to manufacturer's instructions. Briefly slides were blocked for endogenous peroxidase activity and subsequently washed with DAKO wash buffer. Next slides were treated with PSMB5 or PSMB8 primary antibody diluted in DAKO antibody diluent, or negative controls treated with DAKO antibody diluent alone. Slides were again washed with DAKO wash buffer. Slides were then stained with Dako Real Envision Detection system and stained with DAB chromogen. Finally slides were counter-stained using haematoxylin and glass coverslipped.

All slides were analysed by light microscopy, and images acquired at 20x and 40x magnification. Images depicted in results section 3.5.8 are those taken at 40x magnification. Slides were scored semi-quantitatively according to the intensity of the staining: negative, weakly positive, or strongly positive.

2.19 Statistical Analysis

Statistical analysis to determine statistically significant differences between treatment groups in *in vitro* studies was analysed using Prism GraphPad

software, (<http://www.graphpad.com/scientific-software/prism/>), whereby t-test was used and a p value of statistical significance was set at <0.05 with a FDR (false discovery rate) set at 1%. Figures in results section with an overlying asterix (*) represent data-points with p values <0.05.

Statistical analysis for *in vivo* mouse study was completed by Ms. Amanda Christie and Dr. Nancy Kohl at the Lurie Family Imaging Centre. Statistical analysis of whole exome sequencing was performed at the Centre for Cancer Genome Discovery (CCGD) core facility at DFCI. Statistical analysis for gene expression profiling was kindly provided by Dr. Panisinee Lawasut as outlined in methods section 2.12. Statistical analysis of label-free mass spectrometry data was completed by Dr. Paul Dowling using Progenesis LC-MS software as per departmental protocol at Dublin City University as outlined in section 2.15.

Chapter 3

Results

CHAPTER 3. RESULTS

3.1 CHARACTERISATION OF AN ISOGENIC CELL LINE MODEL OF BORTEZOMIB RESISTANCE *IN VITRO* AND *IN VIVO*.

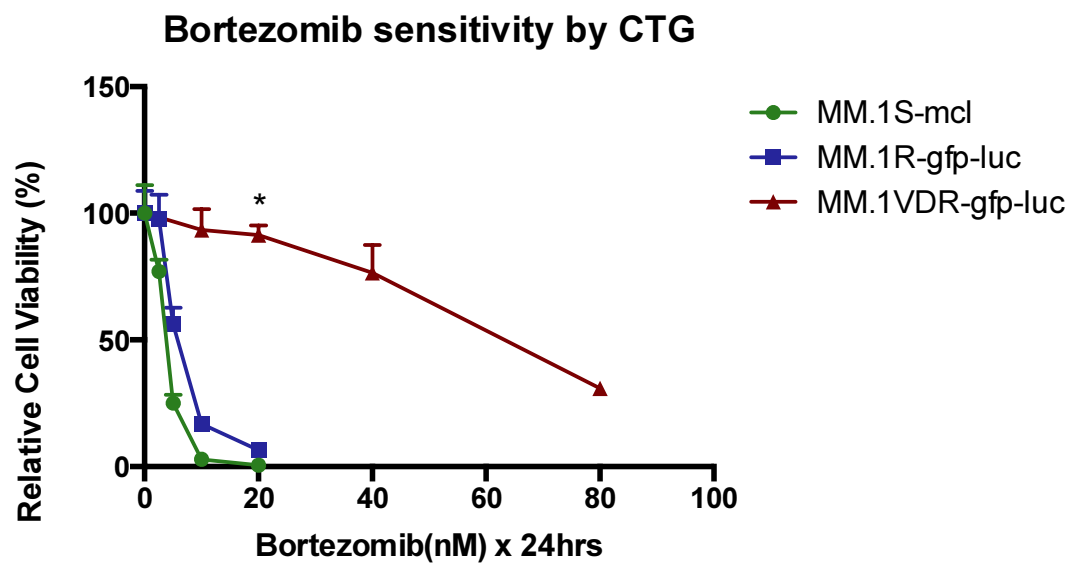
3.1.1 Introduction

As early as 2005, several groups of researchers have been investigating resistance to bortezomib in order to identify targetable molecules conferring resistance in both the *in vitro* and *in vivo* setting in MM, other haematological malignancies, and solid tumours.^[59-61, 63-65, 99-102] A number of *in vitro* isogenic cell line models of bortezomib resistance revealed varying mutations in the PSMB5 gene.^[59-61, 63, 100] However, despite vast *in vitro* evidence, no such mutations have been demonstrated *in vivo* in clinical samples of either newly diagnosed or bortezomib-refractory patients with multiple myeloma.^[67, 69, 103] We set out to examine a further MM-based model of bortezomib resistance generated in our laboratory, and further examine the potential mechanisms of proteasome inhibitor resistance.

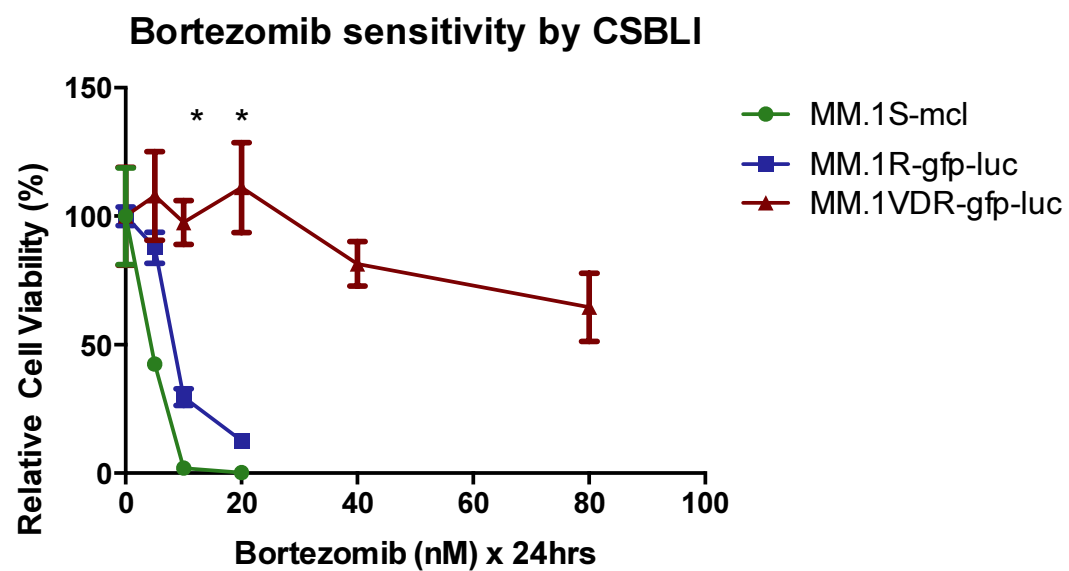
3.1.2 Generation of a cell line model of bortezomib resistance

At the Jerome Lipper Centre for Multiple Myeloma a bortezomib-resistant isogenic cell line mode was generated by Mr Joe Negri by successive rounds of *in vitro* exposure of bortezomib-sensitive MM.1R-gfp-luc (termed MM.1R) cells to increasing bortezomib concentrations. We initially began with pulse exposures of bortezomib 2.5nM, monitoring the cells daily post-exposure for cell viability by direct visualization under light microscopy, in addition to trypan blue staining. Subsequently we incrementally increased bortezomib concentrations as tolerated to a maximum dose of 40nM. Bortezomib resistance for one clone, MM.1VDR-gfp-luc (termed “VDR”, i.e. Velcade- and Dexamethasone-Resistant), was confirmed even after extended *in vitro* culture without bortezomib. The toxicity of bortezomib in VDR was tested using MTT, CSBLI and CTG assays with comparable results for all three assays used (see Materials and Methods 2.7 for details). Figure 3.1.2.1 depicts bortezomib sensitivity data for VDR compared to MM.1R or MM.1S whereby a 12-fold increase in IC₅₀ for bortezomib was observed in VDR cell line compared to either parental cell line.

(a)



(b)



(c)

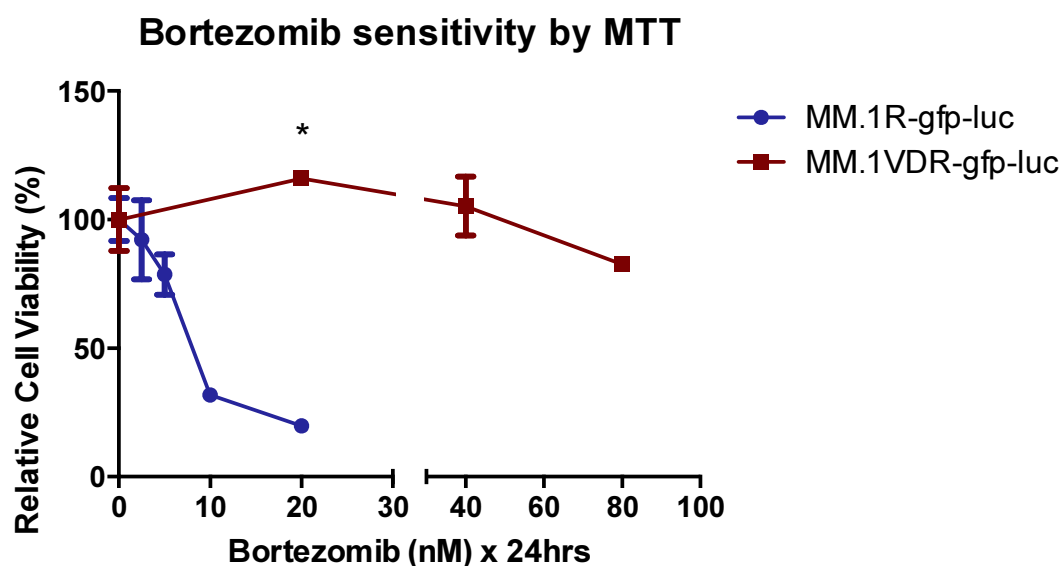


Figure 3.1.2.1 Sensitivity of isogenic cell lines to bortezomib.

Following evolution of one bortezomib resistant clone that we termed VDR, we tested these cells using 3 separate assays. Figure 3.1.2.1a demonstrates cell viability of the 3 cell lines following a Cell Titre Glo Assay, and demonstrates the marked increase in IC₅₀ for bortezomib in VDR cell line. A 12-fold increase in IC₅₀ in VDR (red) was observed, with an IC₅₀ 60nM, versus 5nM for parental MM.1R (blue) or MM.1S (green). This experiment was repeated using (b) a luciferase-based assay (CSBLI) and (c) an MTT assay with comparable results regardless of the assay utilised. *p<0.05 when MM1R compared to VDR.

3.1.3 Response profile of VDR cells to conventional and novel therapies

Given that the VDR cell line was derived from dexamethasone-resistant MM.1R, we examined the cross-resistance of VDR to dexamethasone. In addition, we investigated the sensitivity of this bortezomib-resistant clone to other conventional (doxorubicin, vincristine), novel (vorinostat, lenalidomide, pomalidomide) and investigational (JQ1) therapies. VDR retains its resistance to dexamethasone similar to its parent cell line MM.1R (figure 3.1.3.1.). Doxorubicin and vincristine display comparable toxicity in VDR and parental MM1R. The recently FDA-approved novel therapies lenalidomide and pomalidomide demonstrate similar toxicity in all 3 isogenic lines. MM.1S was slightly more sensitive to the HDAC inhibitor vorinostat compared to either resistant clone, suggesting histone deacetylation may be dysregulated in both MM.1R and VDR (figure 3.1.3.2). Finally the BET-bromodomain inhibitor JQ1 displays marked anti-tumour activity in all three cell lines (figure 3.1.3.2.).

Next, a library of 101 compounds approved by the U.S. FDA for use in clinical oncology was examined by high-throughput CSBLI screening for their relative potencies in MM.1R and VDR. Similar toxicities for the majority of compounds in each cell line were observed (figure 3.1.3.3, a-d). However there were a small number of compounds of the same pharmacological classes that appeared to be more potent in VDR vs. MM.1R cells and these included topoisomerase- (TOP) 1 and -2 inhibitors and the taxanes (figure 3.1.3.4, a,b). While some TOP1 and TOP2 inhibitors were more potent in VDR vs. MM.1R, the TOP2 inhibitor mitoxantrone was highly potent in both cell lines, suggesting TOP2 dysregulation is probably not isolated to the bortezomib-resistant clone (table 3.1.3.2). The taxane, paclitaxel, at the lower concentration of 1nM displayed high potency in VDR compared to MM.1R, however paclitaxel 10nM, docetaxel 1/10nM, and cabazitaxel 1/10nM all induced greater than 90% cell death in both cell lines (table 3.1.3.3). In conclusion, by this large-scale screen, we did not identify a particular class of compounds with high potency solely in bortezomib-resistant VDR.

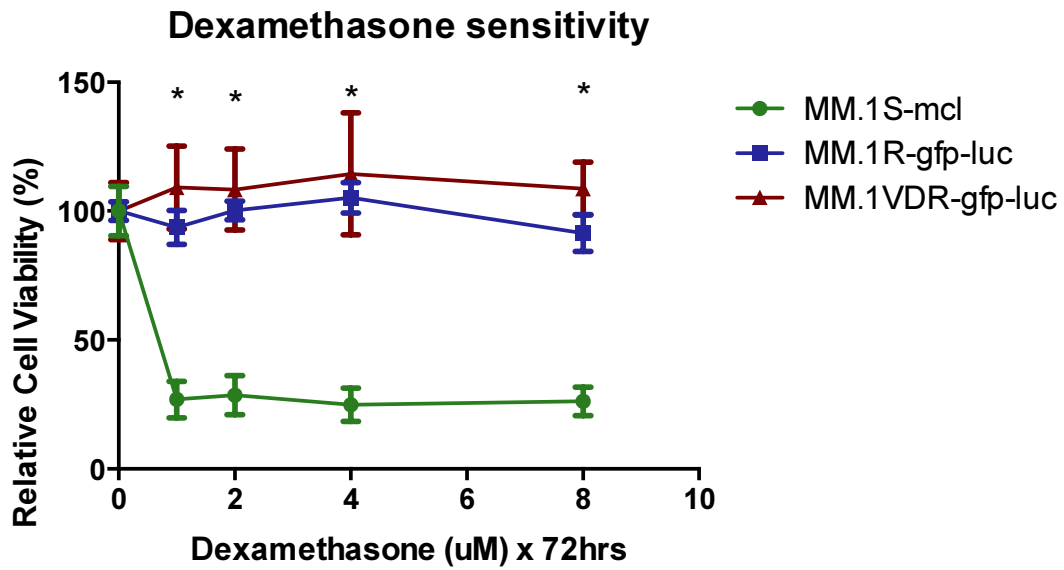


Figure 3.1.3.1 Sensitivity of isogenic cell line model to dexamethasone.

MM.1VDR-gfp-luc retains its resistance to dexamethasone, similar to parental cell line MM.1R-gfp-luc. MM.1S-mcl remains sensitive to dexamethasone. Cell viability was determined by CSBLI. (* $p < 0.05$ for VDR vs. MM.1S).

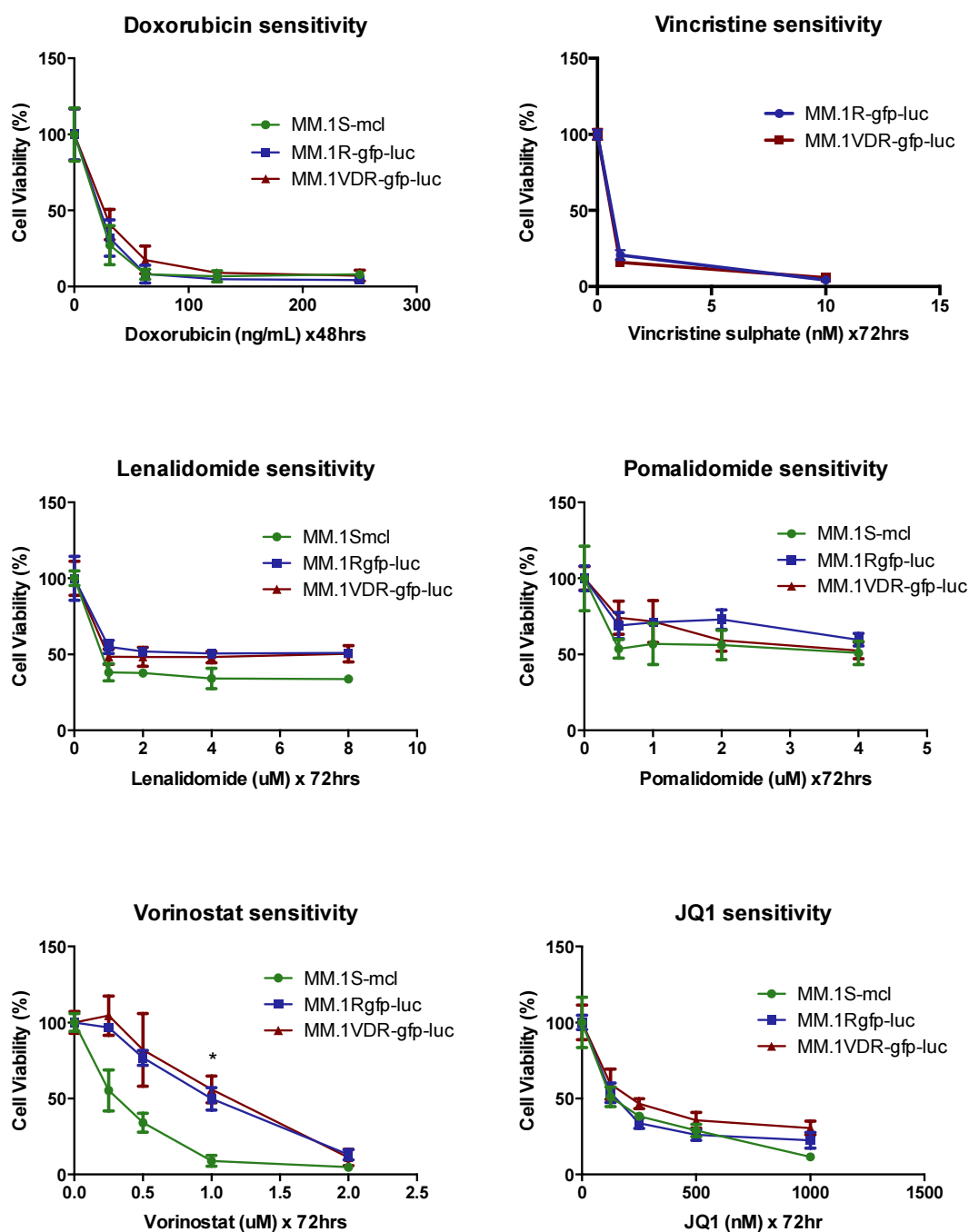
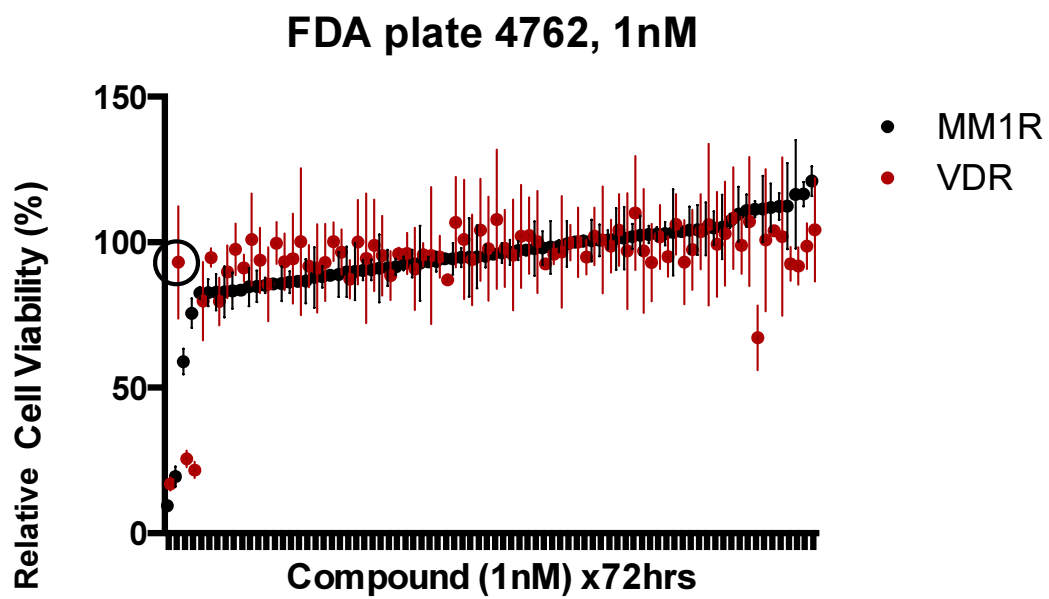


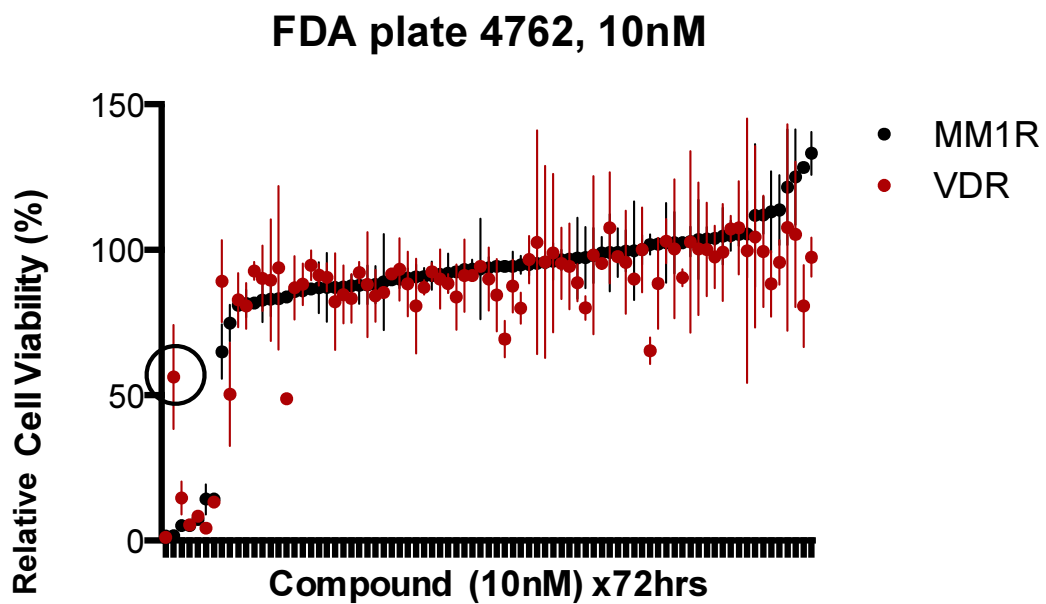
Figure 3.1.3.2. Sensitivity of isogenic cell lines to other therapies.

The toxicity of conventional, novel and investigational reagents to all 3 cells lines is comparable (green=MM.1S, blue= MM.1R and red=VDR), with the exception of MM.1Smcl which displays a greater degree of sensitisation to vorinostat compared to either MM.1R or VDR (* $p < 0.05$). Relative cell viability was determined here by CSBLI in all assays demonstrated.

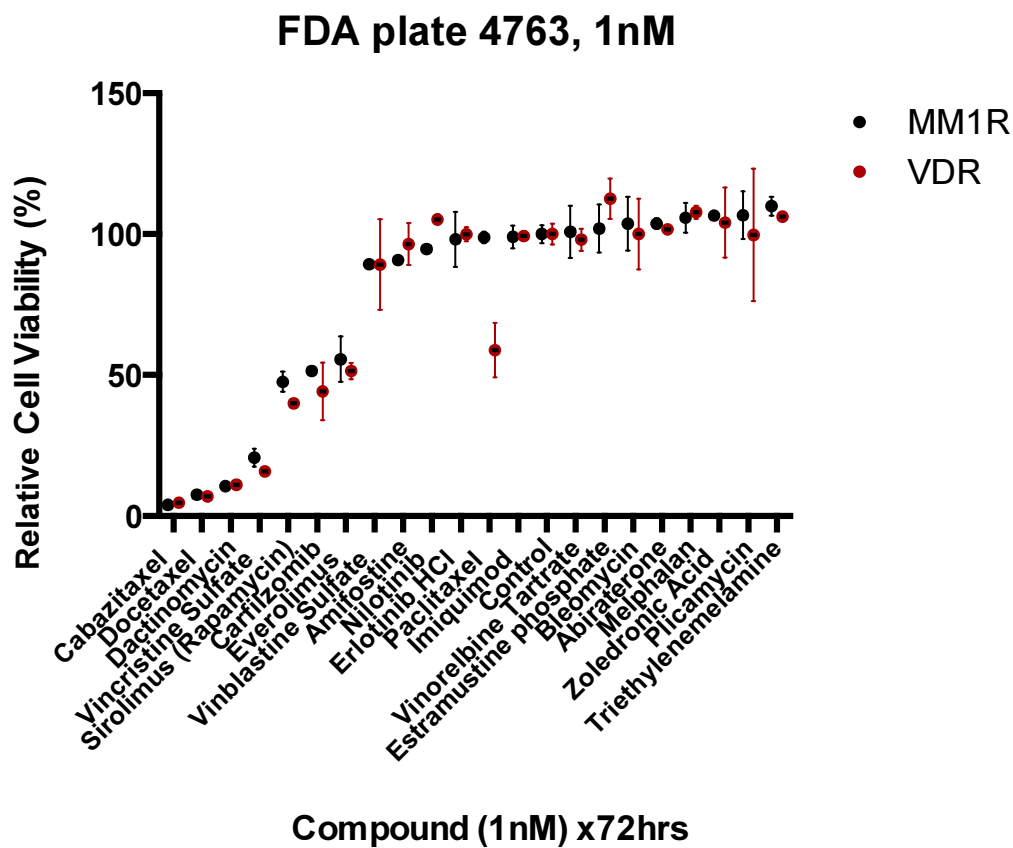
(a)



(b)



(c)



(d)

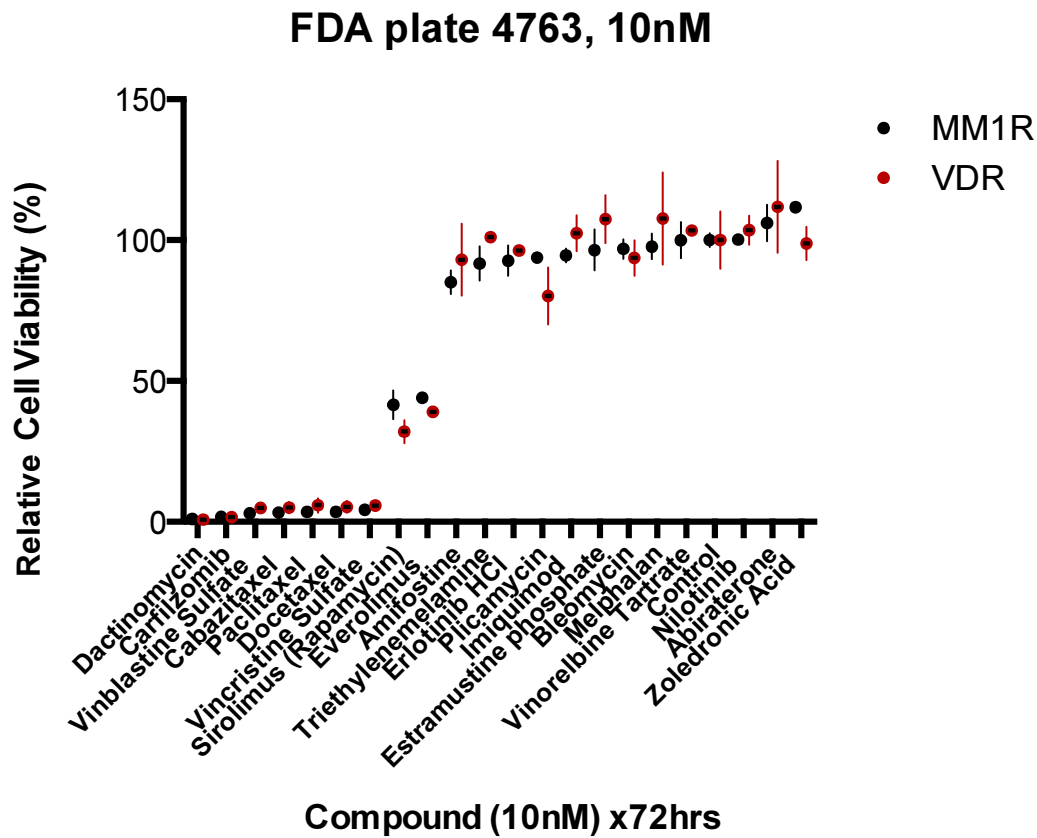
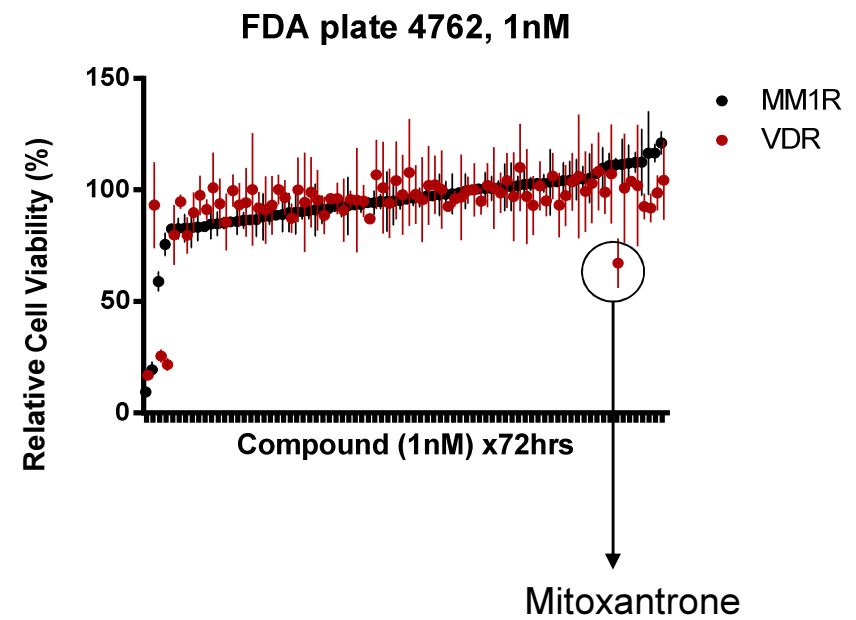
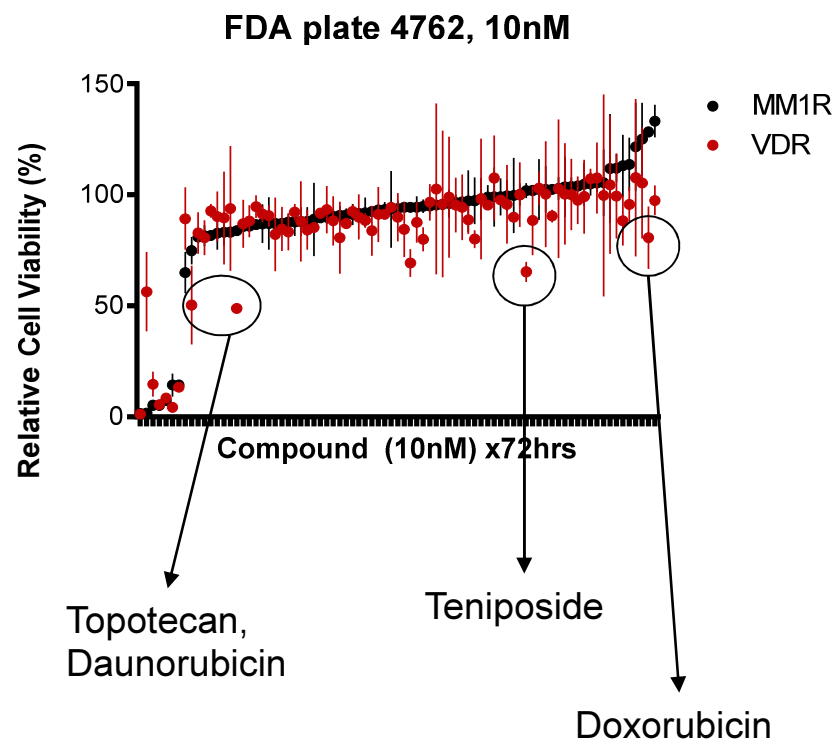


Figure 3.1.3.3 High-throughput screening of FDA-approved compounds for use in oncology.

(a-d) The majority of the 101 FDA-approved compounds tested displayed comparable toxicity in MM1R and VDR in a high throughput screen using CSBLI (results for 1nM and 10nM concentrations shown here). Fig. 3.1.3.3 (a, b): bortezomib was used as a control in FDA plate no. 4762, and again demonstrated resistance to bortezomib in VDR in comparison to MM.1R, highlighted by black circles in plate number 4762.

(a)



(b)

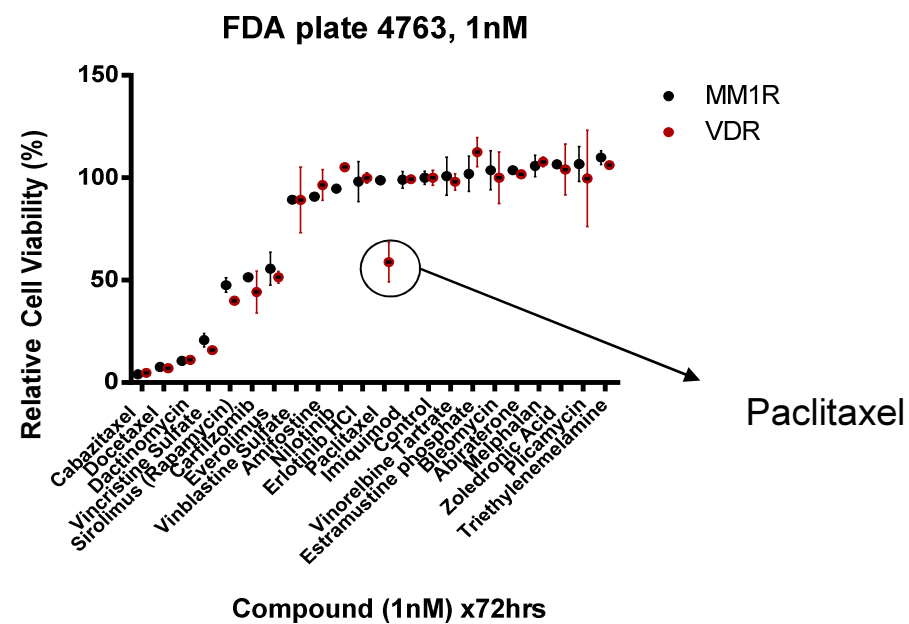
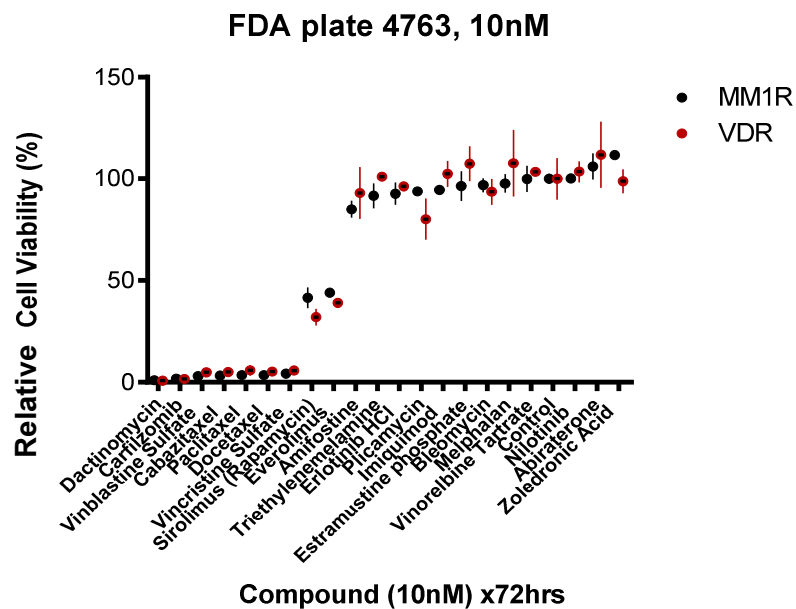


Figure 3.1.3.4 Compounds with differential toxicity in VDR cells vs. MM.1R as determined by high-throughput CSBLI screening.

Specific groups of compounds with similar inhibitor properties exerting a higher degree of cell death in VDR include (a) the topoisomerase (TOP) inhibitors (TOP1 inhibitor topotecan, and TOP2 inhibitors teniposide, daunorubicin, doxorubicin and mitoxantrone) in FDA-plate number 4762, and (b) the taxane paclitaxel in FDA-plate number 4763.

Drug	MM1R Avg % viability +/-SD (1nM)	VDR Avg % viability +/-SD (1nM)	MM1R Avg % viability +/-SD (10nM)	VDR Avg % viability +/-SD (10nM)
TOPI inhibitor				
Irinotecan	87.9 +/-10.4	91.0 +/-15.2	81.7 +/-0.3	92.7 +/-3.1
Topotecan	82.6 +/-2	79.8 +/-13.4	74.9 +/-6.2	50.4 +/-17.8
TOPII inhibitor				
Etoposide	104.9 +/-5.7	99.3 +/-18	125.0 +/-16.4	105.4 +/-25
Teniposide	96.6 +/-4.3	95.6 +/- 19	101.8 +/-3.4	65.3 +/-4.6
Doxorubicin	112.4 +/-14.8	92.5 +/-5.9	128.3 +/-1.7	80.7 +/-14.1
Daunorubicin	98.3 +/-9.1	96.0 +/-3.5	83.8 +/- 1.1	48.8 +/- 1.3
Mitoxantrone	111.3 +/-2.8	67.2 +/-11.1	5.2 +/-0.3	5.5 +/- 0.0

Table 3.1.3.2 Average cell viability by CSBLI of MM.1R or VDR cells following exposure to topoisomerase 1 (TOP1) or topoisomerase 2 (TOP2) inhibitors (1nM and 10nM concentrations).

Both TOPI and TOPII inhibitors demonstrate increased toxicity in VDR compared to MM1R. Topotecan 10nM, teniposide 10nM, and daunorubicin 10nM exert a greater degree of cell death in VDR compared to MM.1R as demonstrated (red). The TOPII inhibitor mitoxantrone 10nM (blue) is highly toxic to both cell lines.

Drug	MM1R Avg % viability +/-SD (1nM)	VDR Avg % viability +/-SD (1nM)	MM1R Avg % viability +/-SD (10nM)	VDR Avg % viability +/-SD (10nM)
Cabazitaxel	3.95 +/-0.33	4.67 +/-0.31	3.30 +/-0.03	5.07 +/-2.06
Docetaxel	7.51 +/-0.53	6.94 +/-0.24	3.61 +/-0.70	5.34 +/-2.05
Paclitaxel	98.8 +/-1.99	58.1 +/-9.65	3.58 +/-0.26	5.91 +/-2.54

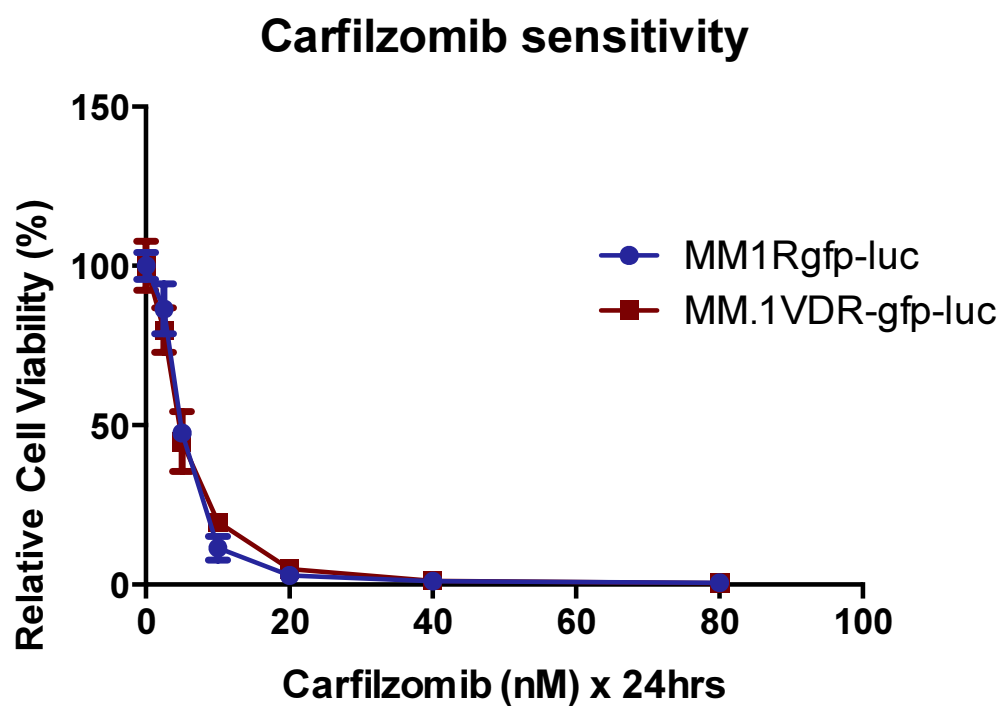
Table 3.1.3.3 Average cell viability by CSBLI of MM.1R or VDR cells following exposure to taxanes.

Paclitaxel 1nM exerted a markedly higher anti-tumour effect in VDR compared to MM.1R as observed (highlighted in red). However, cabazitaxel (1/10nM), docetaxel (1/10nM) and paclitaxel (10nM) all were highly potent inducers of cell death in MM.1R and VDR.

3.1.4 Sensitivity of VDR to novel proteasome inhibitors

Previously documented models of bortezomib resistance in MM and solid tumours were sensitive to the novel and irreversible proteasome inhibitor carfilzomib.^[48, 63] Therefore we next examined the toxicity of second-generation proteasome inhibitors in our model. Carfilzomib, which exhibits irreversible binding to multiple proteasome-associated catalytic subunits, was highly and equally toxic to both MM.1R and VDR cells. However, we observed a marked reduction in sensitivity to the investigational compound MLN2238, a novel orally bioavailable reagent that specifically targets the proteasome beta-5 subunit, suggesting that one mechanism of resistance to bortezomib in VDR can potentially be mediated through the beta-5 proteasome subunit (figure 3.1.4.1).

(a)



(b)

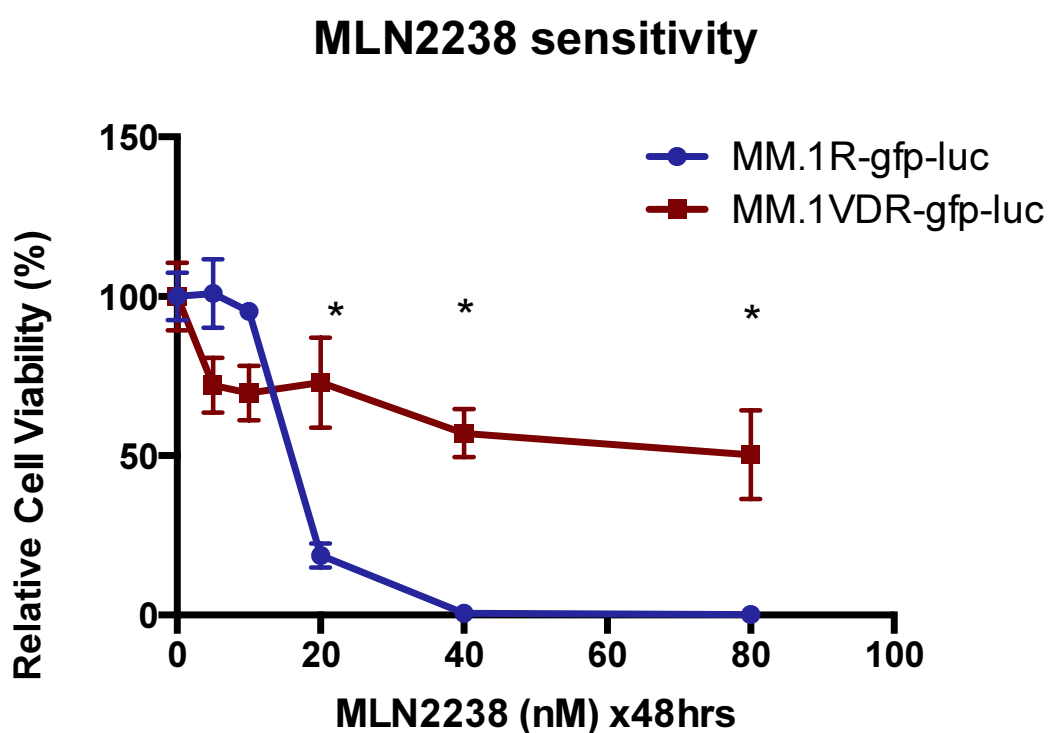


Figure 3.1.4.1 Sensitivity of MM.1R and VDR to second-generation proteasome inhibitors.

MM.1R and VDR were examined for their sensitivity to novel proteasome inhibitors by CSBLI assay. (a) Both cell lines demonstrated exquisite sensitivity to carfilzomib. (b) However VDR demonstrated marked resistance to MLN2238, a novel reagent specifically targeting the beta-5 proteasome subunit, suggesting that resistance to bortezomib in VDR may be at least partially mediated by alterations in PSMB5, (* $p < 0.05$).

3.1.5 The role of p-glycoprotein in bortezomib resistance in VDR.

P-glycoprotein (P-gp) over-expression has been previously well documented for its pertinent role in drug resistance in cancer in the *in vitro* and *in vivo* setting. In particular, very recently the role of P-gp in bortezomib resistance has been delineated and clarified that bortezomib also is subject to pharmacokinetic resistance mediated by P-gp.^[104] We compared the sensitivity of VDR (unknown P-gp expression) and MM cell line RPMI-8226-Dox-40 (also known as “Dox40” with known P-gp over-expression) to bortezomib, MLN2238 (active metabolite of the orally bioavailable proteasome inhibitor MLN-9708) and carfilzomib in combination with the P-gp inhibitor elacridar.

In Dox-40, resistance to bortezomib, MLN2238 and carfilzomib single agent treatment was observed. When we individually combined these agents with the P-gp inhibitor elacridar, resensitisation of Dox40-mcl cells to bortezomib 40nM and carfilzomib 10nM was observed. This suggests that bortezomib and carfilzomib resistance observed in Dox40-mcl may be partially mediated by P-gp, and can be overcome by the addition of a P-gp inhibitor. However concomitant P-gp inhibition with MLN2238 did not induce cell death in Dox40-mcl, suggesting MLN2238 is not a P-gp substrate (figure 3.1.5.1).

VDR again displayed resistance to single agent exposure of bortezomib and MLN2238, and was sensitive to carfilzomib. Bortezomib and elacridar in combination did not result in synergistic cell death in VDR. Similar results were observed for MLN2238 and elacridar in combination in VDR. These results suggest that resistance to bortezomib and MLN2238 in VDR are unlikely to be mediated by P-gp over-expression. Carfilzomib in combination with elacridar did not demonstrate synergistic activity, mainly because the concentrations of carfilzomib used in this assay are highly toxic to VDR cells even without the addition of elacridar (figure 3.1.5.2).

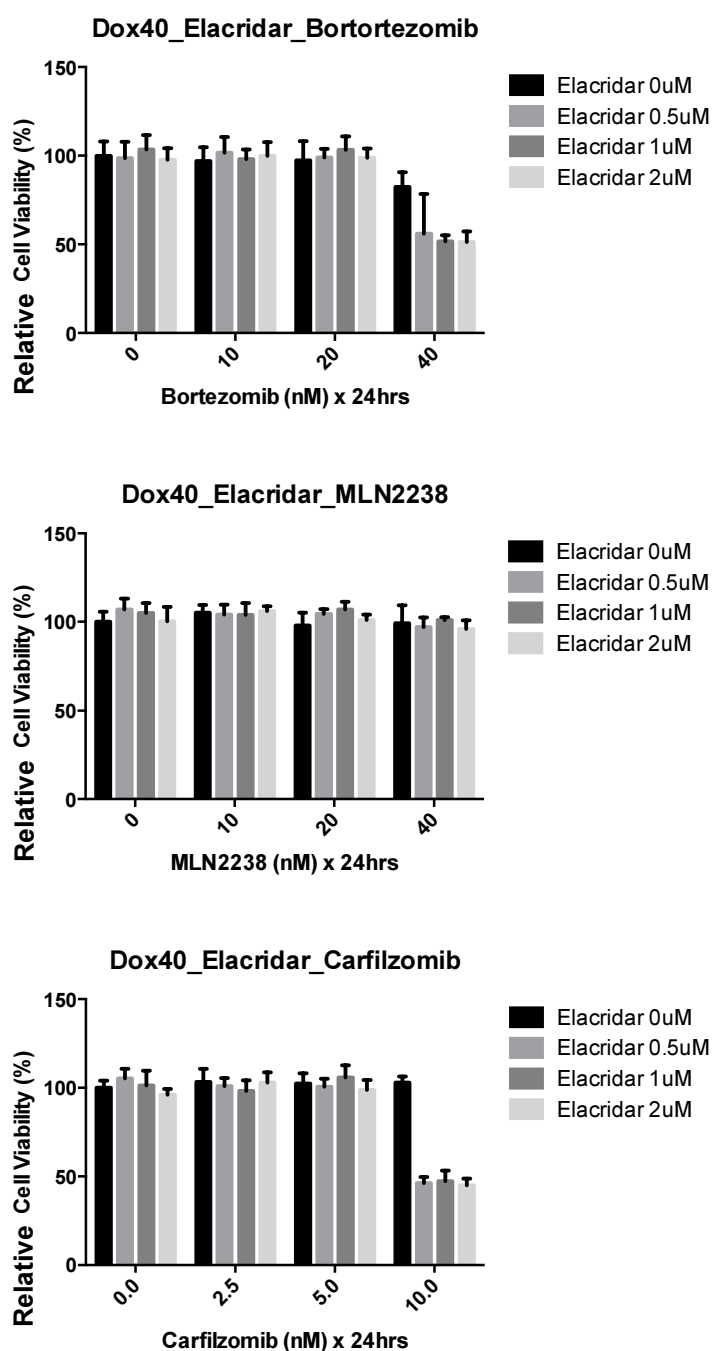


Figure 3.1.5.1 Concomitant P-gp and proteasome inhibition in Dox40-mcl

Dox40-mcl, with known P-gp over-expression, displays resistance to bortezomib, MLN2238 and carfilzomib single agents. Combination of elacridar with carfilzomib 10nM or bortezomib 40nM results in synergistic cell death in Dox40-mcl. However combination of MLN2238 with elacridar does not cause anti-tumour activity in Dox40-mcl.

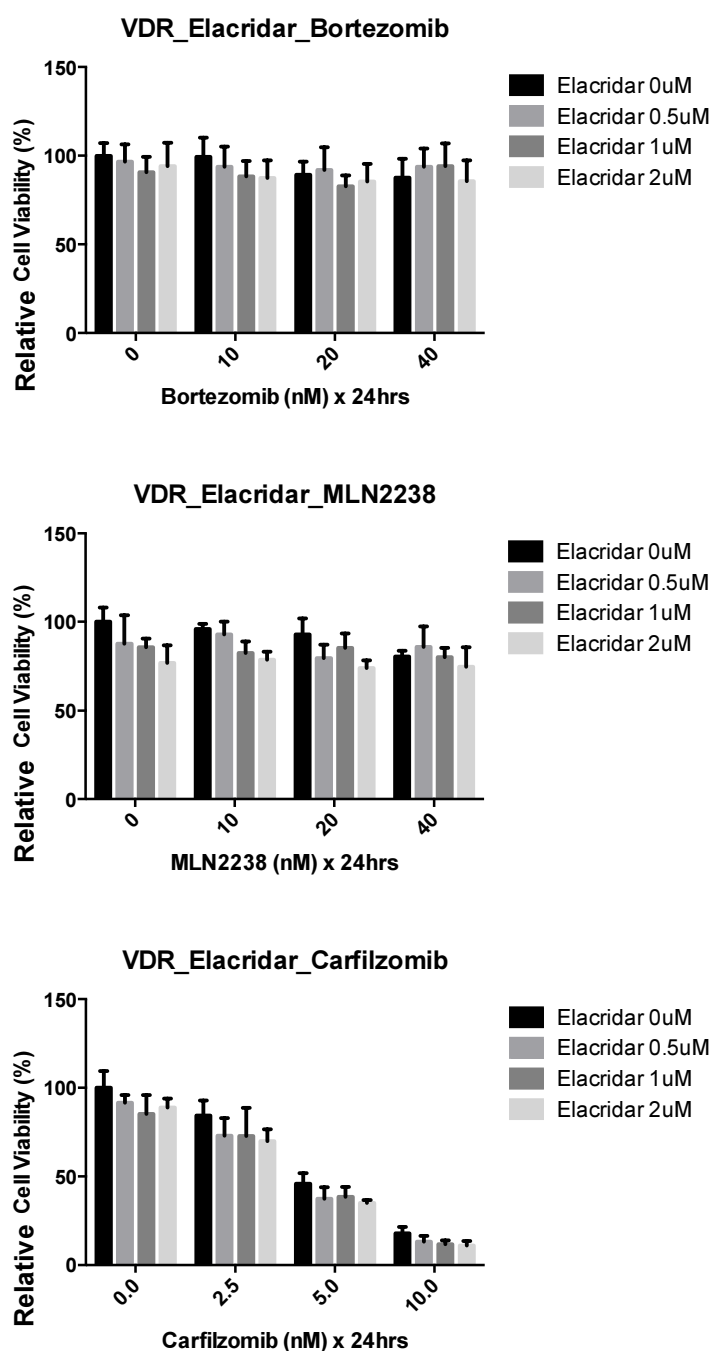


Figure 3.1.5.2 Concomitant P-gp and proteasome inhibition in VDR

Bortezomib or MLN2238 combination with elacridar does not result in death of VDR cells. Synergistic activity of carfilzomib and elacridar in VDR is not observed, mainly because carfilzomib single agent is highly toxic to VDR cells. These results suggest bortezomib and MLN2238 resistance in VDR is not P-gp-mediated.

3.1.6 Baseline proliferation rate of MM.1R and VDR cell lines

To investigate if resistance to bortezomib in VDR was secondary to differences in proliferation rate of VDR compared to MM.1R, we undertook serial measurements of both MM.1R and VDR cell line proliferation rates. MM.1R or VDR cells were plated at a seeding density of 100×10^3 cells/mL in 100uL of RPMI media on a 96-well plate in triplicate for each of the following timeframes of culture: 0, 24, 48, 72 and 96 hours. The cell viability of each condition was measured by CSBLI at the appropriate timepoint (figure 3.1.6 (a)).

In addition one week later, MM.1R and VDR cells were plated in 6-well plates at a seeding density of 250×10^3 cells/mL in biological triplicate and allowed to culture for 0, 24, 48 and 72 hours. In this experiment, at each timepoint the number of cells per condition were physically counted under light microscopy using a haemocytometer, and apoptotic bodies that stained positive for trypan blue were excluded (figure 3.1.6 (b)).

No statistically significant increase in proliferation rate was observed by either means of measurement of proliferation rate in VDR cell line versus MM.1R. Therefore a greater proliferation rate in VDR does not explain its observed resistance to bortezomib.

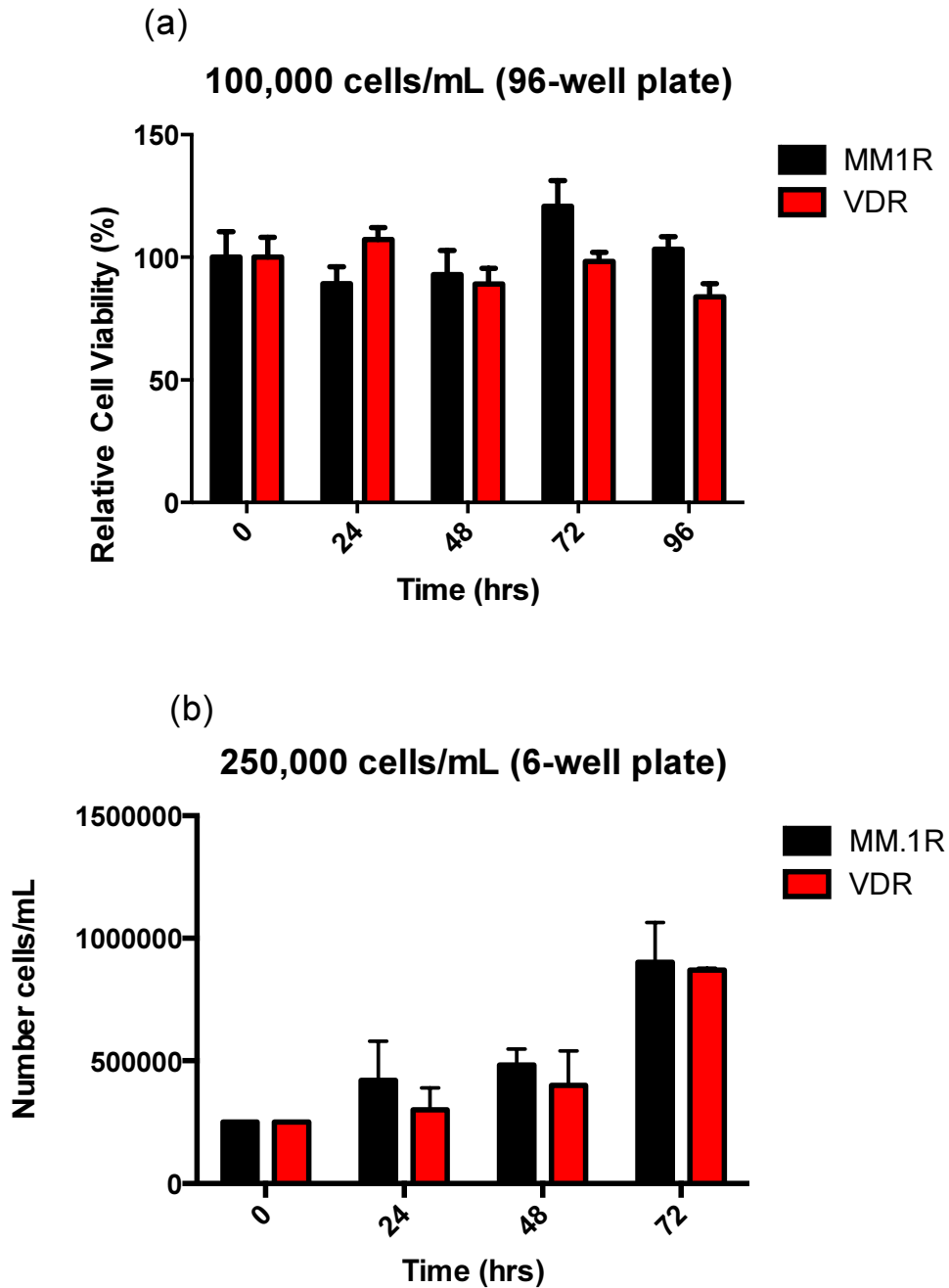


Figure 3.1.6 Baseline proliferation rate of MM.1R and VDR cell lines

(a) MM.1R and VDR were plated in a 96-well plate at a seeding density of 100,000 cells/mL and the cell viability of each cell line measured serially from 0-96 hours by CSBLI.

(b) MM.1R and VDR were plated in a 6-well plate at a seeding density of 250,000 cells/mL and the cells were serially counted using a haemocytometer (apoptotic bodies stained with trypan blue were excluded) from 0-72 hours. No statistically significant difference was found between the different conditions.

3.1.7 Sensitivity of isogenic cell lines MM.1R and VDR to bortezomib and carfilzomib in vivo

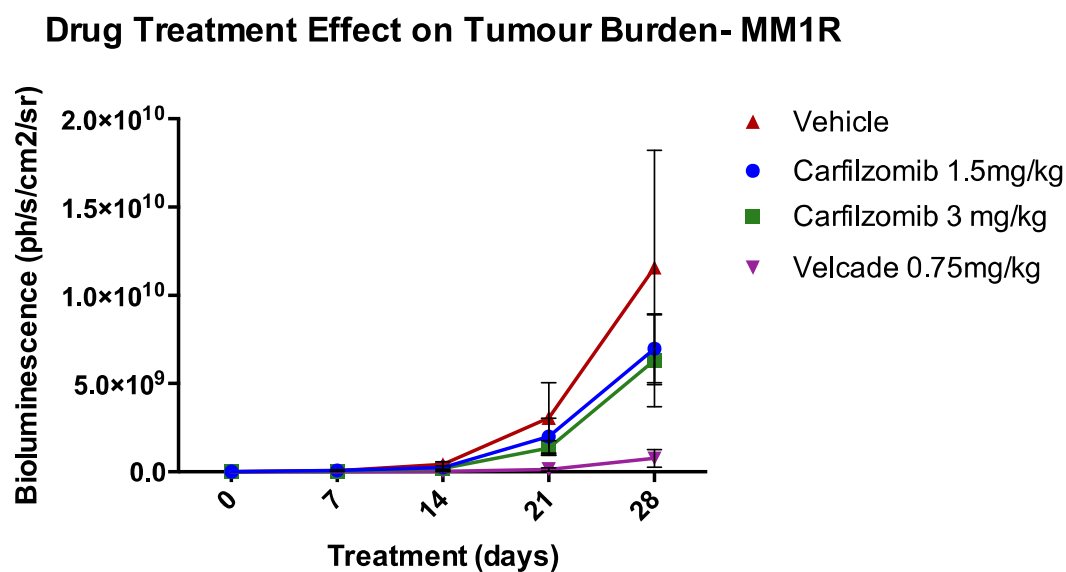
We have demonstrated that VDR cells *in vitro* display resistance to bortezomib regardless of cell viability assay used, but are sensitive to carfilzomib. Therefore we further tested if VDR retains its resistance to bortezomib and sensitivity to carfilzomib *in vivo*, using MM.1R as a control for comparison. 1×10^6 MM.1R or VDR cells were injected via tail vein into SCID-beige mice (see materials and methods 2.8). Drug treatment with vehicle, bortezomib 0.75mg/kg (also known as “Velcade”), carfilzomib 1.5mg/kg or carfilzomib 3mg/kg commenced when whole body bioluminescence imaging studies showed consistent engraftment of luciferase-positive MM cells in the axial skeleton of mice with average signals of at least 10^6 photons/second, and treatment was continued until the mice fulfilled criteria for sacrifice.

In mice bearing MM.1R tumours, there was no statistically significant difference in reduction of tumour burden in any of the drug-treated mice compared to vehicle mice, (figure 3.1.6.1.a). Similarly, in VDR-tumour-bearing mice no reduction in tumour burden was observed in drug-treated mice compared to control mice (figure 3.1.7.1.b).

However, in MM.1R-mice, a statistically significant improvement in overall survival was seen in bortezomib-treated mice compared to vehicle mice or compared to carfilzomib-treated mice (figure 3.1.7.2).

In addition, interestingly, even though there was no significant reduction in tumour burden in drug-treated mice in the VDR arm, both carfilzomib and bortezomib treatment in VDR-mice resulted in a statistically significant higher overall survival compared to control mice (figure 3.1.7.3).

(a)



(b)

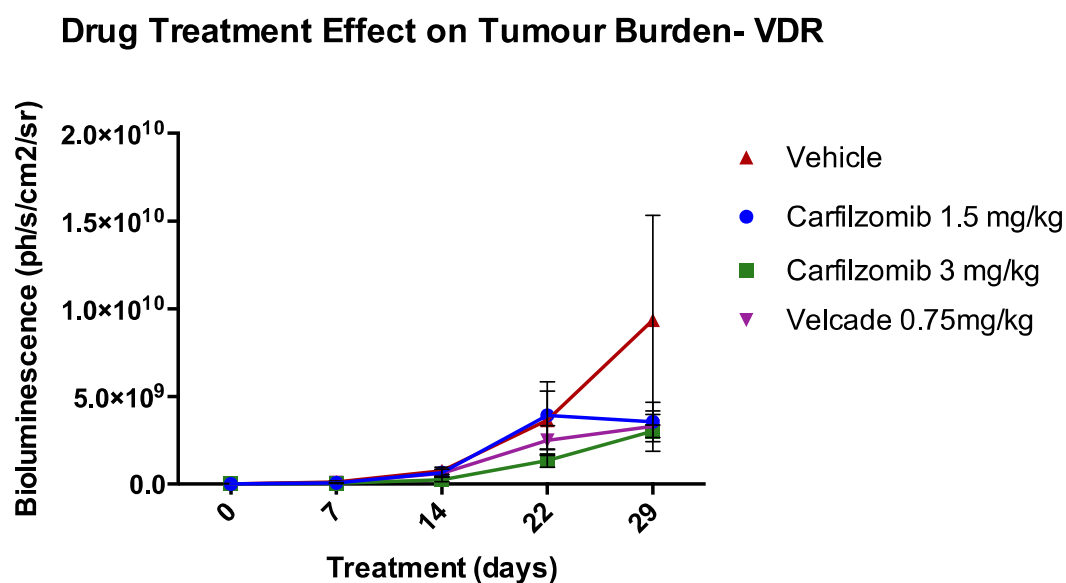


Figure 3.1.7.1 Effect on tumour burden in MM.1R or VDR tumour-bearing mice following proteasome inhibition *in vivo*.

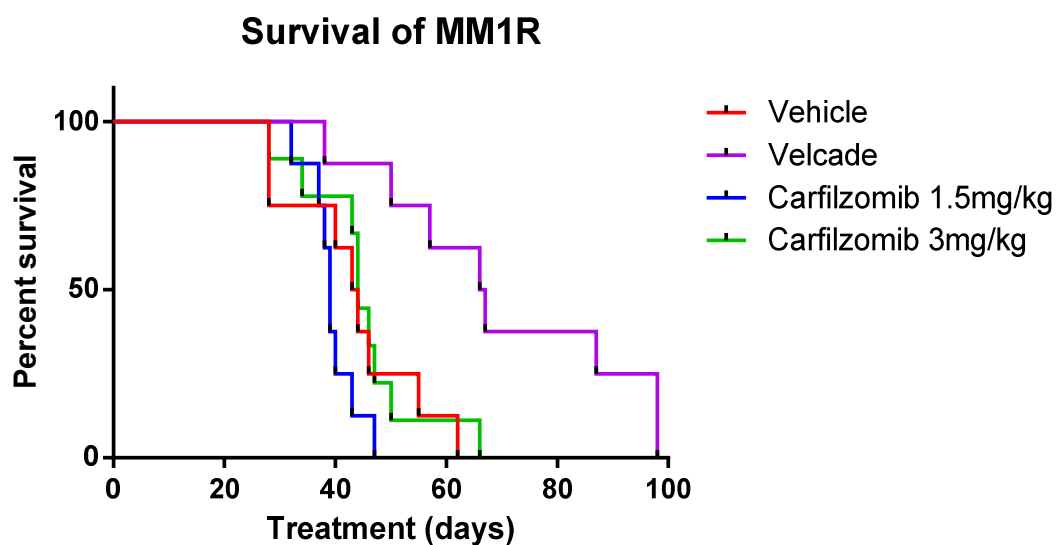
(a) In mice bearing MM.1R tumours, analysis of the data through treatment day 28, the last day when all animals in each of the treatment groups remained on

study, using Tukey's multiple comparison test indicates that none of the groups are statistically significantly different from each other.

(b) In mice bearing VDR tumours, analysis of the data through day 29, the last day when all animals in each of the treatment groups remained on study, using Turkey's multiple comparison test indicates that none of the groups are statistically significantly different from each other.

(Note: Velcade= bortezomib)

(a)

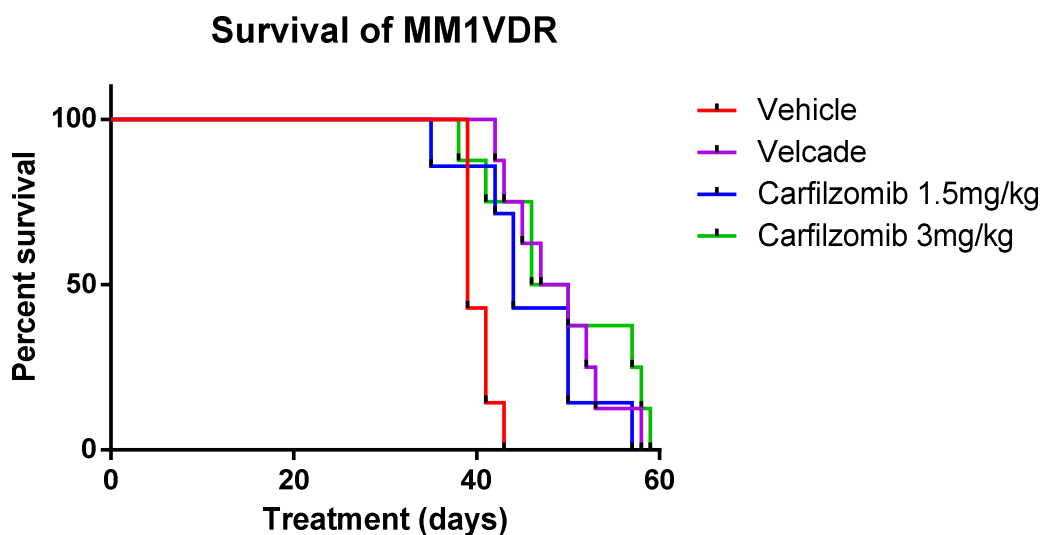


Overall p-value: 0.0006 (Log-rank test). P values for pairwise comparisons are:

MM1R	Velcade	Carfilzomib 1.5mg/kg	Carfilzomib 3mg/kg
Vehicle	0.0048	0.1525	0.6929
Carfilzomib 1.5mg/kg	0.0006		
Carfilzomib 3mg/kg	0.0048	0.0702	

Figure 3.1.7.2 Survival of MM.1R-tumour-bearing mice.

While there was no statistically significant difference in tumour volume among the treatment groups through treatment day 28, the Velcade/bortezomib group had significantly prolonged survival compared to all other groups.



Overall p-value: 0.0006 (Log-rank test). P values for pairwise comparisons are:

MM1VDR	Velcade	Carfilzomib 1.5mg/kg	Carfilzomib 3mg/kg
Vehicle	0.0004	0.0086	0.0063
Carfilzomib 1.5mg/kg	0.4621		
Carfilzomib 3mg/kg	0.5516	0.2661	

Figure 3.1.7.3 Survival of VDR-tumour-bearing mice.

While there was no statistically significant difference in tumour volume among the treatment groups through treatment day 29, all three drug-treated groups had significantly prolonged survival compared to the Vehicle group. (Note: Velcade= bortezomib)

3.1.8 Summary of *in vitro* and *in vivo* studies

In conclusion, VDR demonstrated marked resistance to bortezomib in the *in vitro* setting compared to MM.1R, in a number of toxicological *in vitro* assays tested. VDR retained its resistance to dexamethasone *in vitro*, similar to parental MM.1R. MM.1R and VDR displayed comparable toxicity in a number of conventional and novel therapies examined. Both MM.1R and VDR were more resistant to the HDAC inhibitor vorinostat compared to bortezomib-and-dexamethasone-sensitive MM.1S.

High-throughput screen of a database of compounds with FDA-approval for use in oncology demonstrated that VDR has marked sensitivity to the taxanes and topoisomerase-1 and -2 inhibitors. VDR is highly sensitive to the irreversible proteasome inhibitor carfilzomib but is resistant to another PSMB5-specific proteasome inhibitor MLN2238 *in vitro*.

Bortezomib resistance in VDR did not appear to be mediated by p-glycoprotein. No difference in proliferation rate between MM.1R and VDR was observed, thus proliferation rate does cannot be accountable for the resistance observed.

Finally, an *in vivo* study examining the effect of bortezomib or carfilzomib in MM.1R or VDR did not reveal a statistically significant reduction in tumour burden in either cell lines for any drug treatment or schedule used compared to vehicle mice. However in MM.1R-mice, a statistically significant overall survival was observed in bortezomib treated mice compared to controls and compared to carfilzomib treated mice. In addition, VDR mice displayed a statistically significant improvement in overall survival in both bortezomib treated and carfilzomib treated mice compared to vehicle treated mice.

3.2 WHOLE EXOME SEQUENCING OF MM.1R AND VDR CELL LINES

3.2.1 Introduction

Whole exome sequencing has been used both in the *in vitro* and *in vivo* setting for detection of genomic aberrations and more recently in understanding the evolution of clonal heterogeneity in the setting of multiple myeloma.^[105-108] In particular in recent times the identification of multiple clones in alternating patterns (e.g. linear, branching) and evolution of same clones in MM patients appears to arise not only during the natural course of the disease but also when patients relapse.^{[107] [109]}

We therefore performed whole exome sequencing analysis of the cell lines MM.1R and VDR. The sequencing result for the drug-resistant cell line was compared with the respective drug-sensitive isogenic parental cell line (see materials and methods section 2.10). Whole exome sequencing and resultant statistical analysis were completed by the team at CCGD, and the results interpreted with their expertise and the expertise of Dr Mitsiades.

3.2.2 Frequency of single nucleotide variants observed between isogenic cell lines MM.1R and VDR

There were 28 non-synonymous single nucleotide variants (SNV) observed in the MM.1R vs. VDR comparison, of which 26 were novel mutations. Figure 3.2.2.1 plots the allele fractions of the common mutations between MM.1R and VDR cell lines. The “allele fraction” is a fraction of the sequenced reads from a region that contain a specific allele, which is an estimate of the frequency of this allele in total DNA tested (with no assumptions about copies per cell or number of cells in which the mutation is present). The points on the y-axis correspond to the 28 non-synonymous SNVs present in VDR but not in its parental cell line MM.1R. The points on the X-axis correspond to mutations that were identified only in MM.1R. Finally, the points in the middle of the graph represent mutations that were found in both cell lines, and occur at varying frequency compared to the wild type.

SIFT and Polyphen predictions were obtained for all 28 mutations that are listed in table 3.2.2.1. SIFT (Sorting Intolerant From Tolerant) software predicts

whether an amino acid substitution is likely to affect protein function based on sequence homology and the physico-chemical similarity between the alternate amino acids. The data provided for each amino acid substitution gives a qualitative prediction (either 'tolerated' or 'damaging').^[110] Polyphen-2 is a tool that predicts possible impact of an amino acid substitution on the structure and function of a human protein using physical and comparative considerations.^[111] Of the 28 SNVs detected in VDR but not MM.1R, 7 SNVs were found to be “damaging” by both algorithms, 6 SNVs were found to be “damaging” by one of the algorithms, and the remaining 15 SNVs were found to be “tolerated” by one or both of the algorithms.

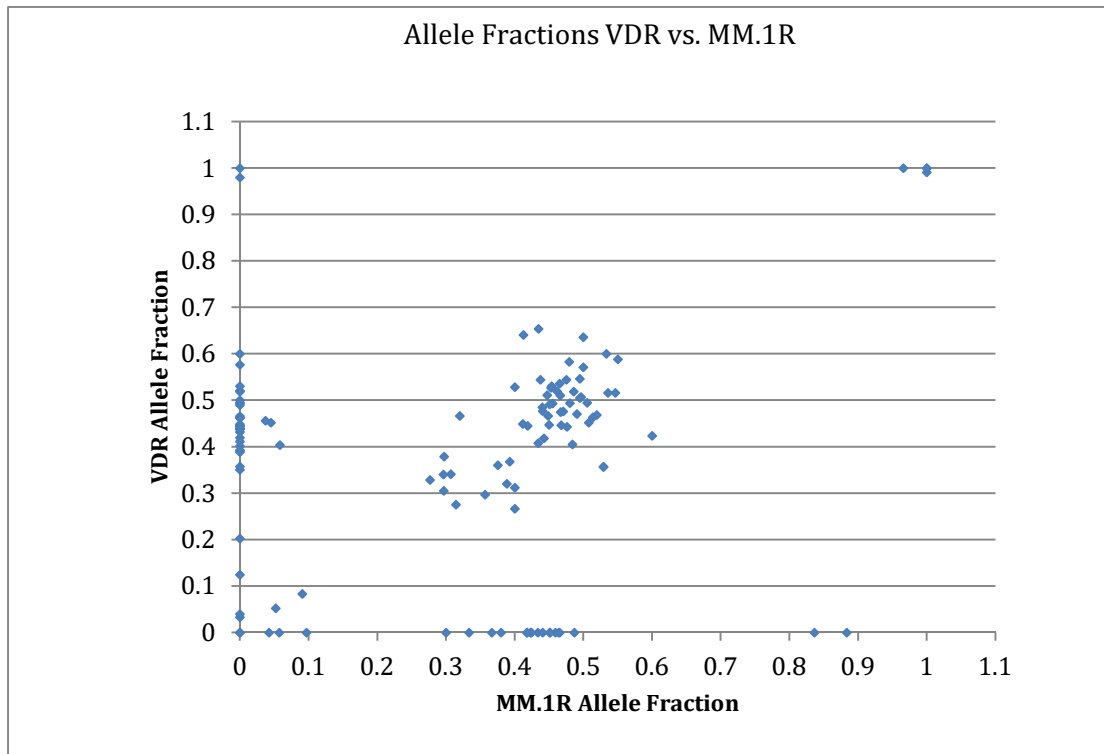


Figure 3.2.2.1 Allele fractions of the common mutations between MM.1R and VDR cell lines. The points on the y-axis correspond to the non-synonymous SNVs present in VDR but not in its parental cell line MM.1R. The points on the x-axis correspond to the non-synonymous SNVs present in MM.1R but not in its bortezomib-resistant counterpart VDR. (Note: “allele fraction” is a fraction of the sequenced reads from a region that contains a specific allele, which is an estimate of the frequency of this allele in total DNA tested).

GENE	CHR	POSITION	AA CHANGE	CODON_CHANGE
SPARCL1	4	g.88415159T>A	p.N265Y	c.(793-795)AAC>TAC
ZER1	9	g.131503072G>T	p.S611Y	c.(1831-1833)TCC>TAC
TPH2	12	g.72366351G>T	p.G221C	c.(661-663)GGT>TGT
MFGE8	15	g.89444941C>A	p.K237N	c.(709-711)AAG>AAT
CCDC113	16	g.58292291A>T	p.E137V	c.(409-411)GAA>GTA
FAM59A	18	g.29890224C>G	p.V109L	c.(325-327)GTG>CTG
ATP5J	21	g.27102074G>A	p.S11F	c.(31-33)TCT>TTT
TTLL1	22	g.43447822C>A	p.K321N	c.(961-963)AAG>AAT
SARS	1	g.109756659C>A	p.D15E	c.(43-45)GAC>GAA
H2AFV	7	g.44874131A>G	p.I119T	c.(355-357)ATT>ACT
ROD1	9	g.114982551G>T	-	-
MKL2	16	g.14312805C>G	p.P215A	c.(643-645)CCA>GCA
PSMB5	14	g.23502844T>C	p.T80A	c.(238-240)ACA>GCA
KCNN3	1	g.154698487C>A	p.A536S	c.(1606-1608)GCC>TCC
TAF5L	1	g.229750100C>T	p.A44T	c.(130-132)GCC>ACC
SEMA4F	2	g.74907071G>A	p.R683H	c.(2047-2049)CGT>CAT
SLC6A18	5	g.1242940C>T	p.P365S	c.(1093-1095)CCC>TCC
GCM2	6	g.10876129A>G	p.S193P	c.(577-579)TCC>CCC
COL9A1	6	g.70992692C>T	-	-
H2AFV	7	g.44874113T>C	p.Q125R	c.(373-375)CAG>CGG
ZER1	9	g.131503073A>G	p.S611P	c.(1831-1833)TCC>CCC
CDK2	12	g.56365357C>A	p.A282D	c.(844-846)GCT>GAT
NCOR2	12	g.124856844T>C	p.K844R	c.(2530-2532)AAG>AGG
C14orf177	14	g.99183598T>C	p.M122T	c.(364-366)ATG>ACG
STAC2	17	g.37374251G>T	p.A89D	c.(265-267)GCT>GAT
ITGB4	17	g.73745009G>A	p.V1067I	c.(3199-3201)GTT>ATT
TMC6	17	g.76118778G>A	p.H379Y	c.(1135-1137)CAC>TAC
ZNF579	19	g.56090288C>T	p.A240T	c.(718-720)GCC>ACC

Table 3.2.2.1 Single nucleotide variants found in VDR but not MM.1R

List of gene mutations identified in bortezomib resistant VDR but not bortezomib sensitive MM.1R. SIFT and Polyphen predictions were obtained for all 28 mutations listed in table 3.2.2.1. Of these, 7 SNVs were found to be damaging by both algorithms (blue), 6 SNVs were found to be damaging by one of the algorithms (red), and the remaining 15 SNVs were found to be tolerated by one or both of the algorithms (green).

3.2.3 Insertions and deletions identified in VDR vs. MM.1R

Besides SNVs, 1 deletion was identified in VDR cell line using Indel Locator (<https://confluence.broadinstitute.org/display/CGATools/Indelocator>), when comparing MM.1R and VDR. No insertions were identified between the MM.1R and VDR comparisons. One deletion was identified in VDR in ABCA7 gene, i.e. ATP-binding cassette sub-family A member 7 gene however, that was not present in MM.1R (table 3.2.3.1).

The ABCA7 gene belongs to a superfamily of ABC (ATP-binding cassette) transporters. The protein products of ABC genes are responsible for transporting numerous substances across cell membranes (both intra- and extra-cellularly). There are 7 ABC subfamilies, of which ABCA7 belongs to the ABC1 subfamily. The ABCA7 protein is expressed at the highest level in peripheral leucocytes, thymus gland, bone marrow and splenic tissue. Kaminski et al first described ABCA7 in 2000 when its role in lipid transport across macrophage membranes was elucidated.^[112]

In 2012 Meurs et al investigated the effect of macrophage ABCA7 knockdown in mice to determine its role in atherosclerosis, given its known involvement in lipid transport. While they did not find a correlation between ABCA7 knockdown and atherosclerosis in the mice, they revealed that concomitant knockdown of ABCA7 and ABCA1 (the promoter of initiating step in cholesterol transport) resulted in massive splenomegaly due to cellular fat accumulation, down-regulation of number of CD3+ T cells, and promoted erythropoietic regulators. Their data suggested that ABCA7 might be involved in splenic proliferation of T cells and erythrocytes.^[113]

In relation to its potential role in cancer pathogenesis, in a cohort of 51 patients with colorectal cancer, a correlation between reduced transcript levels of ABCA7 gene and shortening of disease free interval following treatment has been established ($p=0.033$, log rank test).^[114] However neither ABCA7 gene down-regulation nor deletion in this gene have been implicated in haematological malignancy in the *in vivo* setting to date.

Nucleotide change	Deletion of 44 bases: CGCGG- ctgcgggacacccatgcgcgccatggggctcagccgcgcggtgct -CTGGC
Amino acid change	KETRLrdtmramglsravlw...(+1554 amino acids)...*→KETRLarlvpqlpralpaqr...(+155 amino acids)...*
Gene	ABCA7
Gene Description	ATP-binding cassette sub-family A member 7 (Macrophage ABC transporter)(Autoantigen SS-N)(ABCA-SSN) [Source:UniProtKB/Swiss-Prot;Acc:Q8IZY2]
Protein Family Description	ATP BINDING CASSETTE SUB FAMILY A MEMBER ALTERNATE NAME: ATP BINDING CASSETTE TRANSPORTER
Causes Nonsense Mediated Decay	Yes
Reported in 1000 Genomes	Yes: CTGCGGGACACCATGCGCGCCATGGGGCTCAGCCGCGCGGTGCT/-YRI allele frequency:0.08
SIFT Prediction	DAMAGING

Table 3.2.3.1 Details of deletion in ABCA7 identified in bortezomib-resistant VDR cell line. List of details pertaining to deletion in ABCA7 gene identified in bortezomib-resistant cell line VDR, which was not identified in parental MM.1R. This deletion results in a 1400 amino acid truncation of ABCA7.

3.2.4 Identification of PSMB5 mutation in VDR cell line

Of the 28 SNVs identified in VDR cell line by whole exome sequencing, a gene mutation was noted in the PSMB5 gene. PSMB5 gene is present on chromosome 14 and the SNV involved a threonine to alanine substitution at position 80 on exon 2 (figure 3.2.4.1). PubMed literature review of this mutation revealed that this gene mutation has also been previously identified in a bortezomib-resistant leukaemic cell line, which by 3D *in silico* modelling, appears to alter the bortezomib-PSMB5 binding pocket (see introduction 1.4.1).^[64] MM.1R and VDR cell lines were prepared for Sanger sequencing (see materials and methods section 2.11) and Sanger sequencing that was performed at the Dana-Farber/Harvard Cancer Centre DNA Resource Core confirmed the presence of the PSMB5 mutation in VDR cell line.

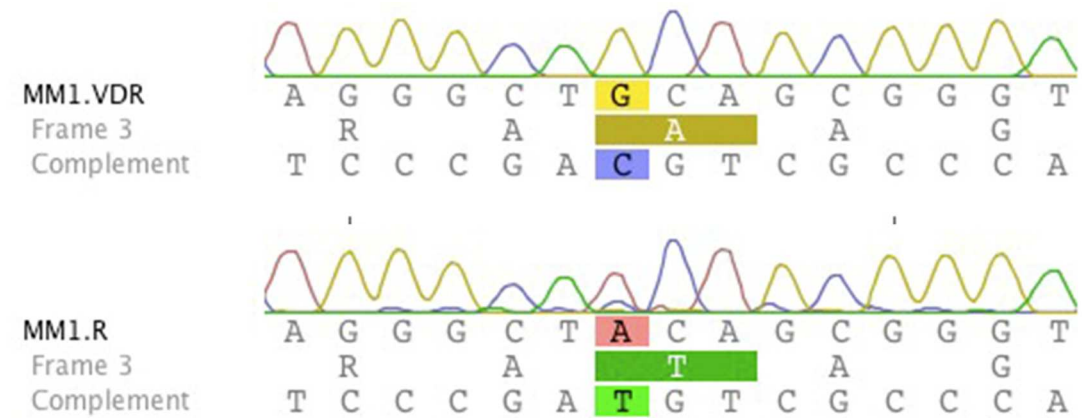


Figure 3.2.4.1 Mutation in PSMB5 gene confirmed by Sanger Sequencing

A threonine to alanine substitution in exon 2 of chromosome 14 initially identified by whole exome sequencing was subsequently validated by Sanger sequencing.

3.2.5 Sensitivity of KMS11 cell line to bortezomib following lentiviral infection with mutPSMB5

Next to determine the potential functional significance of the PSMB5 mutation identified in VDR cell line, we undertook lentiviral infection of mutPSMB5 into bortezomib-sensitive cell lines, to ascertain if over-expression of mutPSMB5 in bortezomib sensitive cell lines rendered them resistant to bortezomib.

We undertook mutPSMB5 lentiviral infection into bortezomib-sensitive cell line KMS11 (see materials and methods section 2.14) to ascertain if over-expression of mutPSMB5 in a bortezomib sensitive cell line could result in altered sensitivity of this cell line to bortezomib. KMS11 cells were infected with a control (BFP) lentivirus, wt-PSMB5 (wild-type), and mutPSMB5, and subsequently treated with bortezomib. We observed a modest reduction in sensitivity of KMS11 cells infected with wtPSMB5 to bortezomib, however an even greater degree of reduction in sensitivity to bortezomib was observed when KMS11 was infected with mutPSMB5 (figure 3.2.5.1).

A trial of infection of both MM.1S and MM.1R cell lines was conducted on 2 separate occasions; however due to exquisite sensitivity of these cell lines to blasticidin and their semi-adherent nature, lentiviral infection was unsuccessful.

In conclusion, our data suggest that over-expression of mutPSMB5 in KMS11 cell line causes a marked reduction in sensitivity to bortezomib compared to KMS11 infected with BFP-control lentivirus.

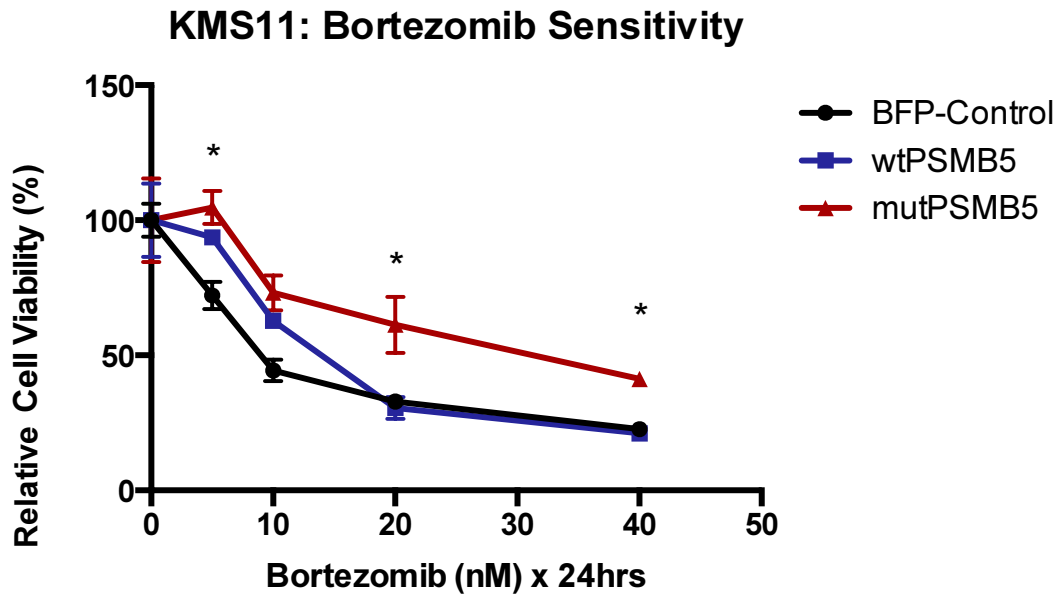


Figure 3.2.5.1 Sensitivity of KMS11 cell line to bortezomib following lentiviral infection

KMS11 cell line was infected with either BFP-control, wild type PSMB5 (wtPSMB5) or mutant PSMB5 (mutPSMB5) and subsequently exposed to bortezomib 0-40nM for 24hrs. Cell viability was subsequently analysed by Cell Titre Glo. (* $p < 0.05$ when comparing BFP-control to mutPSMB5 conditions).

3.2.6 Summary of whole exome sequencing study

We performed whole exome sequencing analysis of the cell lines MM.1R and VDR to determine SNVs, insertions or deletions that were present in bortezomib resistant VDR but not bortezomib-sensitive MM.1R cell line. 28 non-synonymous single nucleotide variants (SNV) were detected in VDR that were not present in MM.1R, of which 26 were novel mutations. SIFT and Polyphen predictions found 7 SNVs to be “damaging” by both algorithms and 6 SNVs were found to be “damaging” by either SIFT or Polyphen algorithms.

A deletion in ABCA7 gene was found in VDR but not MM.1R. The ABCA7 gene belongs to a superfamily of ABC (ATP-binding cassette) transporters. ABCA7 protein is expressed at the highest level in peripheral leucocytes, thymus gland, bone marrow and splenic tissue. In 2012 Meurs et al outlined that concomitant knockdown of ABCA7 and ABCA1 resulted in massive splenomegaly in mice due to cellular fat accumulation, down-regulation of number of CD3+ T cells, and promoted erythropoietic regulators, suggesting that ABCA7 may be involved in splenic proliferation of T cells and erythrocytes.^[113] In a cohort of 51 patients with colorectal cancer, reduced transcript levels of ABCA7 gene has been correlated with shortening of disease free interval in patients with colorectal cancer following treatment ($p=0.033$, log rank test).^[114] However neither ABCA7 gene down-regulation nor deletion in this gene have been implicated in haematological malignancy in the *in vivo* setting to date. Of note, no insertions were identified between the MM.1R and VDR comparisons.

Of the 28 SNVs identified in VDR cell line by whole exome sequencing, a gene mutation was noted in the PSMB5 gene involving a threonine to alanine substitution at position 80 on exon 2. This mutation has been previously described in a bortezomib-resistant leukaemic cell line model, and 3D *in silico* modelling of the mutation appears to alter the bortezomib-PSMB5 binding pocket.^[64] We thus next undertook lentiviral infection of mutPSMB5 into bortezomib-sensitive cell line KMS11, to ascertain if over-expression of mutPSMB5 in KMS11 rendered these cells resistant to bortezomib. We observed a degree of reduction in sensitivity of KMS11 cells infected with wtPSMB5 to

bortezomib, however an even greater degree of reduction in sensitivity to bortezomib was observed when KMS11 was infected with mutPSMB5

In conclusion, our whole exome sequencing results revealed a number of novel SNVs; a deletion of ABCA7 gene whose role in haematological malignancies in the *in vivo* setting is yet to be investigated; and finally that reintroduction of mutPSMB5 into bortezomib-sensitive KMS11 appears to cause a marked reduction in sensitivity of this cell line to bortezomib. The latter finding suggests that mutPSMB5 may play a role in bortezomib resistance in the *in vitro* setting.

3.3 GENE EXPRESSION PROFILING OF MM.1R AND VDR

3.3.1 Introduction

In order to determine the transcriptional profiles of the bortezomib sensitive (MM.1R) and bortezomib resistant (VDR) cell lines, each was cultured in 4 biological replicates at 37°C at a density of 10×10^6 cells per condition for 24 hours, then the cells were collected at 4°C. RNA was extracted using miRNeasy Mini Kit (# 217004) as per protocol, and this was stored at -20°C. Affymetrix oligonucleotide arrays were undertaken at Beth Israel Deaconess Medical Centre Core Genomic Facility using GeneChip Human Gene 1.0 ST Whole Genome Cartridge Gene Arrays (catalogue # 901085), (see materials and methods section 2.12).

In total, 20,724 genes were compared between MM1R and VDR cell lines. Genes from this list were filtered to include only those whereby the difference in fold change between the two conditions was >1.2 and demonstrated a p value ≤ 0.01 , of which 437 transcripts fulfilled these criteria. Of these transcripts, 353 were over-expressed in VDR compared to MM.1R. In comparison only 84 genes were down regulated in VDR compared to MM.1R. The reason for this difference between number of genes up-regulated versus down-regulated is unclear.

Subsequently a number of target transcripts of interest were chosen for shRNA knockdown studies. Briefly, transcripts of particular interest underwent shRNA knockdown and subsequent treatment with bortezomib to determine which genes, following their shRNA knockdown, resulted in resensitisation of VDR cells to bortezomib. PSMB5 transcript was subsequently selected for validation studies, given the fact that bortezomib inhibits the proteasome mainly via PSMB5.

3.3.2 Transcripts over-expressed in VDR compared to MM.1R

By applying the aforementioned cut-off criteria of a fold change >1.2 and an p value ≤ 0.01 , 353 transcripts were found to be over-expressed in bortezomib-resistant cell line VDR compared to its bortezomib-sensitive parental cell line MM.1R, see table 3.3.2.1.

DAVID functional annotation tool (<http://david.abcc.ncifcrf.gov/>) was utilised to determine in which cellular processes transcripts up-regulated in VDR compared to MM.1R are involved, whereby adjusted p value ≤ 0.05 (here p value correlates with strength of association of gene to named cellular process); fold change between control and experimental genes in a given process was ≥ 1.2 ; and the “percentage of genes” equals the total number of genes over-expressed in VDR vs. MM.1R that are involved in a specific pathway. Table 3.3.2.2 reveals all cellular processes in which genes over-expressed in VDR compared to MM.1R are involved. Table 3.3.2.3 lists specific genes over-expressed in VDR involved in 7 separate cellular processes, whereby at least 27 of a total 353 transcripts up-regulated in VDR play a role in each pathway listed.

Pathway analysis again via DAVID functional annotation tool revealed “cellular apoptosis” as a specific pathway in which 4 transcripts up-regulated in VDR play a role. These genes include CFLAR (CASP8 and FADD-like apoptosis regulator), caspase-8 (CASP8, apoptosis-related cysteine peptidase), caspase-10 (CASP10, apoptosis-related cysteine peptidase) and NFKBIA (nuclear factor of kappa light polypeptide gene enhancer in B-cells inhibitor, alpha), (figure 3.3.2.1). Again p value equals ≤ 0.05 for strength of association of each specific gene to cellular apoptosis.

Gene Name	MM.1R Mean Expression	VDR Mean Expression	Fold Change	p value
ALOX5AP	146.31	739.51	5.05	3.15E-04
CALCRL	27.95	133.59	4.78	0.003
SLC7A11	195.74	793.65	4.05	4.00E-06
PSAT1	253.07	919.7	3.63	3.00E-06
MYO1B	77.06	277.52	3.6	2.60E-05
FN1	155.65	536.13	3.44	5.00E-05
CX3CR1	167.41	553.23	3.3	9.00E-06
ALDH1L2	320.77	984.2	3.07	9.00E-06
SOS2	251.8	736.76	2.93	1.70E-05
NLRP11	76.15	220.98	2.9	1.60E-05
STAP1	271.81	776.99	2.86	1.70E-05
CTAGE5	136.97	378.41	2.76	3.30E-05
EML5	79.68	215.86	2.71	3.40E-05
ACTR10	136.6	363.08	2.66	9.54E-04
CD38	288.01	749.34	2.6	1.40E-05
SARS	227.04	557.13	2.45	0.002
DHRS7	172	407.54	2.37	2.34E-04
IDH1	435.4	1031.6	2.37	1.80E-04
PRSS2	98.9	234.49	2.37	3.40E-05
FANCM	169.3	398.69	2.35	2.64E-04
C14orf135	157.77	371.46	2.35	7.60E-05
SEC23A	114.63	268.46	2.34	4.03E-04
TMEM194B	220.88	498.39	2.26	1.42E-04
TUBE1	140.16	314.68	2.25	4.20E-05
STRN3	195.46	438.79	2.24	4.63E-04
PSMC6	444.97	996.13	2.24	1.70E-04
SRP54	320.9	709.69	2.21	2.00E-05
OSBPL6	97.32	215.22	2.21	5.00E-06
FAM172B	85.13	187.5	2.2	9.42E-04
HECTD1	551.33	1211.6	2.2	5.92E-04
PMAIP1	94.27	207.84	2.2	3.38E-04
G2E3	125.73	276.01	2.2	1.59E-04
NFE2L1	163.8	359.63	2.2	4.60E-05
PLEK	126.35	275.22	2.18	0.001
ZNF215	533.23	1160.18	2.18	5.90E-05
RBM23	124.36	267.36	2.15	0.002
CR2	216.88	466.5	2.15	1.60E-04
NLRP14	97.2	206.81	2.13	2.21E-04
TRAPPC6B	171.16	361.81	2.11	0.002
NGDN	114.01	240.86	2.11	0.001
CHMP4A	202.82	427.25	2.11	1.81E-04
NEDD8	500.73	1051.85	2.1	7.03E-04
B3GNT5	103.92	215.92	2.08	2.19E-04
PSMA6	530.11	1095.54	2.07	0.004

Gene Name	MM.1R Mean Expression	VDR Mean Expression	Fold Change	p value
ALS2CR8	114.85	236.97	2.06	0.002
TMEM154	223.98	461.85	2.06	9.00E-06
KLHDC2	268.3	548.07	2.04	1.76E-04
ME1	453.2	924.22	2.04	1.14E-04
SCFD1	214.14	430.08	2.01	9.70E-05
ASNS	635.94	1274.82	2	1.12E-04
CCPG1	448.05	896.15	2	1.80E-05
MBIP	314.1	623.28	1.98	4.31E-04
TXNDC16	120.49	239	1.98	3.82E-04
FBXO34	248.76	487.83	1.96	7.39E-04
C14orf101	172.88	339.68	1.96	2.36E-04
SHMT2	495.49	963.81	1.95	3.39E-04
ADAM23	363.12	703.4	1.94	1.58E-04
PPM1A	191.13	370.98	1.94	3.40E-05
ICAM3	122.86	236.92	1.93	4.00E-04
NETO2	307.65	588.84	1.91	2.00E-04
GALNT3	160	306.34	1.91	7.00E-05
MUDENG	139.03	264.8	1.9	0.004
MNAT1	157.74	299.74	1.9	6.10E-05
PSMB5	188.83	357.69	1.89	4.14E-04
RNASE6	135.81	255.37	1.88	0.005
TIMM9	119.11	223.82	1.88	5.99E-04
SKAP1	128.12	240.13	1.87	5.82E-04
TINF2	189.14	354.1	1.87	1.70E-05
EXOC5	525.64	981.33	1.87	9.00E-06
DDIT4	132.83	247.58	1.86	4.12E-04
HSPA13	548.22	1022.1	1.86	2.22E-04
DDHD1	621.93	1155.6	1.86	1.01E-04
C14orf166	390.9	721.46	1.85	8.70E-04
WARS	191.83	355.78	1.85	1.12E-04
NFKBIA	267.86	492.65	1.84	0.002
FAM126B	364.55	670.49	1.84	5.19E-04
MAP4K5	176.83	326.05	1.84	4.94E-04
CIDEB	209.5	384.97	1.84	4.38E-04
NFE2L2	469.64	862.62	1.84	1.92E-04
SEL1L3	658.64	1210.35	1.84	1.59E-04
GARS	1651.87	3043.57	1.84	3.00E-06
C3orf52	150.91	275.94	1.83	0.002
COQ10B	174.72	318.87	1.83	7.90E-04
ACIN1	176.34	320.26	1.82	0.002
STYX	496.64	904.58	1.82	1.95E-04
COBLL1	173.33	314.08	1.81	7.14E-04
ACSM3	127.44	228.16	1.79	0.008
ARHGAP42	165.86	296.39	1.79	0.001
PPIL5	162.08	290.27	1.79	0.001

Gene Name	MM.1R Mean Expression	VDR Mean Expression	Fold Change	p value
IKZF1	161.27	288.75	1.79	0.001
ALS2	166.31	298.18	1.79	0.001
SV2C	185.14	330.24	1.78	0.003
JKAMP	338.43	604.09	1.78	0.003
PIKFYVE	310.91	550.55	1.77	5.36E-04
RAB30	290.88	515.71	1.77	2.34E-04
MAPRE2	453.06	802.35	1.77	2.31E-04
TM9SF1	133.42	236.58	1.77	6.10E-05
SLCO4C1	210.27	369.57	1.76	0.002
B4GALT3	242.49	427.45	1.76	0.002
BAZ1A	417.76	736.64	1.76	0.001
F2R	138.26	243.56	1.76	9.66E-04
GMPR2	308.19	542.72	1.76	6.12E-04
ERO1L	462.43	815.82	1.76	9.70E-05
RHBDD1	831.6	1465.99	1.76	3.30E-05
DGKA	225.24	391.71	1.74	0.001
WDHD1	787.99	1371.1	1.74	7.88E-04
AIG1	267.4	464.83	1.74	4.20E-05
ITGAV	251.91	435.11	1.73	0.004
AVL9	195.91	339.34	1.73	0.002
TMEM135	153.79	265.76	1.73	0.001
HYOU1	222.19	383.48	1.73	0.001
C14orf145	601.83	1041.27	1.73	0.001
ARID4A	411.29	711.48	1.73	0.001
KIAA0391	140.39	242.53	1.73	4.24E-04
MARS	487.59	842.78	1.73	5.50E-05
GMFB	212.27	366.02	1.72	0.004
ATP6V0A1	367.86	633.05	1.72	0.004
ZFAND1	483.57	833.57	1.72	8.44E-04
AARS	741.12	1271.54	1.72	1.42E-04
SLC1A5	384.23	661.61	1.72	4.50E-05
MTHFD2	1234.19	2128.29	1.72	2.80E-05
INPP5B	167.39	284.95	1.7	9.81E-04
CFLAR	160.35	270.19	1.69	0.003
ESYT1	158.76	267.77	1.69	0.001
HAX1	442.4	747.74	1.69	7.58E-04
CD28	1212.14	2044.23	1.69	6.80E-05
LOC100128364	261.75	439.6	1.68	0.003
ACACA	239.16	401.53	1.68	0.001
DLGAP5	615.3	1036.3	1.68	6.20E-05
TJP1	274.25	457.56	1.67	0.006
SLC41A2	298.67	498.31	1.67	0.003
NCOA7	155.23	259.48	1.67	0.002
EDEM1	694.57	1156.66	1.67	0.002
KIAA0586	266.57	445.64	1.67	8.52E-04

Gene Name	MM.1R Mean Expression	VDR Mean Expression	Fold Change	p value
PPP2R3C	200.86	332.67	1.66	0.002
ERV3	173.42	288.36	1.66	8.05E-04
PSME1	659.04	1096.24	1.66	4.80E-04
RASA2	567.12	943.19	1.66	1.49E-04
CLK1	414.82	683.4	1.65	0.001
GTF3C3	744.22	1225.52	1.65	4.75E-04
MAPK1IP1L	263.45	433.95	1.65	1.42E-04
ARHGAP5	167.57	274.65	1.64	0.002
DCBLD1	403.56	661.76	1.64	0.001
PRMT5	198.65	326.14	1.64	5.78E-04
OAS1	267.7	439.78	1.64	3.91E-04
RAB3GAP1	300.02	489.56	1.63	0.009
OCLN	178.09	289.82	1.63	0.008
GALNT1	320.47	522.07	1.63	0.001
SNX6	338.13	552.4	1.63	3.03E-04
ATIC	798.97	1303.35	1.63	1.04E-04
DPY19L1	445.02	721.9	1.62	0.006
ITGA6	451.31	729.28	1.62	0.005
ZNF322A	290.22	469.47	1.62	0.004
CREB3L2	300.65	486.25	1.62	0.002
TES	617.33	998.86	1.62	7.07E-04
SERPINE2	359.73	583.91	1.62	4.89E-04
WIP1	506.12	817.41	1.62	5.10E-05
HIAT1	464.48	748.94	1.61	0.005
CAMK2D	219.87	354.97	1.61	0.002
RGS2	402.62	647.39	1.61	2.54E-04
BZW1L1	788.19	1268.18	1.61	1.35E-04
ALCAM	401.28	642.67	1.6	0.001
ACSL3	477.98	765.59	1.6	1.16E-04
DCLRE1A	205.46	326.5	1.59	0.013
GOLGA6L5	376.37	599.75	1.59	0.009
YARS	503.11	800.1	1.59	0.001
HMGCS1	720.51	1142.74	1.59	3.69E-04
SPATS2L	697.79	1109.16	1.59	4.90E-05
PGD	537.22	847.89	1.58	0.003
FASTKD2	212.39	336.12	1.58	0.001
TTC35	432.94	678.25	1.57	0.007
C2orf60	198.2	310.38	1.57	0.005
NT5DC1	303.59	476.89	1.57	0.004
NHEJ1	209.18	327.36	1.56	0.005
CYP20A1	312.49	488.04	1.56	0.002
SLC7A1	191.31	298.61	1.56	4.67E-04
STRADB	235.38	363.96	1.55	0.008
VPS41	644.04	1000.83	1.55	0.007
LANCL1	276.65	428.8	1.55	0.004

Gene Name	MM.1R Mean Expression	VDR Mean Expression	Fold Change	p value
AGA	221.22	342.24	1.55	0.002
SLC7A5	314.07	485.69	1.55	0.002
OR2D2	184.96	285.17	1.54	0.008
CARS	200.22	308.21	1.54	0.004
WDFY1	196.05	302.61	1.54	0.002
WIPF1	1257.31	1932.86	1.54	0.001
RPE	438.61	676.21	1.54	7.23E-04
TSEN15	589.1	907.47	1.54	2.22E-04
SEL1L	1329.39	2050.47	1.54	1.89E-04
KIAA1598	231.23	352.97	1.53	0.013
KLF3	355.45	542.93	1.53	0.002
AP1AR	228.17	349.17	1.53	1.87E-04
OS9	361.59	550.49	1.52	0.002
KBTBD8	347.05	525.97	1.52	0.002
ADAM9	580.77	879.34	1.51	0.003
ANKRD44	251.95	380.62	1.51	0.002
HCLS1	668.57	1009.03	1.51	0.001
C4orf52	312.41	472.85	1.51	3.47E-04
SCD	1517.8	2285.6	1.51	2.74E-04
CWC22	570.43	857.44	1.5	0.007
NR1D2	228.93	343.52	1.5	0.005
KTN1	924.61	1384.68	1.5	0.005
FAM171B	267.68	401.94	1.5	0.002
MFSD6	231.1	346.89	1.5	0.001
DNAJB9	255.26	381.91	1.5	9.89E-04
DNAJC10	1463.37	2195.66	1.5	1.78E-04
COPG	302.22	450.58	1.49	0.008
SESTD1	276.47	412.09	1.49	0.008
CASP10	354.25	528.85	1.49	0.004
C5orf33	509.9	758.67	1.49	0.003
METTL4	303.77	453.36	1.49	0.003
PRKRA	322.36	479.95	1.49	0.002
FKBP3	252.26	374.97	1.49	0.001
PRPS1	422.07	628.16	1.49	9.37E-04
PIK3CG	1030.47	1534.82	1.49	3.21E-04
CDKN3	577.95	859.89	1.49	1.60E-05
AP3M2	222.05	328.65	1.48	0.013
CAPRIN2	301.91	447.84	1.48	0.011
GDAP2	240.55	355.53	1.48	0.008
C14orf106	536.38	795.72	1.48	0.003
ZCCHC8	217.64	322.97	1.48	5.51E-04
ITGA4	1369.17	2024.5	1.48	1.54E-04
TAPT1	256.95	381.01	1.48	1.50E-04
MCTP2	223.43	327.95	1.47	0.014
PRMT3	304.07	446.35	1.47	0.007

Gene Name	MM.1R Mean Expression	VDR Mean Expression	Fold Change	p value
PDIA4	945.12	1388.35	1.47	3.00E-04
HIST1H1E	1505.06	2204.64	1.46	0.009
CIR1	380.13	556.67	1.46	0.004
CALCOCO2	411.33	599.24	1.46	0.003
TMED10	602.28	882.02	1.46	0.002
PSME2	557.51	813.72	1.46	9.79E-04
ANLN	608.29	890.52	1.46	9.27E-04
HERPUD2	266.41	388.55	1.46	8.28E-04
PABPN1	378.64	554.44	1.46	2.08E-04
TMX4	385.67	559.14	1.45	0.012
CNIH	479.57	693.19	1.45	0.007
KIDINS220	498.2	724.18	1.45	0.007
SLC35A5	244.32	354.42	1.45	0.007
KLHL5	315.53	458.09	1.45	0.006
PRPF39	295.77	428.16	1.45	0.006
WDR41	361.29	523.86	1.45	0.005
FBXW7	313.16	453.21	1.45	0.003
CCL3	3190.87	4614	1.45	0.002
CYP2R1	242.84	351.08	1.45	0.002
FNDC3A	819.76	1186.02	1.45	7.39E-04
OXA1L	618.88	899.62	1.45	3.40E-04
HMGCR	537.1	775.55	1.44	0.008
LMBRD2	474.81	682.47	1.44	0.006
RPL18AP3	723.35	1040.95	1.44	0.006
WDR48	331.37	476.38	1.44	0.005
ERGIC3	811.26	1166	1.44	0.005
EXOC6	249.03	359.35	1.44	0.004
CLIP1	254.23	365.53	1.44	0.004
GLB1	255.16	367.78	1.44	0.003
ZDBF2	993.17	1426.48	1.44	2.54E-04
CTBS	280.24	401.82	1.43	0.013
HUS1	433.64	619.03	1.43	0.009
ERN1	307.62	440.49	1.43	0.006
MAN1A2	427.35	611.44	1.43	0.006
WDR12	895.54	1276.83	1.43	0.004
OAT	245.11	350.04	1.43	0.004
KLHL12	321.81	459.58	1.43	0.004
KLHL2	341.32	487.84	1.43	0.003
FDPS	522.5	749.36	1.43	0.002
ERLEC1	362.36	517.95	1.43	0.002
POLR3C	623.06	892.92	1.43	0.001
BCL2L1	392.78	562.77	1.43	1.04E-04
FAM18B2	330.17	469.78	1.42	0.009
C17orf75	264.96	375.57	1.42	0.006
ORC2L	492.57	700.59	1.42	0.004

Gene Name	MM.1R Mean Expression	VDR Mean Expression	Fold Change	p value
STRBP	943.71	1339.05	1.42	0.003
ATF2	748.32	1061.12	1.42	0.002
IRF4	1237.57	1763.01	1.42	8.10E-05
ARIH2	245.45	346.22	1.41	0.011
HIBADH	276.53	388.65	1.41	0.009
TMEM19	365.81	516.2	1.41	0.008
FAM107B	493.96	698.08	1.41	0.004
CREB1	1094.32	1545.07	1.41	0.003
HDDC2	282.67	399.43	1.41	5.35E-04
RCN1	1220.99	1725.89	1.41	1.17E-04
NIN	287.4	401	1.4	0.007
PTER	290.5	406.15	1.4	0.006
UFM1	480.8	674.92	1.4	0.006
PSMA3	420.21	590.1	1.4	0.006
ASAH1	569.6	799.59	1.4	0.005
NCSTN	345.85	482.76	1.4	0.005
NCOA2	454.92	636.79	1.4	0.004
MLH1	410.86	576.2	1.4	0.001
PMS1	683.35	954.58	1.4	6.57E-04
SENP2	423.92	595.59	1.4	5.51E-04
BARD1	756.77	1063.25	1.4	1.30E-05
SAP130	502.36	699.49	1.39	0.012
BAT1	490.94	680.76	1.39	0.004
FNDC3B	584.45	815	1.39	0.003
INSIG1	698.94	972.96	1.39	0.003
TARS	1496.96	2082.91	1.39	0.002
LMAN2	396.33	551.46	1.39	0.002
SLC38A2	2149.68	2980.95	1.39	8.79E-04
CCL5	571.54	791.8	1.39	3.21E-04
MT01	324.23	446.43	1.38	0.006
RAD17	334.1	461.45	1.38	0.005
DCPS	270.88	375.05	1.38	0.002
CASP8	572.29	792.46	1.38	0.002
PLDN	371.32	512.97	1.38	8.86E-04
C7orf44	415.21	570.63	1.37	0.009
GPBP1L1	452.68	619.62	1.37	0.008
ATM	456.05	626.53	1.37	0.005
NDUFS1	837.44	1144.37	1.37	0.004
INO80D	361.48	496.26	1.37	0.004
TRIP13	590.76	808.5	1.37	0.003
JAK1	1011.64	1386.68	1.37	0.002
APLP2	359.57	493.54	1.37	0.001
XPOT	1225.84	1677.43	1.37	2.07E-04
PRNP	409.23	558.39	1.36	0.014
MACC1	885.59	1205.32	1.36	0.009

Gene Name	MM.1R Mean Expression	VDR Mean Expression	Fold Change	p value
MBNL2	587.92	797.49	1.36	0.006
C11orf24	481.2	655.46	1.36	0.004
ORMDL1	300.29	406.9	1.36	0.004
UBE2Q2	303.3	413.56	1.36	0.002
GLS	839.2	1140.48	1.36	7.81E-04
HSD17B7	524.93	716.29	1.36	5.31E-04
BICD1	290.55	394.06	1.36	2.24E-04
TCEA1	1051.35	1427.66	1.36	4.50E-05
FAM106A	352.65	474.78	1.35	0.004
SSFA2	366.25	496.25	1.35	0.001
CCL3L1	3665.55	4957.23	1.35	9.56E-04
EDEM3	1354.23	1823.97	1.35	5.04E-04
DPM1	842.22	1126.14	1.34	0.008
KLHL6	1010.3	1357.64	1.34	0.007
AAAS	412.74	554.69	1.34	0.005
DOCK8	488.55	654.85	1.34	0.002
FAIM3	502.66	672.47	1.34	8.16E-04
ELMO1	1050.28	1403.05	1.34	7.21E-04
NARS	1169.41	1567.76	1.34	6.69E-04
HIVEP1	732.16	975.34	1.33	0.005
PNN	2074.1	2750.5	1.33	9.99E-04
C12orf45	861.63	1145.75	1.33	5.10E-05
XPR1	649.33	855.69	1.32	0.002
USP3	567.99	750.64	1.32	0.002
RAPGEF2	329.65	435.28	1.32	0.001
CALM3	366.16	478.61	1.31	0.009
GOPC	616.89	810.61	1.31	0.008
ABHD3	575.88	753.42	1.31	0.003
CDK13	385.27	505.68	1.31	0.003
AGPS	968.14	1271.59	1.31	0.002
KIAA1715	466.52	609.36	1.31	7.95E-04
NIF3L1	605.95	791.31	1.31	5.70E-04
PDCD4	845.36	1100.12	1.3	0.002
RQCD1	397.47	513.95	1.29	0.003
CPT2	538.88	695.58	1.29	4.48E-04
RPL36AL	2812.52	3613.56	1.28	0.001
CLIC4	1277.77	1639.22	1.28	1.30E-04
TMX1	1702.8	2153.85	1.26	4.82E-04
PDK1	2165.14	2673.11	1.23	3.59E-04

Table 3.3.2.1 Transcripts over-expressed in VDR compared to MM.1R. In total 353 transcripts exhibited a gene fold change >1.2 in VDR compared to MM.1R where $p \leq 0.01$.

G.O. ID	GO Term for Cellular Process	Gene Count	% of total	P Value
GO:0009057	Macromolecule Catabolic Process	34	9.66	5.724E-05
GO:0008104	Protein Localization	33	9.38	0.001
GO:0044265	Cellular Macromolecule Catabolic Process	32	9.09	7.884E-05
GO:0006508	Proteolysis	32	9.09	0.025
GO:0046907	Intracellular Transport	29	8.24	1.851E-04
GO:0010033	Response To Organic Substance	28	7.95	0.002
GO:0051603	Proteolysis Involved In Cellular Protein Catabolic Process	27	7.67	2.452E-04
GO:0044257	Cellular Protein Catabolic Process	27	7.67	2.647E-04
GO:0030163	Protein Catabolic Process	27	7.67	4.231E-04
GO:0015031	Protein Transport	27	7.67	0.007
GO:0045184	Establishment Of Protein Localization	27	7.67	0.008
GO:0042981	Regulation Of Apoptosis	27	7.67	0.014
GO:0043067	Regulation Of Programmed Cell Death	27	7.67	0.015
GO:0010941	Regulation Of Cell Death	27	7.67	0.016
GO:0007049	Cell Cycle	26	7.39	0.016
GO:0043632	Modification-Dependent Macromolecule Catabolic Process	24	6.82	0.002
GO:0019941	Modification-Dependent Protein Catabolic Process	24	6.82	0.002
GO:0016192	Vesicle-Mediated Transport	24	6.82	0.002
GO:0010605	Negative Regulation Of Macromolecule Metabolic Process	23	6.53	0.045
GO:0033554	Cellular Response To Stress	22	6.25	0.006
GO:0022402	Cell Cycle Process	21	5.97	0.012
GO:0044093	Positive Regulation Of Molecular Function	20	5.68	0.032
GO:0006915	Apoptosis	20	5.68	0.039
GO:0012501	Programmed Cell Death	20	5.68	0.045
GO:0006396	RNA Processing	19	5.40	0.032
GO:0019220	Regulation Of Phosphate Metabolic Process	18	5.11	0.021
GO:0051174	Regulation Of Phosphorus Metabolic Process	18	5.11	0.021
GO:0043085	Positive Regulation Of Catalytic Activity	18	5.11	0.038
GO:0070727	Cellular Macromolecule Localization	17	4.83	0.011
GO:0042325	Regulation Of Phosphorylation	17	4.83	0.030
GO:0034613	Cellular Protein Localization	16	4.55	0.022
GO:0043066	Negative Regulation Of Apoptosis	15	4.26	0.014
GO:0043069	Negative Regulation Of Programmed Cell Death	15	4.26	0.016
GO:0060548	Negative Regulation Of Cell Death	15	4.26	0.016
GO:0000278	Mitotic Cell Cycle	15	4.26	0.020
GO:0044092	Negative Regulation Of Molecular Function	14	3.98	0.020
GO:0045859	Regulation Of Protein Kinase Activity	14	3.98	0.025
GO:0043549	Regulation Of Kinase Activity	14	3.98	0.032
GO:0051338	Regulation Of Transferees Activity	14	3.98	0.042
GO:0034660	Norma Metabolic Process	13	3.69	0.003

G.O. ID	GO Term for Cellular Process	Gene Count	% of total	P Value
GO:0006511	Ubiquitin-Dependent Protein Catabolic Process	13	3.69	0.004
GO:0051726	Regulation Of Cell Cycle	13	3.69	0.040
GO:0006399	Trna Metabolic Process	12	3.41	2.897E-05
GO:0043086	Negative Regulation Of Catalytic Activity	12	3.41	0.027
GO:0051247	Positive Regulation Of Protein Metabolic Process	11	3.13	0.027
GO:0043161	Proteasomal Ubiquitin-Dependent Protein Catabolic Process	10	2.84	2.350E-04
GO:0010498	Proteasomal Protein Catabolic Process	10	2.84	2.350E-04
GO:0048193	Golgi Vesicle Transport	10	2.84	0.001
GO:0007346	Regulation Of Mitotic Cell Cycle	10	2.84	0.004
GO:0032940	Secretion By Cell	10	2.84	0.027
GO:0043039	Trna Aminoacylation	9	2.56	3.613E-06
GO:0006418	Trna Aminoacylation For Protein Translation	9	2.56	3.613E-06
GO:0043038	Amino Acid Activation	9	2.56	3.613E-06
GO:0051789	Response To Protein Stimulus	9	2.56	0.002
GO:0006887	Exocytosis	9	2.56	0.002
GO:0051186	Cofactor Metabolic Process	9	2.56	0.046
GO:0006986	Response To Unfolded Protein	8	2.27	0.001
GO:0006732	Coenzyme Metabolic Process	8	2.27	0.037
GO:0070647	Protein Modification By Small Protein Conjugation Or Removal	8	2.27	0.046
GO:0051351	Positive Regulation Of Ligase Activity	7	1.99	0.004
GO:0051340	Regulation Of Ligase Activity	7	1.99	0.006
GO:0010564	Regulation Of Cell Cycle Process	7	1.99	0.029
GO:0031400	Negative Regulation Of Protein Modification Process	7	1.99	0.035
GO:0051436	Negative Regulation Of Ubiquitin-Protein Ligase Activity During Mitotic Cell Cycle	6	1.70	0.010
GO:0031145	Anaphase-Promoting Complex-Dependent Proteasomal Ubiquitin-Dependent Protein Catabolic Process	6	1.70	0.010
GO:0051444	Negative Regulation Of Ubiquitin-Protein Ligase Activity	6	1.70	0.012
GO:0051352	Negative Regulation Of Ligase Activity	6	1.70	0.012
GO:0051437	Positive Regulation Of Ubiquitin-Protein Ligase Activity During Mitotic Cell Cycle	6	1.70	0.012
GO:0007229	Integrin-Mediated Signalling Pathway	6	1.70	0.014
GO:0051443	Positive Regulation Of Ubiquitin-Protein Ligase Activity	6	1.70	0.014
GO:0032386	Regulation Of Intracellular Transport	6	1.70	0.015
GO:0051439	Regulation Of Ubiquitin-Protein Ligase Activity During Mitotic Cell Cycle	6	1.70	0.015
GO:0031397	Negative Regulation Of Protein Ubiquitination	6	1.70	0.018
GO:0051438	Regulation Of Ubiquitin-Protein Ligase Activity	6	1.70	0.022
GO:0034097	Response To Cytokine Stimulus	6	1.70	0.023
GO:0031398	Positive Regulation Of Protein Ubiquitination	6	1.70	0.029
GO:0006865	Amino Acid Transport	6	1.70	0.037

G.O. ID	GO Term for Cellular Process	Gene Count	% of total	P Value
GO:0051640	Organelle Localization	6	1.70	0.040
GO:0048278	Vesicle Docking	5	1.42	0.002
GO:0022406	Membrane Docking	5	1.42	0.003
GO:0034976	Response To Endoplasmic Reticulum Stress	5	1.42	0.005
GO:0006984	ER-Nuclear Signalling Pathway	5	1.42	0.005
GO:0051783	Regulation Of Nuclear Division	5	1.42	0.027
GO:0007088	Regulation Of Mitosis	5	1.42	0.027
GO:0006892	Post-Golgi Vesicle-Mediated Transport	5	1.42	0.030
GO:0045454	Cell Redox Homeostasis	5	1.42	0.040
GO:0006739	NADP Metabolic Process	4	1.14	0.004
GO:0034620	Cellular Response To Unfolded Protein	4	1.14	0.009
GO:0030968	Endoplasmic Reticulum Unfolded Protein Response	4	1.14	0.009
GO:0006904	Vesicle Docking During Exocytosis	4	1.14	0.012
GO:0051053	Negative Regulation Of DNA Metabolic Process	4	1.14	0.045
GO:0046496	Nicotinamide Nucleotide Metabolic Process	4	1.14	0.048
GO:0006769	Nicotinamide Metabolic Process	4	1.14	0.048
GO:0048199	Vesicle Targeting, To, From Or Within Golgi	3	0.85	0.024
GO:0034612	Response To Tumour Necrosis Factor	3	0.85	0.028
GO:0045069	Regulation Of Viral Genome Replication	3	0.85	0.032

Table 3.3.2.2 Cellular processes in which genes over-expressed in VDR compared to MM.1R are involved (genes included demonstrate fold change >1.2 and p value ≤ 0.01). Functional annotation analysis via DAVID literature mining software revealed 96 cellular processes in which genes over-expressed in VDR vs. MM1R are involved, (where p value for strength of association <0.05). Note: “% genes” equals the number of genes involved in stated cellular process expressed as a percentage of total 353 genes up-regulated in VDR. (<http://david.abcc.ncifcrf.gov/>)

G.O. ID	Cellular Process	Gene Count	% Genes	P Value	Gene IDs
GO:0009057	Macromolecule Catabolic Process	34	9.66	5.724E-05	USP3, MLH1, NEDD8, EDEM3, EDEM1, ERLEC1, OS9, DCPS, PSMB5, G2E3, FBXW7, ARIH2, UFM1, CASP8, PPIL5, CTBS, ADAM9, HECTD1, AGA, RNASE6, UBE2Q2, ATM, WDR48, NCSTN, SENP2, MNAT1, PSMC6, PSMA6, PSME1, PSME2, PSMA3, KLHL12, FBXO34, BARD1
GO 0008104	Protein Localization	33	9.38	0.001	ALS2, OXA1L, PLDN, SNX6, AP1AR, HMP4A, NFKBIA, NEDD8, PDIA4, LMAN2, KLHL2, MUDENG, OS9, AP3M2, GOPC, PIKFYVE, TIMM9, TMED10, EXOC6, EXOC5, TINF2, SEC23A, SRP54, STAP1, PLEK, VPS41, STRADB, SENP2, SCFD1, RAB30, FBX034, COPG, F2R
GO:0044265	Cellular Macromolecule Catabolic Process	32	9.09	7.884E-05	USP3, MLH1, NEDD8, EDEM3, EDEM1, ERLEC1, OS9, DCPS, PSMB5, G2E3, FBXW7, ARIH2, UFM1, CASP8, PPIL5, ADAM9, HECTD1, RNASE6, UBE2Q2, ATM, WDR48, NCSTN, SENP2, MNAT1, PSMC6, PSMA6, PSME1, PSME2, PSMA3, KLHL12, FBXO34, BARD1
GO:0006508	Proteolysis	32	9.09	0.025	USP3, NEDD8, EDEM3, EDEM1, ERLEC1, OS9, PSMB5, G2E3, FBXW7, ARIH2, UFM1, PRSS2, CASP8, PPIL5, ADAM9, HECTD1, CFLAR, CR2, ADAM23, UBE2Q2, NCSTN, SENP2, WDR48, CASP10, PSMC6, PSMA6, PSME1, PSME2, PSMA3, KLHL12, FBXO34, BARD1

G.O. ID	Cellular Process	Gene Count	% Genes	P Value	Gene IDs
GO:0046907	Intracellular Transport	29	8.24	1.851E-04	ALS2, TMX1, PLDN, CPT2, SNX6, NFKBIA, BCL2L1, KLHL2, MUDENG, AP3M2, GOPC, PIKFYVE, TIMM9, TMED10, WIPF1, EXOC5, XPOT, SEC23A, PABPN1, SRP54, STAP1, VPS41, STRADB, WIPI1, SCFD1, AAAS, COPG, BAT1, F2R
GO:0010033	Response To Organic Substance	28	7.95	0.002	ME1, HMGC1, NFKBIA, CALCOCO2, NEDD8, ASNS, EDEM3, PMAIP1, BCL2L1, CCL5, EDEM1, ASAH1, PRKRA, CASP8, CREB3L2, IDH1, ERO1L, ADAM9, STRN3, HCLS1, CREB1, AARS, ACACA, HERPUD2, CD38, ERN1, NFE2L2, F2R
GO:0051603	Proteolysis Involved In Cellular Protein Catabolic Process	27	7.67	2.452E-04	USP3, NEDD8, EDEM3, EDEM1, ERLEC1, OS9, PSMB5, FBXW7, ARIH2, G2E3, UFM1, CASP8, PPIL5, ADAM9, HECTD1, UBE2Q2, NCSTN, SENP2, WDR48, PSMC6, PSME1, PSMA6, PSME2, PSMA3, KLHL12, FBXO34, BARD1
GO:0044257	Cellular Protein Catabolic Process	27	7.67	2.647E-04	USP3, NEDD8, EDEM3, EDEM1, ERLEC1, OS9, PSMB5, FBXW7, ARIH2, G2E3, UFM1, CASP8, PPIL5, ADAM9, HECTD1, UBE2Q2, NCSTN, SENP2, WDR48, PSMC6, PSME1, PSMA6, PSME2, PSMA3, KLHL12, FBXO34, BARD1

Table 3.3.2.3 Cellular processes in which genes over-expressed in VDR compared to MM.1R are involved (genes included demonstrate fold change >1.2, p value ≤ 0.01). Specific genes up-regulated in VDR compared to MM.1R and their association with specified cellular processes. Note: “% genes” equals

the number of genes involved in stated cellular process expressed as a percentage of total 353 genes up-regulated in VDR.
(<http://david.abcc.ncifcrf.gov/>)

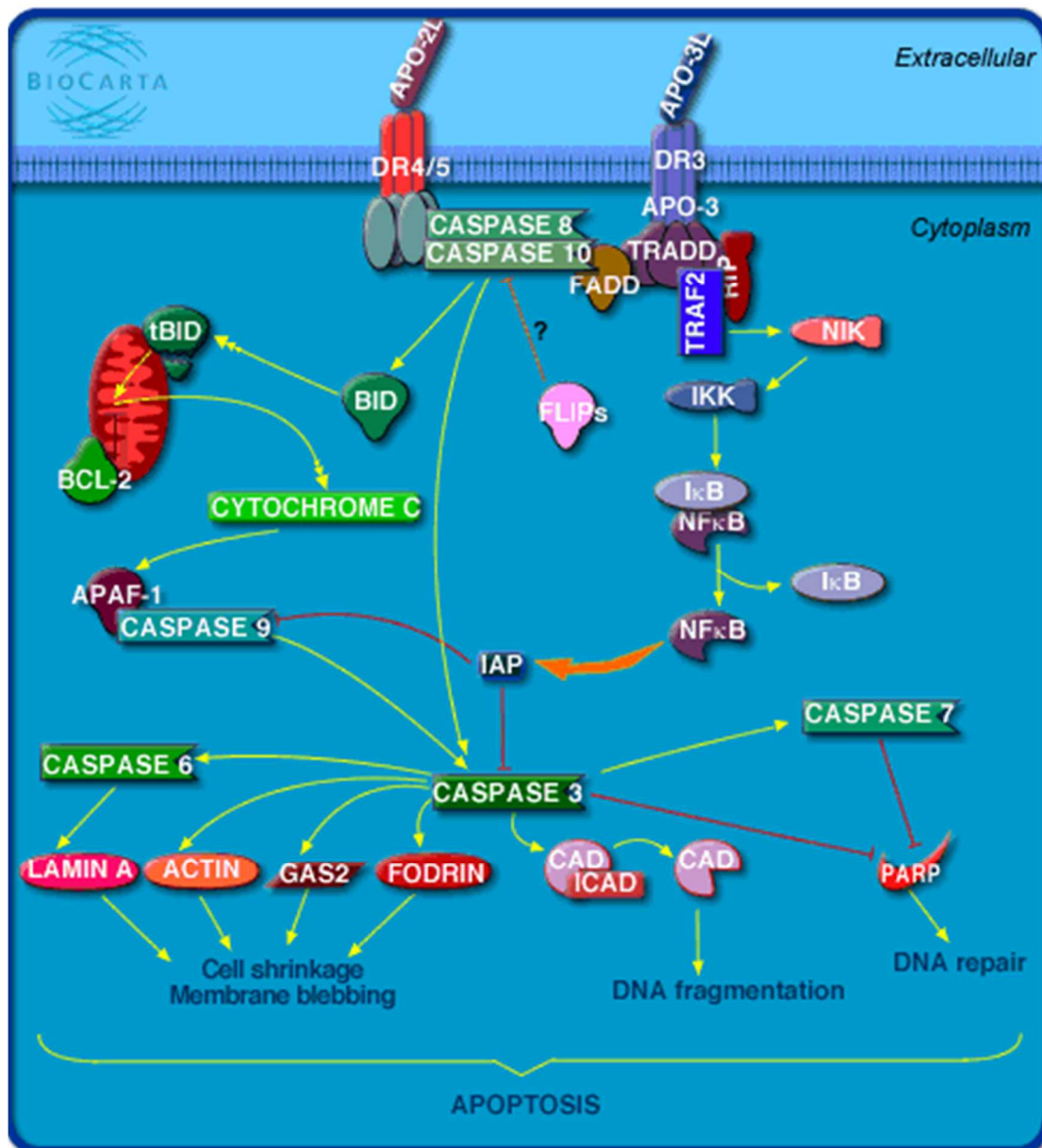


Figure 3.3.2.1 Genes up-regulated in VDR compared to MM.1R and their role in cellular apoptosis.

DAVID functional annotation tool revealed 4 genes up-regulated in VDR compared to MM.1R that share an intracytoplasmic role in cellular apoptosis. These transcripts include CFLAR, CASP8, CASP10 and NFKBIA.

(<http://david.abcc.ncifcrf.gov/>)

3.3.3 Transcripts downregulated in VDR compared to MM.1R

In contrast to the 353 transcripts upregulated in VDR compared to MM.1R, only 84 genes were downregulated in the resistant cell line compared to bortezomib-sensitive MM.1R. The difference in the number of genes upregulated compared to downregulated comparative analysis is unclear. It is not due to a difference in proliferation rate between the two cell lines as none is evident (results section 3.16). Again for all 84 genes downregulated in VDR cell line, the list includes only genes with a fold change difference <1.2 in VDR compared to MM.1R where p value ≤ 0.01 , (table 3.3.3.1).

Again the list of transcripts downregulated in VDR compared to MM.1R was analysed for their involvement in cellular processes in Homo Sapiens. Transcripts down-regulated in VDR are noted to participate in a number of cellular processes mainly concerned with the immune system for example antigen processing and presentation, immune response, T cell differentiation and T cell selection, (table 3.3.3.2).

Table 3.3.3.3 demonstrates a list of specific genes down-regulated in VDR compared to MM.1R and their association with specified cellular processes where by at least 5% of genes down-regulated in VDR are involved in a common cellular process. Genes listed here are involved in cellular process of antigen processing and presentation ($n=10$ genes or 11.9% of total genes, $p=3.98E-03$), or the immune response ($n=5$ genes or 5.95% of total genes, $p=5.61E-04$).

Finally figure 3.3.3.1 depicts the location of CD74 (CD74 molecule, MHC complex, class 2 invariant chain) and HLA-DRA (major histocompatibility complex, class 2, RD alpha) in the antigen processing and presentation pathway, both of which are also down-regulated in VDR compared to MM.1R.

Gene ID	MM.1R Mean Expression	VDR Mean Expression	Fold Change	P value
THEMIS	147.37	31.82	-4.63	0.01
ARHGEF6	337.95	74.04	-4.56	0.01
AHNAK	190.53	62.87	-3.03	1.29E-03
RNU4ATAC	453.17	153.06	-2.96	0.01
HLA-DPA1	710.08	251.09	-2.83	0.01
HLA-DRA	1274.44	473.54	-2.69	7.98E-04
CDH2	318.44	123.57	-2.58	0.01
HLA-DPB1	265.13	110.12	-2.41	0.01
C21orf99	177.36	73.77	-2.4	9.99E-04
CD74	2148.22	918.07	-2.34	1.12E-04
CD52	590.79	270.07	-2.19	4.89E-03
RPL31	406.9	189.37	-2.15	1.10E-05
SNCAIP	204.72	96.25	-2.13	1.39E-03
CASP6	271.51	129.27	-2.1	1.52E-03
NR3C1	298.54	148.13	-2.02	2.60E-03
CCDC99	1029.95	514.94	-2	5.16E-04
HBD	357.94	182.13	-1.97	0.01
ADAM28	324.18	165.96	-1.95	0.01
DHFR	1510.04	836.36	-1.81	0.02
FOLH1	381.36	215.43	-1.77	0.01
KDELC1	899.14	514.68	-1.75	6.82E-04
CCDC29	312.23	178.57	-1.75	7.58E-04
SULF1	508.46	290.37	-1.75	0.01
PEG10	724.45	417.18	-1.74	0.01
JAKMIP2	454.14	262.66	-1.73	0.01
LCP2	1066.65	618.98	-1.72	2.19E-04
TTC1	538.07	313.77	-1.71	1.59E-04
CHRNA5	361.11	210.98	-1.71	0.02
TEX15	371.39	220.38	-1.69	0.01
ANXA6	662.62	393.45	-1.68	4.29E-03
DUSP1	350.96	208.36	-1.68	0.02
CNN2	316.26	189.14	-1.67	0.02
GNPDA1	318.06	195.64	-1.63	3.82E-03
SPARC	298.09	189.23	-1.58	0.02
CLINT1	1229.64	790.27	-1.56	1.69E-04
LILRB4	457.61	294.73	-1.55	0.01
MAL2	782.55	510.6	-1.53	5.38E-04
YBX1P2	1180.96	771.65	-1.53	0.01
SNORD47	964.09	628.2	-1.53	0.01
TNFAIP3	637.85	415.79	-1.53	0.01
RASGRP3	1328.08	871.14	-1.52	1.08E-03
TCF4	396.83	261.57	-1.52	0.01
SLU7	299.57	198.61	-1.51	0.01
PTTG1	541.21	360.42	-1.5	2.96E-03
YIPF5	800.43	536.67	-1.49	1.97E-03

Gene ID	MM.1R Mean Expression	VDR Mean Expression	Fold Change	P value
HEMGN	432.9	289.71	-1.49	0.01
RPL26L1	505.79	344.62	-1.47	2.40E-03
SCARNA9	2711.77	1861.79	-1.46	0.03
MGAT5	341.12	233.13	-1.46	0.03
SLC9A9	406.55	280.62	-1.45	0.02
RARS	693.94	482.2	-1.44	0.02
AKT3	371.64	258.73	-1.44	0.02
SAMHD1	1702.67	1193.62	-1.43	1.63E-03
HAPLN4	402.91	282.61	-1.43	0.01
SNORD75	500.36	349.56	-1.43	0.02
LRRFIP1	878.74	617.46	-1.42	0.01
SSBP2	1153.5	816.48	-1.41	6.73E-04
EIF2AK2	1047.85	744.38	-1.41	1.22E-03
TRAM2	1126.94	801.62	-1.41	1.64E-03
MAF	803.15	569.52	-1.41	0.01
VIM	1566.36	1115.95	-1.4	2.05E-03
SLC17A7	4551	3265.07	-1.39	3.75E-03
C20orf103	757	549.81	-1.38	1.86E-03
ERGIC1	438.96	318.89	-1.38	1.97E-03
WBP1	738.53	533.3	-1.38	0.01
NBPF15	1655.5	1200.46	-1.38	0.01
RBM27	699.25	507.4	-1.38	0.03
FMN1	654.97	478.87	-1.37	4.18E-03
UBLCP1	470.02	343.63	-1.37	0.01
G3BP1	1085.28	789.47	-1.37	0.01
LARP1	637.13	464.03	-1.37	0.01
NFIL3	1328.63	969.84	-1.37	0.01
ACTG1	1057.05	769	-1.37	0.02
ARL6IP5	1527.02	1119.84	-1.36	6.57E-04
DOCK2	480.24	353.36	-1.36	0.01
UBE2E1	947.75	700.41	-1.35	4.64E-04
LOC51152	1332.27	983.73	-1.35	4.23E-03
IFNG	723.73	535.27	-1.35	0.02
ATP6V0E1	1311.93	982.19	-1.34	1.74E-04
BARX2	428.34	321.18	-1.33	1.83E-03
C7orf11	5095.03	3855.56	-1.32	2.81E-03
BASP1	527.27	401.79	-1.31	7.31E-04
SLC30A1	510.86	392.15	-1.3	1.19E-03
MGST3	1275.71	1013.36	-1.26	9.30E-05

Table 3.3.3.1 Transcripts down-regulated in VDR compared to MM.1R

84 transcripts were found to be down-regulated in bortezomib-resistant VDR compared to parental MM.1R.

G.O. ID	GO Term for Cellular Process	Gene Count	% Genes	P Value
GO:0006955	Immune Response	10	11.90	3.98E-03
GO:0019882	Antigen Processing And Presentation	5	5.95	5.61E-04
GO:0002504	Antigen Processing And Presentation Of Peptide Or Polysaccharide Antigen Via MHC Class II	4	4.76	4.53E-04
GO:0043383	Negative T Cell Selection	3	3.57	7.29E-04
GO:0043368	Positive T Cell Selection	3	3.57	7.29E-04
GO:0045058	T Cell Selection	3	3.57	3.36E-03
GO:0030217	T Cell Differentiation	3	3.57	0.04
GO:0031641	Regulation Of Myelination	2	2.38	0.03
GO:0045059	Positive Thymic T Cell Selection	2	2.38	0.03
GO:0019886	Antigen Processing And Presentation Of Exogenous Peptide Antigen Via MHC Class II	2	2.38	0.04
GO:0045060	Negative Thymic T Cell Selection	2	2.38	0.04
GO:0002495	Antigen Processing And Presentation Of Peptide Antigen Via MHC Class II	2	2.38	0.04
GO:0033574	Response To Testosterone Stimulus	2	2.38	0.04

Table 3.3.3.2 Pathway analysis of transcripts down-regulated in VDR compared to MM.1R. Down-regulated VDR transcripts are noted to participate in the cellular processes listed. Note: “% genes” equals the number of genes involved in stated cellular process expressed as a percentage of total 84 genes down-regulated in VDR. (<http://david.abcc.ncifcrf.gov/>)

G.O. Term ID	G.O. Term for Cellular Process	Gene Count	% of Total Genes	P Value	Gene IDs
GO:0006955	Immune Response	10	11.90	3.98E-03	THEMIS, LILRB4, IFNG, SAMHD1, HLA-DPA1, HLA-DPB1, NFIL3, CD74, HLA-DRA, LCP2
GO:0019882	Antigen Processing and Presentation	5	5.95	5.61E-04	IFNG, HLA-DPA1, HLA-DPB1, CD74, HLA-DRA

Table 3.3.3.3 Cellular processes in which genes down-regulated in VDR compared to MM.1R are involved (genes included demonstrated fold change >1.2, p value ≤ 0.01). List of specific genes down-regulated in VDR compared to MM.1R and their association with specified cellular processes where by at least 5% of genes down-regulated in VDR are involved in a common cellular process. (<http://david.abcc.ncifcrf.gov/>)

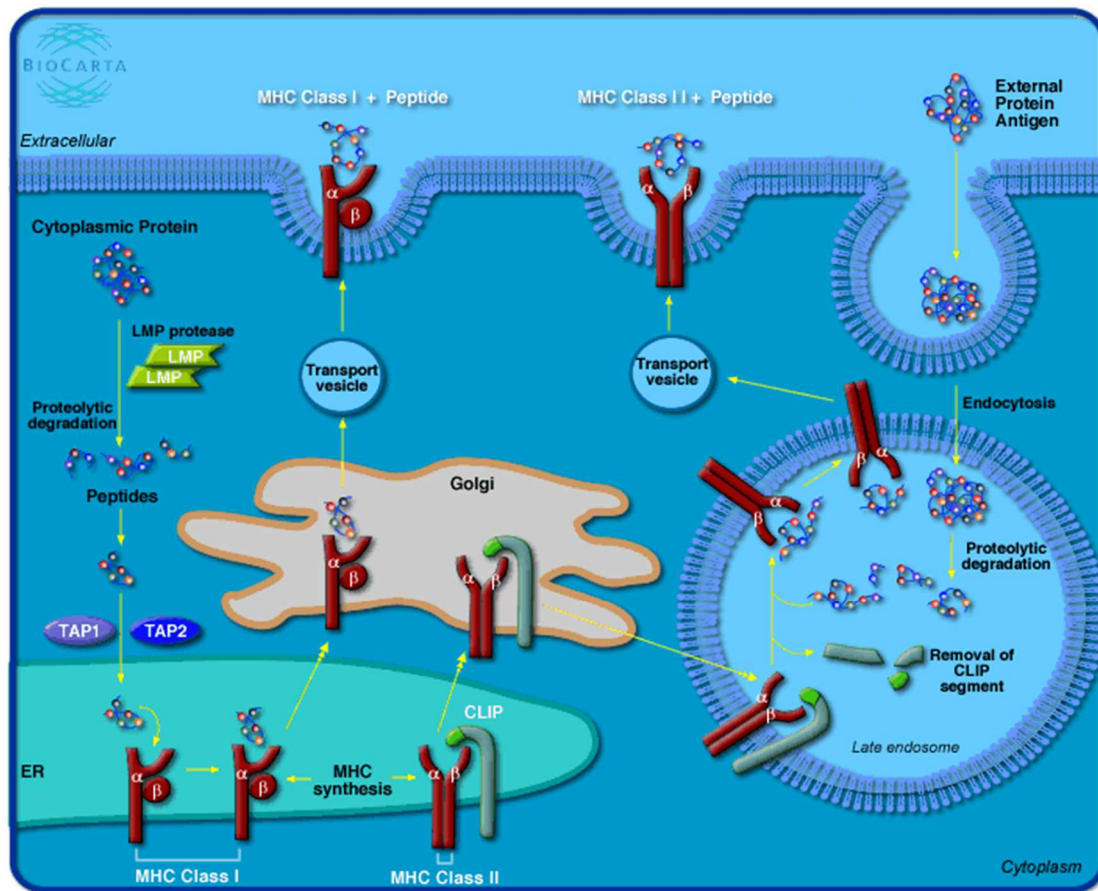


Figure 3.3.3.1 Transcripts down-regulated in VDR involved in the cellular process “Antigen Processing and Presentation”. 2 transcripts that were found to be down-regulated in VDR were identified in the DAVID functional annotation tool analysis as having known involvement in the process of antigen processing and presentation. These transcripts include CD74 (CD74 molecule, MHC complex, class 2 invariant chain) and HLA-DRA (major histocompatibility complex, class 2, RD alpha). (<http://david.abcc.ncifcrf.gov/>)

3.3.4 Identification of transcripts of interest for shRNA knockdown screening

Given the large number of genes over-expressed in VDR compared to MM.1R, an shRNA knockdown screen of genes upregulated in VDR was undertaken to determine which genes, following their shRNA knockdown, had the potential to desensitise VDR cells to bortezomib. The transcripts were selected from the list of genes up-regulated in VDR with fold change >1.2 (table 3.3.2.1).

The transcript selection process for targeted shRNA knockdown was conducted as follows (see table 3.3.4.1 for complete list):

1. We compared the following two lists: transcripts up-regulated in VDR vs. MM.1R compared to proteins up-regulated in VDR vs. MM.1R (see table 3.4.2.1 “Individual candidate biomarkers over-expressed in VDR vs. MM.1R identified by label-free mass spectrometry” for transcripts; for all proteins fold change>1.2 and p value <0.05). Genes and transcripts that were concordantly over-expressed at both the transcriptional and molecular level in VDR vs. MM.1R were selected for shRNA knockdown screening, (n=8).
2. Transcripts with at least > 2-fold mean expression in VDR versus MM.1R, (n=7).
3. From the list of transcripts up-regulated in VDR vs. MM.1R, we identified 3 target genes for which the chemical inhibitor of their molecular products are currently commercially available, (n=3).
4. Finally, 9 additional transcripts up-regulated in VDR vs. MM.1R were selected from the complete list of genes over-expressed in VDR vs. MM.1R, as shRNA constructs for hairpins for these genes were already available in the laboratory (n=9)

Gene Name	MM.1R Mean Expression	VDR Mean Expression	Fold Change	P Value
NEDD8	500.73	1051.85	2.1	7.03E-04
PSMB5	188.83	357.69	1.89	4.14E-04
HYOU1	222.19	383.48	1.73	1.18E-03
PSME1	659.04	1096.24	1.66	4.80E-04
HCLS1	668.57	1009.03	1.51	1.15E-03
PDIA4	945.12	1388.35	1.47	3.00E-04
PSME2	557.51	813.72	1.46	9.79E-04
PSAT1	253.07	919.7	3.63	3.00E-06
ALOX5AP	146.31	739.51	5.05	3.15E-04
CALCRL	27.95	133.59	4.78	2.54E-03
MYO1B	77.06	277.52	3.6	2.60E-05
FN1	155.65	536.13	3.44	5.00E-05
CX3CR1	167.41	553.23	3.3	9.00E-06
ALDH1L2	320.77	984.2	3.07	9.00E-06
PRSS2	98.9	234.49	2.37	3.40E-05
PIK3CG	1030.47	1534.82	1.49	3.21E-04
BCL2L1	392.78	562.77	1.43	1.04E-04
SLC7A11	195.74	793.65	4.05	4.00E-06
ASNS	635.94	1274.82	2	1.12E-04
SKAP1	128.12	240.13	1.87	5.82E-04
TINF2	189.14	354.1	1.87	1.70E-05
NFKBIA	267.86	492.65	1.84	2.12E-03
ERO1L	462.43	815.82	1.76	9.70E-05
CEP128	601.83	1041.27	1.73	1.17E-03
PRMT5	198.65	326.14	1.64	5.78E-04
RGS2	402.62	647.39	1.61	2.54E-04
SLC7A1	191.31	298.61	1.56	4.67E-04

Table 3.3.4.1 Transcripts over-expressed in VDR compared to MM.1R that were selected for shRNA knockdown screening.

Red= transcripts over-expressed in VDR with concordant up-regulation at the protein level in VDR (as identified by label-free mass spectrometry), compared to parental MM.1R respectively. (Expression level, fold change and p value stated represent those at the transcript level). (n=8)

Blue= transcripts with > 2-fold over-expressed in VDR vs. MM.1R. (n=7)

Wine= chemical inhibitors commercially available for the molecular product of these transcripts. (n=3)

Green= genes up-regulated in VDR vs. MM.1R where fold change >1.2 and p value ≤ 0.01 and constructs for these hairpins available in the lab (n=9)

3.3.5 Results of shRNA knockdown screen

As described above, 27 genes were selected for shRNA knockdown studies (Table 3.3.4.1). 5 different hairpins were utilised for knockdown of each specific gene. The shRNA knockdown screen was completed at the DFCI RNA Interference (RNAi) Screening Facility. Cells were plated at a density of 400×10^3 cells/mL in 384-well-plates, in the presence of polybrene, subsequently infected with lentiviral vectors and then selected using puromycin 2.5ug/mL (control wells). Additionally, duplicate plates were analysed for the response of VDR cells to bortezomib 50nM (the IC₂₀ for MM1VDR, for 24hrs) following shRNA knockdown with selected gene targets (see materials and methods section 2.13).

Table 3.3.5.1 lists target genes whereby shRNA knockdown of named gene and subsequent treatment with bortezomib 50nM resulted in >40% cell death (i.e. less than 60% cell viability) in VDR cells following their shRNA knockdown. Only genes whereby the latter criteria were fulfilled by 2 or > hairpins for a given gene are included. If ≤ 1 gene hairpin resulted in >40% cell death, these genes were not considered significant. 11 genes fulfilled these criteria.

Figure 3.3.5.1 depicts the percentage cell viability of VDR following shRNA knockdown of 11 genes listed in table 3.3.5.1 for each individual hairpin compared to empty vector or Lac-Z control vectors. 11 out of a total 27 genes resulted in >40% cell death of VDR cells following their shRNA knockdown with above named gene and subsequent treatment with bortezomib. Empty vector and Lac-Z served as controls.

Clone ID	Symbol	NCBI Gene ID	Relative % Cell Viability	SD
TRCN0000003920	PSMB5	5693	6.26	0.506
TRCN0000352618	PSMB5	5693	11.14	1.093
TRCN0000003916	PSMB5	5693	14.21	0.997
TRCN0000003919	PSMB5	5693	72.73	4.972
TRCN0000003917	PSMB5	5693	76.59	3.439
TRCN0000150510	ALDH1L2	160428	15.14	7.212
TRCN0000154597	ALDH1L2	160428	31.05	19.589
TRCN0000179462	ALDH1L2	160428	63.29	3.838
TRCN0000151018	ALDH1L2	160428	78.90	3.677
TRCN0000155970	ALDH1L2	160428	88.55	4.441
TRCN0000286357	FN1	2335	47.82	4.296
TRCN0000293840	FN1	2335	48.16	6.404
TRCN0000293839	FN1	2335	52.95	2.776
TRCN0000293790	FN1	2335	55.39	6.240
TRCN0000286356	FN1	2335	819.20	1502.732
TRCN0000430313	PIK3CG	5294	43.61	2.373
TRCN0000199330	PIK3CG	5294	44.21	5.673
TRCN0000195574	PIK3CG	5294	58.38	3.286
TRCN0000414541	PIK3CG	5294	73.25	5.201
TRCN0000196870	PIK3CG	5294	79.87	2.669
TRCN0000058080	PSME1	5720	47.10	2.490
TRCN0000307152	PSME1	5720	48.23	48.596
TRCN0000290074	PSME1	5720	54.97	0.851
TRCN0000290008	PSME1	5720	72.29	3.894
TRCN0000058082	PSME1	5720	81.02	3.429
TRCN0000033499	BCL2L1	598	34.09	2.682
TRCN0000299588	BCL2L1	598	50.09	6.195
TRCN0000299586	BCL2L1	598	72.83	7.909
TRCN0000033503	BCL2L1	598	95.52	15.252
TRCN0000033502	BCL2L1	598	96.14	5.331
TRCN0000430774	SKAP1	8631	33.30	4.725
TRCN0000006372	SKAP1	8631	54.91	1.093
TRCN0000006369	SKAP1	8631	83.12	1.281
TRCN0000416504	SKAP1	8631	90.96	5.039
TRCN0000435304	SKAP1	8631	107.99	5.851
TRCN0000010448	TINF2	26277	39.59	1.009
TRCN0000039988	TINF2	26277	48.09	3.268
TRCN0000218178	TINF2	26277	67.37	3.484
TRCN0000039990	TINF2	26277	76.79	2.344
TRCN0000230466	TINF2	26277	82.93	5.436

Clone ID	Symbol	NCBI Gene ID	Relative % Cell Viability	SD
TRCN0000078149	ALOX5AP	241	40.73	4.037
TRCN0000078150	ALOX5AP	241	46.14	3.451
TRCN0000078152	ALOX5AP	241	82.93	5.652
TRCN0000078151	ALOX5AP	241	95.38	5.026
TRCN0000078148	ALOX5AP	241	98.37	5.846
TRCN0000142061	CEP128	145508	42.04	4.316
TRCN0000141520	CEP128	145508	45.38	3.412
TRCN0000144988	CEP128	145508	72.10	3.371
TRCN0000145094	CEP128	145508	75.97	5.388
TRCN0000144220	CEP128	145508	82.62	3.343
TRCN0000356922	CX3CR1	1524	46.58	2.845
TRCN0000011309	CX3CR1	1524	52.63	5.111
TRCN0000356923	CX3CR1	1524	64.41	7.534
TRCN0000011312	CX3CR1	1524	74.70	3.289
TRCN0000356860	CX3CR1	1524	79.59	9.859
TRCN0000000000	EMPTY	-1	101.35	4.50
TRCN0000000000	EMPTY	-1	101.45	3.21
TRCN0000000000	EMPTY	-1	91.64	11.82
TRCN0000000000	EMPTY	-1	90.12	9.99
TRCN0000000000	EMPTY	-1	101.70	6.18
TRCN0000072240	lacZ	-15	93.14	7.02
TRCN0000072236	lacZ	-15	78.41	2.20
TRCN0000072242	lacZ	-15	84.85	2.75
TRCN0000072242	lacZ	-15	78.52	5.86
TRCN0000072236	lacZ	-15	85.73	10.27

Table 3.3.5.1 Results of shRNA knockdown screen. List of 5 hairpins/clone IDs for individual genes, NCBI gene ID, and relative cell viability of VDR cells following their shRNA knockdown with each individual hairpin and subsequent bortezomib treatment. Note: blue text represents shRNAs that when incorporated into VDR cells and VDR subsequently exposure to bortezomib 50nM for 24 hours, results in <60% cell viability of VDR cells (or >40% cell death). Relative cell viability of control (“empty” vector or lac Z also included).

Cell Viability Post-shRNA knockdown + Bortezomib Treatment

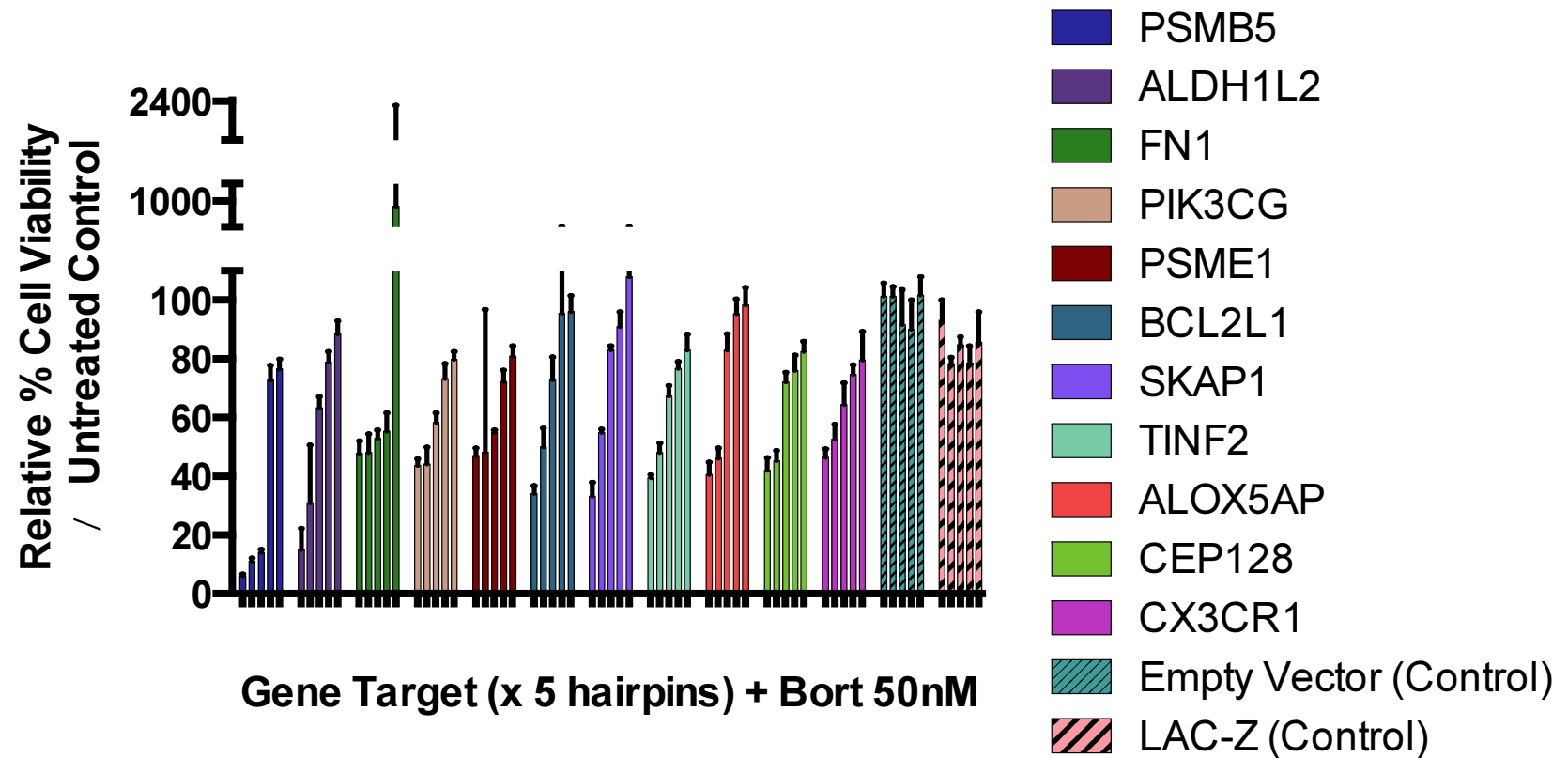


Figure 3.3.5.1 Relative cell viability of VDR cells following shRNA knockdown of select target genes and subsequent treatment with bortezomib 50nM for 24 hours. Figure depicts the percentage cell viability of VDR following shRNA knockdown of 11 genes or control genes (those listed in table 3.3.5.1) for each 5 individual hairpins divided by untreated control. In total, 11 out of 27 genes resulted in >40% relative cell death of VDR cells following their shRNA knockdown with above named gene and subsequent treatment with bortezomib. Empty vector and LAC-Z served as control genes and are also depicted here. (Note: “relative cell viability” here represents the percentage of treated MM cells divided by percentage of untreated MM cells.)

3.3.6 Validation of shRNA knockdown of PSMB5

Given the known inhibitory effect of bortezomib on PSMB5 specifically as it's major mode of cell death of myeloma cells, and the success of PSMB5 shRNA knockdown in resensitising VDR cells to bortezomib, we chose to validate this gene knockdown.

MM.1R and VDR cells again underwent shRNA knockdown of PSMB5 or control vector. First, cell lysates were collected following shRNA knockdown of PSMB5 or control vector, and immunoblot confirmed the successful shRNA knockdown of PSMB5 gene in MM.1R and VDR for PSMB5- associated hairpins E, F, G and H (see materials and methods 2.13), (Figure 3.3.6.1).

Figure 3.3.6.2 depicts the cell viability of MM1R and VDR following PSMB5 knockdown with control hairpins or PSMB5 hairpins and subsequent bortezomib treatment (0-20nM). In MM.1R, shRNA knockdown did not alter sensitivity to bortezomib. In VDR, shRNA knockdown of PSMB5-hairpins E, H and G followed by treatment with bortezomib 20nM and 40nM resulted in significant increase in cell death of VDR cells compared to controls.

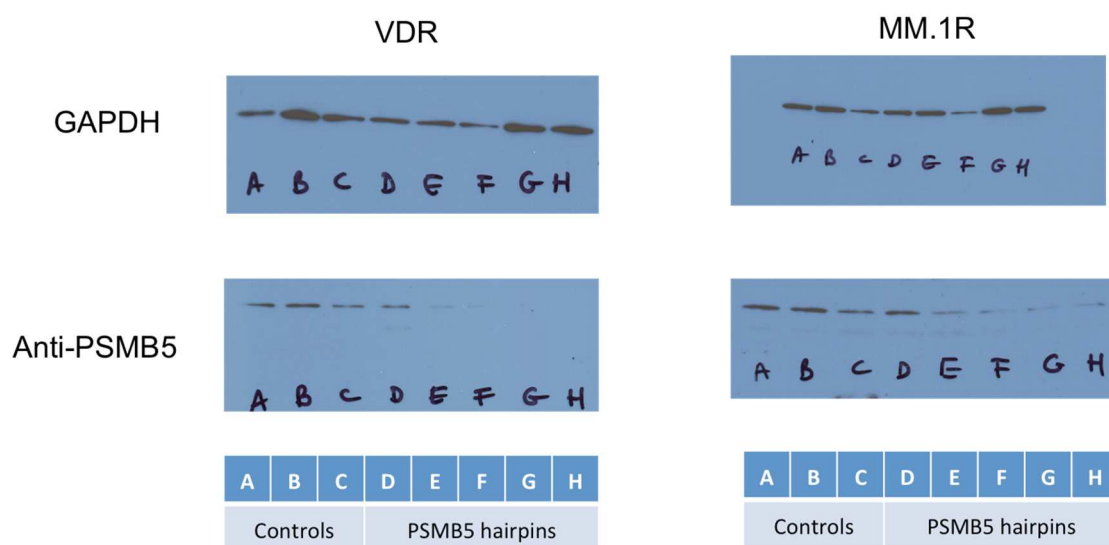
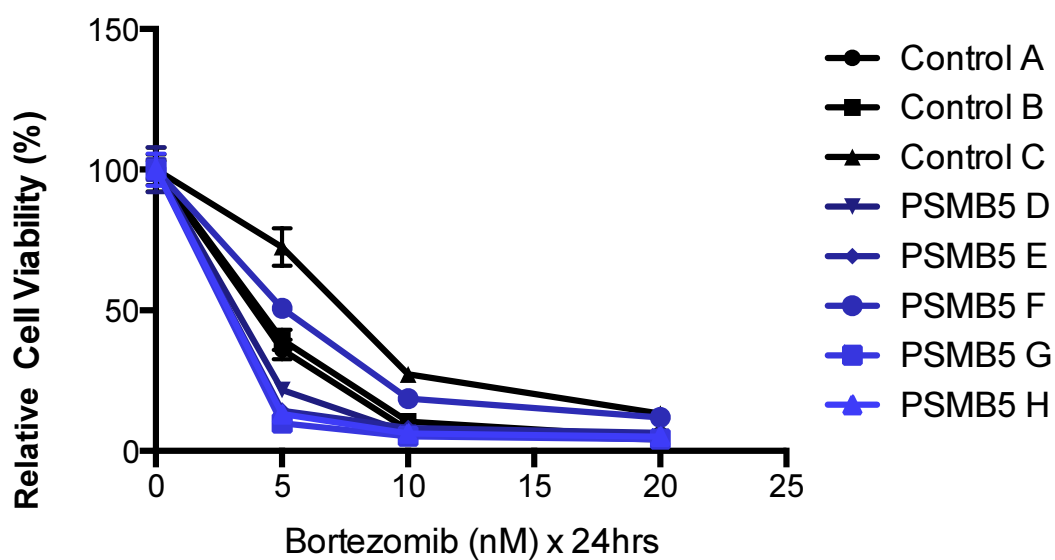


Figure 3.3.6.1: Validation of knockdown of PSMB5 in MM1R and VDR by Western Blot. MM.1R and VDR cell lysates were probed with anti-GAPDH (Control) and PSMB5 antibody and developed on film via chemiluminescence, which confirmed successful shRNA knockdown of PSMB5 gene in MM.1R and VDR for PSMB5- associated hairpins E, F, G and H.

(A)

MM.1R following shRNA knockdown



(B)

VDR following shRNA knockdown

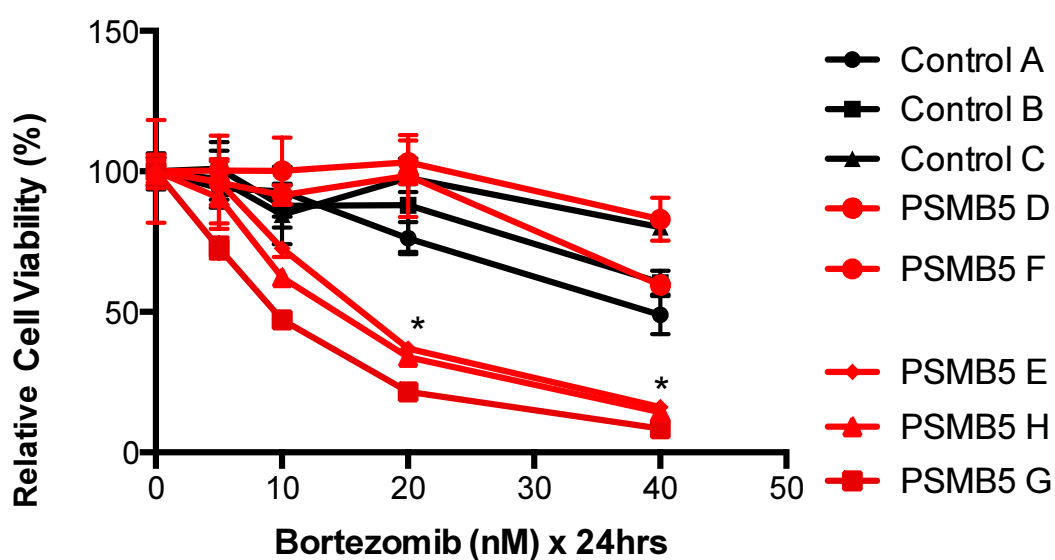


Figure 3.3.6.2: Cell viability of VDR and MM1R following PSMB5 knockdown post-bortezomib treatment. (A) In MM.1R, shRNA knockdown did not alter sensitivity to bortezomib. **(B)** In VDR, shRNA knockdown of PSMB5-hairpins E, H and G followed by treatment with bortezomib 20nM and 40nM resulted in significant increase in cell death of VDR cells compared to controls. (Note: *= $p < 0.05$ for PSMB5 hairpins E, G, H compared to control vector).

3.3.7 Conclusion of gene expression profiling studies

In summary, 20,724 genes were evaluated in MM1R versus VDR cell lines. Genes whereby fold change between the two conditions was >1.2 and demonstrated a p value ≤ 0.01 , of which 437 transcripts fulfilled this criteria, were included for further studies. 353 were over-expressed in VDR compared to MM.1R. In comparison only 84 genes were down-regulated in VDR compared to MM.1R. The reasoning for the discrepancy between number of genes up-regulated versus down-regulated is unclear.

Pathway analysis again via DAVID functional annotation tool revealed “cellular apoptosis” as a specific pathway in which 4 transcripts up-regulated in VDR play a role. These genes include CFLAR, CASP8, CASP10, and NFKBIA. By comparison, VDR transcripts that were down-regulated compared to MM.1R were noted to participate in a number of cellular processes mainly concerned with the immune system for example antigen processing and presentation, immune response, T cell differentiation and T cell selection, with specific attention to the antigen-presenting pathway that involved CD74 and HLA-DRA.

A number of specific genes were selected for an shRNA knockdown screen, that included transcripts over-expressed in VDR with concordant up-regulation at the protein level in VDR (as identified by label-free mass spectrometry), transcripts with > 2 -fold over-expressed in VDR vs. MM.1R, transcripts whereby chemical inhibitors are currently commercially available for the molecular product of these transcripts, and a set of transcripts for which shRNAs were available were selected from the complete list of all genes up-regulated in VDR vs. MM.1R where fold change >1.2 and p value ≤ 0.01 . Of 27 genes investigated in the shRNA screen, which involved shRNA knock down of a specific target, with 5 hairpins in use for each target individually, 11 genes were found to, following shRNA knockdown and subsequent treatment with bortezomib (IC_{20}), result in $>40\%$ cell death of VDR cells compared to control hairpins.

Given that bortezomib specifically binds PSMB5 in myeloma cell lines and thus induces cell death secondary to inhibition of the proteasome pathway, we chose

to further validate the role of PSMB5 knockdown in resensitisation of VDR cells to bortezomib. First we demonstrated successful shRNA knockdown of PSMB5 in MM.1R and VDR by immunoblot. Secondly, we demonstrated that shRNA knockdown of PSMB5 and subsequent treatment of VDR cells (used at even lower concentrations of bortezomib compared to initial screen: 50nM vs. 20-40nM), resulted in significant resensitisation of VDR to bortezomib.

Our validation studies were somewhat limited by the technical challenge of shRNA knockdown of semi-adherent cell lines, which when not adherent to the surface of the tissue culture flask, prove to be much more difficult to successfully infect with lentivirus and then subsequent selection initially resulted in cell death of almost all cells. We overcame this difficulty by centrifuging the tissue culture plates following infection with lentivirus for 30 minutes post-infection, to allow both virus and cells to adhere to the base of the plates.

Future work could include validation studies of the remaining 10 genes that, following their shRNA knockdown, resulted in a marked increase in sensitivity to bortezomib in otherwise bortezomib-resistant VDR cells.

3.4 PROTEOMIC PROFILE OF MM.1R AND VDR BY LABEL-FREE MASS SPECTROMETRY

3.4.1 Introduction

The role of gene expression profiling in MM patients for number of years as a highly valued predictor of clinical outcome and response to therapy has been well documented.^[115, 116] More recently, advances in determining the proteomic profile of MM patients by label-free mass spectrometry has provided the field of haematology research with insight into biomarkers predicting response to therapy.^[117] Therefore we next examined the proteomic profiles of the isogenic cell lines MM.1R and VDR, in addition to investigating the proteins differentially expressed following their treatment with bortezomib.

We incubated MM.1R or VDR cells at equal cell densities over-night to allow the cells to adhere and subsequently exposed them to bortezomib 40nM for 8 hours in culture (or media only was added to the controls). Subsequently all conditions were collected, counted and stored as cell pellets at -80°C in preparation for label-free mass spectrometry (see Materials and Methods 2.15). We first compared the proteomic profiles of MM.1R vs. VDR without drug treatment, next each cell line following bortezomib treatment compared to its respective control, and finally comparison of both cell lines following bortezomib treatment (see table 3.4.1.1 for overview of comparative analyses).

Comparative Analyses		
MM.1R	vs.	VDR
MM.1R	vs.	MM.1R + bortezomib
VDR	vs.	VDR + bortezomib
MM1R + bortezomib	vs.	VDR + bortezomib

Table 3.4.1.1 Comparative analyses following label-free mass spectrometry. The conditions used for comparative analysis of VDR with and without bortezomib treatment compared to respective MM.1R controls, that allowed us determine which proteins were differentially expressed in the comparisons outlined in this table.

3.4.2 Proteins over-expressed in VDR vs. MM.1R

3.4.2.1 Individual proteins over-expressed in VDR vs. MM.1R

We identified 238 proteins differentially expressed in the MM.1R vs. VDR comparison. Of these, 106 proteins had the highest expression level in VDR compared to MM.1R ($p < 0.05$), of which 36 of these had a fold change > 2 (table 3.4.2.1). Two proteins displayed very high protein fold changes in VDR compared to MM.1R (> 200 fold change for each, $p < 0.05$). These included:

- (a) Ubiquitin-conjugating enzyme E2 N (UBE2N/ Ubc13) displayed a 433-fold change increase in VDR ($p = 0.04$). This protein plays a major role in protein polyubiquitination in preparation for degradation, in addition to activation of NF- κ B *in vitro*. A small molecule inhibitor specifically targeting this protein is presently commercially available and has been shown to be a successful anti-tumour agent in diffuse large B cell lymphoma *in vitro*.^[118] However, it is important to note that the baseline expression level of this protein was almost zero in MM.1R, and thus the high protein fold change detected in VDR is potentially misleading as UBE2N levels are low also in VDR at baseline in comparison to other molecules detected by this method of quantification of protein abundance.
- (b) SH3 domain-binding glutamic acid-rich-like protein 3 (SH3BGRL3) had a 215-fold increase in VDR vs. MM.1R ($p = 0.04$), an anti-apoptotic molecule that safeguards both normal and cancer cells from tumour-necrosis-factor (TNF)-induced apoptosis.^[119] On review of the raw data of protein abundance, SH3BGRL3 has a very low expression level in MM.1R and markedly high expression levels in VDR, similar to the baseline expression levels of most proteins within this analysis, thereby encouraging the validity of this result.

In relation to both proteins UBE2N and SH3BGRL3, an alternative explanation for the very high fold change observed in VDR may be that these proteins are not expressed at all in MM.1R however are expressed in VDR, which in contrast suggests a high potential for this protein in bortezomib resistance in VDR. Initial

examination into whether or not these proteins are implicated in bortezomib pathogenesis in VDR should be first initiated by validating their expression levels by immunoblot.

CCL3/MIP1- α (C-C motif ligand 3/ macrophage inflammatory protein 1-alpha) was over-expressed in VDR compared to MM.1R with a 22-fold change ($p=0.013$). CCL3 has been well documented previously in its role as a stimulator of osteoclastogenesis, inhibition of osteoblastogenesis, and thus its contribution to myelomatous bone disease.^[85, 120] This protein is highly expressed in myeloma cell lines and an inhibitor of CLL1, through which CCL3, is signals in currently in pre-clinical investigation and has shown promising anti-myelomatous and anti-osteolytic effects in a MM *in vivo* mouse model.^[121] In the setting of the bone marrow microenvironment *in vivo*, CCL3 could potentially markedly augment the proliferation capacity and pro-osteolytic activity of VDR cells given its marked over-expression compared to bortezomib sensitive MM.1R.

In addition, other proteins which are well known for their role in MM pathogenesis, for example NEDD8, were found to be over-expressed 2.1-fold in VDR ($p=0.003$). The success of NEDD8 inhibition by its selective inhibitor, MLN4924 has been well documented and is now in phase 1 clinical trials for relapsed/refractory MM and lymphoma. ^[34] In addition, PSMB5 protein had a 3.8-fold increase expression level in VDR vs. MM.1R ($p=0.0004$).

Accession	Confidence score	Anova (p)	Max. fold change	Uniprot Symbol
P61088	103.07	0.048	433.75	UBE2N
Q9H299	35.23	0.048	215.94	SH3BGRL3
P10147	51.45	0.013	22.89	CCL3
Q9Y4L1	194.58	0.026	14.12	HYOU1
Q9BVA1	1284.26	0.001	8.17	TUBB2B
P62304	36.51	0.028	7.30	SNRPE
P04792	105.07	0.009	6.48	HSPB1
Q9UKY7	295	0.026	5.46	CDV3
P28074	229.32	4.36E-04	3.85	PSMB5
P54868	41.02	1.84E-04	3.71	HMGCS2
Q14697	181.31	0.046	3.44	GANAB
P14314	132.46	0.043	3.17	PRKCSH
P13667	450.83	0.024	3.06	PDIA4
P55327	106.56	0.022	2.80	TPD52
Q9Y2X3	70.75	0.004	2.77	NOP58
P11021	1044.05	0.041	2.73	HSPA5
P07237	643.13	0.031	2.71	P4HB
P62333	31.69	0.001	2.59	PSMC6
Q86V88	48.62	0.005	2.46	MDP1
Q12906	155.64	0.013	2.42	ILF3
P54819	84.55	0.021	2.39	AK2
P28070	162.73	0.001	2.36	PSMB4
Q15084	173.87	0.050	2.31	PDIA6
P08670	199.19	0.046	2.29	VIM
Q8NBS9	491.28	0.046	2.22	TXNDC5
P63241	222.76	0.008	2.21	EIF5A
Q00688	91.4	0.001	2.20	FKBP3
Q14061	90.99	0.033	2.18	COX17

Accession	Confidence score	Anova (p)	Max. fold change	Uniprot Symbol
P10809	942.81	0.010	2.16	HSPD1
P27797	167.72	0.049	2.14	CALR
Q15843	50.64	0.004	2.14	NEDD8
Q9UL46	514.43	1.51E-04	2.11	PSME2
P61604	235.75	0.001	2.07	HSPE1
Q9BY43	118.65	0.001	2.06	CHMP4A
O75874	97.43	0.003	2.02	IDH1
P62937	840.02	0.009	2.00	PPIA

Table 3.4.2.1 Individual candidate biomarkers over-expressed in VDR vs. MM.1R identified by label-free mass spectrometry. 106 proteins were over-expressed in VDR compared to parental MM.1R and those with protein fold change ≥ 2 are shown ($p < 0.05$). UBE2N and SH3BGRL3 are markedly over-expressed in VDR compared to MM.1R. NEDD8 and PSMB5, as anticipated, are also over-expressed in the VDR cell line.

3.4.2.2 Functional protein-association mapping of proteins over-expressed in VDR vs. MM.1R

In addition, functional protein association mapping of proteins with known direct interactions as demonstrated by STRING networking ("Search Tool for the Retrieval of Interacting Genes/Proteins", <http://string-db.org/>) revealed the heat shock proteins (HSP) (HSPB1, HSPE1, HSPD1, HSPA5) as a highly interactive group of potential biomarkers that were over-expressed in VDR compared to MM.1R, that had direct protein-to-protein interactions with a number of other molecules that were concomitantly over-expressed in VDR (figure 3.4.2.2.1). The heat shock proteins have been well documented for their role in MM pathogenesis and specific inhibitors of HSP90AA1 (heat shock 90kDa AA1) protein have completed phase 1 clinical trials.^[122-125] HSP90AA1 itself was not identified as having statistically significant over-expression in VDR, however over-expression of HSPE1, HSPD1 and HSPD5, which interact with HSP90AA1 was observed (see figure 3.4.2.2.2 for interaction modelling).

Using the DAVID functional annotation tool (<http://david.abcc.ncifcrf.gov/>) a number of proteins over-expressed in VDR compared to MM.1R were involved in a number of cellular processes implicated in the pathogenesis of malignancy including regulation of apoptosis, regulation of cellular metabolic processes, cellular homeostasis, cell cycle process, and proteasomal ubiquitin-dependent protein catabolic process, adjusted p value <0.05 (table 3.4.2.2.1).

Finally, 4 proteins that have established involvement in the proteasome-ubiquitination pathway are displayed in Figure 3.4.2.2.3, which again are over-expressed in VDR compared to MM.1R by label-free mass spectrometry (with fold change >2, p<0.05) were found to be involved in the proteasome-ubiquitination pathway, and these include PSME2, PSMC6, PSMB4 and PSMB5.

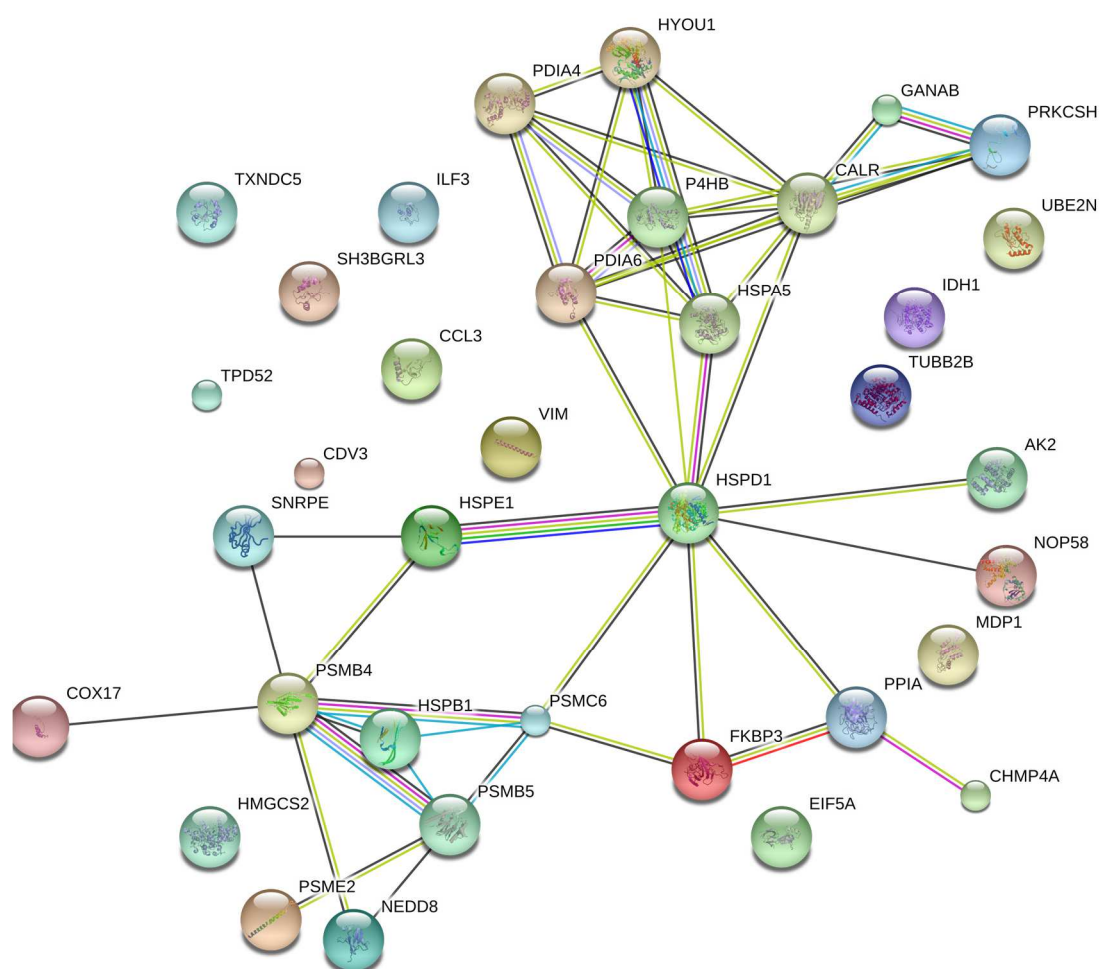


Figure 3.4.2.2.1 Overview of proteins over-expressed in VDR compared to MM.1R.

A number of proteins demonstrated statistically significant over-expression in VDR compared to MM.1R. Functional protein association mapping of proteins with known direct interactions as demonstrated by STRING networking revealed the heat shock proteins (HSPB1, HSPE1, HSPD1, HSPA5) as highly interactive group of biomarkers that were over-expressed in VDR compared to MM.1R, that had direct protein-to-protein interactions with a number of other molecules that were concomitantly over-expressed in VDR, (www.string-db.org).

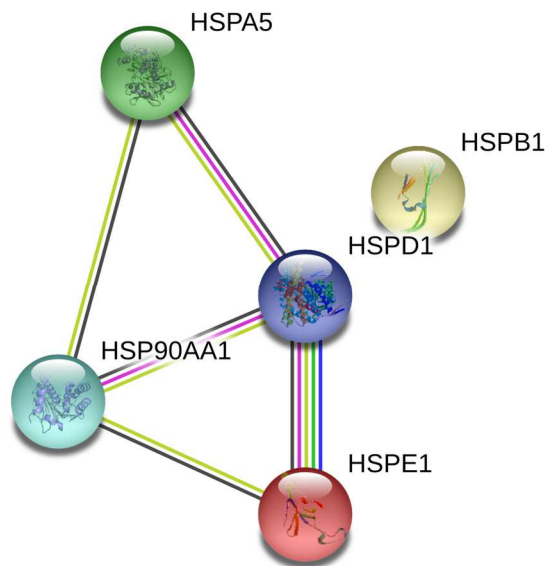


Figure 3.4.2.2.2 Known interactions of heat shock proteins

While HSP90AA1 was not detected in our list of proteins over-expressed in VDR, 3 heat shock proteins that are known to interact with HSP90AA1 were over-expressed in VDR compared to MM.1R. These include HSPE1, HSPD1 and HSPA5, (www.string-db.org).

Cellular Process	Protein Count	Adjusted p value (Benjamini)
Protein folding	6	0
Positive regulation of ligase activity	5	0
Regulation of ubiquitin-protein ligase activity	5	0
Regulation of ligase activity	5	0
Positive regulation of protein ubiquitination	5	0
Regulation of cellular protein metabolic process	8	0.01
Positive regulation of cellular protein metabolic process	6	0.01
Positive regulation of protein metabolic process	6	0.01
Cell redox homeostasis	5	0.01
Positive regulation of ubiquitin-protein ligase activity	5	0.01
Regulation of protein ubiquitination	5	0.01
Cellular homeostasis	7	0.02
Negative regulation of cellular protein metabolic process	5	0.02
Positive regulation of protein modification process	5	0.02
Negative regulation of protein metabolic process	5	0.02
Anaphase-promoting complex-dependent proteasomal ubiquitin-dependent protein catabolic process	4	0.02
Negative regulation of ubiquitin-protein ligase activity during mitotic cell cycle	4	0.02
Negative regulation of ubiquitin-protein ligase activity	4	0.02
Negative regulation of ligase activity	4	0.02
Positive regulation of ubiquitin-protein ligase activity during mitotic cell cycle	4	0.02
Regulation of ubiquitin-protein ligase activity during mitotic cell cycle	4	0.02
Negative regulation of protein ubiquitination	4	0.02
Positive regulation of catalytic activity	7	0.03
Cell cycle process	7	0.04
Proteasomal protein catabolic process	4	0.04
Proteasomal ubiquitin-dependent protein catabolic process	4	0.04

Table 3.4.2.2.1 Proteins over-expressed in VDR vs. MM.1R that are involved in a common cellular processes as demonstrated by DAVID functional annotation tool.

Proteins over-expressed in VDR compared to MM.1R are involved in a number of cellular processes including regulation of apoptosis and regulation of protein ubiquitination (adjusted p value <0.05). (*david.abcc.ncifcrf.gov*).

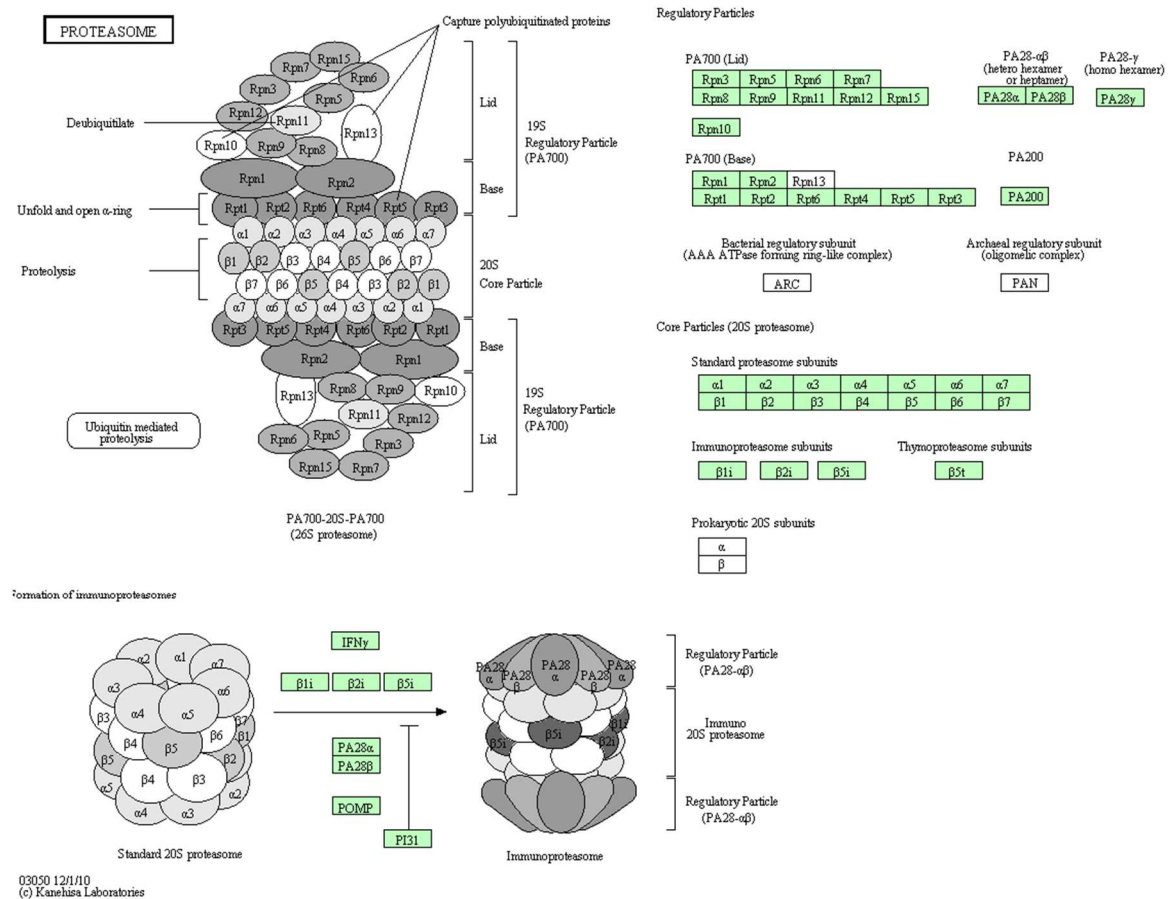


Figure 3.4.2.2.3: A number of proteins over-expressed in VDR compared to MM.1R by label-free mass spectrometry (with fold change >2, p<0.05) were found to be involved in the proteasome-ubiquitination pathway. These proteins include PSME2, PSMC6, PSMB4 and PSMB5. (*david.abcc.ncifcrf.gov*).

3.4.3 Proteins down-regulated in VDR compared to MM.1R

We found 238 proteins in total differentially expressed in the MM.1R vs. VDR comparison. Of these 132 were down-regulated in VDR compared to MM.1R, of which 44 had a fold change ≥ 1.5 where $p < 0.05$ (table 3.4.3.1).

Three proteins that were found to be down-regulated in VDR compared to MM.1R at the protein level by label-free mass spectrometry (fold change > 2 , $P < 0.05$) were found to be involved in aminoacyl tRNA biosynthesis. These proteins include IARS (isoleucyl-tRNA synthetase), RARS (arginyl-tRNA synthetase) and LARS (leucyl-tRNA synthetase), (figure 3.4.3.1).

Finally we additionally examined both proteins up-regulated and down-regulated in VDR compared to MM.1R using DAVID functional annotation tool to determine which cellular pathways are involved in the complete list of statistically significant proteins both over-expressed and down-regulated in VDR compared to MM.1R. Table 3.4.3.2 lists the cellular processes potentially perturbed in VDR, either secondary to their over-expression or down-regulation compared to MM.1R. These processes involved the mitotic cell process, negative regulation of protein metabolic and protein modification processes, and both positive and negative regulation of ubiquitination.

Accession	Confidence score	Anova (p)	Max fold change	Uniprot
P50224	51.33	7.85E-04	15.95	SULT1A3
Q09666	513.52	2.60E-06	7.12	AHNAK
Q9Y5X3	79.17	0.01	3.24	SNX5
P82970	42.85	1.94E-04	3.10	HMG5
P46926	116.08	0.01	2.53	GNPDA1
P24941	95.46	0.04	2.31	CDK2
Q53GG5	44.86	8.29E-04	2.24	PDLIM3
P78347	61.60	0.03	2.15	GTF2I
O75461	30.94	3.12E-04	2.01	E2F6
P41252	295.37	3.22E-04	1.93	IARS
P21333	3263.52	4.63E-04	1.90	FLNA
P48539	206.65	0.01	1.90	PCP4
O14974	128.16	2.26E-03	1.89	PPP1R12A
P54136	213.18	3.96E-04	1.86	RARS
Q9H4M9	80.51	0.01	1.85	EHD1
P36405	90.34	0.03	1.83	ARL3
P51965	56.16	2.43E-03	1.80	UBE2E1
P09525	40.73	0.05	1.79	ANXA4
P80723	211.18	1.10E-03	1.79	BASP1
P11413	92.65	0.01	1.79	G6PD
O15247	82.44	1.28E-03	1.78	CLIC2
P78417	172.01	0.01	1.77	GSTO1
Q9P2J5	325.70	9.78E-04	1.74	LARS
Q32MZ4	184.84	0.02	1.74	LRRFIP1

Accession	Confidence score	Anova (p)	Max fold change	Uniprot
P50224	51.33	7.85E-04	15.95	SULT1A3
Q09666	513.52	2.60E-06	7.12	AHNAK
Q9Y5X3	79.17	0.01	3.24	SNX5
P82970	42.85	1.94E-04	3.10	HMG5
P46926	116.08	0.01	2.53	GNPDA1
P24941	95.46	0.04	2.31	CDK2
Q53GG5	44.86	8.29E-04	2.24	PDLIM3
P78347	61.60	0.03	2.15	GTF2I
O75461	30.94	3.12E-04	2.01	E2F6
P41252	295.37	3.22E-04	1.93	IARS
P21333	3263.52	4.63E-04	1.90	FLNA
P48539	206.65	0.01	1.90	PCP4
O14974	128.16	2.26E-03	1.89	PPP1R12A
P54136	213.18	3.96E-04	1.86	RARS
Q9H4M9	80.51	0.01	1.85	EHD1
Q99439	129.52	1.37E-03	1.71	CNN2
Q8IXM2	177.80	2.06E-03	1.66	BAP18
Q5JTH9	46.25	0.01	1.66	RRP12
Q9Y3Z3	155.89	2.04E-03	1.63	SAMHD1
Q14320	212.18	2.83E-03	1.62	FAM50A
O43598	120.27	0.01	1.62	RCL
Q5VW32	50.81	0.01	1.60	BROX
Q13576	67.22	1.76E-03	1.60	IQGAP2
P36873	123.85	0.01	1.60	PPP1CC
P78406	67.08	0.02	1.59	RAE1

Accession	Confidence score	Anova (p)	Max fold change	Uniprot
P50224	51.33	7.85E-04	15.95	SULT1A3
Q09666	513.52	2.60E-06	7.12	AHNAK
Q9Y5X3	79.17	0.01	3.24	SNX5
P82970	42.85	1.94E-04	3.10	HMG5
P46926	116.08	0.01	2.53	GNPDA1
P24941	95.46	0.04	2.31	CDK2
Q53GG5	44.86	8.29E-04	2.24	PDLIM3
P78347	61.60	0.03	2.15	GTF2I
O75461	30.94	3.12E-04	2.01	E2F6
P41252	295.37	3.22E-04	1.93	IARS
P21333	3263.52	4.63E-04	1.90	FLNA
P48539	206.65	0.01	1.90	PCP4
O14974	128.16	2.26E-03	1.89	PPP1R12A
P54136	213.18	3.96E-04	1.86	RARS
Q9H4M9	80.51	0.01	1.85	EHD1
O43252	81.58	0.01	1.56	PAPSS1
Q9UM54	64.55	0.01	1.55	MYO6
P35659	226.23	0.01	1.55	DEK
Q9NT62	45.03	0.02	1.53	ATG3
Q08209	62.44	2.75E-03	1.53	PPP3CA
P30041	390.10	0.02	1.52	PRDX6
P08133	914.79	1.36E-03	1.51	ANXA6
P52701	30.94	2.76E-03	1.51	MSH6
Q9NR46	61.24	0.03	1.50	SH3GLB2
Q96C23	247.61	0.02	1.50	GALM

Table 3.4.3.1 Proteins down-regulated in VDR compared to MM.1R by label free mass spectrometry. 44 proteins were down-regulated in VDR compared to MM.1R with a fold change ≥ 1.5 ($p < 0.05$).

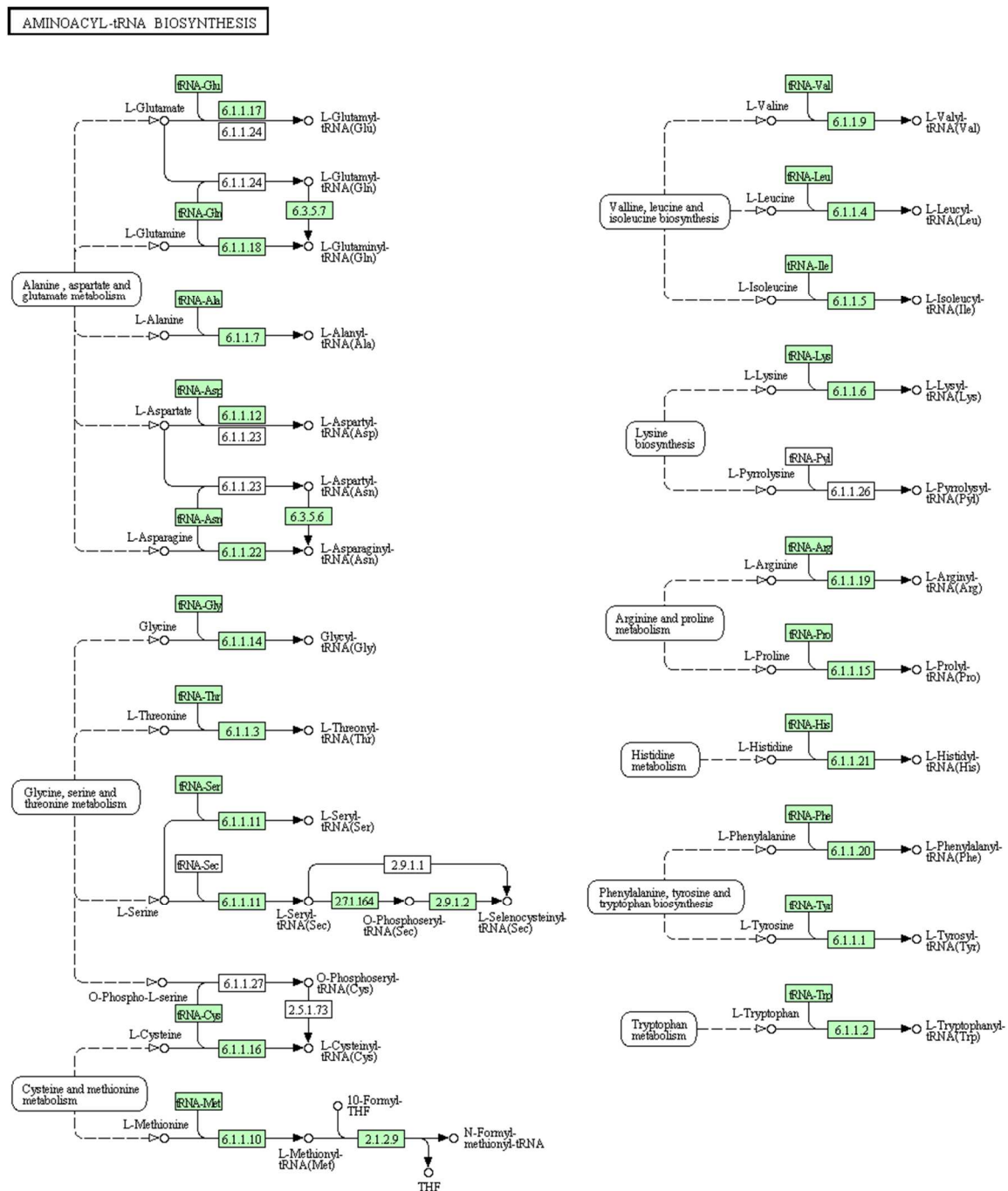


Figure 3.4.3.1: Proteins down-regulated in VDR vs. MM.1R by mass spectrometry. Three proteins that were found to be down-regulated in VDR compared to MM.1R at the protein level by label-free mass spectrometry (fold change >2, P<0.05) were found to be involved in aminoacyl tRNA biosynthesis. These proteins include IARS (isoleucyl-tRNA synthetase), RARS (arginyl-tRNA synthetase) and LARS (leucyl-tRNA synthetase), (*david.abcc.ncifcrf.gov*).

Cellular Process	Protein Count	Adjusted p value (Benjamini)
Regulation of ligase activity	6	0.01
Regulation of ubiquitin-protein ligase activity	6	0.01
Positive regulation of protein ubiquitination	6	0.01
Negative regulation of protein metabolic process	8	0.01
Positive regulation of ligase activity	6	0.01
Cell cycle	14	0.01
Positive regulation of ubiquitin-protein ligase activity	6	0.01
Cell cycle process	12	0.01
Regulation of protein ubiquitination	6	0.01
Cell redox homeostasis	6	0.01
Positive regulation of ubiquitin-protein ligase activity during mitotic cell cycle	5	0.02
Negative regulation of protein modification process	6	0.02
Negative regulation of ligase activity	5	0.02
Negative regulation of ubiquitin-protein ligase activity	5	0.02
Negative regulation of cellular protein metabolic process	7	0.02
Negative regulation of ubiquitin-protein ligase activity during mitotic cell cycle	5	0.02
Anaphase-promoting complex-dependent proteasomal ubiquitin-dependent protein catabolic process	5	0.02
Regulation of ubiquitin-protein ligase activity during mitotic cell cycle	5	0.02
Negative regulation of protein ubiquitination	5	0.02
Mitotic cell cycle	9	0.02
Regulation of cellular protein metabolic process	10	0.02
Negative regulation of macromolecule metabolic process	12	0.04
Positive regulation of cellular protein metabolic process	7	0.04

Table 3.4.3.2: Proteins both over-expressed and down-regulated in VDR compared to MM.1R. The cellular processes in which these proteins are involved are listed, with corresponding number of proteins involved in each given pathway, and associated adjusted p value (<0.05).

3.4.4 Individual biomarkers down-regulated in MM.1R or VDR following bortezomib treatment

3.4.4.1 Overview of proteins downregulated following bortezomib treatment in MM.1R or VDR

Following bortezomib treatment, 212 proteins in MM.1R and only 35 proteins in VDR were down-regulated post-treatment compared to their respective bortezomib-untreated controls ($p < 0.05$). Furthermore, comparing bortezomib-treated MM.1R to bortezomib-treated VDR, 109 proteins out of a total 323 were downregulated in bortezomib-treated-VDR compared to bortezomib-treated-MM.1R (see table 3.4.4.1.1 for contrast in number of proteins suppressed in MM.1R compared to VDR following bortezomib treatment).

Table 3.4.4.1.2 displays proteins downregulated in MM.1R following bortezomib treatment with protein fold change ≥ 1.5 , ($n=48$ out of a total 212) compared to MM.1R control. In contrast table 3.4.4.1.3 displays proteins downregulated in VDR following bortezomib treatment again with fold change ≥ 1.5 ($n=20$ out of a total 35) compared to VDR control.

On review of proteins that were down-regulated in bortezomib-treated VDR compared to bortezomib-treated MM.1R, a total of 109 proteins were downregulated in bortezomib-treated VDR (table 3.4.4.1.4 highlights 63 of these proteins which had a fold change ≥ 1.5 where $p < 0.05$). The remaining 46 proteins demonstrated a 1.20-1.49 reduction in fold change in bortezomib-treated VDR where $p < 0.05$.

DAVID functional annotation tool allowed us to review proteins down-regulated following bortezomib treatment in either cell lines. A number of proteins involved in the proteasome structure were suppressed in both bortezomib-treated MM.1R and bortezomib-treated VDR (see figure 3.4.4.1.1 and figure 3.4.4.1.2).

Comparative Analysis	Number of proteins up-regulated following bortezomib treatment	No. of proteins down-regulated following bortezomib treatment
MM.1R vs. MM.1R + Bort.	161	212
VDR vs. VDR + Bort.	79	35
MM.1R + Bort vs. VDR + Bort	214 (VDR + Bort)	109 (VDR + Bort)

Table 3.4.4.1.1 Total number of proteins differentially expressed in MM.1R or VDR following bortezomib treatment.

In MM.1R 212 proteins were down-regulated post-treatment with bortezomib in stark contrast to VDR, whereby 35 proteins were down-regulated post-bortezomib, compared to their respective bortezomib-untreated controls ($p < 0.05$). By comparing bortezomib-treated MM.1R to bortezomib-treated VDR, 214 proteins out of a total 323 differentially expressed in this comparison remained elevated in bortezomib-treated-VDR compared to bortezomib-treated-MM.1R. (*D.E. = differentially expressed*).

Accession	Confidence score	Anova (p)	Max fold change	Description
P02765	64.74	8.74E-04	Infinity	AHSG
Q9UKY7	58.70	0.01	Infinity	CDV3
Q13492	32.34	0.01	Infinity	PICALM
P09382	36.27	0.05	947.70	LGALS1
Q9Y6G9	70.28	2.03E-04	20.81	DYNC1LI1
P28062	59.75	1.46E-03	8.37	PSMB8
P10599	55.07	0.03	7.86	TXN
P28074	229.32	7.47E-04	4.66	PSMB5
P25788	165.92	6.88E-05	3.97	PSMA3
P25787	158.03	4.78E-03	3.61	PSMA2
P60900	460.16	1.68E-04	3.35	PSMA6
Q6JBY9	43.43	2.63E-03	2.88	RCSD1
Q07960	44.79	0.04	2.71	ARHGAP1
O00193	45.80	0.01	2.51	SMAP
P06730	48.87	4.66E-03	2.42	EIF4E
P28066	253.11	8.73E-05	2.22	PSMA5
P26583	225.32	1.97E-05	2.21	HMGB2
O14818	244.26	4.43E-04	2.21	PSMA7
P49721	239.73	1.22E-04	2.12	PSMB2
P07384	89.88	0.03	2.06	CAPN1
P25789	129.57	4.03E-03	2.04	PSMA4
P20618	173.37	1.14E-04	1.97	PSMB1
P25786	90.58	2.26E-03	1.87	PSMA1
P78347	61.60	0.03	1.86	GTF2I
P28072	113.95	1.47E-04	1.85	PSMB6
P41227	47.58	0.02	1.84	NAA10
Q9BPX5	70.88	0.01	1.78	ARPC5L
Q9UNM6	45.13	0.01	1.73	PSMD13
Q9UBW5	166.24	1.25E-03	1.71	BIN2
P62899	42.76	6.78E-04	1.69	RPL31
Q9BRA2	50.94	0.05	1.66	TXNDC17
Q9UM54	64.55	0.01	1.64	MYO6
P37837	100.71	0.04	1.64	TALDO1
P13798	32.54	0.02	1.62	APEH
P32969	142.28	0.02	1.61	RPL9
P23381	112.78	0.01	1.59	WARS
P48739	94.78	0.02	1.58	PITPNB
P12081	47.24	3.77E-03	1.55	HARS
O60232	132.48	0.01	1.54	SSSCA1
P60228	37.07	0.01	1.54	EIF3E
Q08J23	64.93	0.02	1.54	NSUN2
P11766	31.90	0.02	1.51	ADH5
Q92499	37.88	0.01	1.51	DDX1

Accession	Confidence score	Anova (p)	Max fold change	Description
P14868	121.89	4.48E-03	1.51	DARS
P15374	129.68	2.65E-03	1.51	UCHL3
P55060	95.42	0.01	1.50	CSE1L
Q8N1G4	33.07	0.04	1.50	LRRC47
P62244	198.59	2.91E-03	1.50	RPS15A

Table 3.4.4.1.2 List of proteins downregulated in MM.1R following bortezomib treatment compared to untreated control MM.1R. Proteins downregulated in MM.1R following bortezomib treatment with protein fold change ≥ 1.5 , (n=48, out of a total 212 proteins where remaining protein fold change ranges from 1.2-1.49).

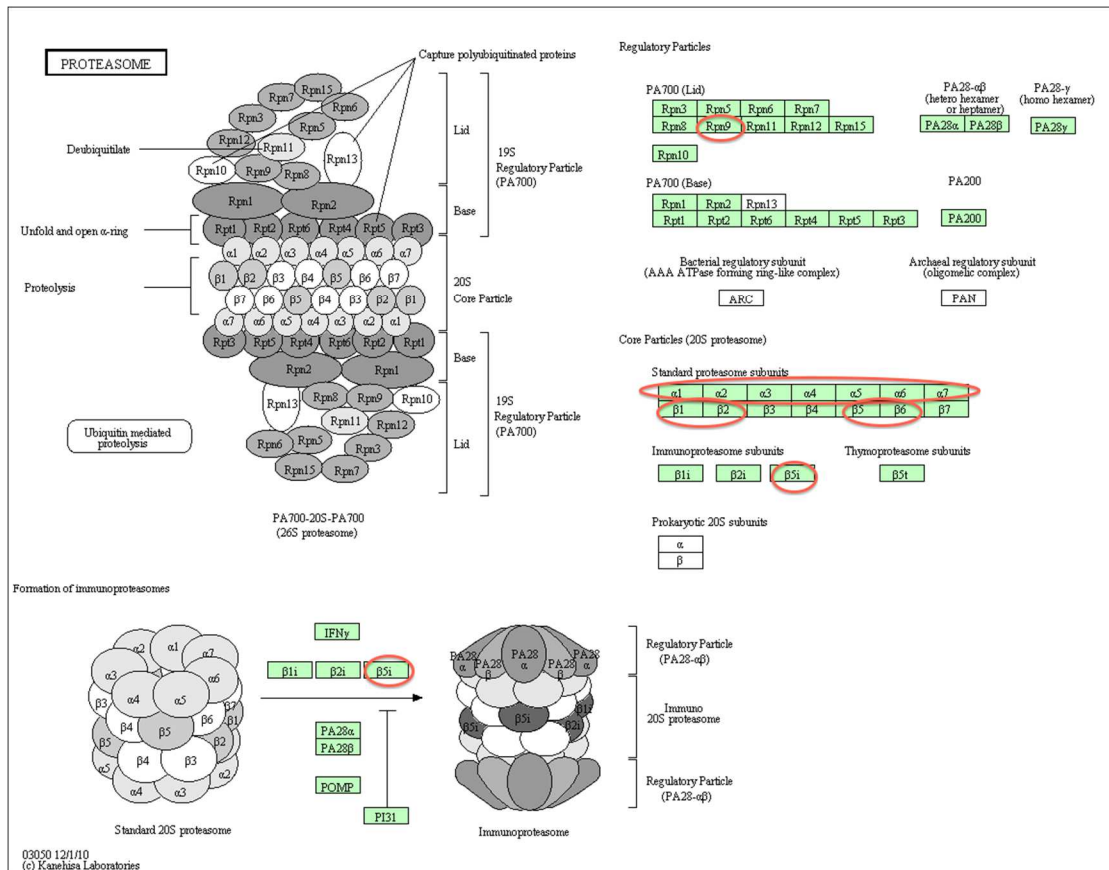


Figure 3.4.4.1.1 Proteins down-regulated in bortezomib-treated MM.1R compared to untreated MM.1R and their role in the proteasome structure.

PSMD13, PSMA1, PSMA2, PSMA3, PSMA4, PSMA5, PSMA6, PSMA7, PSMB1, PSMB2, PSMB5, PSMB6, PSMB8 were all found to be down-regulated in bortezomib-treated MM.1R compared to untreated MM.1R (red circles). (david.abcc.ncifcrf.gov).

Accession	Confidence score	Anova (p)	Fold change	Description
Q9P016	30.50	0.01	8.27	THYN1
P28062	94.33	3.35E-04	8.03	PSMB8
P25787	158.03	3.25E-03	3.47	PSMA2
Q8NB66	31.28	0.04	2.99	UNC13C
P36405	90.34	0.01	2.57	ARL3
P17066	1623.81	0.02	2.25	HSPA6
P23193	103.13	1.41E-03	2.16	TCEA1
P62633	61.67	0.02	2.09	CNBP
Q01469	200.21	3.59E-03	1.88	FABP5
P09429	432.76	0.02	1.75	HMGB1
P07339	77.68	0.02	1.74	CTSD
P25788	165.92	0.01	1.74	PSMA3
P25789	129.57	0.01	1.73	PSMA4
P60900	460.16	0.01	1.70	PSMA6
P28066	253.11	0.01	1.68	PSMA5
P20618	173.37	0.01	1.63	PSMB1
Q16576	45.39	1.33E-03	1.60	RBBP7
Q06203	225.07	0.01	1.60	PPAT
O14818	244.26	0.01	1.55	PSMA7
Q14258	32.26	0.04	1.51	TRIM25

Table 3.4.4.1.3 List of proteins downregulated in VDR following bortezomib treatment compared to untreated control VDR cells. Proteins downregulated in VDR following bortezomib treatment with protein fold change ≥ 1.5 , (n=20, out of a total 35 proteins where remaining protein fold change ranges from 1.2-1.49).

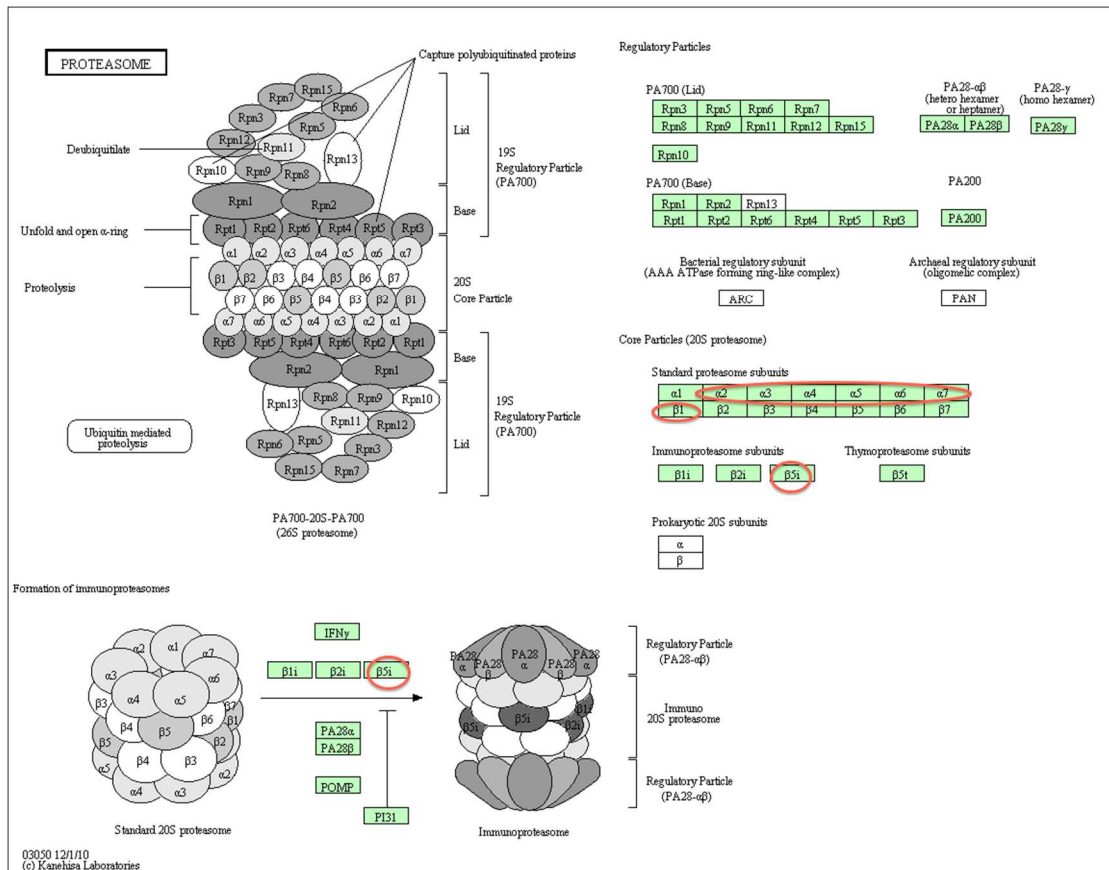


Figure 3.4.4.1.2: Proteins down-regulated in bortezomib-treated VDR compared to untreated VDR.

It is interesting to note that many of the proteasome- α subunits again are down-regulated in bortezomib-treated VDR (similar to bortezomib-treated MM.1R). In addition PSMB8 (or beta-5-immunoproteasome subunit) was down-regulated in bortezomib-treated VDR. PSMB5 however was not downregulated in bortezomib-treated VDR.

Accession	Confidence score	Anova (p)	Fold change	Description
P20839	141.62	3.20E-03	Infinity	IMPDH1
P17066	1710.71	2.21E-06	132.16	HSPA6
Q8IYS1	63.84	0.05	21.31	PM20D2
Q9NX09	59.24	3.17E-04	8.67	DDIT4
Q9P016	30.50	0.01	7.78	THYN1
Q09666	513.52	4.71E-07	6.82	AHNAK
P26010	702.26	2.14E-04	6.27	ITGB7
P09496	35.72	0.02	4.53	CLTA
P04792	105.07	0.02	4.51	HSPB1
Q9Y5P6	36.83	2.57E-03	4.49	GMPPB
Q96AQ6	293.23	0.01	4.38	PBXIP1
P36405	90.34	0.01	3.54	ARL3
P25685	615.68	8.00E-04	3.45	DNAJB1
O95817	54.09	0.02	3.43	BAG3
P08107	2066.62	3.43E-05	3.07	HSPA1A
P01591	234.45	1.12E-03	2.78	IGJ
P49916	48.71	0.03	2.75	LIG3
P82970	120.54	0.01	2.67	HMGH5
Q06413	43.61	4.03E-04	2.60	MEF2C
P62979	389.92	2.86E-03	2.49	RPS27A
O15247	82.44	0.01	2.45	CLIC2
P42677	171.67	0.01	2.38	RPS27
O14530	42.99	1.57E-05	2.15	TXNDC9
Q9Y2S6	43.52	0.02	2.14	TMA7
P14210	33.66	0.02	2.10	HGF
Q14493	54.23	0.01	2.01	SLBP
P46926	116.08	0.03	1.97	GNPDA1
O75461	30.94	2.10E-03	1.93	E2F6
Q07960	132.89	0.05	1.92	ARHGAP1
Q13616	43.40	0.05	1.91	CUL1
P13645	367.62	0.04	1.90	KRT10
P19388	33.00	1.97E-03	1.87	POLR2E
Q9H4M9	80.51	0.01	1.85	EHD1
P78347	61.60	3.27E-03	1.84	GTF2I
Q8I WV8	30.51	9.45E-04	1.84	UBR2
P07900	2804.88	4.39E-06	1.81	HSP90AA1
O95373	150.95	3.78E-03	1.77	IPO7
P41252	295.37	5.53E-04	1.77	IARS
Q99439	296.52	3.15E-03	1.74	CNN2

Accession	Confidence score	Anova (p)	Fold change	Description
Q53GG5	44.86	0.04	1.74	PDLIM3
P51965	56.16	2.52E-04	1.74	UBE2E1
P11413	92.65	3.58E-04	1.72	G6PD
Q16576	45.39	1.07E-03	1.71	RBBP7
Q9Y3Z3	217.50	2.25E-04	1.70	SAMHD1
Q712K3	31.74	0.03	1.70	UBE2R2
P54136	213.18	0.02	1.68	RARS
P50579	116.24	0.01	1.67	METAP2
P80723	266.80	0.01	1.65	BASP1
Q08209	62.44	0.02	1.65	PPP3CA
Q8IXM2	177.80	0.02	1.64	BAP18
P21333	3807.26	1.96E-03	1.64	FLNA
Q9ULX3	31.58	0.03	1.63	NOB1
Q8IWS0	34.76	0.01	1.63	PHF6
P36873	123.85	1.29E-04	1.57	PPP1CC
Q9Y265	32.86	3.49E-03	1.57	RUVBL1
Q6PKG0	44.78	0.03	1.57	LARP1
Q92598	854.52	0.01	1.57	HSPH1
Q14974	102.94	0.01	1.56	KPNB1
P62633	115.82	0.05	1.56	CNBP
P22059	49.84	2.28E-03	1.55	OSBP
Q01469	264.74	0.04	1.54	FABP5
P08133	1077.65	1.28E-05	1.53	ANXA6
P35908	395.74	0.03	1.52	KRT2

Table 3.4.4.1.4 Proteins down-regulated in bortezomib-treated VDR compared to bortezomib-treated MM.1R. List of proteins down-regulated ≥ 1.5 -fold in bortezomib-treated VDR compared to bortezomib-treated MM.1R by label free mass spectrometry ($p < 0.05$).

3.4.4.2 Functional annotation analysis of proteins down-regulated following bortezomib treatment in VDR compared to bortezomib-treated MM.1R.

Functional annotation analysis of the proteins downregulated in bortezomib-treated VDR compared to bortezomib-treated MM.1R revealed 59 pathways in which these proteins are involved and included positive regulation of protein ubiquitination, negative regulation of programmed cell death, proteasomal protein catabolic process, cell cycle processes and positive regulation of ubiquitin-protein ligase activity. For all cellular processes identified the adjusted Benjamini p value was <0.05 , (see table 3.4.4.2.1).

Taking a closer look, we found 5 proteins that are down-regulated in bortezomib-treated VDR compared to bortezomib-treated MM.1R in the MAP-kinase signalling pathway (figure 3.4.4.2.1). The MAP-kinase signalling pathway, when altered, is well documented for its role in carcinogenesis. These proteins including FLNA, HSP72/HSPA6, PPP3C, MEF2C and HSP27/HSPB1 may potentially contribute to bortezomib refractoriness in VDR.

Cellular Process	Count	Adjusted p value (Benjamini)
Long-term strengthening of neuromuscular junction	4	3.79E-04
Regulation of synaptic growth at neuromuscular junction	4	4.39E-04
Anti-apoptosis	9	5.43E-04
Cell cycle	14	8.86E-04
Regulation of ubiquitin-protein ligase activity	6	9.63E-04
Regulation of ligase activity	6	9.65E-04
Mitotic cell cycle	10	9.74E-04
Positive regulation of ligase activity	6	9.94E-04
Regulation of ubiquitin-protein ligase activity during mitotic cell cycle	6	1.01E-03
Response to unfolded protein	6	1.01E-03
Cell cycle process	12	1.04E-03
Positive regulation of protein ubiquitination	6	1.06E-03
Positive regulation of ubiquitin-protein ligase activity	6	1.13E-03
Positive regulation of ubiquitin-protein ligase activity during mitotic cell cycle	6	1.23E-03
Regulation of synaptogenesis	4	2.12E-03
Regulation of protein ubiquitination	6	2.14E-03
Response to protein stimulus	6	2.76E-03
Regulation of synapse organization	4	2.82E-03
Negative regulation of apoptosis	9	3.03E-03
Negative regulation of cell death	9	3.07E-03
Negative regulation of programmed cell death	9	3.17E-03
Negative regulation of protein metabolic process	7	3.17E-03
Negative regulation of protein modification process	6	3.18E-03
ER-associated protein catabolic process	4	3.29E-03
Regulation of synapse structure and activity	4	3.29E-03

Cellular Process	Count	Adjusted p value (Benjamini)
Anaphase-promoting complex-dependent proteasomal ubiquitin-dependent protein catabolic process	5	3.35E-03
Negative regulation of ubiquitin-protein ligase activity during mitotic cell cycle	5	3.35E-03
Regulation of skeletal muscle fibre development	4	3.42E-03
Negative regulation of ubiquitin-protein ligase activity	5	3.62E-03
Negative regulation of ligase activity	5	3.62E-03
Regulation of skeletal muscle tissue development	4	4.77E-03
Negative regulation of protein ubiquitination	5	4.94E-03
Regulation of striated muscle cell differentiation	4	0.01
Positive regulation of synaptic transmission	4	0.01
Ubiquitin-dependent protein catabolic process	7	0.01
Positive regulation of transmission of nerve impulse	4	0.01
Regulation of muscle cell differentiation	4	0.01
Positive regulation of neurological system process	4	0.01
Negative regulation of macromolecule metabolic process	11	0.01
Translational elongation	5	0.01
Proteasomal protein catabolic process	5	0.01
Proteasomal ubiquitin-dependent protein catabolic process	5	0.01
Negative regulation of cellular protein metabolic process	6	0.01
Regulation of developmental growth	4	0.01
Positive regulation of protein modification process	6	0.01
Regulation of striated muscle tissue development	4	0.02
Regulation of muscle development	4	0.02

Cellular Process	Count	Adjusted p value (Benjamini)
Regulation of protein modification process	7	0.02
Protein ubiquitination	5	0.02
Protein modification by small protein conjugation	5	0.03
Regulation of synaptic transmission	5	0.03
Translation	7	0.03
Regulation of synaptic plasticity	4	0.03
Positive regulation of cellular protein metabolic process	6	0.03
Regulation of cellular protein metabolic process	8	0.04
Regulation of transmission of nerve impulse	5	0.04
Positive regulation of protein metabolic process	6	0.04
Regulation of neurological system process	5	0.04
Protein modification by small protein conjugation or removal	5	0.04

Table 3.4.4.2.1 Functional annotation analysis of proteins down-regulated in bortezomib-treated VDR vs. bortezomib-treated MM.1R

A large number of pathways were identified by DAVID functional annotation analysis generated from the list of proteins that were down-regulated in bortezomib-treated VDR vs. bortezomib-treated MM.1R including a number of proteins involved in negative regulation of macromolecule metabolic process, cell cycle processes and anti-apoptotic processes. (*david.abcc.ncifcrf.gov*).

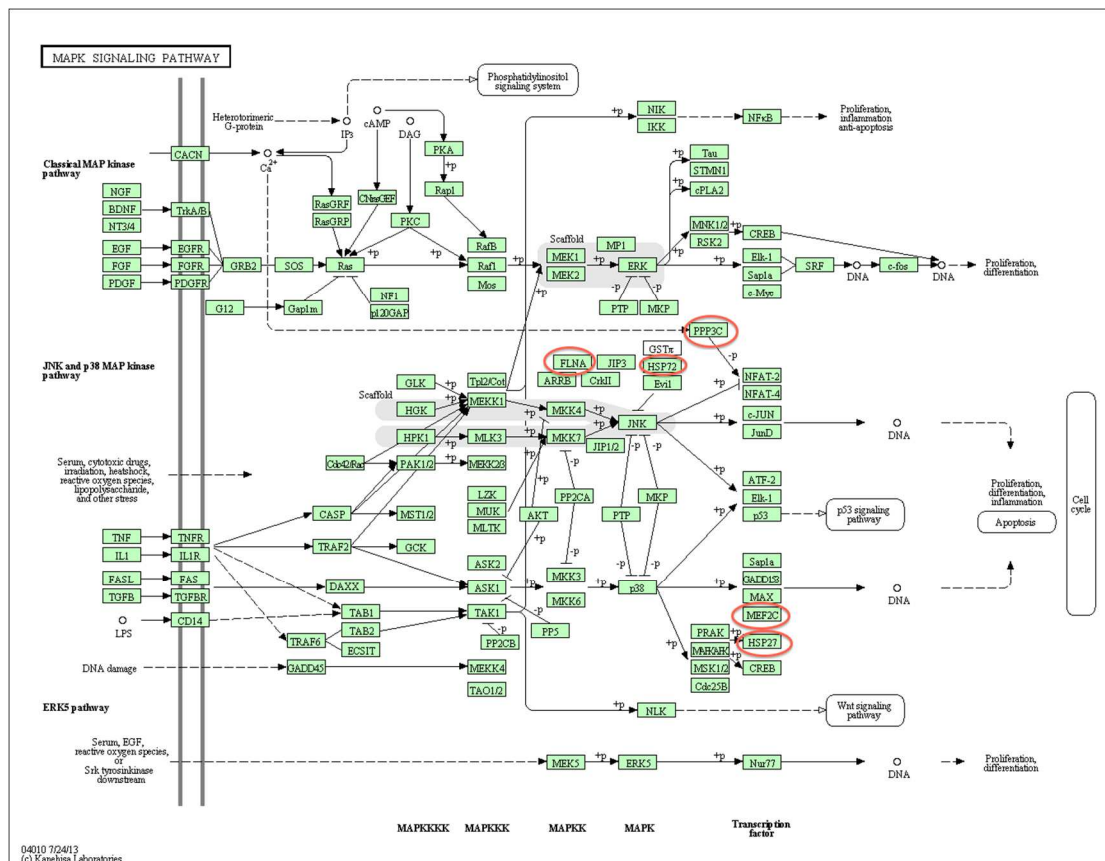


Figure 3.4.4.2.1 Involvement of proteins down-regulated in bortezomib-treated VDR compared to bortezomib-treated MM.1R in the MAP-kinase signalling pathway.

Five proteins were found to be suppressed in bortezomib-treated VDR compared to bortezomib-treated MM.1R and these are visualised in this figure as to their location in the MAP-kinase signalling pathway, which when altered, is well documented for its role in carcinogenesis. These proteins include FLNA, HSP72/HSPA6, PPP3C, MEF2C and HSP27/HSPB1. (*david.abcc.ncifcrf.gov*).

3.4.5 Proteins over-expressed in bortezomib treated VDR compared to bortezomib treated MM.1R

3.4.5.1 Individual proteins over-expressed in bortezomib treated VDR compared to bortezomib treated MM.1R

On review of proteins up-regulated in bortezomib-treated VDR compared to bortezomib-treated MM.1R we found 215 proteins up-regulated in bortezomib-treated VDR, of which 78 proteins had a fold change ≥ 2 ($p < 0.05$), (see table 3.4.5.1.1).

Again PSMB5 was over-expressed in bortezomib-treated VDR compared to bortezomib treated MM.1R (13.04 fold change, $p = 3.90E-05$). Additionally, the protein responsible for trypsin-like protein cleavage at the $\beta 2$ -subunit, PSMB7, was over-expressed in bortezomib-treated VDR and demonstrated a 16-fold increase compared to bortezomib-treated MM.1R ($p = 0.009$). Finally, the protein responsible for chymotrypsin-like proteolytic cleavage at the β -1 subunit, PSMB6, was also upregulated in by 2.32 fold ($p = 0.001$) in bortezomib-treated VDR compared to bortezomib-treated MM.1R.

While NEDD8 did not meet our cut-off criteria for inclusion of proteins of interest (i.e. fold change ≥ 2), on examination of the remaining 134 protein with a fold change between 1.20 and 1.99, NEDD8 was found to be over-expressed in bortezomib-treated VDR compared to bortezomib-treated MM.1R, fold change 1.98 ($p = 0.008$). This suggests that addition of a NEDD8-activating enzyme inhibitor may be useful in the setting of bortezomib resistant MM, however this would be dependent on bone marrow microenvironmental effects. We have demonstrated that the NEDD8-activating enzyme inhibitor MLN4924 was subject to HS-5 stromal cell induced drug resistance in the VDR cell line (figure 3.5.3.1), and despite combination of MLN4924 with bortezomib, resistance to this agent persisted in the presence of HS-5 stromal cells (figure 3.5.3.2), (see chapter 5 results section). Therefore this point again emphasizes the need to consider the bone marrow environmental impact on drug sensitivity testing when considering novel therapies under investigation for the treatment of multiple myeloma.

Previously we demonstrated that CCL3 is up-regulated in VDR at baseline compared to MM.1R (table 3.4.2.1), a protein known to be involved in stimulating MM cell growth and worsening osteolytic bone disease. When MM.1R and VDR were treated with bortezomib, CCL3 remained markedly over-expressed in bortezomib-treated VDR compared to bortezomib-treated MM.1R (fold change 3.55, $p=0.016$). Thus bortezomib resistance in VDR may potentially be augmented by its over-expression of CCL3, which remains elevated despite bortezomib treatment.

GSTP1 (glutathione s-transferase pi 1) is an enzyme that detoxifies carcinogens and variances of its detoxifying ability can be altered further by the GSTP1 rs1695 polymorphism,^[126] although this polymorphism has not yet been demonstrated in myeloma cell lines. It has been shown to inhibit JNK1 (c-Jun N-terminal kinase) and alter kinase signalling *in vitro*.^[127] Over-expression of the GSTP1 gene has been implicated in progression of multiple myeloma and has been suggested as a target biomarker for treatment of both MM and acute myeloid leukaemia.^[128, 129] We noted that GSTP1 was over-expressed in bortezomib-treated VDR compared to bortezomib-treated MM.1R (fold change 2.76, $p=0.004$).

Accession	Confidence score	Anova (p)	Max fold change	Uniprot symbol
P53041	61.35	0.008	672.24	PPP5C
Q13442	47.1	0.029	307.61	PDAP1
P05386	51.02	0.027	244.17	RPLP1
Q96L21	49.53	1.970E-05	102.37	RPL10L
P02765	237.58	3.160E-05	68.64	AHSG
P68371	1806.16	0.023	47.22	TUBB4B
P63241	328.31	0.008	24.98	EIF5A
Q8IX21	31.4	0.011	19.41	FAM178A
P06454	472.07	0.003	18.93	PTMA
P60709	1076.4	0.001	18.63	ACTB
Q9Y6G9	70.28	3.104E-04	17.91	DYNC1LI1
O15355	107.34	0.024	17.09	PPM1G
P07437	2236.97	4.535E-04	16.55	TUBB
Q99436	59.41	0.009	16.43	PSMB7
P84085	51.84	0.028	13.79	ARF5
P28074	264.99	3.900E-05	13.04	PSMB5
P29966	80.86	1.962E-04	12.20	MARCKS
P33316	104.54	0.025	10.91	DUT
Q7Z6G8	31.43	0.005	10.32	ANKS1B
Q15121	50.98	0.040	9.76	PEA15
P49207	90.9	0.001	9.58	RPL34
Q9P2T1	39.43	0.003	9.48	GMPR2
Q6P2Q9	44.64	2.229E-04	9.42	PRPF8
P06733	1810.85	3.854E-04	8.90	ENO1
Q9BVA1	1433.96	4.240E-05	8.05	TUBB2B
P53999	300.23	0.044	7.91	SUB1
P61978	407.98	0.009	7.25	HNRNPK
P31949	83.22	0.001	7.05	S100A11
P55327	167.97	0.020	7.01	TPD52
O60841	77.7	0.017	6.98	EIF5B
Q969Q0	91.64	0.009	5.73	RPL36AL
O60493	53.96	0.002	5.59	SNX3
Q16186	75.82	0.032	5.23	ADRM1
P07384	89.88	0.008	5.17	CAPN1
Q9BW85	47.41	0.023	4.95	CCDC94
P61513	46.11	0.029	4.50	RPL37A
P68366	733.08	0.028	4.37	TUBA4A
Q6JBY9	43.43	0.003	3.91	RCSD1
P25788	165.92	2.364E-04	3.73	PSMA3
P35241	219.37	2.549E-04	3.72	RDX
P46779	233.2	0.001	3.69	RPL28
P35527	355.4	0.025	3.67	KRT9
P31948	598.47	0.016	3.55	STIP1

Accession	Confidence score	Anova (p)	Max fold change	Uniprot symbol
P10147	51.45	0.039	3.51	CCL3
P52566	285.3	3.534E-04	3.46	ARHGDIB
P60900	542.5	3.770E-04	3.41	PSMA6
Q9BY43	165.87	2.773E-04	3.36	CHMP4A
Q86V88	48.62	0.002	3.18	MDP1
Q9Y5B9	30.97	0.011	2.99	SUPT16H
P54868	41.02	2.510E-05	2.97	HMGCS2
P31146	979.24	0.009	2.96	CORO1A
P25787	203.79	0.004	2.88	PSMA2
P52565	229.83	0.005	2.88	ARHGDIA
Q00688	163.97	0.001	2.83	FKBP3
Q14103	276.02	0.023	2.80	HNRNPD
P09211	1156.32	0.004	2.76	GSTP1
P20073	153.12	0.046	2.65	ANXA7
P41250	320.35	0.030	2.62	GARS
O75874	97.43	0.001	2.47	IDH1
Q01081	76.53	0.006	2.42	U2AF1
Q9UL46	603.72	5.380E-05	2.39	PSME2
Q99959	62.08	0.004	2.33	PKP2
P28072	238.37	0.001	2.32	PSMB6
Q9NZB2	86.82	0.007	2.29	FAM120A
Q15637	48.07	0.049	2.28	SF1
P49721	239.73	3.156E-04	2.28	PSMB2
Q06323	820.35	0.001	2.09	PSME1
O15372	36.84	0.007	2.07	EIF3H
P30043	104.8	5.770E-06	2.06	BLVRB
P06744	430.26	0.036	2.03	GPI
P28066	283.21	0.001	2.01	PSMA5
O14818	244.26	0.001	2.00	PSMA7

Table 3.4.5.1.1 Proteins upregulated in bortezomib-treated VDR compared to bortezomib-treated MM.1R by label free mass spectrometry

Proteins listed include those with fold change ≥ 2 where $p < 0.05$. Proteins with fold change $> 1,000$ were excluded from this analysis. Of particular interest, PSMB5 and CCL3 remained upregulated in bortezomib-treated VDR compared to bortezomib-treated MM.1R.

3.4.5.2 Functional protein association mapping of protein classes over-expressed in bortezomib-treated VDR compared to bortezomib-treated MM.1R

Functional protein association mapping of proteins identified by mass spectrometry over-expressed in bortezomib-treated-VDR compared to bortezomib-treated-MM.1R revealed 3 specific groups of molecules (figure 3.4.5.2.1).

EIF5A (eukaryotic initiation factor 5A) was over-expressed in bortezomib-treated VDR compared to bortezomib-treated MM.1R and demonstrated multiple interactions with other proteins over-expressed in bortezomib-treated VDR. This molecule has been previously documented to play a major role in MM pathogenesis and a specific nanoparticle inhibitor has been developed to abrogate EIF5A expression, which results in concomitant NF- κ B inhibition and demonstrated a significant reduction in tumour burden in two mouse models of multiple myeloma.^[130] Not only was this protein up-regulated in bortezomib-treated VDR compared to bortezomib-treated MM.1R, but also on review of baseline protein expression for each cell line, EIF5A is also up-regulated in VDR compared to MM.1R at baseline by a factor of 2.21 fold ($p=0.008$), (see table 3.4.2.1).

In addition, a number of 60S ribosomal-associated proteins were over-expressed in bortezomib-treated VDR (RPLP1, RPL34, RPL10L and RPL36AL). The exact role of these proteins in MM pathogenesis is not well documented, however RPLP1 appears to play a role in circumventing cellular senescence and is known to be over-expressed in human gynaecological and colon cancers.^[131, 132]

Finally, multiple proteasome-related subunits formed a core group of molecules with multiple direct protein interactions, in particular the β -proteasome subunit PSMB5, PSMB6 and PSMB7. PSMB2, PSME1, PSME2, PSMA2, PSMA3 and PSMA7 also formed central connections within these pathways.

In addition, of the 72 proteins which were upregulated in bortezomib-treated VDR compared to bortezomib-treated MM.1R (where fold change ≥ 2), functional annotation analysis via DAVID revealed a number of cellular processes in which

these proteins are involved including negative regulation of protein ubiquitination, negative regulation of cellular protein metabolic process and cell cycle processes (table 3.4.5.2.1).

Finally, 2 proteins with established involvement in the glycolysis pathway were found to be over-expressed in bortezomib-treated VDR compared to bortezomib-treated MM.1R. These include glucose phosphate isomerase (GPI) and enolase (ENO1). GPI is an enzyme early on in the glycolysis cycle that converts glucose-6-phosphate to fructose-6-phosphate (and vice versa). ENO1 plays a role in the second last step of pyruvate generation, by converting 2-phosphoglycerate to phosphoenolpyruvate (prior to conversion of the latter by pyruvate kinase to pyruvate), (figure 3.4.5.2.2), (*david.abcc.ncifcrf.gov*) .

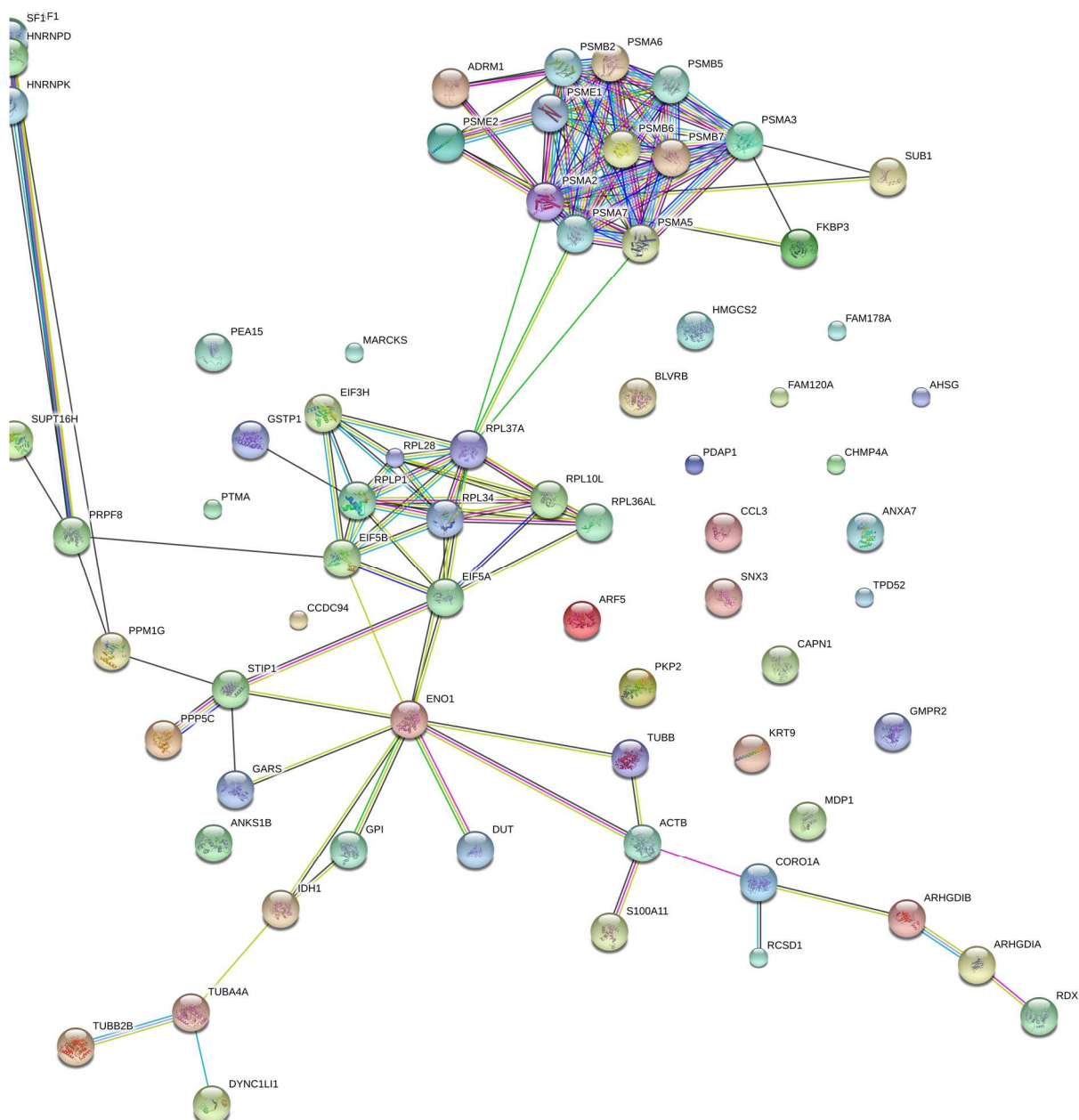


Figure 3.4.5.2.1 Direct protein-protein interactions of proteins over-expressed in bortezomib-treated-VDR compared to bortezomib-treated MM.1R. Functional protein association mapping of proteins identified by mass spectrometry over-expressed in bortezomib-treated-VDR compared to bortezomib-treated-MM.1R. In particular, EIF5A demonstrated multiple interactions with other proteins over-expressed in bortezomib-treated VDR. Multiple proteasome-related subunit molecules formed a core group of proteins with multiple direct interactions. Finally a number of 60S-ribosomal proteins formed a third group of interacting molecules. (*www.string-db.org*).

Cellular process	Count	Adjusted p value (Benjamini)
Regulation of ubiquitin-protein ligase activity during mitotic cell cycle	11	9.78E-11
Positive regulation of ubiquitin-protein ligase activity during mitotic cell cycle	11	1.04E-10
Positive regulation of ubiquitin-protein ligase activity	11	1.05E-10
Negative regulation of protein ubiquitination	11	1.08E-10
Positive regulation of ligase activity	11	1.09E-10
Negative regulation of ubiquitin-protein ligase activity	11	1.33E-10
Negative regulation of ligase activity	11	1.33E-10
Regulation of ubiquitin-protein ligase activity	11	1.62E-10
Negative regulation of ubiquitin-protein ligase activity during mitotic cell cycle	11	1.94E-10
Anaphase-promoting complex-dependent proteasomal ubiquitin-dependent protein catabolic process	11	1.94E-10
Regulation of ligase activity	11	2.13E-10
Positive regulation of protein ubiquitination	11	2.79E-10
Regulation of protein ubiquitination	11	1.50E-09
Proteasomal protein catabolic process	11	1.68E-09
Proteasomal ubiquitin-dependent protein catabolic process	11	1.68E-09
Negative regulation of protein modification process	11	7.30E-09
Positive regulation of cellular protein metabolic process	12	3.63E-07
Negative regulation of cellular protein metabolic process	11	3.64E-07
Mitotic cell cycle	14	4.29E-07
Negative regulation of protein metabolic process	11	4.38E-07
Positive regulation of protein modification process	11	4.38E-07
Positive regulation of protein metabolic process	12	4.63E-07
Cell cycle process	16	9.94E-07
Ubiquitin-dependent protein catabolic process	11	4.51E-06
Regulation of cellular protein metabolic process	14	5.95E-06
Negative regulation of catalytic activity	11	1.43E-05
Regulation of protein modification process	11	2.43E-05
Cell cycle	16	4.66E-05
Negative regulation of molecular function	11	6.84E-05
Translation	10	4.66E-04
Negative regulation of macromolecule metabolic process	13	2.65E-03
Positive regulation of catalytic activity	11	2.73E-03
Modification-dependent macromolecule catabolic process	11	5.86E-03
Modification-dependent protein catabolic process	11	0.01
Positive regulation of molecular function	11	0.01
Proteolysis involved in cellular protein catabolic process	11	0.01

Cellular process	Count	Adjusted p value (Benjamini)
Cellular protein catabolic process	11	0.01
Cellular macromolecule catabolic process	12	0.01
Protein catabolic process	11	0.01
Macromolecule catabolic process	12	0.01
Protein polymerization	4	0.02
Positive regulation of macromolecule metabolic process	12	0.03

Table 3.4.5.2.1 Functional annotational analysis of proteins upregulated in bortezomib-treated VDR compared to bortezomib-treated MM.1R.

72 proteins were upregulated in bortezomib-treated VDR compared to bortezomib-treated MM.1R and functional annotation analysis revealed a number of cellular processes in which these proteins are involved. (david.abcc.ncifcrf.gov/) .

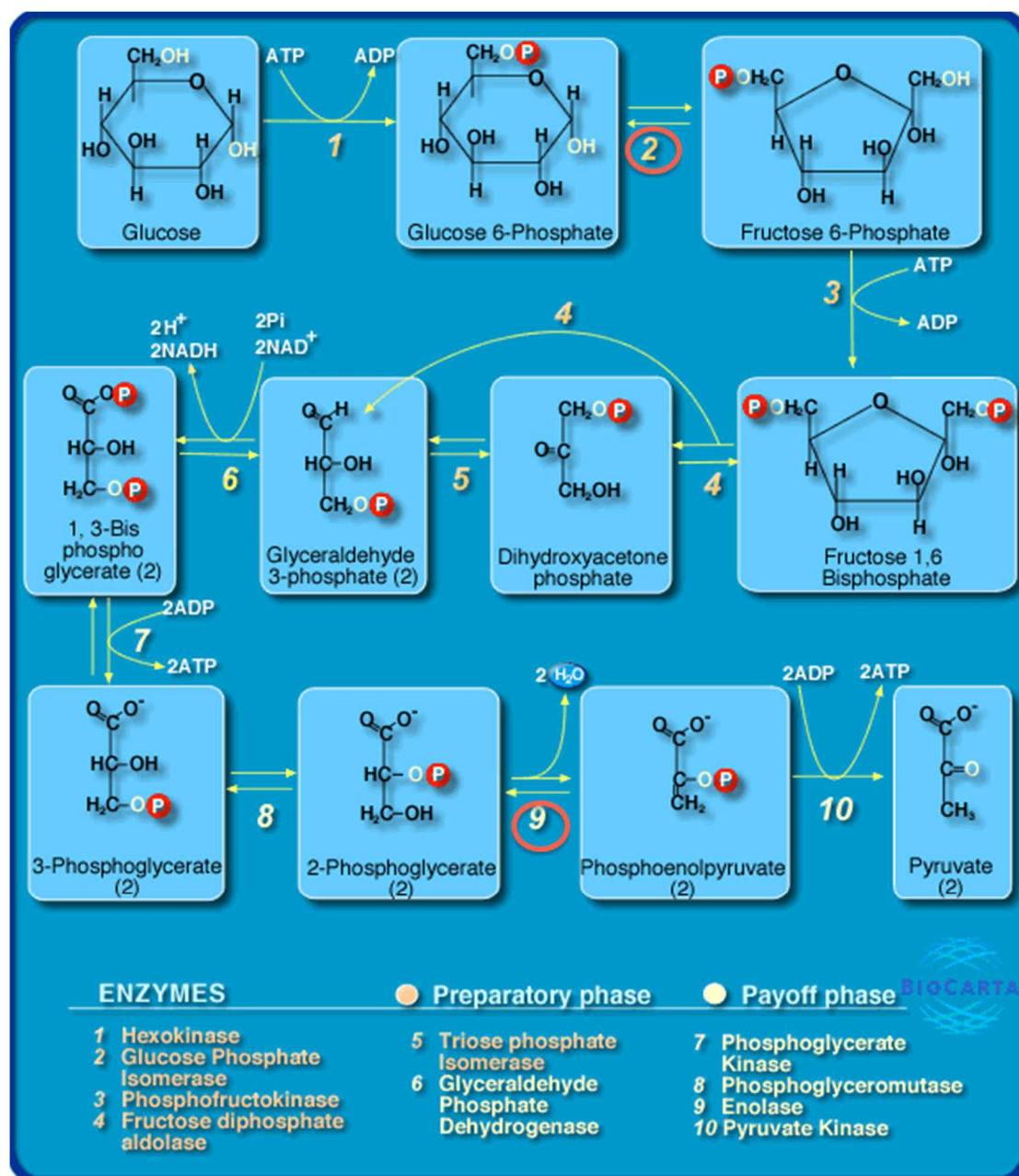


Figure 3.4.5.2.2: Proteins over-expressed in bortezomib-treated VDR compared to bortezomib-treated MM.1R.

Two proteins that were found to be over-expressed in bortezomib-treated VDR compared to bortezomib-treated MM.1R ($p < 0.05$) included glucose phosphate isomerase (GPI) and enolase (ENO1), of which have known involvement in the glycolysis pathway. (david.abcc.ncifcrf.gov/). Red circles indicate proteins identified by label-free mass spectrometry i.e. “2”/GPI and “9”/ENO1.

3.4.6 PSMB5 protein expression in MM.1R and VDR with and without bortezomib treatment

The proteomic expression of a number of the catalytic subunits of the proteasome, including the $\beta 5$, $\beta 5i$, $\beta 1$ and $\beta 1i$ subunits, has been previously demonstrated by 2D-gel electrophoresis to be abolished following a 4-hour treatment with bortezomib in bortezomib-sensitive MM.1S cells (see introduction 1.3.4).^[55] In our study, at baseline, PSMB5 was over-expressed in VDR compared to MM.1R (PSMB5 is over-expressed 3.85-fold in VDR compared to MM.1R, $p=4.36E-04$). Following bortezomib treatment PSMB5 was suppressed by a factor of 4.65 fold in MM.1R treated with bortezomib compared to untreated control MM.1R ($p=7.47E-04$), whereas VDR displayed only a 1.34 decrease in PSMB5 expression compared to untreated VDR control ($p=0.03$). Finally, by comparing bortezomib-treated MM.1R to bortezomib-treated VDR, PSMB5 expression was down-regulated by 13 fold when directly comparing the two cell lines post-treatment ($p=3.90E-05$). These results suggest that bortezomib resistance in VDR may potentially be mediated through PSMB5, evidenced by over-expression of PSMB5 in VDR at baseline compared to MM.1R, and minimal reduction in PSMB5 expression in VDR despite bortezomib treatment (figure 3.4.6.1).

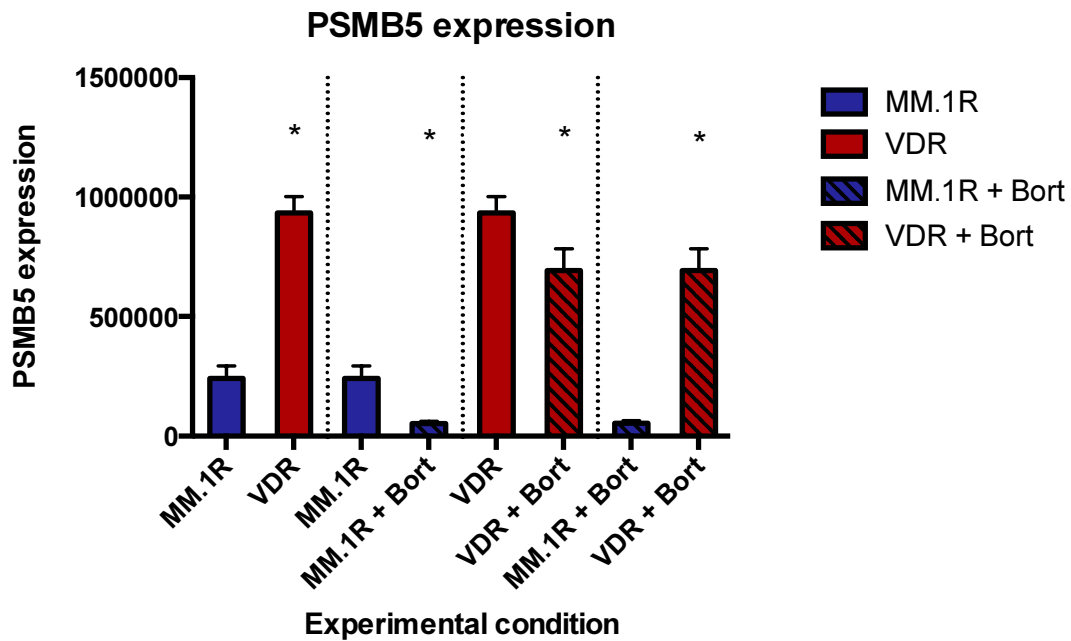


Figure 3.4.6.1 Summary of PSMB5 protein expression at baseline and following bortezomib treatment in MM.1R or VDR. At baseline, PSMB5 is over-expressed 3.85-fold in VDR compared to MM.1R. When MM.1R is treated with bortezomib, PSMB5 is suppressed as demonstrated by a 4.66 reduction in fold change, however to a lesser degree when VDR is treated with bortezomib (reduction in fold change is 1.34-fold). By direct comparison of bortezomib-treated VDR compared to bortezomib-treated MM.1R, a 13.04-fold difference in PSMB5 expression is observed, where PSMB5 remains markedly elevated in bortezomib-treated VDR, supporting the role of PSMB5 dysregulation in VDR as a potential mechanism for bortezomib resistance in this cell line.

3.4.7 Immunoblot validation of proteins differentially expressed in VDR compared to MM.1R

Following review of our proteomic datasets a number of specific molecules of interest were validated by western blot analysis, including:

- PSMB5
- NEDD8

PSMB5 was over-expressed in VDR compared to MM.1R at baseline, and this was validated by western blot for PSMB5. In addition, NEDD8 was found to be over-expressed by mass spectrometry in VDR compared to MM.1R and again this was validated by immunoblot (table 3.4.7.1).

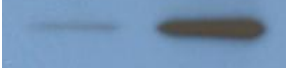



	Protein of interest		GAPDH	
	MM.1R vs. VDR		MM.1R vs. VDR	
PSMB5				
NEDD8				

Table 3.4.7.1 Validation of proteins of interest identified by label-free mass spectrometry.

Over-expression of PSMB5 and NEDD8 was validated in VDR compared to MM.1R by immunoblot.

3.4.8 Summary of proteomic profiling studies

We examined the proteomic profiles of the isogenic cell lines MM.1R and VDR, in addition to investigating the proteins differentially expressed following their treatment with bortezomib.

We identified 238 proteins differentially expressed in the MM.1R vs. VDR comparison. CCL3 demonstrated a 22-fold higher expression level in VDR compared to MM.1R. This protein has been previously documented to contribute to myelomatous bone disease, and an inhibitor of CLL1 through which CCL3 signals is currently in pre-clinical investigation that has shown promising anti-myelomatous and anti-osteolytic effects in a MM *in vivo* mouse model. Further studies could include examining the sensitivity of VDR cells to bortezomib in the presence of a CCL1 inhibitor. In addition NEDD8 and PSMB5 were also found to be over-expressed in VDR when compared to MM.1R.

Functional protein association mapping of proteins by String software revealed the heat shock proteins as a common subgroup of proteins over-expressed in VDR. DAVID functional annotation tool revealed a number of proteins over-expressed in VDR that are involved in apoptosis, regulation of cellular metabolic processes, cellular homeostasis, cell cycle process and proteasomal ubiquitin-dependent protein catabolic process.

Of the 238 proteins in total differentially expressed in the MM.1R vs. VDR comparison, 132 were down-regulated in VDR compared to MM.1R. Three proteins that were found to be down-regulated in VDR compared to MM.1R were found to be involved in aminoacyl tRNA biosynthesis, and these included IARS, RARS and LARS.

Following bortezomib treatment, 212 proteins in MM.1R and only 35 proteins in VDR were down-regulated post-treatment compared to their respective bortezomib-untreated controls. Furthermore, comparing bortezomib-treated MM.1R to bortezomib-treated VDR, 109 proteins out of a total 323 were downregulated in bortezomib-treated-VDR compared to bortezomib-treated-

MM.1R, of which 63 demonstrated a fold change ≥ 1.5 (where $p < 0.05$). DAVID functional annotation tool again allowed us to review proteins down-regulated following bortezomib treatment in either cell line. A number of proteins involved in the proteasome structure were suppressed in both bortezomib-treated MM.1R and bortezomib-treated VDR compared to their respective untreated controls. PSMD13, PSMA1, PSMA2, PSMA3, PSMA4, PSMA5, PSMA6, PSMA7, PSMB1, PSMB2, PSMB5, PSMB6, PSMB8 were all found to be down-regulated in bortezomib-treated MM.1R compared to untreated MM.1R; PSMB5 however was not down-regulated in bortezomib-treated VDR compared to untreated VDR control.

Taking a closer look, we found 5 proteins that were down-regulated in bortezomib-treated VDR compared to bortezomib-treated MM.1R that are involved in the MAP-kinase signalling pathway, which when altered, is well documented for its role in carcinogenesis. These proteins including FLNA, HSP72/HSPA6, PPP3C, MEF2C and HSP27/HSPB1 that are differentially expressed in bortezomib-treated VDR compared to bortezomib-treated MM.1R warrant further investigation to establish if they play a role in bortezomib refractoriness in VDR.

We found 215 proteins up-regulated in bortezomib-treated VDR compared to bortezomib-treated MM.1R, of which 78 proteins had a fold change ≥ 2 . These included PSMB5, PSMB7 (responsible for trypsin-like protein cleavage at the $\beta 2$ -subunit) and PSMB6 (responsible for chymotrypsin-like proteolytic cleavage at the $\beta 1$ -subunit). In addition CCL3 was markedly over-expressed in bortezomib-treated VDR compared to bortezomib-treated MM.1R. This again poses the question as to whether or not the addition of a CCL1 inhibitor may have the potential to overcome bortezomib resistance in VDR. Finally we noted that GSTP1 was over-expressed in bortezomib-treated VDR compared to bortezomib-treated MM.1R, a protein whose over-expression has been implicated in both the progression of multiple myeloma, and has been suggested as a target biomarker for treatment of both MM and acute myeloid leukaemia.

EIF5A (eukaryotic initiation factor 5A) was over-expressed in bortezomib-treated VDR compared to bortezomib-treated MM.1R. A specific nanoparticle inhibitor has previously been developed to abrogate EIF5A expression, which results in concomitant NF- κ B inhibition, and also demonstrated a significant reduction in tumour burden in two mouse models of multiple myeloma.^[130] Not only was this protein up-regulated in bortezomib-treated VDR compared to bortezomib-treated MM.1R, but also over-expressed in VDR compared to MM.1R at baseline. This raises the question whether EIF5A could act as an additional potential regulator for bortezomib refractoriness in the VDR cell line.

Finally, PSMB5 is over-expressed 3.85-fold in VDR compared to MM.1R at baseline. When MM.1R is treated with bortezomib, PSMB5 is suppressed as demonstrated by a 4.66 reduction in fold change, however to a lesser degree (1.34-fold) when VDR is treated with bortezomib. By direct comparison of bortezomib-treated VDR compared to bortezomib-treated MM.1R, a 13-fold increase in PSMB5 expression is observed in bortezomib-treated VDR, supporting the role of PSMB5 dysregulation in VDR as a potential mechanism for bortezomib resistance in this cell line.

3.5 FUNCTIONAL STUDIES AND POTENTIAL ROLE OF THE BONE MARROW MICROENVIRONMENT IN THE PATHOGENESIS OF BORTEZOMIB RESISTANCE IN VDR

3.5.1 Introduction

While we have demonstrated the toxicological profile of the VDR cell line to conventional and novel therapies, and examined its genetic mutations, gene expression and proteomic profiles in comparison to parental MM.1R, we cannot consider the cell line model as an entity independent of its microenvironment. As outlined in the introduction (section 1.6), myeloma cells co-exist with surrounding accessory cells, many of which appear to stimulate their growth. The bone marrow microenvironment plays a major role in resistance mechanisms in MM by either direct or indirect interactions between bone marrow stromal cells and tumour cells.^[73, 133] Bortezomib has been shown to abrogate protective effects conferred by stromal cells to tumour cells *in vitro*, in particular in relation to IL-6 signalling.^[134] Therefore we examined the effect of HS-5 stromal cells in co-culture with our bortezomib-resistant clone, VDR.

We examined the sensitivity of the isogenic cell line model to conventional and novel therapies in the presence and absence of HS-5 stromal cells. We examined the baseline proliferation rate of both MM.1R and VDR. We then investigated the effect of osteoblasts on the proliferation rate of the MM cell lines to ascertain if the stromal-induced effects were specific to HS-5 cells or merely a cell-to-cell ratio effect. We furthermore examined the effect of osteoblasts on the drug sensitivity of VDR cell line to a number of therapies.

Finally, given that there was marked overexpression of PSMB5 at the proteomic and transcript levels, in addition to the finding of a PSMB5 mutation in the VDR cell, we hypothesised if bortezomib resistance could potentially be overcome by up-regulating the PSMB5 immunoproteasome counterpart, PSMB8. By pre-treating VDR cells with interferon-gamma, we observed an increase in sensitivity of VDR cells to bortezomib, potentially by up-regulation of PSMB8 as demonstrated by western blot. While interferon-gamma did not completely

resensitise VDR to bortezomib, it appears to have the potential to play a role in over-coming bortezomib resistance in VDR. To test our hypothesis in the *in vivo* setting, we ran immunohistochemistry on bone marrow trephines of patients with bortezomib-refractory multiple myeloma, which revealed PSMB8 was present in the bone marrow of this patient group. These data support a role for the use of PSMB8 inhibitors in the setting of bortezomib resistance *in vivo*.

3.5.2 Effect of HS-5 stromal cells on sensitivity of MM1R and VDR to bortezomib and carfilzomib

We first investigated the sensitivity of MM.1R and VDR cells to either bortezomib or carfilzomib following their co-culture with immortalised bone marrow stromal cells, i.e. HS-5 cell line. HS-5 cells were plated in a 96 well-plate and allowed to adhere for 6 hours. Next MM.1R or VDR cells were added and cultured in the presence or absence of HS-5 cells, and co-cultures were performed for 24, 48 and 72 hours each. Finally each co-culture condition was treated with bortezomib 0-80nM or carfilzomib 0-20nM for 24hours. Then cell viability was analysed by CSBLI, (see materials and methods 2.7).

We observed no change in the sensitivity of MM.1R to bortezomib despite its co-culture with HS-5 stromal cells. VDR retained the same degree of resistance to bortezomib following HS-5 co-culture, (figure 3.5.2.1). Interestingly MM.1R cells appeared to display resistance to carfilzomib following their co-culture with HS-5 cells, and the degree of resistance to carfilzomib increased with duration of preceding co-culture time. The mechanism for this observation is not clear. Finally VDR cells retained their sensitivity to carfilzomib despite their co-culture with HS-5 cells, (figure 3.5.2.2).

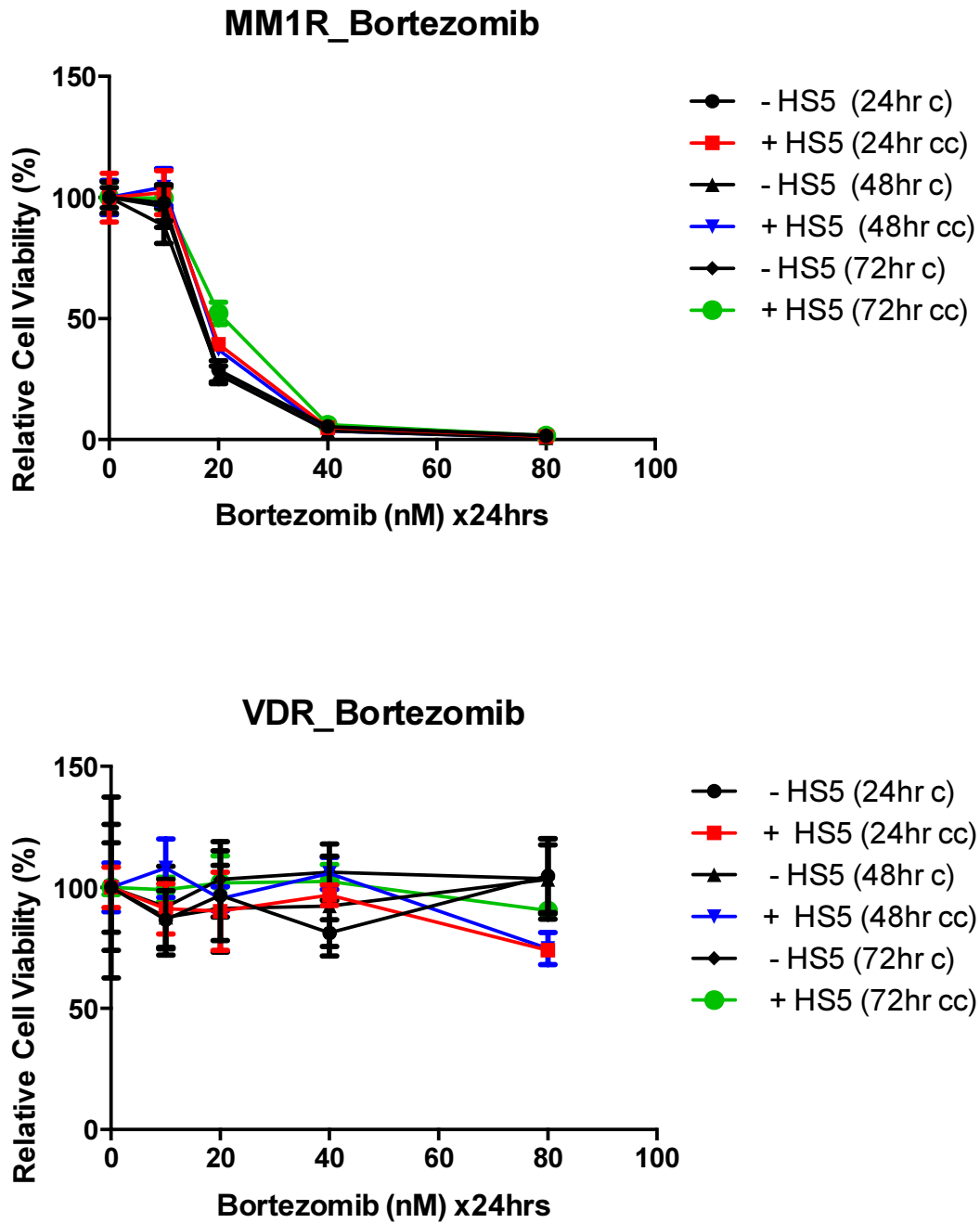


Figure 3.5.2.1: Co-culture of MM.1R and VDR with HS-5 stromal cells and subsequent bortezomib treatment.

No change in the sensitivity of MM.1R to bortezomib was observed despite its co-culture with HS-5 stromal cells. VDR retained the same degree of resistance to bortezomib following its co-culture with HS-5 cells. (Note: c= monoculture; cc=co-culture).

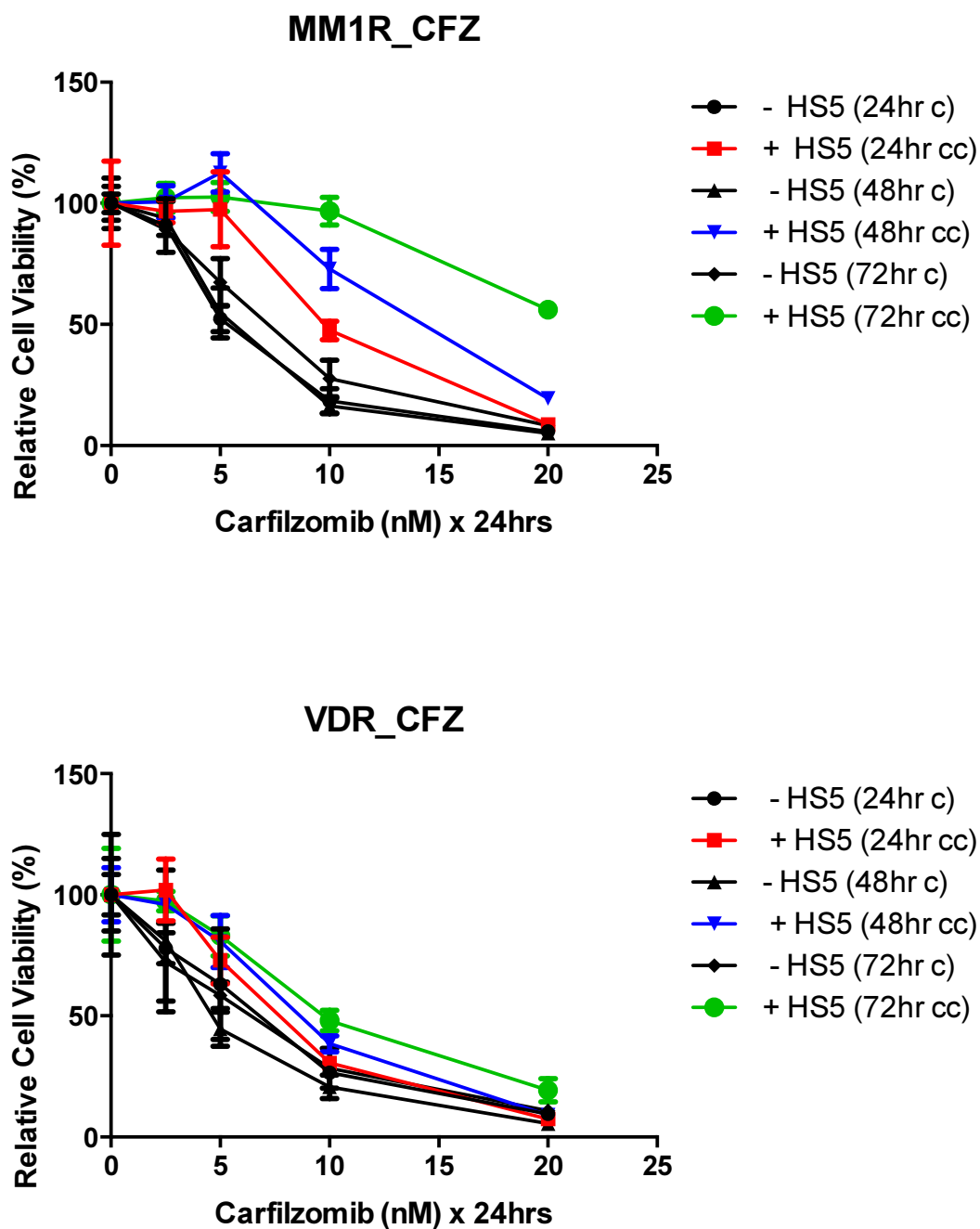


Figure 3.5.2.2: Co-culture of MM.1R and VDR with HS-5 stromal cells and subsequent carfilzomib treatment.

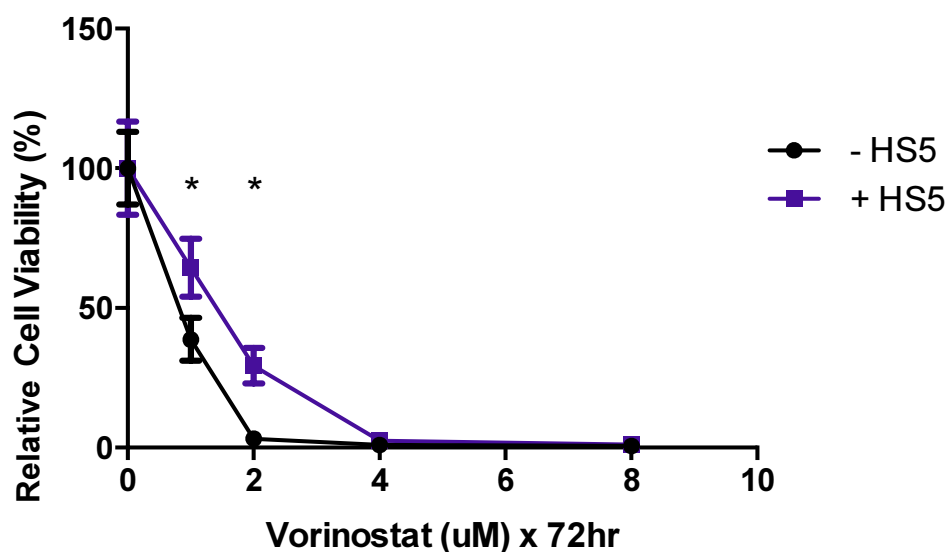
MM.1R cells appeared to display reduced sensitivity to carfilzomib following their co-culture with HS-5 cells, and reduced sensitivity to carfilzomib was observed with increased duration of co-culture time. VDR cells retained their sensitivity to carfilzomib despite their co-culture with HS-5 cells (Note: c= monoculture; cc=co-culture, CFZ= carfilzomib).

3.5.3 Investigation of the role for combination therapies to overcome bortezomib resistance in VDR cells in co-culture with HS-5 stromal cells

We next examined the effect of HS-5 stromal cells on the sensitivity of VDR cells to novel therapies. We found that the presence of HS-5 stromal cells in co-culture with VDR caused resistance to both the novel FDA-approved HDAC inhibitor vorinostat, and resistance to NEDD8-activating enzyme inhibitor MLN4924, (a reagent in which a phase 1 clinical trials for multiple myeloma and lymphoma has been completed with results pending), (figure 3.5.3.1). We next tested the combination of these two agents with bortezomib in our *in vitro* model in co-culture with HS-5 stromal cells. The protective effect conferred to the VDR cells by HS-5 stromal cells was not overcome by combination of either vorinostat or MLN4924 with bortezomib, (figure 3.5.3.2).

(a)

Vorinostat sensitivity in VDR in the presence of HS-5



(b)

MLN4924 sensitivity in VDR in the presence of HS-5

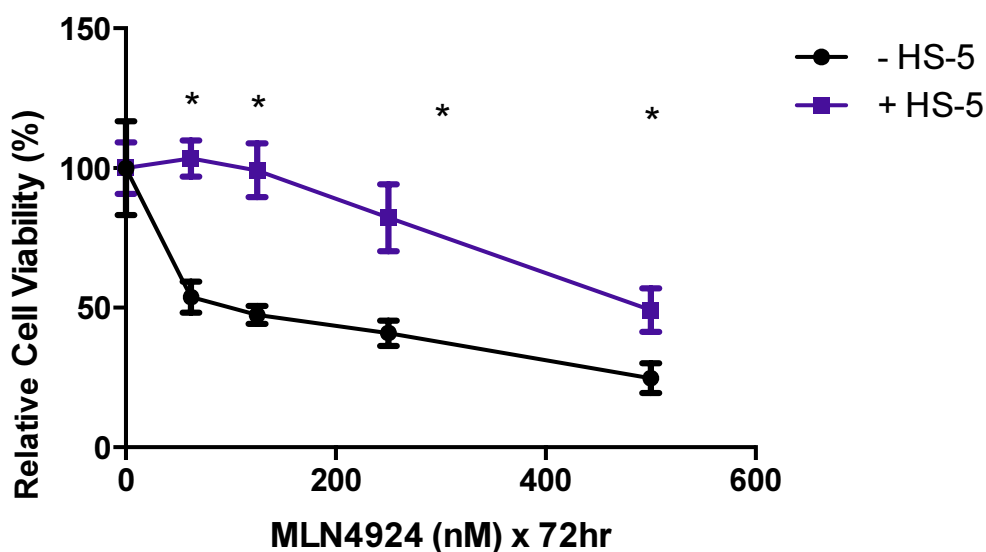


Figure 3.5.3.1 Effect of HS-5 stromal cells on efficacy of novel and investigational reagents in VDR.

The presence of HS-5 stromal cells in co-culture with VDR cells for 24 hours prior to treatment with either (a) vorinostat or (b) MLN4924 causes a reduction in sensitivity of VDR cells to vorinostat 1/2uM and MLN4924 (62.5-500nM) as demonstrated by CSBLI analysis .

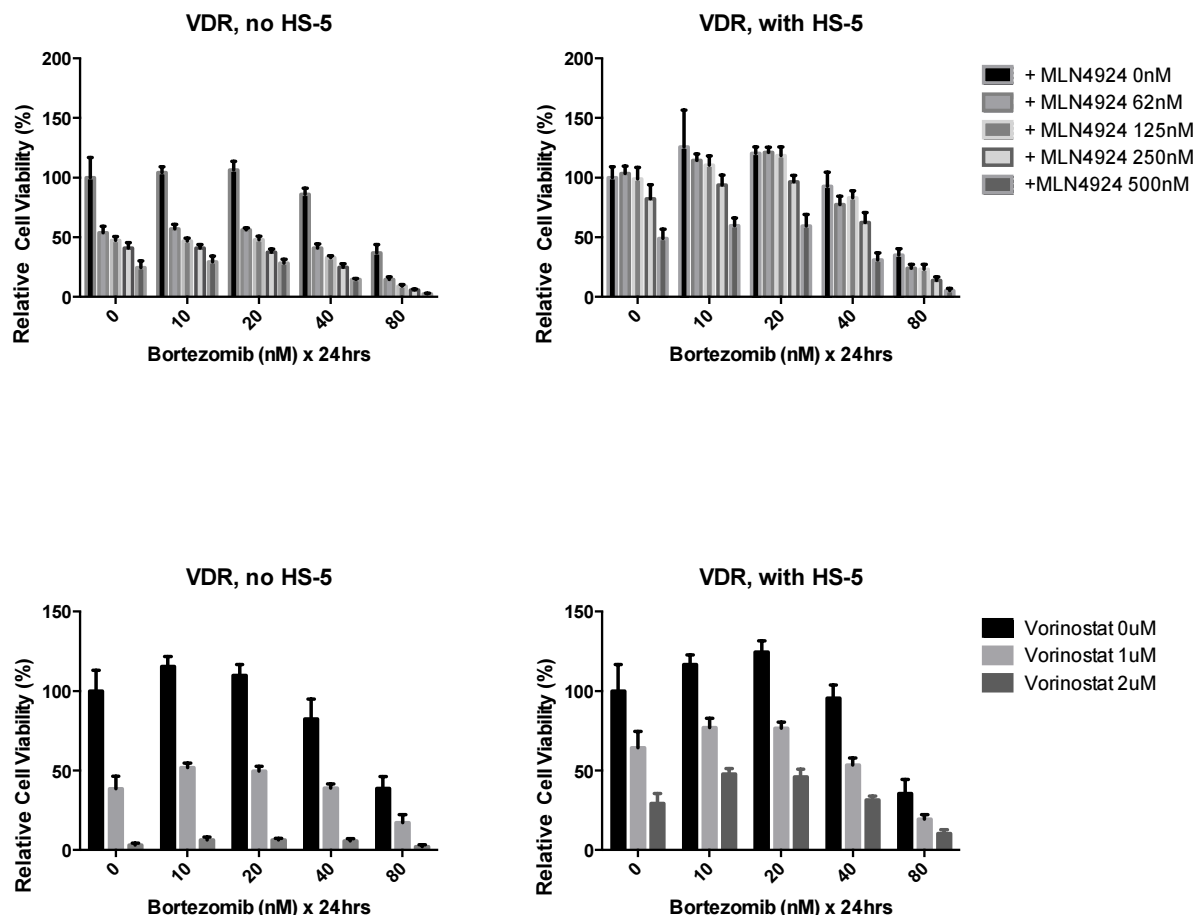


Figure 3.5.3.2 Effect of HS-5 stromal cells on efficacy of novel and investigational reagents in combination with bortezomib.

VDR cells were cultured alone or in the presence of HS-5 stromal cells for 24hours with subsequent 72-hour treatment with either MLN4924 or vorinostat alone, and each in combination with bortezomib 0-80nM for 24hours. Again by CSBLI a marked reduction in sensitivity of VDR cells in co-culture for either reagent is observed despite their combination with bortezomib, suggesting that the bone marrow microenvironment also confers resistance to bortezomib-containing combination regimens in VDR cells *in vitro*.

3.5.4 Effect of osteoblasts on proliferation rate and sensitivity of MM.1S, MM.1R and VDR to therapies *in vitro*

In order to examine further bone marrow accessory cells involvement in bortezomib resistance we next undertook a series of experiments to examine the potential role that osteoblasts play in the pathogenesis of bortezomib resistance.

We first examined the baseline effect of osteoblast-like cell line hFob (immortalised human foetal osteoblast-like 1.19 cells) on the proliferation rate of a number of multiple myeloma cell lines (n=8). On day 1 hFob was plated at a seeding density of 40,000 cells/mL and allowed to adhere overnight. The following day MM cell lines were added in triplicate at a seeding density of 20,000 cells/mL and cultured alone or in the presence of hFob cells for 24 and 48-hours. The bortezomib resistant cell line VDR displayed a marked increase in cell viability when co-cultured in the presence of hFob cell line at both 24 and 48-hour timepoints (figure 3.5.4.1), (see Materials and Methods 2.3 and 2.7 for further information of co-culture methods).

Next we examined the sensitivity of MM.1S, MM.1R and VDR to novel and conventional therapies following their co-culture with hFob cells. Again hFob cells were plated and allowed to adhere for 6 hours, before the addition of MM.1S, MM.1R or VDR to the plates, and each of the 3 cell lines were cultured alone or in the presence of hFob cells for 24 hours prior to treatment with either conventional (dexamethasone, doxorubicin), novel (bortezomib, lenalidomide, vorinostat) or investigational (JQ1) therapies. For this experiment the cells were plated in a 1:1 ratio to avoid MM cell overgrowth in the plates. We made a number of observations from these studies: firstly MM.1S appeared to be the cell line that was most susceptible to changes in drug sensitivity when co-cultured with hFob cells, and this was observed in treatments with dexamethasone, doxorubicin and vorinostat. In addition resistance to doxorubicin was evident in MM.1R and VDR cells in co-culture with hFob also. No change in sensitivity of any cell line to lenalidomide, JQ1 or bortezomib was observed when in co-culture with hFob (figure 3.5.4.2).

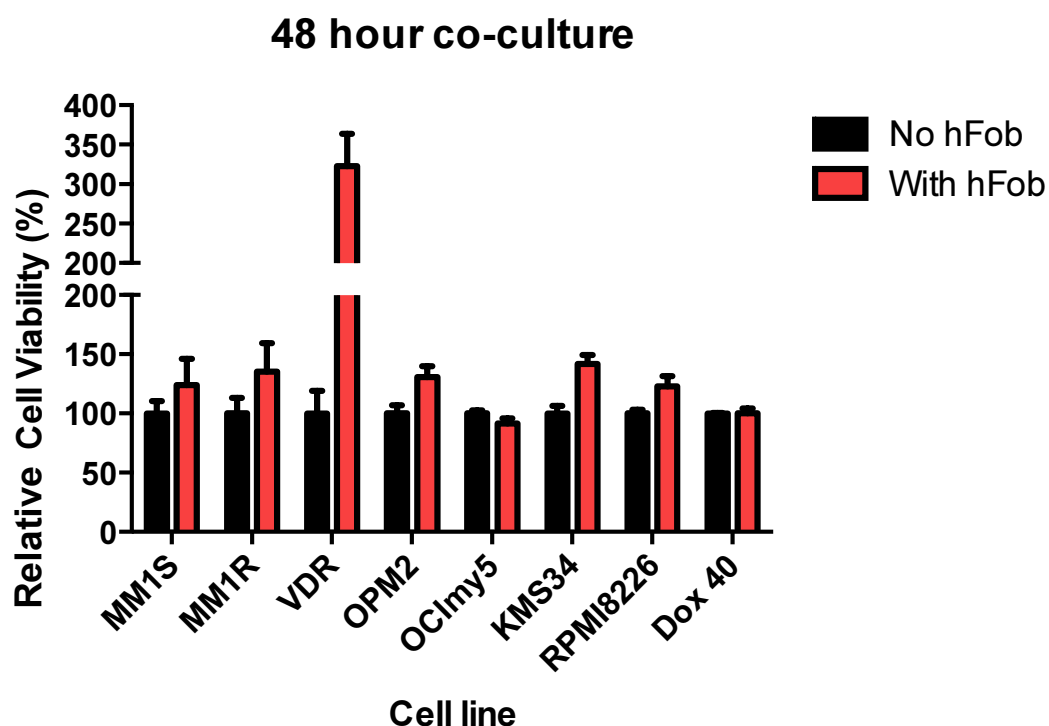
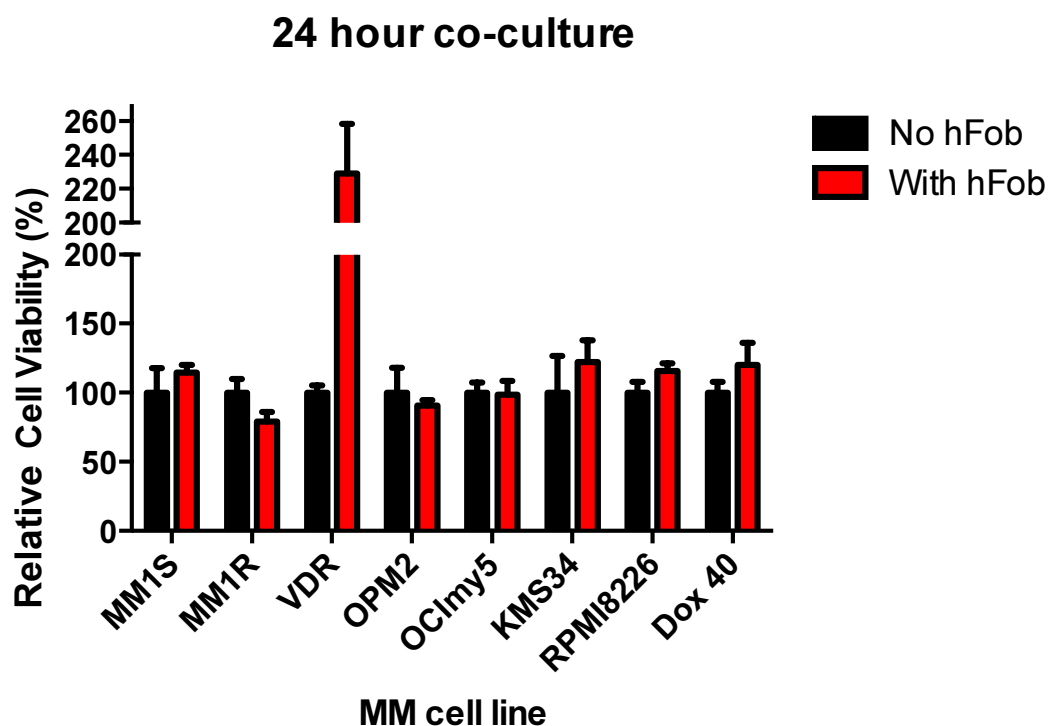


Figure 3.5.4.1: Relative cell viability of MM cell lines following their co-culture with immortalised human foetal osteoblast-like cell line hFob. VDR cell line in co-culture with hFob 1.1.9 revealed a marked increase in relative cell viability compared to VDR in culture alone after 24 and 48 hours.

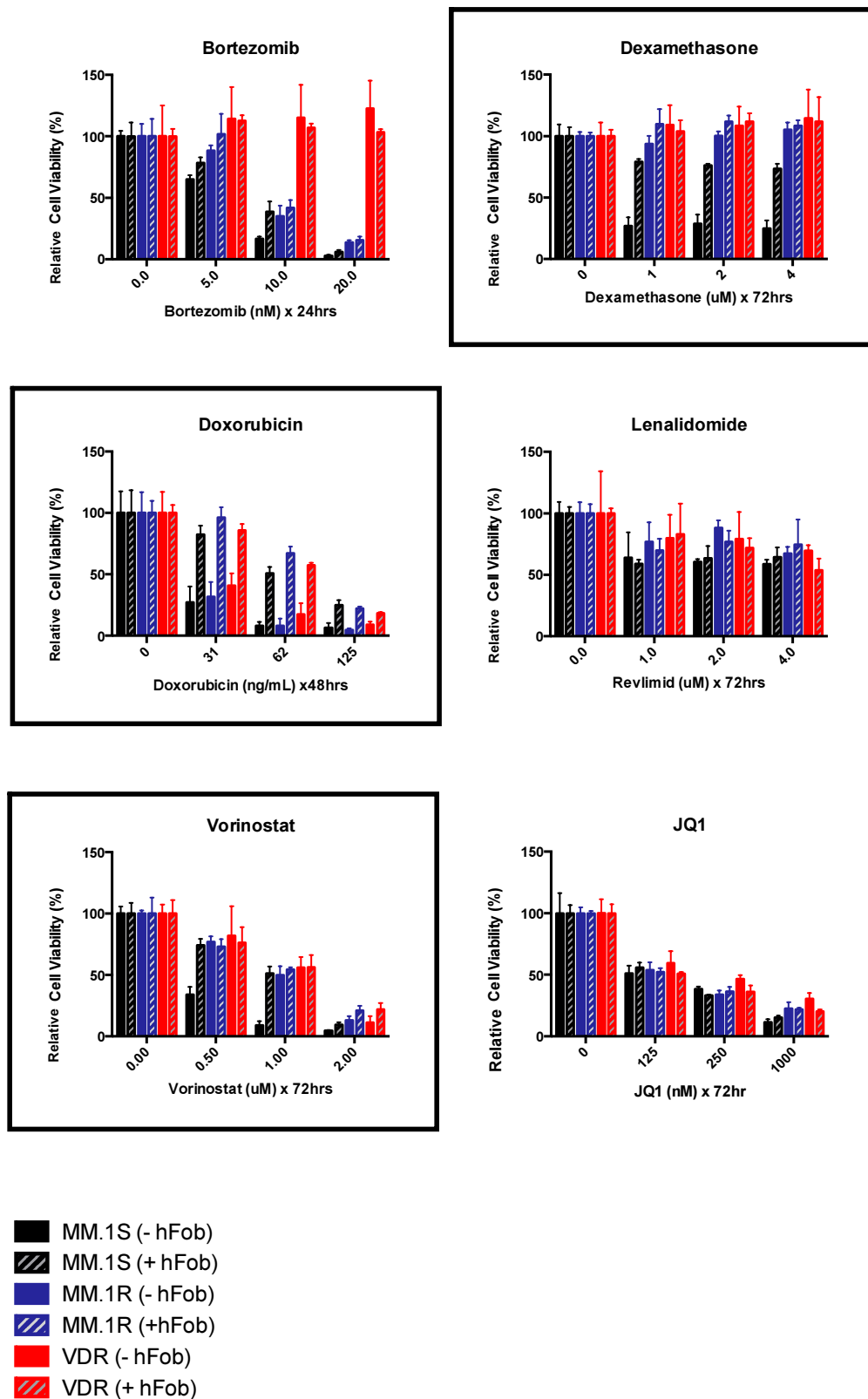


Figure 3.5.4.2: Sensitivity of MM.1S, MM.1R and VDR to novel and conventional therapies following co-culture with hFob cells. MM.1S, MM.1R and VDR cells were cultured in the presence and absence of hFob cells and subsequently treated with bortezomib, dexamethasone, doxorubicin,

lenalidomide, vorinostat or JQ1. (Note 1: Black= MM.1S, Blue= MM.1R, Red= VDR; Solid=no hFob; Stripes= Plus hFob). (Note 2: black squares indicate observations of drug resistance in MM.1S cell line in co-culture with hFob).

3.5.5 Role of direct cell-to-cell contact in osteoblast-like cell-induced drug resistance in MM.1S

As we observed a change in the drug sensitivity in MM.1S to a number of reagents following their co-culture with osteoblast-like cells hFob, we next determined whether or not direct cell to cell contact was necessary for this observation to occur.

Transwell plates were used to culture MM.1S cells in the presence and absence of hFob cells, those in co-culture were not however in direct contact (see Materials and Methods section 2.16). The cellular compartments were treated with doxorubicin, vorinostat or lenalidomide as previously described. Once treatment was complete, the viability of the MM.1S cells was analysed by CSBLI.

We again observed a significant reduction in sensitivity of MM.1S to doxorubicin when MM.1S was in co-culture with hFob but without direct cell-to-cell contact, suggesting that direct cell-to-cell contact is not essential for hFob-induced doxorubicin resistance in MM.1S. No change in sensitivity was observed in MM.1S cells treated with vorinostat when in co-culture with hFob, suggesting that direct cell-to-cell contact is necessary in osteoblast-induced resistance to vorinostat. Finally, as a control, MM.1S cells were co-cultured without direct cell-to-cell contact also with hFob, and treated with lenalidomide. Our previous observation, i.e. no change in sensitivity to lenalidomide when the cells are in direct contact with hFob, was confirmed in the transwell experiment (Figure 3.5.5.1).

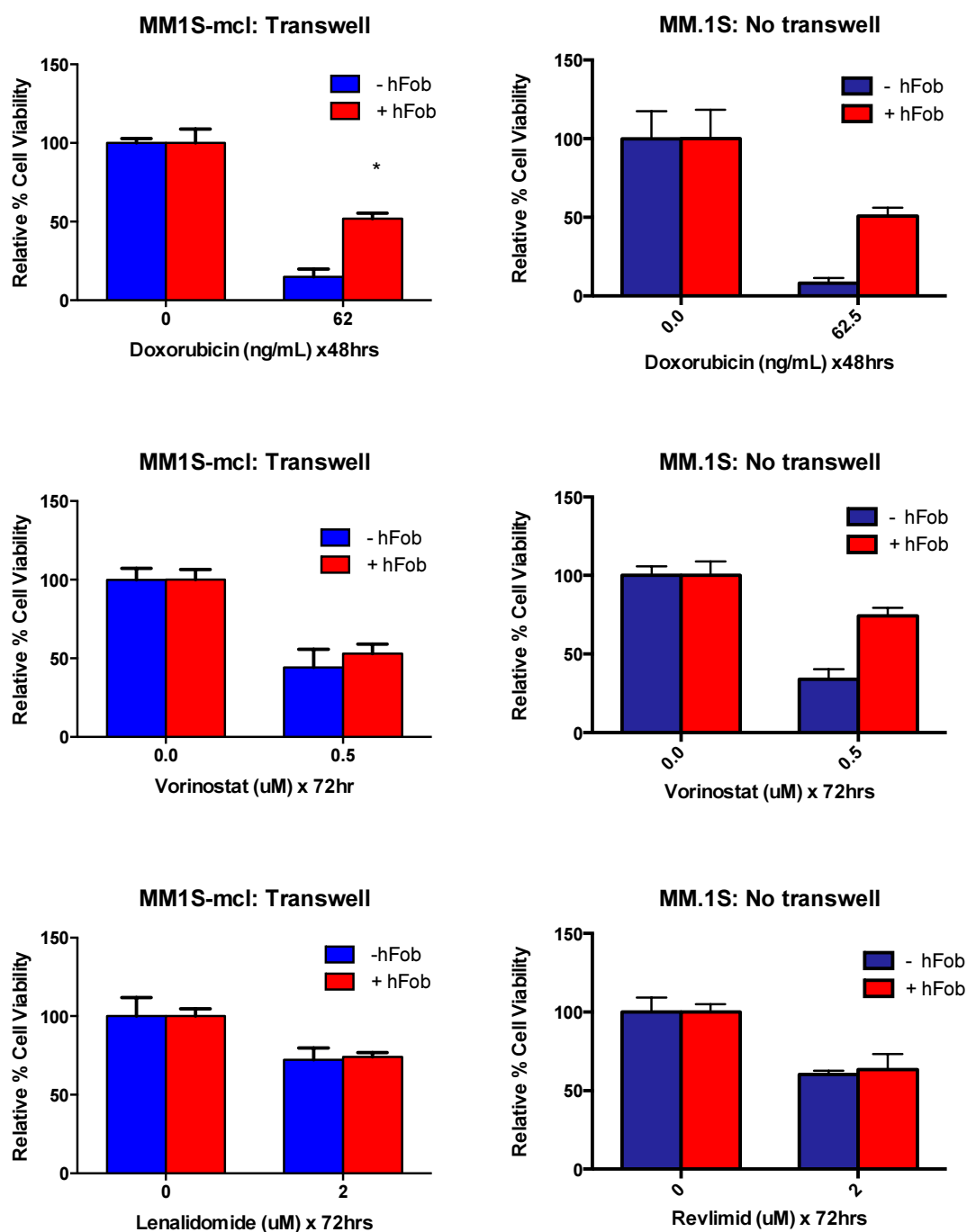


Figure 3.5.5.1: Assessment of sensitivity of MM.1S cells to doxorubicin, vorinostat or lenalidomide in co-culture with hFob in Transwell System.

MM.1S cells were co-cultured with hFob in a transwell system without direct cell-to-cell contact and the cell viability of MM.1S examined by CSBLI following treatment with doxorubicin, vorinostat or lenalidomide. (*= $p < 0.05$). Previous co-cultures without transwell are depicted here on the right for comparative purposes.

3.5.6 Role of cell-to-accessory cell ratio and protein content in observed osteoblast-like cell-induced resistance

To determine if resistance observed in MM.1S cells co-cultured in the presence of osteoblasts is secondary to local mass effect or MM cell to accessory cell ratio, we further tested the validity of the previous results by adding luciferase negative MM cells to luciferase positive MM.1S-mcl cells instead of osteoblasts to determine whether or not the prior results could be replicated simply by adding the same number of myeloma cells to the co-culture condition that equals the cell volume of osteoblasts.

In order to achieve this we first determined the protein content of myeloma cells and osteoblasts. Equal numbers (1×10^6) of RPMI-8226 myeloma cells and osteoblasts were counted, and stored as described at -80°C in cell pellets in preparation for protein quantification (see materials and methods 2.9). The protein content of osteoblast-like hFob 1.19 cells was approximately 5 times greater than that of RPMI8226 MM cells (figure 3.5.6.1).

Next we determined if luciferase negative myeloma cells, plated in a ratio of equal protein content to hFob, replicated the resistance observed in MM.1S-mcl cells in co-culture with hFob. Therefore we plated either 1,000 hFob cells or 5,000 luciferase negative MM.1S cells in 96-well plates, and as before allowed MM.1S-mcl (luciferase positive) cells to co-culture with hFob or non-luciferase MM.1S, and subsequently treated each condition with doxorubicin or vorinostat.

We found that MM.1S-mcl cells again displayed resistance to vorinostat or doxorubicin when co-cultured in the presence of hFob, however these results were not replicated when co-cultured in the presence of non-luciferase MM.1S cells. These results suggest that the observation of hFob-induced resistance to MM.1S is not secondary to local mass effect (figure 3.5.6.2).

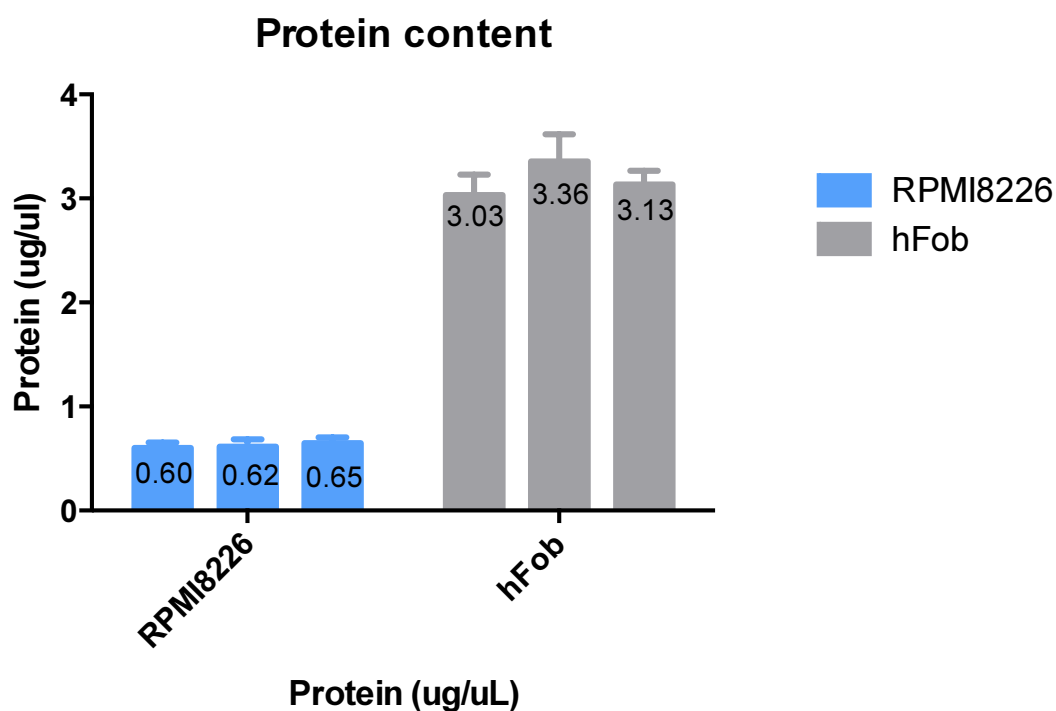


Figure 3.5.6.1 Protein content of RPMI8226 myeloma cells and hFob cells

1 x10⁶ RPMI8226 MM cells and hFob cells were counted in biological triplicate, and the protein content of each biological triplicate was measured in technical replicate. Values shown represent the average protein content in ug/uL per equal cell number of technical triplicates for each respective biological replicate.

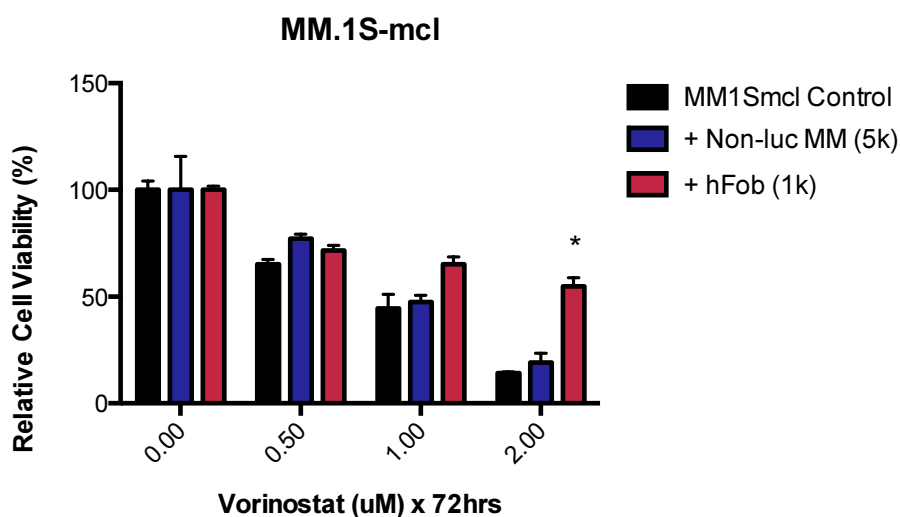
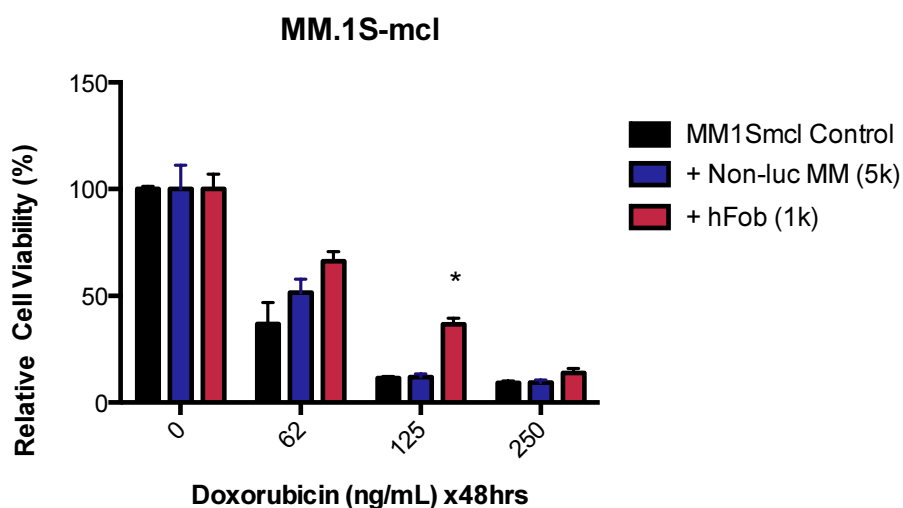


Figure 3.5.6.2: Determining if local mass effect of luciferase-negative cells can replicate the resistance observed in MM.1S following its co-culture with hFob.

MM.1S-mcl positive cells were co-cultured with luciferase-negative MM.1S cells (i.e. “Non-luc MM”) or hFob cells at equal protein volumes and subsequently treated with doxorubicin or vorinostat. The resistance observed to doxorubicin or vorinostat in MM.1S-mcl in co-culture with hFob was not replicated when MM.1S-mcl cells were co-cultured with luciferase-negative cells. (*= $p < 0.05$ when comparing MM.1S-mcl control to MM.1S + hFob).

3.5.7 Upregulation of PSMB8 by interferon-gamma increases the sensitivity of VDR cell lines to bortezomib

Bortezomib principally inhibits the proteasome by binding the PSMB5 subunit of the 20S core particle. Given that there is marked over-expression of PSMB5 in VDR cells, in addition to an inherent mutation of PSMB5, we speculated as to whether or not upregulation of the immunoproteasome subunit PSMB8 (or LMP7 or $\beta 5i$) that is analogous to PSMB5 proteasome subunit could result in resensitisation of VDR cells to bortezomib.

The immunoproteasome has been well documented for its role in MHC Class-I antigen presentation. Immunoproteasome subunit generation is induced in cells by the presence of interferon-gamma. Once generated, immunoproteasome subunits are introduced into newly generated proteasome 20S cores instead of constitutive subunits. Even though interferon- gamma results in replacement of constitutive subunits with immunoproteasome subunits into the proteasome structure, its presence does not appear to alter the overall content of $\beta 5$, $\beta 1$ or $\beta 2$ mRNA within cells. In fact following interferon-gamma stimulation of cells, cells are found to contain proteasomes with a mixture of $\beta 5$, $\beta 1$ and $\beta 2$ subunits, or $\beta 5i$, $\beta 1i$ and $\beta 2i$ subunits.^[54] We investigated whether or not we could overcome bortezomib resistance in VDR cells by inducing the immunoproteasome subunit PSMB8 via interferon gamma, and allow proteasome inhibition in the VDR cells to occur through the $\beta 5i$ subunit, namely PSMB8.

On day 1 MM1R and VDR cells were plated in 96-well plates in the absence or presence of interferon-gamma (0 or 200U/mL for 48hours). After 48 hours the cells were treated with bortezomib for 24 hours and the cell viability measured by CTG.

We found that the addition of interferon gamma to MM.1R cells did not change its sensitivity to bortezomib. In VDR we noted an increased sensitivity for bortezomib at dose concentrations of 20, 40 and 80nM when the cells were pre-treated with interferon-gamma 200IU/mL, (figure 3.5.7.1). Subsequent western blot of the aforementioned conditions confirmed up-regulation of PSMB8 in VDR cells pre-treated with interferon gamma, consistent with the possibility that the

increased sensitivity of VDR cells to bortezomib that were pre-treated with interferon gamma may be in part mediated by PSMB8 up-regulation. We also observed down-regulation of PSMB5 in MM.1R and VDR following interferon-gamma treatment. We assessed whether or not accumulation of polyubiquitinated proteins occurred in MM.1R and VDR cell with interferon-gamma pre-treatment prior to bortezomib treatment. We observed a modest degree of accumulation of poly-ubiquitinated proteins in VDR cells following treatment with bortezomib when they were pre-treated with interferon gamma, suggesting that the proteasome-ubiquitination pathway is at least partially activated in VDR cells when PSMB8 is up-regulated (figure 3.5.7.2).

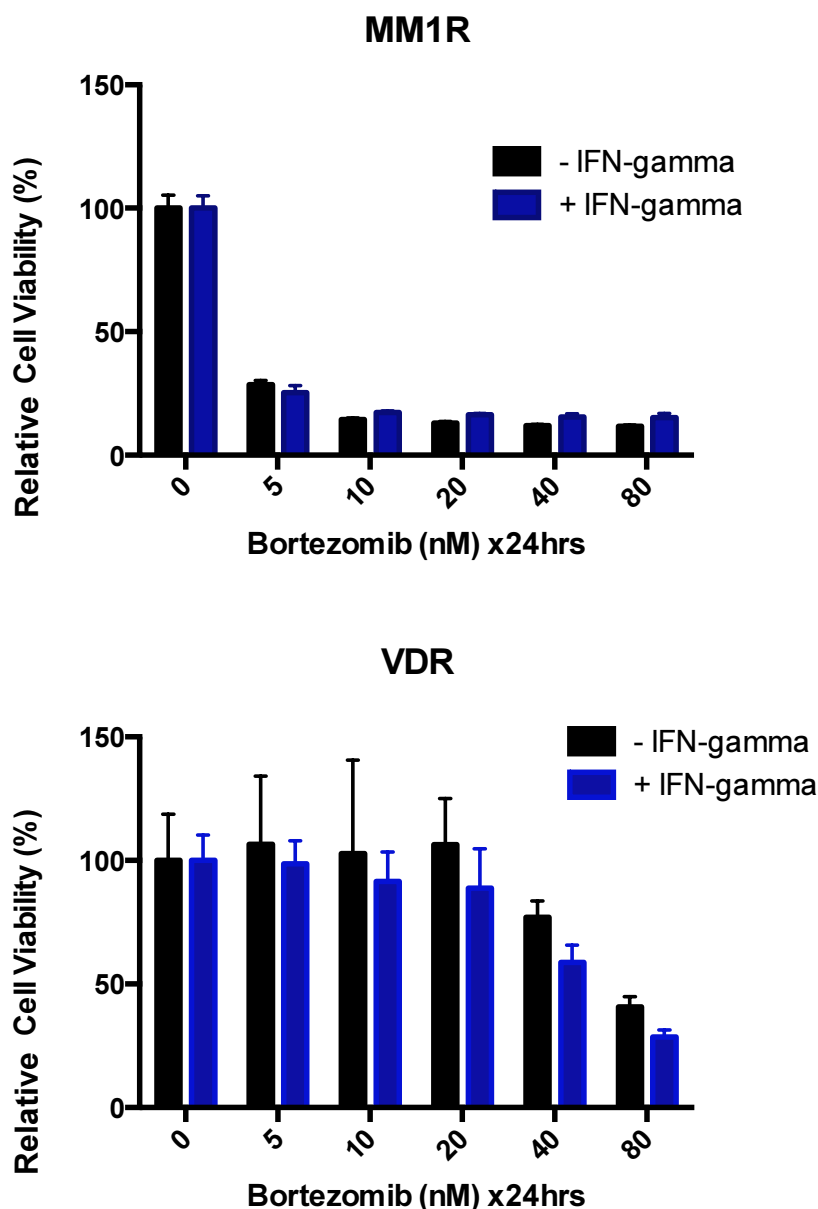


Figure 3.5.7.1 Pre-treatment of VDR cells with interferon gamma results in increased sensitivity of VDR cells to bortezomib.

MM.1R or VDR cells were pre-treated with interferon gamma 200IU/mL and subsequently treated with bortezomib as illustrated for 24 hours. Pre-treatment of VDR cells with interferon-gamma resulted in increased sensitivity of VDR cells to bortezomib as demonstrated, however p value for “- IFN-gamma” vs. “+IFN-gamma” were not statistically significant.

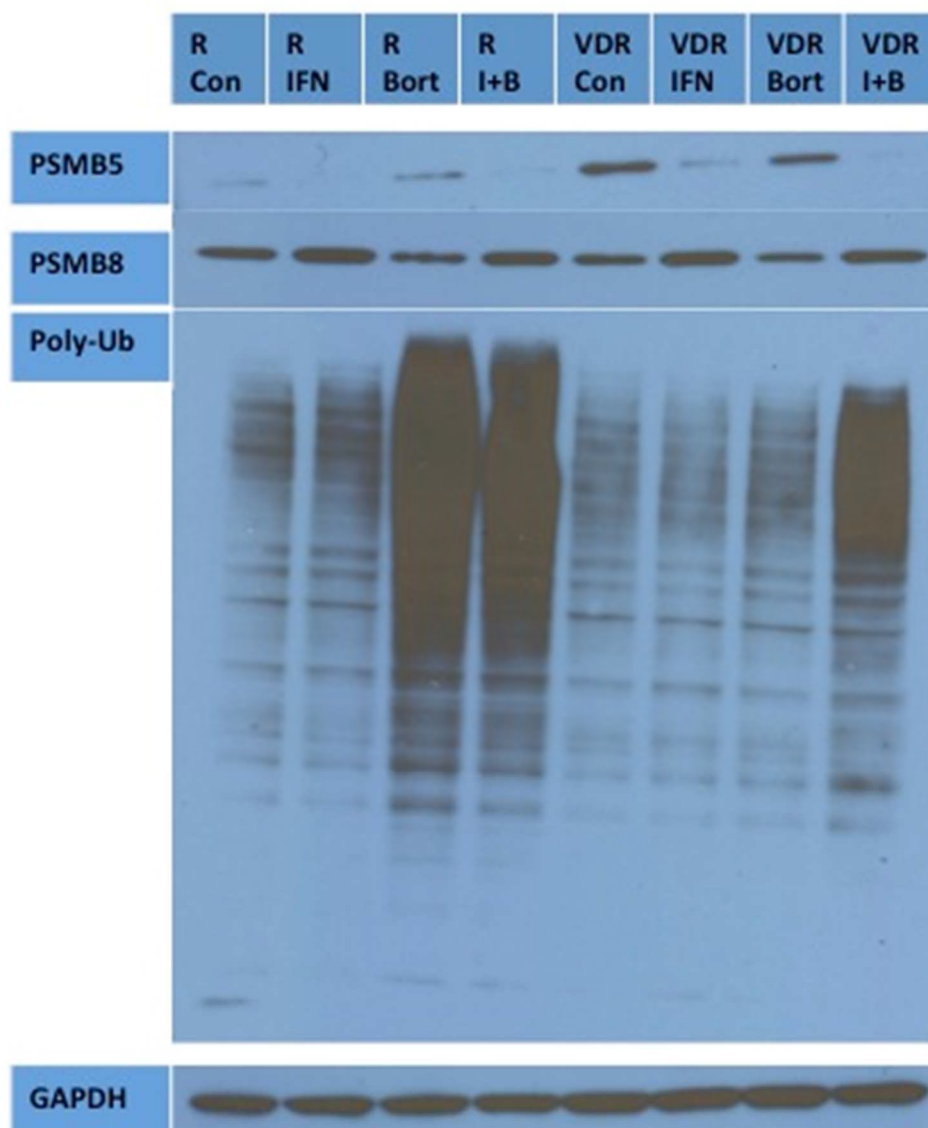


Figure 3.5.7.2: Interferon gamma results in up-regulation of PSMB8 and down-regulation of PSMB5 in both MM.1R and VDR cell lines.

MM.1R or VDR cell lines were treated alone or in combination with interferon gamma or bortezomib. Interferon gamma, both in the presence and absence of bortezomib (20nM for MM.1R, 80nM for VDR) resulted in modest up-regulation of PSMB8 and down-regulation of PSMB5. Additionally, an increase in poly-ubiquitinated protein accumulation was observed following bortezomib treatment in VDR cells that had been pre-treated with interferon gamma.

Figure legend:

R= MM.1R; Con= Control; I/ IFN= Interferon gamma; B/Bort= Bortezomib

3.5.8 PSMB5 and PSMB8 expression *in vivo*

Our previous results suggest that PSMB5 is over-expressed and mutated *in vitro* in VDR cells. By pre-treating VDR cells with interferon-gamma, which appears to upregulate the immunoproteasome counterpart PSMB8, we observed partial resensitisation of VDR cells to bortezomib. In order to investigate the importance of this observation in the *in vivo* setting, we performed immunohistochemistry (IHC) on a number of samples from patients with multiple myeloma for PSMB5 and PSMB8 expression levels.

Clinical data and bone marrow trephine slides from the multiple myeloma biobank were kindly provided by Dr. Kay Reen Ting and Dr. Colm Cosgrove at Dublin City University. Patient samples selected were as follows: 7 diagnostic samples of patients who achieved at least VGRP following a bortezomib-based regimen; 6 diagnostic samples of patients who received a bortezomib-based regimen and subsequently relapsed, and finally 7 samples from patients who relapsed following a bortezomib-based regimen (6 of which correlate to the latter diagnostic samples), (see materials and methods section 2.1.7). Response criteria were defined by IMWG response criteria in multiple myeloma. Immunohistochemistry was performed as per departmental protocol (materials and methods section 2.18).

A number of interesting observations were made. PSMB5 is expressed in both diagnostic samples of bortezomib-responders and bortezomib-non-responders. In this matched comparison, in 3 out of 7 samples tested, PSMB5 expression is reduced at time of relapse in bortezomib-non-responders compared to the corresponding diagnostic samples (table 3.5.8.1). PSMB8 was expressed in all diagnostic samples of bortezomib-responders and in 5 out of 6 diagnostic samples of bortezomib-non-responders. PSMB8 expression was markedly reduced in relapsed samples of bortezomib-non-responders compared to their correlating diagnostic sample. However in 2 out of 7 samples, PSMB8 was still expressed at time of relapse in bortezomib non-responders. In one of the latter samples, PSMB8 expression was negative at diagnosis and positive at time of relapse (table 3.5.8.2).

In summary PSMB5 was over-expressed and PSMB8 suppressed in bortezomib refractory patients at time of relapse. In VDR we demonstrated over-expression of PSMB5 at the protein level, have outlined its potential role in bortezomib resistance *in vitro*, and the potential to overcome this resistance by up-regulation of PSMB8 using interferon-gamma. Therefore perhaps pre-treatment with interferon gamma and subsequent bortezomib treatment would increase the efficacy of bortezomib in bortezomib-refractory myeloma *in vivo*.

In addition PSMB8 appears to be strongly expressed at diagnosis in both bortezomib-responders and bortezomib non-responders supporting the role for a PSMB8-specific inhibitor *in vivo*. PSMB8 inhibitors are now currently commercially available and under investigation in the pre-clinical setting, for example PR-924 has been documented for its efficacy in multiple myeloma in the *in vitro* and *in vivo* setting in a SCID-hu mouse model of plasmacytoma xenografts.^[58] Our *in vivo* data support the suggestion by Singh et al to assess the efficacy of PSMB8 inhibitors in the *in vivo* setting for treatment of newly diagnosed multiple myeloma, alone or perhaps in combination with bortezomib, to achieve dual PSMB5 and PSMB8 inhibition. In two of the bortezomib-refractory samples at time of relapse, PSMB8 was over-expressed, also supporting a role for PSMB8 inhibitors in relapsed and refractory disease.

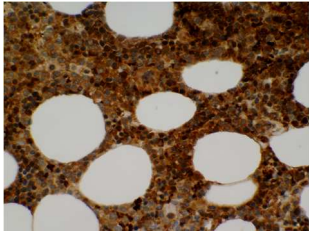
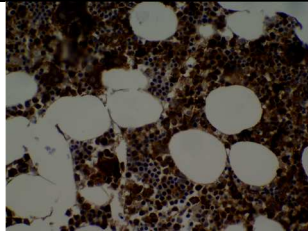
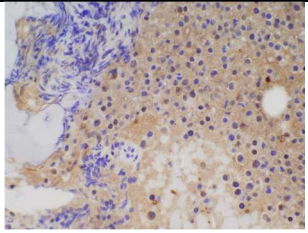
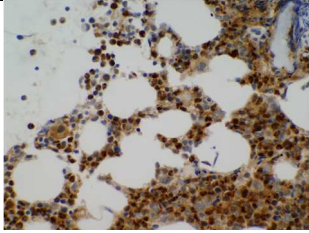
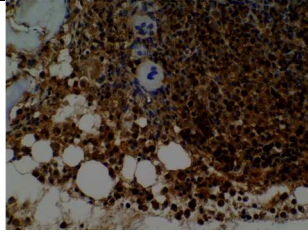
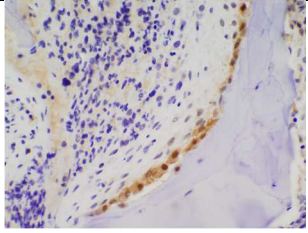
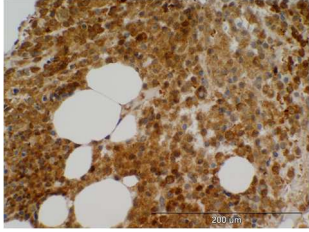
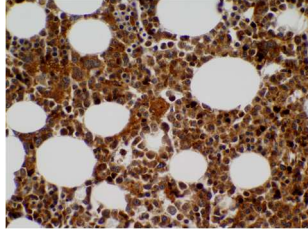
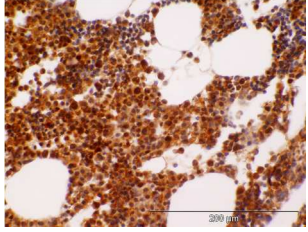
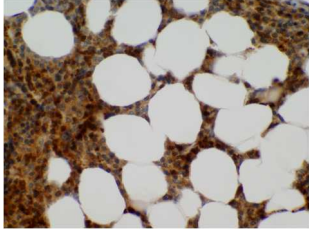
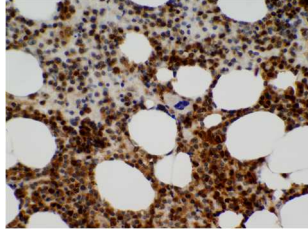
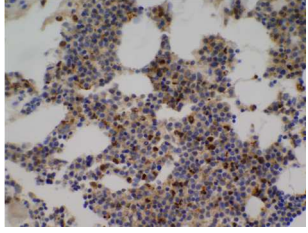
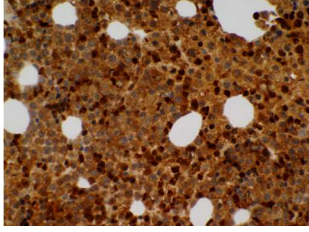
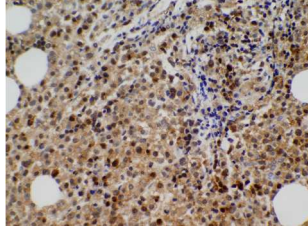
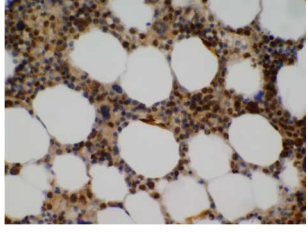
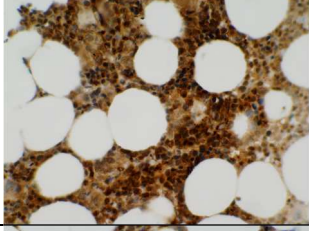
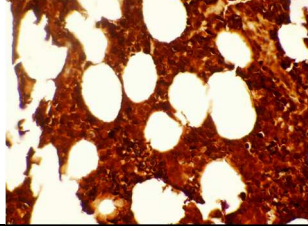
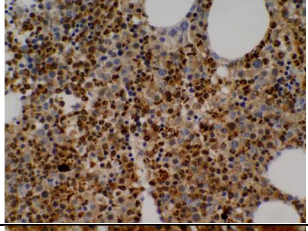
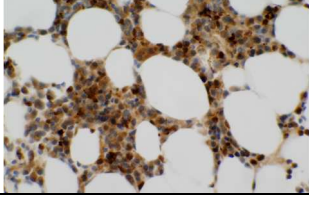
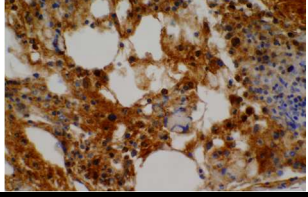
Anti-PSMB5	Diagnostic: Responder	Diagnostic: Non-Responder	Relapsed: Non-Responder
Sample 1			
Sample 2			
Sample 3			
Sample 4			
Sample 5			
Sample 6			
Sample 7		Sample not available.	

Table 3.5.8.1: Immunohistochemistry of bone marrow trephines of multiple myeloma patients stained for PSMB5.

PSMB5 expression was examined in known bortezomib responders on diagnostic bone marrow trephine samples, and also on diagnostic samples of known bortezomib non-responders with paired samples at time of relapse. A comparative diagnostic sample was not available for sample 7 non-responder.

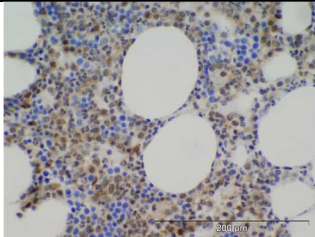
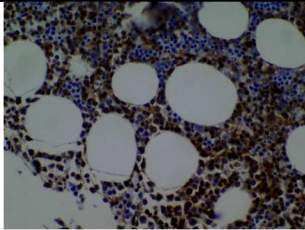
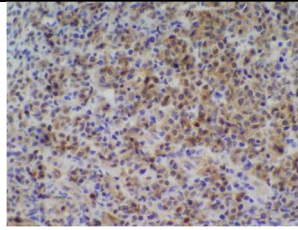
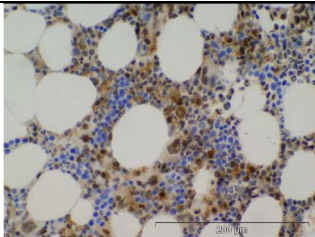
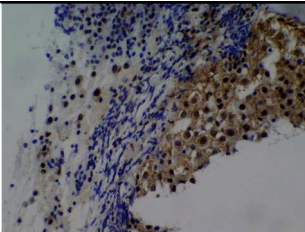
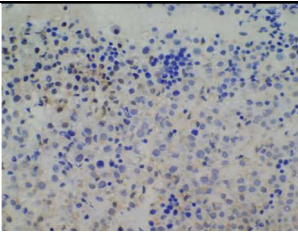
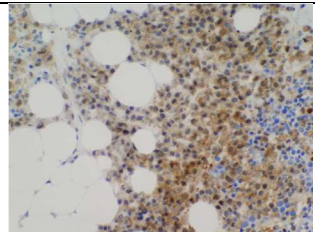
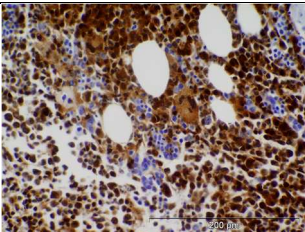
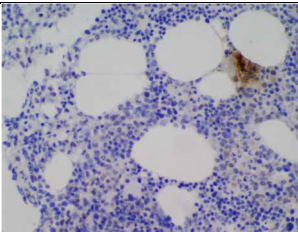
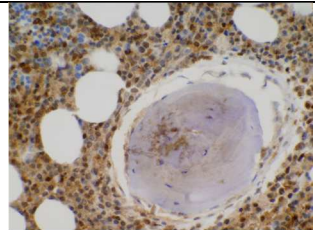
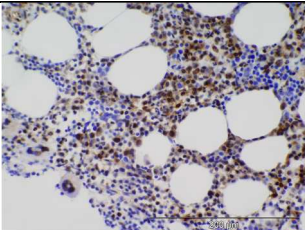
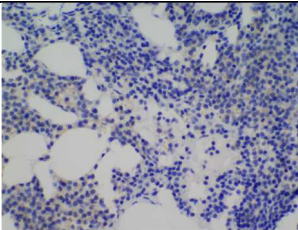
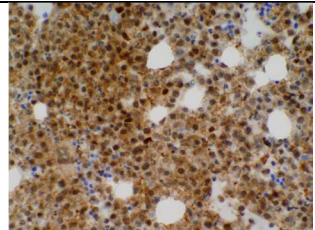
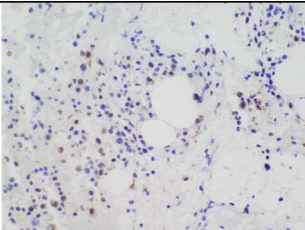
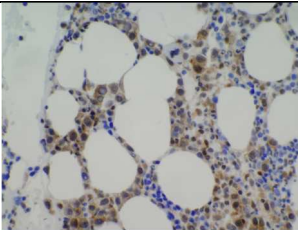
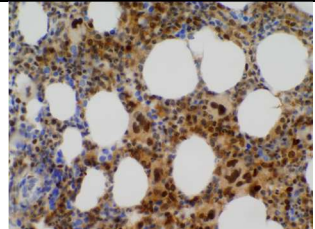
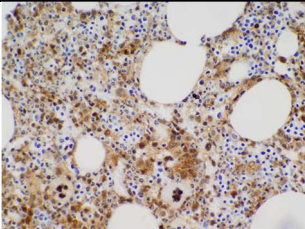
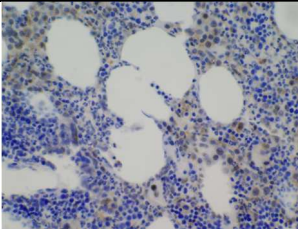
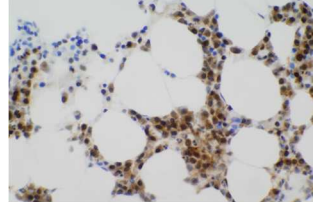
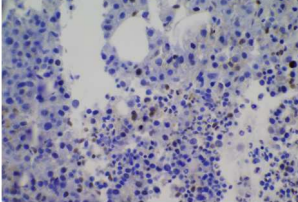
Anti-PSMB8	Diagnostic: Responder	Diagnostic: Non-Responder	Relapsed: Non-Responder
Sample 1			
Sample 2			
Sample 3			
Sample 4			
Sample 5			
Sample 6			
Sample 7		Sample not available.	

Table 3.5.8.2: Immunohistochemistry of bone marrow trephines of multiple myeloma patients stained for PSMB8.

PSMB8 expression was examined in known bortezomib responders on diagnostic bone marrow trephine samples, and also on diagnostic samples of known bortezomib non-responders with paired samples at time of relapse. A comparative diagnostic sample was not available for sample 7 non-responder.

3.5.9 Summary of functional studies

As previously outlined, the bone marrow microenvironment plays a major role in resistance mechanisms in MM by either direct or indirect interactions between bone marrow stromal cells and tumour cells. We thus undertook a number of functional studies to further explore the mechanism of bortezomib resistance in VDR.

We examined the sensitivity of the isogenic cell line model to conventional and novel therapies in the presence and absence of HS5 stromal cells. In relation to the sensitivity of MM.1R or VDR to proteasome inhibitors, we observed no change in the sensitivity of MM.1R to bortezomib despite its co-culture with HS-5 stromal cells, VDR retained the same degree of resistance to bortezomib following its co-culture with HS-5 cells, MM.1R cells appeared to display reduced sensitivity to carfilzomib following their co-culture with HS-5 cells, (the mechanism for which remains unclear) however VDR cells retained their sensitivity to carfilzomib despite their co-culture with HS-5 cells. VDR cells were found to demonstrate resistance to vorinostat and MLN4924 when co-cultured in the presence of HS-5 cells, and combination of bortezomib with either agent was not sufficient to overcome the resistance observed. These data emphasise the potent effect of the bone marrow microenvironment in drug resistance to bortezomib when it is used alone or in combination with other novel therapies.

We then investigated the effect of osteoblasts on the proliferation rate of the MM cells lines to ascertain if the stromal-induced effects were specific to HS5 cells or merely a cell-to-cell ratio effect. The bortezomib resistant cell line VDR displayed a marked increase in cell viability when co-cultured in the presence of hFob cell line compared to all other cell line tested. We furthermore examined the effect of osteoblasts on the drug sensitivity of MM.1S, MM.1R and VDR cell lines to a number of therapies. Interestingly MM.1S appeared to be the cell line that was most susceptible to changes in drug sensitivity when co-cultured with hFob cells, and this was observed in treatments with dexamethasone, doxorubicin and

vorinostat. In addition resistance to doxorubicin was evident in both MM.1R and VDR cells in co-culture with hFob. Transwell system was subsequently used to determine whether or not the observed resistance in MM.1S required direct cell-to-cell contact; we observed direct cell-to-cell contact appeared to be necessary for osteoblast-induced resistance to vorinostat in MM.1S, but was not necessary for osteoblast-induced resistance to doxorubicin in MM.1S. The resistance observed to doxorubicin or vorinostat in MM.1S-mcl in co-culture with hFob was not replicated when MM.1S-mcl cells were co-cultured with luciferase-negative cells, suggesting that this phenomenon is not a mass related effect secondary to the size of the osteoblast-like cells.

Given that there was marked overexpression of PSMB5 at the proteomic and transcript levels, in addition to the finding of a PSMB5 mutation in the VDR cell, we hypothesised if bortezomib resistance could potentially be overcome by up-regulating the PSMB5 immunoproteasome counterpart, PSMB8. By pre-treating VDR cells with interferon-gamma, we observed an increase in sensitivity of VDR cells to bortezomib and an increase in poly-ubiquitinated proteins, potentially by upregulation of PSMB8 as demonstrated by western blot. While interferon-gamma pre-treatment and subsequent PSMB8 over-expression did not completely resensitise VDR to bortezomib, it appears to have the potential to play a role in over-coming bortezomib resistance in VDR.

Finally, we ran immunohistochemistry on bone marrow trephines of patients with bortezomib-sensitive (diagnostic samples) and bortezomib-refractory (diagnostic and relapsed samples) multiple myeloma. PSMB5 was over-expressed and PSMB8 suppressed in bortezomib refractory patients at time of relapse. Thus perhaps pre-treatment of multiple myeloma patients with interferon gamma and could resensitise these patients to bortezomib, as demonstrated by our *in vitro* model. In addition PSMB8 appears to be strongly expressed at diagnosis in both bortezomib-responders and bortezomib non-responders supporting the role for use of PSMB8 inhibitors *in vivo*.

Chapter 4

Discussion

CHAPTER 4. DISCUSSION

4.1 CHARACTERISATION OF AN ISOGENIC CELL LINE MODEL OF BORTEZOMIB RESISTANCE IN VITRO AND IN VIVO.

4.1.1 Introduction

Multiple myeloma is an incurable malignancy characterised by uncontrolled proliferation of terminally differentiated B-lymphocytes, or plasma cells. The spectrum of abnormal plasma cell differentiation ranges from monoclonal gammopathy of uncertain significance, to smouldering myeloma, to fully active myeloma requiring treatment with chemotherapy. Major advances have been made in the past 10 years in particular in relation to the FDA approval of a number of novel therapies for the treatment of myeloma. Bortezomib now forms the cornerstone of combination therapies for the management of newly diagnosed and relapsed and refractory myeloma. However once patients develop resistance to bortezomib-containing regimens, the overall survival is dismal. Therefore for the purpose of this thesis we undertook a study of a cell line model of bortezomib resistance in order to further decipher potential intrinsic and extrinsic mechanistic pathways implicated in bortezomib resistance. We examined the toxicological profile of bortezomib-resistant VDR at baseline. We examined the sensitivity of VDR to bortezomib *in vivo*. We undertook whole exome sequencing, gene expression profiling and label-free mass spectrometry to identify mutations, genes or proteins respectively that may contribute to bortezomib resistance intrinsically. We examined extrinsic factors that may contribute to bortezomib resistance by examining the effect of bone marrow accessory cells on drug sensitivity in VDR cell line. Finally we examined bone marrow trephine samples of specific proteasome-associated subunits for their expression levels in patients with bortezomib-refractory myeloma. Overall, bortezomib resistance appears to be multifactorial, and intrinsic resistance mechanisms are further compounded by extrinsic factors in the local bone marrow microenvironment. Efforts to overcome these mechanisms of drug resistance will likely require the use of target-specific combination regimes to overcome specific resistance pathways that are altered.

4.1.2 The use of cell line models to examine bortezomib resistance *in vitro* and *in vivo*

As outlined in the introduction, patients with myeloma who relapse following treatment with novel therapies, have a very poor overall survival. This was outlined very explicitly by Kumar et al in their informative study of the prognosis of multiple myeloma patients when they no longer respond to novel therapies such as lenalidomide or bortezomib, whereby the overall survival in this group is approximately 9 months.^[4] It is essential that we continue in our efforts to provide our patients with better treatment options once they reach the inevitable drug-refractory stage of their illness, and given bortezomib forms the cornerstone of myeloma combination regimens, we chose to study resistance to bortezomib. Preclinical investigation of a bortezomib-resistant cell line, VDR, which had been generated in the laboratory of Dr Mitsiades therefore formed the cornerstone of this thesis.

We and others have used *in vitro* cell line models to study bortezomib resistance in multiple myeloma, and many groups have used cell line models to investigate drug resistance to other therapies for use in myeloma, such as lenalidomide and vorinostat.^[65, 135-137] Indeed a cell line model of carfilzomib resistance has also been developed from human lung and colonic adenocarcinoma cell lines to examine carfilzomib-resistance mechanisms in solid tumours.^[138] While these cell line models provide us with vast information pertaining to resistance mechanisms in the *in vitro* setting, one must take into account the pertinent role of the bone marrow microenvironment in multiple myeloma pathogenesis and drug resistance, in addition to factors in the bone marrow that attempt to deter myeloma cell growth.^[139-145] All in all, clonal myeloma cells and their bone marrow microenvironment should for all intents and purposes, be considered a collective entity in our efforts to study resistance mechanisms, as previously outlined by Schuler et al.^[146] Perhaps a more efficacious mode of investigating drug resistance in myeloma should involve the co-culture of myeloma cell lines on HS-5 stromal cells, or alternatively co-culturing myeloma cell lines on bone marrow stromal cells isolated from patients with multiple myeloma, and then exposing these cells to successive rounds of incremental doses of bortezomib.

Alternatively one could extract CD138-positive cells from bone marrow aspirates of multiple myeloma patients rather than using a cell line model, and successively expose these cells to bortezomib. However the latter may prove technically challenging, as CD138-positive plasma cells from patients do not proliferate readily in the *in vitro* setting, likely because they lack the supportive network of the bone marrow microenvironment.

Perhaps an *in vivo* model would be more efficacious in order to more truly reflect the bone marrow microenvironmental changes. A number of models may be suitable, such as the SCID-hu model that reflects bone disease similar to patients, or xenogeneic models in humanized mice that appropriately mirror the human bone marrow microenvironment. However these models do not come without their own limitations, such as restricted availability of human bone chips and huge laboratory expense for these preclinical models respectively.^[146]

Despite recent advances in preclinical models of multiple myeloma, cell line monoculture models remain the gold standard for preclinical studies of multiple myeloma pathogenesis and drug resistance mechanisms, and while they have their own set of limitations, their use in myeloma research has lead to the identification of a number of novel therapies for use in multiple myeloma patients.^[147]

4.1.3 Variations in the sensitivity of bortezomib-resistant cells to other therapies *in vitro*

As outlined in results section 1, VDR displays a 12-fold increase in IC₅₀ for bortezomib compared to parental MM.1R, and retains its resistance to dexamethasone similar to MM.1R (figures 3.1.2.1 and 3.1.3.1). Given that both cell lines are resistant to dexamethasone one could argue that biomarkers identified in both cell lines as potential targets of bortezomib resistance may in fact represent dexamethasone resistance biomarkers, and this is one limitation of our study. Therefore in all biomarker studies, we compared the differences in VDR compared to MM.1R cell line. Biomarkers that were present in both cell lines were not selected for further studies as these were assumed to be dexamethasone-resistance-associated targets.

On examining the cell line model for differences in sensitivity to other novel and conventional therapies, we made a number of interesting observations (figure 3.1.3.2). All three cell lines (MM.1S, MM.1R and VDR) displayed similar efficacy in the *in vitro* setting to the immunomodulators lenalidomide and pomalidomide, conventional therapies such as doxorubicin and vincristine, and the novel BET2-bromodomain inhibitor JQ1. In contrast, both MM.1R and VDR were less sensitive to the HDAC inhibitor vorinostat compared to MM.1S. By inhibition of HDAC1 and HDAC2, cellular apoptosis results.^[148] However in MM.1R and VDR it is unclear if responsiveness to HDAC inhibitors is due more so to HDAC1, HDAC2 or both equally.

4.1.4 Potential FDA-approved compounds that overcome bortezomib resistance in VDR

In order to examine a broader range of compounds for their toxicity to VDR cells, we chose to run a larger scale toxicity assay involving the use of FDA-approved data sets (figure 3.1.3.3). The purpose again here was to identify compounds that were more efficacious in VDR compared to the MM.1R cell line. 101 compounds in total were examined. While the majority of compounds demonstrated comparable toxicity in both cell lines, two specific groups emerged as demonstrating a higher relative percentage cell death in the VDR cell line compared to MM.1R. These included the taxanes and the topoisomerase inhibitors and each will be discussed in more detail.

Taxanes exert their anti-cancer effects principally by interrupting normal microtubule structure. A number of taxanes have been FDA-approved for their use in cancer treatment and those tested in this assay included cabazitaxel, docetaxel and paclitaxel. Paclitaxel and docetaxel are widely used in cancer of the ovary, stomach, lung, breast and prostate. Resistance to the taxanes is thought to be principally mediated by p-glycoprotein.^[149] Paclitaxel inhibits the G2/M stage of normal cell cycle and thus cells cannot form a normal apparatus of mitosis.^[150] Docetaxel works by similar means to paclitaxel by promoting the stabilisation of microtubules and ultimately also causing G2/M cell cycle arrest. However docetaxel is much more potent than paclitaxel, i.e. smaller doses of

docetaxel cause a greater degree of cell death than an equivalent dose of paclitaxel. This is reflected in our FDA-dataset results: 1nM of docetaxel results in >90% cell death of both VDR and MM.1R cells, whereas paclitaxel 1nM causes <50% cell death of either VDR or MM.1R cells. The reason why the taxanes were identified as a specific group with higher toxicity in VDR than MM.1R: 1nM of paclitaxel caused a much greater reduction in relative percentage viability in VDR (58.1%; SD9.65) compared to MM.1R (98.8%; SD 1.99). However 10nM paclitaxel caused >90% cell death in both cell lines, thus the taxanes are in fact efficacious to both bortezomib-sensitive MM.1R and bortezomib-resistant VDR (table 3.1.3.3).

Cabazitaxel, a novel taxane that functions similarly to docetaxel, is a poor p-glycoprotein substrate and thus is less susceptible to p-glycoprotein mediated drug resistance. Cabazitaxel has recently been documented for its efficacy in phase 1 clinical trials in castration-resistant prostate cancer.^[151, 152] In our cell line model, MM.1R and VDR were both highly sensitive to the novel taxane cabazitaxel, at both 1nM and 10nM concentrations.

In summary, while VDR appears to be more sensitive to paclitaxel 1nM than MM.1R, paclitaxel 10nM, cabazitaxel 1nM and 10nM, and docetaxel 1nM and 10nM all appear to be highly potent to both MM.1R and VDR cell lines. While we cannot conclude that the taxanes may overcome bortezomib resistance (i.e. they appear to be overall equally toxic to both MM.1R and VDR), we have demonstrated that the taxanes exert a high degree of relative reduction in cell viability in both myeloma cell lines, and support the use of taxanes in multiple myeloma treatment. Paclitaxel in combination with gemcitabine for example has been investigated in phase 2 clinical trials in patients with relapsed multiple myeloma. This was a small study involving 12 patients only; interestingly one patient achieved a complete remission with 98% reduction in serum M protein and percentage plasma cells in the bone marrow, and furthermore achieved a 6 month complete remission. While this study was quite limited in terms of numbers, the overall result concluded that this combination regimen was tolerated well by patients and is an active regimen in relapsed and refractory myeloma.^[153]

The topoisomerase inhibitors also appeared to exert a greater reduction in relative cell viability in VDR compared to MM.1R cell line, therefore this finding was also examined in greater detail. Topoisomerase 1 (TOP1) causes relaxation of DNA coils in replicating cells, and when TOP1 is inhibited, excess torsional strain within the DNA template results in arrest of the movement of the replication fork, DNA double-strand breaks and sequential cell death.^[154] Topoisomerase 2 (TOP2) is an enzyme that untangles DNA which involves a transient DNA break in order to achieve successful DNA unknotting. Inhibition of TOP2 occurs whilst TOP2 attempts to untangle knotted DNA at the point of transient DNA breakage, with subsequent generation of permanent DNA double-strand breaks in the genome, next resulting in the formation of further insertions, deletions and genomic aberrations, and finally initiation of apoptotic events which cause cell death.^[155] In our set of drugs analysed for their toxicity in MM.1R and VDR, TOP1 inhibitors included irinotecan and topotecan. TOP2 inhibitors included etoposide, teniposide, doxorubicin, daunorubicin and mitoxantrone.

No differences in toxicity between MM.1R and VDR were observed in treatment with irinotecan, etoposide, doxorubicin or mitoxantrone at either 1nM or 10nM concentrations tested. Topotecan, teniposide and daunorubicin at a 10nM concentration exerted a much greater reduction in relative cell viability in VDR compared to MM.1R, (74.9% \pm 6.2 versus 50.4% \pm 17.8 for topotecan; 101.8% \pm 03.4 versus 65.3% \pm 4.6 for teniposide; and 83.8% \pm 1.1 vs. 48.8% \pm 1.3 for daunorubicin), (table 3.1.3.2). Therefore topoisomerase inhibitors as a group appeared to display greater toxicity in VDR compared to MM.1R at 10nM concentrations. However, it is important to note that mitoxantrone was highly toxic to both MM.1R (5.2% cell viability post treatment), and VDR (5.5% cell viability post treatment). Mitoxantrone was created in the 1980s as a doxorubicin analogue with reduced cardiac side effects compared to doxorubicin. It has a prolonged half-life ranging from almost 9 hours to 9 days. It intercalates DNA, similar to doxorubicin, but also exhibits additional modes of action such as altering the immune response by suppressing cytokine secretion.^[156] This may in part explain its toxicity in myeloma cell lines MM.1R

and VDR. In conclusion, topotecan, teniposide and daunorubicin were identified by our screen as drugs that appear to exhibit greater reduction in relative cell viability in VDR compared to MM.1R, however topoisomerase inhibitors as a whole do not appear to be more efficacious in their toxicity in VDR over MM.1R. Mitoxantrone appears to be the most potent TOP inhibitor of all drugs tested, suggesting a role for its use preferentially to other TOP inhibitors in multiple myeloma.

4.1.5 The efficacy of novel proteasome inhibitors in the setting of bortezomib resistance *in vitro*

VDR cell line demonstrated marked resistance to bortezomib in the *in vitro* setting. Therefore we examined 2 further proteasome inhibitors available in the laboratory for their toxicity to VDR cells, carfilzomib and ixazomib (MLN2238), (figure 3.1.4.1). Carfilzomib is an irreversible panproteasome inhibitor and has been FDA-approved for use in multiple myeloma therapy. Ixazomib is a novel orally bioavailable proteasome inhibitor which reversibly inhibits the beta-5 subunit specifically, similar to bortezomib, and is currently in phase 3 clinical trials for treatment of multiple myeloma.^[51] Carfilzomib displayed marked toxicity to VDR cell line, as well as parental MM.1R. Interestingly, VDR displayed significant resistance to ixazomib (MLN2238). Stessman et al reported on a bortezomib resistant cell line in 2013, which displayed cross-resistance to both carfilzomib and MLN2238. Their cell line, termed BzR, displayed increased levels of PSMB5 compared to parental bortezomib-sensitive cell line, similar to VDR, however no mutations of the PSMB5 gene were detected.^[101] Therefore perhaps resistance to bortezomib and MLN2238 in VDR is mediated by mutPSMB5 gene in VDR, however this remains to be fully elucidated.

4.1.6 P-glycoprotein does not mediate bortezomib resistance in VDR

P-glycoprotein (P-gp) acts as an efflux pump to shunt drugs out of the cell as a mechanism of drug resistance. Recently our group published on the role of P-gp in bortezomib resistance in myeloma, and demonstrated that bortezomib is subject to pharmacokinetic resistance mediated by P-gp. This work suggested a role for the combination of a P-gp inhibitor with bortezomib in P-gp positive

myeloma.^[104] Therefore we wanted to ascertain whether or not a P-gp inhibitor in combination with bortezomib would resensitise the VDR cells to bortezomib. We therefore compared the sensitivity of VDR (unknown P-gp expression) and Dox40 (known to over-express P-gp) myeloma cell lines to combinations of bortezomib or carfilzomib or MLN2238, with the P-gp inhibitor elacridar (figure 3.1.5.1 and figure 3.1.5.2). In Dox40 cell line, sensitisation to bortezomib and carfilzomib were observed when either agent was used in combination with elacridar. Concomitant P-gp inhibition with MLN2238 did not cause any relative reduction in cell viability in Dox40, suggesting MLN2238 is not a P-gp substrate, or perhaps Dox40 is also resistant to MLN2238 and the mechanism of resistance is not P-gp mediated. In the VDR cell line, we observed no change in sensitivity of VDR to bortezomib or MLN2238 when combined with elacridar, suggesting resistance to either agent is not P-gp mediated. Finally carfilzomib resulted in marked reduction in relative cell viability again in VDR, however no synergistic effect was observed in combination with elacridar. These results suggest that the drug efflux pump P-glycoprotein does not mediate bortezomib resistance in VDR.

4.1.7 The *in vivo* efficacy of bortezomib and carfilzomib in bortezomib-resistant VDR cell line

As previously outlined in this section, while cell line models are the gold standard for investigating drug resistance mechanisms in the present day, we further explored to sensitivity of VDR to bortezomib in the *in vivo* setting, in order to establish how these cells respond to bortezomib when bone marrow microenvironmental changes are taken into account. SCID-beige mice were injected with MM.1R or VDR cells, allowing them to home their natural environment, the bone marrow, and this was confirmed by whole body bioluminescence imaging prior to commencement of treatment with bortezomib or carfilzomib(section 3.1.7).

Bortezomib displayed the greatest reduction in tumour burden compared to vehicle or carfilzomib in MM.1R mice, however unusually the degree of reduction in tumour burden with MM.1R was not found to be statistically significant. Carfilzomib appeared to cause a greater reduction in tumour burden than vehicle

in MM.1R mice however again this reduction was not statistically significant. Interestingly, the overall survival for bortezomib-treated MM.1R mice significantly exceeded overall survival in MM.1R mice treated with either vehicle or carfilzomib, (bortezomib vs. vehicle: $p=0.0048$; bortezomib vs. carfilzomib 1.5mg/kg: $p=0.0006$; bortezomib vs. carfilzomib 3mg/kg: $p=0.0048$). This is quite interesting in light of the fact that we also observed HS-5 stromal cell-induced resistance to carfilzomib in MM.1R cell line (Results section 3.5.2, figure 3.5.5.2), whereby 24hour co-culture of MM.1R with HS-5 cells reduced the sensitivity of MM.1R to carfilzomib, and prolonged co-culture with HS-5 by up to 48 and 72 hours prior to treatment with carfilzomib resulted in even greater reduction in the sensitivity of MM.1R to carfilzomib. The efficacy of carfilzomib in the *in vitro* setting, in preclinical mouse models and in clinical trials have been well documented and lead to the rapid FDA approval of this drug for the treatment of multiple myeloma.[20, 47, 48, 157-160] It is unclear why in our study MM.1R cell line did not show comparable toxicity to carfilzomib compared to bortezomib in the setting of HS-5 stromal cell co-culture or in the *in vivo* mouse model. It may be worthwhile exploring the possible reason for this finding in future studies. One possible explanation may be that the MM.1R cell line, over time, developed a clone resistant to carfilzomib, that is only apparent when the cells are in a co-culture system with HS-5 stromal cells or grown in the bone marrow of mice *in vivo*. Clonal heterogeneity is becoming a more and more apparent factor in myeloma disease progression, and perhaps our findings represent this phenomenon. Further studies may help to explain these findings.

In VDR, while both carfilzomib and bortezomib appeared to induce a greater reduction in tumour burden in VDR compared to control, again the p value for degree of reduction in tumour burden with either treatment was not significant. This data suggests that VDR is likely somewhat resistant to bortezomib in the *in vivo* setting, and possibly also resistant to carfilzomib. However in contrast, both carfilzomib and bortezomib treatment in VDR mice resulted in a statistically significant increase in overall survival in VDR mice (vehicle vs. bortezomib: $p=0.0004$; vehicle vs. carfilzomib 1.5mg/kg: $p=0.0086$; vehicle vs. carfilzomib 3mg/kg: $p=0.0063$). No significant difference in overall survival was observed

between bortezomib-treated and carfilzomib-treated VDR mice (for both 1mg/kg and 3mg/kg dosing regimens). Overall, the resistance of VDR to bortezomib was not as pronounced in the *in vivo* setting. These data suggest that perhaps elements of the bone marrow microenvironment that are present in the *in vivo* setting can overcome, to a certain degree, resistance mechanisms that are at play in the *in vitro* setting.

4.2 MUTATIONAL ALTERATIONS IN MM.1R AND VDR AS IDENTIFIED BY WHOLE EXOME SEQUENCING

4.2.1 Introduction to whole exome sequencing

Whole exome sequencing has been used both in the *in vitro* and *in vivo* setting in the investigation of multiple myeloma pathogenesis as outlined in the introduction. Quite interestingly, yet not surprisingly, the evidence for clonal heterogeneity in myeloma has recently been documented by a number of groups. The clonal evolution in myeloma in any given patient helps explain why patients relapse in myeloma; the majority of the malignant plasma cells initially respond to treatment, with a small number of resistant cells remaining indolent in the bone marrow, until such time when this residual clone proliferates and the patient relapses and is refractory to drugs to which they initially responded. In fact Melchor et al demonstrated that at diagnosis, between 2 and 6 clones are present in myeloma patients, and clonal heterogeneity can occur either by a branching (subclone) or linear (new clone) patterns.^[107] This new finding helps explain how resistant clones are generated. It is not clear however in our model of bortezomib resistance, whether repetitive exposure of MM.1R to bortezomib resulted in the generation of a new (linear) clone, i.e. VDR, or whether the VDR clone was present at baseline in MM.1R and following recurrent bortezomib treatment, a VDR clone that was present but not apparent at baseline subsequently emerged.

Whole exome sequencing is used to capture the coding regions of a particular genome, called the exome. It is anticipated that genetic mutations resulting in disease for the most part are associated with mutations of the exome, i.e. variants in protein-coding regions of the genome. A large group of sequence reads consisting of varying lengths and arrangements are produced by whole exome sequencing runs. The sequence reads are aligned to known sequence references and abnormal alleles are recognised and recorded. Filters are applied that characterise the variant alleles identified and these include qualitative scores (based on coverage depth), and criteria that imply significance (such as frequency of alleles, anticipated consequences on protein structure). Given the vast quantity of information provided by whole exome sequencing many new

technologies are currently being developed to interpret the results. The first occasion in which next generation sequencing was used to correlate a gene mutation with a disease process was in 2010, when mutation of *DHODH* gene was found to cause postaxial acrofacial dysostosis syndrome, a rare familial disorder characterised by abnormalities of the face, limbs and eyes. Whole exome sequencing was used in the next 12 months to identify the genetic causes of 12 further disorders of Mendelian inheritance.^[161]

Whole exome sequencing has also been used to seek out genetic mutations in multiple myeloma patients that contribute to disease pathogenesis. Chapman et al revealed a number of important findings in their study in 2011. Eleven distinct mutations of genes involved in the NF- κ B pathway were found to play a role in initiation of this pathway in patients with multiple myeloma. Mutations of BRAF kinase were also identified in 4% of patients, suggesting a novel role for BRAF inhibitors in multiple myeloma.^[67]

We therefore undertook whole exome sequencing of our cell line model of bortezomib resistance, which was completed at the Centre for Cancer Genome Discovery Core Facility at Dana-Faber Cancer Institute in order to identify which gene mutations were present in bortezomib-resistant VDR cell line but absent in MM.1R.

4.2.2 Single nucleotide variants identified in bortezomib-resistant VDR but not MM.1R

As outlined in results section 3.2.2, 28 non-synonymous single nucleotide variants were identified in bortezomib resistant VDR that were not identified in MM.1R. A non-synonymous variation involves a nucleotide mutation that changes the amino acid sequence of a protein. Single nucleotide variants (SNVs) differ to single nucleotide polymorphisms (SNPs), in that SNPs are polymorphisms that by definition are variable sites within or between populations, whereas SNVs make no assumption about degree of polymorphism.

Of the 28 SNVs identified in VDR but not MM.1R, 26 of these mutations were identified as novel mutations by COSMIC (Catalogue of Somatic Mutations in Cancer) database. Two mutations were identified by dbSNP (Single Nucleotide

Polymorphism Database) database (hosted by the National Centre for Biotechnology Information (NCBI) in collaboration with the National Human Genome Research Institute (NHGRI)), and these included two distinct mutations of H2AFV gene (dbSNP IDs: rs114398265 and rs1802437). SIFT and polyphen predictions were obtained for all SNVs identified as outlined in table 3.2.2.1. Seven SNVs were found to be “damaging” by both SIFT and PolyPhen predictions and these genes will now be discussed in detail. Note all seven of these genes were classified as novel mutations based on search criteria in dbSNP and COSMIC databases. Each gene was researched in PubMed under the terms “gene, cancer”, “gene, myeloma”, “gene, mutation”.

SPARCL1 (secreted protein, acidic and rich in cysteine-like 1) gene was found to bear a mutation in VDR that was not present in MM.1R. This missense mutation involved an asparagine to tyrosine substitution in the gene and has not been previously identified. SPARCL1 wild type has been shown to reduce cellular adhesion and prevent migration of fibroblasts. The way in which SPARCL1 controls migration and adhesion has not been fully elucidated. We do know that SPARCL1 binds to type 1 collagen, a constituent of extracellular matrix that promotes migration of tumour cells and tumour cell invasion.^[162-164] SPARCL1 gene has been recently cited in relation to a number of cancers. In colorectal cancer, Yu et al in 2011 suggested that the combination of high p53 levels and low SPARCL1 levels collectively could provide a valuable tool as a prognostic indicator as an adjunct to TNM (tumour-metastasis-node) staging in colorectal cancer.^[165] Zhang et al in 2011 demonstrated that SPARCL1 is poorly expressed in normal colorectal tissue, strongly positive in primary colorectal tumour sites and again at very low levels in distant lymph node positive for metastatic disease, suggesting that SPARCL1 upregulation in colorectal cancer is an early event in the development of this type of cancer, and possibly has oncogenic characteristics that contribute to disease progression.^[166] It has previously been documented also that SPARCL1 is markedly suppressed in a number of cancer cell lines including colon cancer (SW480), lymphoblastic leukaemia (Molt 4), chronic myeloid leukaemia (K-562), lung cancer (A549) and melanoma (6361) compared to normal tissues, and that SPARCL1 negatively regulates cellular

proliferation.^[167] More recently however, SPARCL1 expression in human gliomas has been shown to correlate with tumour grade, whereby no more than 25% of normal brain, grade 1 or grade 2 astrocytomas express SPARCL1, whereas >75% of grade 3 astrocytomas or glioblastomas (aggressive brain tumour with very poor prognosis) were positive for SPARCL1 expression.^[168] Again in contrast to this latter study, low levels of SPARCL1 were found to correlate with development of lymph node metastases and poor tumour grade in breast cancer, this data was published more recently in 2013.^[169] More interestingly, in prostate cancer, SPARCL1, which is known to be suppressed in prostate cancer, in the *in vivo* setting over-expression of SPARCL1 resulted in suppression of prostate cancer metastasis in an *in vivo* mouse model.^[170] In conclusion, low levels of SPARCL1 appear to occur in a number of cancer cell lines, in colon cancer levels are high in the primary tumour and low in lymph node metastases, and in prostate cancer SPARCL1 over-expression in an *in vivo* model appears to suppress prostate cancer migration and metastases *in vivo*. The role of the SPARCL1 mutation in VDR is not yet known. However one should consider the role of SPARCL1 in multiple myeloma pathogenesis. One could hypothesise that if SPARCL1 mutation in VDR is present in patients with multiple myeloma, perhaps the mutated form of SPARCL1 no longer functions normally to bind collagen type 1 in the bone marrow microenvironment, potentially promoting myeloma cell invasion *in vivo*. This hypothesis could be further explored in future work.

ZER1 (Zyg-11 Related, Cell Cycle Regulator) gene was also found to have a novel mutation in VDR cell line, another missense mutation involving a serine to tyrosine substitution. ZER1 is thought to be involved in encoding a subunit of the E3 ubiquitin complex. ZER1 has been documented to be up-regulated at early stage of bladder cancer and down-regulated at later stage bladder cancer.^[171] The role of the ZER1 mutation in VDR is not clear.

TPH2 (tryptophan hydroxylase) gene is mutated in VDR cell line involving a serine to tyrosine substitution (similar to ZER1 mutation). TPH2 gene encodes a protein that catalyses the rate limiting step in the biosynthesis of serotonin, an

endogenous neurotransmitter. Little to no information is available in relation to the role of this gene in cancer pathogenesis or multiple myeloma.

MFGE8 (Milk Fat Globule-EGF Factor 8 Protein, or lactadherin) gene was also mutated in VDR cell line. This mutation involved a cysteine to alanine substitution. Following PubMed literature review, MFGE8 appears to play a role in promotion of dietary triglyceride absorption and obesity.^[172] Tibaldi et al recently showed by immunohistochemistry that MFGE8 is over-expressed in 45% of ovarian cancer samples tested in their study, and also over-expressed in triple negative breast cancer. Furthermore this group identified antibodies to MFGE8 that inhibited survival, migration and adhesion of cell line models of ovarian cancer and triple-negative breast cancer, suggesting a role for MFGE8 antibodies in solid tumour cancer of the ovary and breast.^[173] MFGE8 has also recently been found to promote osteoclastogenesis.^[174] Osteoclasts are well documented for their role in myeloma cell promotion in the bone marrow microenvironment. The potential role of mutated MFGE8 in myeloma should be further examined.

CCDC113 (Coiled-Coil Domain-Containing Protein) gene also harboured a missense mutation in VDR cell line involving an alanine to threonine substitution. CCDC113 appears to play a role in cilia formation and does not appear to play a role in cancer pathogenesis or in multiple myeloma.

FAM59A (GRB2 associated, regulator of Erk/MAPK1, or GAREM) gene was found to have a mutation in VDR that involved a cysteine to glycine substitution. FAM59A gene encodes a protein that functions in the epidermal growth factor receptor (EGFR) pathway. The EGFR pathway is known to regulate normal cell proliferation but also has been implicated in the development of many types of malignancies. The protein product of FAM59A promotes signalling of the MAPK/ERK (mitogen-activated protein kinases/extracellular signal related kinases) pathway.^[175] The MAPK/ERK pathway allows signalling from the cell surface via a cell surface receptor that is transmitted to the DNA of the cell nucleus. Essentially a molecule binds a receptor on the cell surface and triggers a message to be sent to the DNA that results in the expression of a protein, causing

an alteration in the cell, such as cell division. If one of the proteins in this pathway contains a mutation then the message being transferred to the DNA can become fixed in an “on” or alternatively “off” state, and this step is sometimes an initiation step in cancer development. Interestingly, in our proteomic analysis of MM.1R plus bortezomib vs. VDR plus bortezomib treatment, we found a number of proteins that were suppressed in bortezomib-treated VDR compared to bortezomib-treated MM.1R (figure 3.4.2.1) suggesting that the MAP-kinase signalling pathway is perturbed between the two cell lines after they have been treated with bortezomib. Further studies are required to determine whether or not the mutation of FAM59A/ GAREM gene contributes to bortezomib resistance in VDR, hypothetically by altering the EGFR and/or MAP-kinase signalling pathway in VDR cells.

ATP5J (ATP Synthase, H⁺ Transporting, Mitochondrial Fo Complex, Subunit F6) gene also harboured a mutation in VDR cell line that was not present in MM.1R. This involved a point mutation, with the substitution of a guanine for an alanine at position g.27102074 in chromosome 21. The amino acid substitution involved a serine to phenylalanine exchange. ATP5J gene is known to function as a subunit of a complex structure (the mitochondrial ATP synthase Fo complex) that is responsible for synthesis of ATP. A recent study of the STAT (Signal Transducer and Activator of Transcription) pathway, which is known for its role in the pathogenesis of many haematopoietic malignancies, revealed ATP5J is one of a number of STAT-p53 target genes with altered platelet expression in patients with myeloproliferative disorders compared to platelets from healthy donors.^[176] This study concluded that these target genes, including ATP5J, via recruitment of p53, could represent a novel molecular means of abnormal transcription in haematological cancers. Again, it is unclear if the ATP5J mutation in VDR cell line could also alter STAT-p53 signalling, however this could be considered in future studies.

4.2.3 Deletion in ABCA7 gene identified in VDR cell line

While no insertions were identified in VDR compared to MM.1R, a deletion in ABCA7 gene was identified in VDR cell line that was not present in MM.1R (table

3.2.3.1). The ABCA7 gene belongs to a superfamily of ABC (ATP-binding cassette) transporters. The protein products of ABC genes as outlined in the results section 3.2.3 are responsible for transporting numerous substances across cell membranes (both intra- and extra-cellularly).

There are 7 ABC subfamilies, of which ABCA7 belongs to the ABC1 subfamily. The ABCA7 protein is expressed at highest levels in peripheral leucocytes, thymus gland, bone marrow and splenic tissue. Kaminski et al first described ABCA7 in 2000 when its role in lipid transport across macrophage membranes was elucidated.^[112]

In 2012 Meurs et al investigated the effect of macrophage ABCA7 knockdown in mice to determine its role in atherosclerosis, given its known involvement in lipid transport. While they did not find a correlation between ABCA7 knockdown and atherosclerosis in the mice, they revealed that concomitant knockdown of ABCA7 and ABCA1 (the promoter of initiating step in cholesterol transport) resulted in massive splenomegaly due to cellular fat accumulation, down-regulation of number of CD3+ T cells, and promoted erythropoietic regulators. Their data suggested that ABCA7 might be involved in splenic proliferation of T cells and erythrocytes.^[113]

In relation to its potential role in cancer pathogenesis, in a cohort of 51 patients with colorectal cancer, a correlation between reduced transcript levels of ABCA7 gene and a reduction in disease free interval following treatment has been established ($p=0.033$, log rank test).^[114] However neither ABCA7 gene down-regulation nor deletion in this gene have been implicated in haematological malignancy in the *in vivo* setting to date.

In conclusion, it may be worthwhile examining CD138-positive cells in multiple myeloma patients for deletions in ABCA7 gene and suppressed transcript levels as, in the *in vitro* setting in VDR, deletion in ABCA7 is associated with bortezomib resistance, and one could hypothesise that low transcript levels may also associated with a shorter disease-free interval in myeloma, similar to what has been observed in colorectal cancer.

4.2.4 *In vitro* and *in vivo* significance of mutPSMB5 identified in VDR

Of the 28 SNVs identified in VDR cell line by whole exome sequencing, a gene mutation was noted in the PSMB5 gene involving a threonine to alanine substitution at position 80 on exon 2 (figure 3.2.4.1). Initially, this gene mutation was reported by COSMIC database as a “novel” mutation, however it subsequently transpired that this mutation has been previously described in a bortezomib-resistant leukaemic cell line model.^[64] The reason for this false call as a “novel” mutation was that when this mutation was published in the literature, the cleaved version of PSMB5 was documented, rather than the complete gene, therefore mutPSMB5 in VDR was called as “novel” by COSMIC rather than known. All SNVs detected by whole exome sequencing were reviewed in collaboration with CCGD core facility to ensure all other mutations documented as “novel” were truly novel. No further SNVs reported in the list generated by WES required revision of terminology in terms of their novelty or lack thereof. 3D *in silico* modelling of the PSMB5 mutation identified by Franke et al in their leukaemic cell line model was shown to alter the bortezomib-PSMB5 binding pocket.^[64]

We thus next undertook lentiviral infection of mutPSMB5 into bortezomib-sensitive cell lines. We initially attempted to over-express mutPSMB5 in MM.1S and MM.1R cell lines, given these are the parental and grand-parental cell lines respectively of VDR. However these cells were remarkably sensitive to blasticidin, which was used to select the clone infected with muPSMB5 lentivirus. Also, given the semi-adherent nature of these cells, difficulty with lentiviral infection was also thought to play a role in poor infection rates in these cell lines given the poor cell-to-lentivirus contact of the non-adherent cells.

Instead KMS11 was infected with mutPSMB5 to ascertain if over-expression of mutPSMB5 in KMS11 rendered these cells resistant to bortezomib. We observed a degree of reduction in sensitivity of KMS11 cells infected with wtPSMB5 to bortezomib. However an even greater degree of reduction in sensitivity to bortezomib was observed when KMS11 was infected with mutPSMB5 (figure 3.2.5.1). The latter finding suggests that mutPSMB5 may play a role in

bortezomib resistance and may partially explain the resistance of VDR to bortezomib in the *in vitro* setting.

4.3 TRANSCRIPTIONAL PROFILE OF ISOGENIC CELL LINE MODEL OF BORTEZOMIB RESISTANCE

4.3.1 Introduction to gene expression profiling

Gene expression profiling as outlined in the introduction section has lead major advances in deciphering the pathogenesis of cancer, allowing specific pathways to be targeted so that novel therapies can be developed for the treatment of a multitude of cancers, in addition to identifying which genes when their expression is altered correlate with a worse or better prognosis. We therefore undertook gene expression profiling of MM.1R and VDR cell lines to determine which genes were differentially expressed between the bortezomib-sensitive and bortezomib-resistant clone (section 3.3). Affymetrix oligonucleotide arrays were undertaken at Beth Israel Deaconess Medical Centre Core Genomics facility.

20,724 genes were differentially expressed between MM1R and VDR cell lines. Genes whereby fold change between the two conditions was >1.2 and demonstrated a p value ≤ 0.01 were included for further studies. In total 437 transcripts fulfilled these criteria. Of these, 353 were over-expressed in VDR compared to MM.1R (table 3.3.2.1). In comparison only 84 genes were down-regulated in VDR compared to MM.1R (table 3.3.3.1). The reasoning for the discrepancy between number of genes up-regulated versus down-regulated is unclear. Genes that were over-expressed or down-regulated were analysed by DAVID functional annotation tool to determine which pathways were implicated in groups of transcripts that were differentially expressed.

4.3.2 Pathways associated with genes over-expressed in VDR compared to MM.1R

Pathway analysis via DAVID functional annotation tool revealed “cellular apoptosis” as a specific pathway in which 4 transcripts up-regulated in VDR play a role. These genes include CFLAR, CASP8, CASP10, and NFKBIA (figure 3.3.2.1). NF-kappaB proteins are involved in immune responses, cell proliferation and cellular apoptosis in normal cells. NF-kappaB itself is well documented for its

role in multiple myeloma pathogenesis in particular by protecting malignant plasma cells from apoptosis and promoting myeloma cell proliferation. One suggested mechanism of action of the proteasome inhibitor bortezomib is through the NF- κ B/I κ B complex by hindering degradation of I κ B α and thus augmenting myeloma cell apoptosis.^[177] I-kappa-B-alpha, the gene product of NFKBIA, is known to bind NF-kappaB, which prevents activation of NF-kappaB and suppresses apoptosis in B-cell neoplasms. It is not clear why caspase 8 (CASP8) and caspase 10 (CASP10) are also concomitantly upregulated in VDR, as this suggests a greater degree of apoptosis in VDR compared to MM.1R. CFLAR (CASP8 And FADD-Like Apoptosis Regulator, or c-FLIP) gene is also upregulated in VDR compared to MM.1R and also involved in the apoptosis pathway. CFLAR (also known as c-FLIP) was recently found to play a pertinent role in acute promyelocytic leukaemia, whereby PML-retinoic acid receptor α (PMLRAR α) joins with Fas and inhibits Fas-associated apoptosis by generating an inhibitory complex of apoptosis with c-FLIP (i.e. CFLAR).^[178] C-FLIP (CFLAR) has been shown to inhibit caspase-8 and promote cell survival,^[179] but has also been shown to activate caspase-8 to induce cellular apoptosis.^[180] In VDR, one could hypothesise that c-FLIP plays a role in stabilising caspase-8 and promoting VDR survival. Further studies are warranted to determine the role of these genes in multiple myeloma, and whether or not they contribute to drug resistance to bortezomib *in vivo*.

4.3.3 Pathways associated with genes down-regulated in VDR compared to MM.1R

Transcripts that were down-regulated in VDR compared to MM.1R were noted to participate in a number of cellular processes mainly concerned with the immune system for example antigen processing and presentation, immune response, T cell differentiation and T cell selection. In particular 2 genes, CD74 and HLA-DRA, were identified by DAVID functional annotation tool to be involved in “antigen processing and presentation”, ($p=5.61E-04$), (table 3.3.3.3).

The protein product of CD74 (CD74 Molecule, Major Histocompatibility Complex, Class II Invariant Chain) gene is known to play a pivotal role in MCH class II

antigen presentation, acting as a chaperone that helps regulate the immune response. The protein product also acts as a receptor on the cell surface for the MIF (macrophage migration inhibitory factor) cytokine that promotes cell survival and proliferation.^[181] Interestingly, PubMed search of “CD74” and “myeloma” revealed that a CD74 monoclonal antibody, milatuzumab, has been developed and has recently completed phase 1 clinical trials for use in relapsed and refractory multiple myeloma. The novel agent was well tolerated, and while no tangible responses (measured by criteria of European Group for Blood and Marrow Transplantation) were observed, disease stabilisation was observed in 26% of patients, suggesting its role for use in refractory myeloma, in particular in combination with other therapies.^[182] In VDR cell line, CD74 was down-regulated suggesting that perhaps CD74 expression is lost later on in the disease process by the time resistant clones have evolved. Perhaps this is why no quantifiable response was detected in the aforementioned phase 1 clinical trial, as perhaps malignant plasma cells later in the disease potentially lose CD74 expression. It is not clear why it would be beneficial to malignant clones to lose a cell surface marker that promotes cell survival and proliferation, presumably later in the disease alternative means of survival are at play. While CD74 does not appear to be associated with bortezomib resistance, it appears to be over-expressed in MM.1R clone compared to VDR, suggesting perhaps that milatuzumab should preferentially be utilised in newly diagnosed myeloma.

4.3.4 shRNA knockdown studies of genes up-regulated in VDR

A number of specific genes were selected for a shRNA knockdown screen, to determine which genes, following their shRNA knockdown, might resensitise VDR to bortezomib. This included the following: (i) transcripts over-expressed in VDR with concordant up-regulation at the protein level in VDR (as identified by label-free mass spectrometry), (ii) transcripts with > 2-fold over-expression in VDR vs. MM.1R, (iii) transcripts whereby chemical inhibitors are currently commercially available for the molecular product of these transcripts, and (iv) a number of transcripts for which shRNAs were available in the laboratory (table

3.3.4.1). All genes chosen were selected from the complete list of genes up-regulated in VDR vs. MM.1R where fold change >1.2 and p value ≤ 0.01 . Of 27 genes investigated in the shRNA screen, 11 genes were found, following shRNA knockdown and subsequent treatment with bortezomib (IC₂₀), to result in >40% cell death of VDR cells compared to control hairpins. These included PSMB5, ALDH1L2, FN1, PIK3CG, PSME1, BCL2L1, SKAP1, TNF2, ALOX5AP, CEP128 and CX3CR1 (figure 3.3.5.1). A number of these targets will be discussed in more detail including PIK3CG, BCL2L1 and PSMB5.

4.3.4.1 Effect of shRNA knockdown of PIK3CG on VDR cells

Following shRNA knockdown of PIK3CG, in 3 of 5 hairpins used, we observed resensitisation of VDR to bortezomib. Phosphatidylinositol 3-kinase (PI3K) signalling in recent years has been well documented for its role in multiple myeloma pathogenesis by promoting cell growth, survival and migration, and thus multiple PI3K inhibitors to various PI3K isoforms have been developed. CAY10505 has been developed as a specific inhibitor of PIK3CG. However a recent study revealed PIK3CA as the most successful PI3K target for inhibition in order to induce maximum cell death in myeloma cell lines, for which an inhibitor is also available.^[183] However bortezomib-refractory cell lines were not used in this study, therefore perhaps the PIK3CG isoform holds greater importance later in the disease process. Our data suggest a role for PIK3CG inhibitor CAY10505 in combination with bortezomib in bortezomib-refractory myeloma, however further studies are warranted to validate this hypothesis.

4.3.4.2 shRNA knockdown of BCL2L1 resensitises VDR to bortezomib

BCL2L1 (Bcl2-Like 1) gene, following its shRNA knockdown, also resensitised VDR to bortezomib. The protein generated by BCL2L1 forms part of the Bcl2 family of proteins. BCL2L1 is known to be a potent inhibitor of cell death by inhibiting caspase activation. A very recent study examining the gene expression profile of various stages of myeloma development (i.e. MGUS to SMM to MM) revealed BCL2L1 as a target gene upregulated on progression from MGUS to either smouldering myeloma or multiple myeloma.^[184] Two small molecule inhibitors of BCL2L1, that also inhibit Bcl2, have been documented for their relative potencies in preclinical models of myeloma *in vitro* and *in vivo*. These

include ABT-737 documented for its efficacy in cell line models *in vitro*,^[185] and gossypol acetate, a naturally occurring compound extracted from the cotton plant, documented for its potency both *in vitro* and *in vivo* in the pre-clinical setting.^[186]

4.3.4.3 shRNA knockdown of PSMB5 resensitises VDR to bortezomib

Given that PSMB5 was found in our studies to be over-expressed at the transcript level (table 3.3.2.1), protein level (table 3.4.2.1), and harbours a genetic mutation (table 3.2.2.1), we chose to further validate PSMB5 knockdown and subsequent resensitisation of VDR cells to bortezomib. First we demonstrated successful shRNA knockdown of PSMB5 in MM.1R and VDR by immunoblot (figure 3.3.6.1). Secondly, we demonstrated that shRNA knockdown of PSMB5 and subsequent treatment of VDR cells (used at even lower concentrations of bortezomib compared to initial screen: 50nM vs. 20-40nM), resulted in significant resensitisation of VDR to bortezomib (figure 3.3.6.2b). shRNA knockdown of PSMB5 in MM.1R did not alter the sensitivity of MM.1R cells to bortezomib (figure 3.3.6.2a).

Our validation studies were somewhat limited by the technical challenge of shRNA knockdown of semi-adherent cell lines, which when not adherent to the surface of the tissue culture flask, prove to be much more difficult to successfully infect with lentivirus, and subsequent selection with blasticidin initially resulted in cell death of almost all cells. We overcame this difficulty by centrifuging the tissue culture plates following infection with lentivirus for 30 minutes post-infection, to allow both virus and cells to adhere to the base of the plates.

Our data clearly indicate the potent role of PSMB5 in bortezomib resistance in the *in vitro* setting. Perhaps an alternative inhibitor of the proteasome such as a PSMB8 inhibitor may be useful in the setting of over-expression and mutation of PSMB5 gene.

4.4 PROTEOMIC PROFILING OF ISOGENIC CELL LINE MODEL OF BORTEZOMIB RESISTANCE

4.4.1 Introduction to proteomic profiling in MM.1R and VDR

We examined the proteomic profiles of the isogenic cell lines MM.1R and VDR, in addition to investigating the proteins differentially expressed following treatment of each cell line with bortezomib. Label-free mass spectrometry has been developed to determine the proteins differentially expressed in cell lines, tissue culture supernatant, solid tumours, cell lines of haematological malignancies and tissues derived from human samples including serum, to allow us to gain a greater understanding of cancer pathogenesis at the molecular level. Our group in particular have recently published on the use of label-free mass spectrometry in identifying biomarkers predicting response to thalidomide-based therapy in multiple myeloma patients.^[117] We identified 106 proteins over-expressed (table 3.4.2.1) and 132 proteins down-regulated (table 3.4.3.1) in VDR compared to MM.1R.

4.4.2 Protein expression in VDR compared to MM.1R

4.4.2.1 CCL3 is over-expressed in VDR vs. MM.1R at the protein level

One protein of particular interest, CCL3, demonstrated a 22-fold higher expression level in VDR compared to MM.1R. CCL3/MIP1- α (C-C motif ligand 3/macrophage inflammatory protein 1-alpha) was over-expressed in VDR compared to MM.1R with a 22-fold change ($p=0.013$). CCL3 has been well documented previously in its role as a stimulator of osteoclastogenesis, inhibition of osteoblastogenesis, and thus contribution to myelomatous bone disease.^[85, 120] This protein is highly expressed in myeloma cell lines and an inhibitor of CLL1 through which CCL3 signals is currently in pre-clinical investigation and has shown promising anti-myelomatous and anti-osteolytic effects in a MM *in vivo* mouse model.^[121] CCL3 is markedly over-expressed in bortezomib-resistant VDR, suggesting a role for this inhibitor in relapsed and refractory myeloma, if CLL3 is found to be over-expressed in malignant clones of multiple myeloma patients. Further studies could include examining the sensitivity of VDR cells to bortezomib in the presence of a CCL1 inhibitor.

4.4.2.2 The heat shock proteins are over-expressed in VDR vs. MM.1R

A group of proteins identified by String software revealed the heat shock proteins as a particular group that are over-expressed in VDR compared to MM.1R (figure 3.4.2.2.1). The heat shock proteins are known to be expressed in response to external stimuli such as drugs and have been well documented for their role in multiple myeloma pathogenesis. Indeed a specific heat shock protein inhibitor of HSP90AA1 has undergone phase 1 clinical trials and shows promising results for its use in relapsed and refractory myeloma. [122-125] While HSP90AA1 was not over-expressed at a statistically significant level in VDR compared to MM.1R, over-expression of HSPE1, HSPD1 and HSPD5, all of which interact with HSP90AA1, are over-expressed in VDR compared to MM.1R, suggesting a potential role for HSP90 inhibitors in bortezomib-refractory multiple myeloma.

4.4.2.3 Aminoacyl-tRNA biosynthesis-associated molecules are down-regulated in VDR compared to MM.1R.

Aminoacyl-tRNA is an amino acid bound to transfer RNA that is delivered to the ribosome for integration of the amino acid into a polypeptide during protein synthesis. Three proteins that were found to be down-regulated in VDR compared to MM.1R were found to be involved in aminoacyl-tRNA biosynthesis, and these included IARS, RARS and LARS (figure 3.4.3.1). PubMed search of “IARS”/ “RARS”/ “LARS” in combination with the term “myeloma” did not reveal any associations of these proteins with myeloma pathogenesis. However a large study involving 1064 cases of patients with breast cancer and 1073 cancer-free controls revealed that functional polymorphisms of LARS and RARS were associated with a risk of developing breast cancer. In particular for RARS, the finding was statistically significant (OR = 1.17, 95% CI = 1.02-1.35).[187] The role of these proteins in the pathogenesis of myeloma and/or resistance to proteasome inhibitors remains to be elucidated.

4.4.3 Protein expression in bortezomib-treated VDR and bortezomib-treated MM.1R

4.4.3.1 Proteasome-associated subunits are suppressed following bortezomib treatment in MM.1R and VDR

Following bortezomib treatment, 212 proteins were down-regulated in MM.1R compared to untreated control (table 3.4.4.1.2), and in VDR 35 proteins were down-regulated compared to untreated controls (table 3.4.4.1.3). By comparing bortezomib-treated MM.1R to bortezomib-treated VDR, 109 proteins out of a total 323 were downregulated in bortezomib-treated-VDR compared to bortezomib-treated-MM.1R, of which 63 demonstrated a fold change ≥ 1.5 (where $p < 0.05$), (table 3.4.4.1.4).

DAVID functional annotation tool revealed a number of proteins involved in the proteasome structure were suppressed in both bortezomib-treated MM.1R and bortezomib-treated VDR compared to their respective untreated controls. PSMD13, PSMA1, PSMA2, PSMA3, PSMA4, PSMA5, PSMA6, PSMA7, PSMB1, PSMB2, PSMB5, PSMB6, PSMB8 were all found to be down-regulated in bortezomib-treated MM.1R compared to untreated MM.1R (table 3.4.4.1.1). PSMA3, PSMA4, PSMA6, PSMA5, PSMB1 and PSMA7 were down-regulated in bortezomib-treated VDR compared to untreated VDR (table 3.4.4.1.3). However PSMB5, through which bortezomib principally acts, was not down-regulated in bortezomib-treated VDR compared to untreated VDR control, suggesting that PSMB5 dysregulation is also evident at the protein level in VDR cell line.

4.4.3.2 Proteins of the MAP-kinase signalling pathway are down-regulated in bortezomib-treated VDR vs. bortezomib-treated MM.1R

We identified 5 proteins that were down-regulated in bortezomib-treated VDR compared to bortezomib-treated MM.1R that are involved in the MAPK (mitogen-activated protein kinases) signalling pathway (figure 3.4.4.2.1). The MAPK pathway is well documented for its role in carcinogenesis. At baseline, the MAPK pathway allows transduction of a message from outside the cell to be transmitted into the cell nucleus by a cell surface receptor that results in a change in the DNA in the nucleus, such as signalling a command to cause cell

division. This is of particular importance in cancer pathogenesis, whereby an alteration in the MAPK signalling pathway causes uncontrolled cell turnover. A large number of compounds have been developed to inhibit the MAPK pathway to overcome cancer, the first of which was sorafenib which was developed for use in numerous cancers including hepatocellular cancer^[188] and renal cell carcinoma.^[189]

The proteins down-regulated in bortezomib-treated VDR compared to bortezomib-treated MM.1R that have known involvement in the MAPK signalling pathway include FLNA, HSP72/HSPA6, PPP3C, MEF2C and HSP27/HSPB1. The most important of these targets appears to be MEF2C (Myocyte Enhancer Factor 2C). MEF2C has been shown to regulate differentiation of monocytes preferably to granulocytes, and the oncogene c-Jun is a pivotal downstream modulator of MEF2C.^[190] Furthermore, another player in the MAPK pathway, ERK5, has been shown to direct haematopoiesis toward the malignant monocytic clone in acute myeloid leukaemia (AML), of which MEF2C is the direct downstream target, and this group have suggested further investigation of MEF2C as a target molecule for treatment in AML.^[191] MEF2C is downregulated in bortezomib-treated VDR compared to bortezomib-treated MM.1R (2.60 fold change, $p=4.03E-04$). MEF2C was not identified as differentially expressed in VDR compared to MM.1R at baseline. It is unclear why MEF2C is down-regulated in bortezomib-treated VDR compared to bortezomib-treated MM.1R, as, if it is thought to act as an oncogene, then one would expect it to be upregulated. Further work may help outline the role of MEF2C in the pathogenesis of haematological malignancies.

4.4.3.3 CCL3 is up-regulated in bortezomib-treated VDR compared to bortezomib-treated MM.1R

We found 215 proteins up-regulated in bortezomib-treated VDR compared to bortezomib-treated MM.1R, of which 78 proteins had a fold change ≥ 2 .

Again CCL3 was significantly over-expressed in bortezomib-treated VDR compared to bortezomib-treated MM.1R (fold change 3.51, $p=0.039$), (we previously observed CCL3 at baseline is over-expressed in VDR compared to MM.1R, section 4.4.2.1). As bortezomib treatment does not appear to suppress CCL3 protein levels, this again poses the question as to whether or not the

addition of a CCL1 inhibitor (through which CCL3 signals) may have the potential to overcome bortezomib resistance in VDR.

4.4.3.4 EIF5A is up-regulated in bortezomib-treated VDR compared to bortezomib-treated MM.1R

EIF5A (eukaryotic initiation factor 5A) was over-expressed in bortezomib-treated VDR compared to bortezomib-treated MM.1R (24.9 fold change, $p=0.008$, table 3.4.5.1.1). EIF5A is known to be subject to post-translational modification to hypusine from a conserved lysine. Hypusinated EIF5A has been documented to be involved in cancer cell proliferation, promotion of oncogenes and neoplastic change in cells of the haematopoietic system. A specific nanoparticle inhibitor, SNSO1, has previously been developed to abrogate hypusinated EIF5A expression, which results in concomitant NF- κ B inhibition, and also demonstrated a significant reduction in tumour burden in two mouse models of multiple myeloma.^[130] Not only was this protein up-regulated in bortezomib-treated VDR compared to bortezomib-treated MM.1R, but also over-expressed in VDR compared to MM.1R at baseline (2.21 fold change, $p=0.008$, table 3.4.2.1). Given the over-expression of EIF5A in VDR at baseline, and its persistent over-expression despite bortezomib treatment, in comparison to these conditions in MM.1R respectively, one could hypothesis that in myeloma, EIF5A plays a role in bortezomib refractoriness. It may be worthwhile examining the potency of SNSO1 nanoparticle in VDR cell line for its relative toxicity to VDR cells, in addition to examining the expression level of EIF5A in bone marrow biopsies of patients with bortezomib-refractory multiple myeloma, in order to clarify its potential role on the treatment of bortezomib refractory myeloma *in vivo*.

4.4.4 Potential significance of PSMB5 in bortezomib resistance

Given that bortezomib specifically inhibits the proteasome through PSMB5 we summarise here the PSMB5 protein expression levels from all mass spectrometry results available in this study. PSMB5 is over-expressed 3.85-fold in VDR compared to MM.1R at baseline ($p=4.36E-04$), table 3.4.2.1). When MM.1R is treated with bortezomib, PSMB5 is suppressed as demonstrated by a 4.66 reduction in fold change ($p=7.47E-04$), (table 3.4.4.1.2). However PSMB5 is suppressed to a much lesser degree in VDR following its treatment with

bortezomib (1.34-fold, p value is not significant). By direct comparison of bortezomib-treated VDR compared to bortezomib-treated MM.1R, a 13-fold increase in PSMB5 protein expression is observed in bortezomib-treated VDR compared to bortezomib-treated MM.1R ($p=3.9E-05$), (table 3.4.5.1.1).

Furthermore, we previously noted PSMB5 is over-expressed also at the transcript level in VDR compared to MM.1R, (fold change 1.89, $p=4.14E-04$), (table 3.3.2.1); and shRNA knockdown of PSMB5 partially resensitised VDR to bortezomib (figure 3.3.6.2). PSMB5 gene in VDR cell line harbours a genetic mutation that has been previously documented for its potential role in altering the bortezomib-binding pocket in PSMB5 (section 3.2.4), and introduction of this mutant PSMB5 into bortezomib-sensitive KMS11 cells reduces the sensitivity of KMS11 to bortezomib (figure 3.2.5.1).

In conclusion, PSMB5 appears to be over-expressed in VDR compared to MM.1R at baseline at the transcript and protein level. Bortezomib treatment does not appear to suppress PSMB5 protein in VDR compared to MM.1R. One could hypothesise that these findings are due to the mutation present in VDR that is absent in MM.1R. Interestingly, in our *in vivo* study the degree of refractoriness to bortezomib observed in VDR did not mirror the *in vitro* level of refractoriness, (i.e. no significant reduction in tumour burden was identified in VDR-mice between vehicle, carfilzomib and bortezomib treatments (figure 3.1.7.1), and overall survival in VDR mice treated with both bortezomib and carfilzomib was significantly greater than vehicle-treated VDR-mice (figure 3.1.7.3)).

The *in vivo* study suggests that mechanisms of bortezomib-refractoriness observed *in vitro* can potentially be overcome in the *in vivo* setting, and perhaps this is why PSMB5 mutations have not been found to be significant in patients with multiple myeloma. One possible mechanism to explain this is the fact that immunoproteasome subunit PSMB8 is expressed in the *in vivo* setting in patients with multiple myeloma, therefore even if PSMB5 is over-expressed and mutated, then perhaps bortezomib can inhibit the proteasome through PSMB8. This hypothesis requires clarification by further studies examining specific

proteasome subunit expression levels in VDR cells following bortezomib treatment.

4.5 THE ROLE OF THE BONE MARROW MICROENVIRONMENT AND ITS FURTHER CONTRIBUTION TO DRUG RESISTANCE

4.5.1 Introduction

As previously outlined, the bone marrow microenvironment plays a major role in multiple myeloma pathogenesis by either direct or indirect interactions between bone marrow stromal cells and malignant plasma cells. One major blockade to advances in the study of multiple myeloma pathogenesis and drug resistance mechanisms is the difficulty of laboratory-based culturing of malignant plasma cells that have been extracted from the bone marrow of patients with multiple myeloma. Outside their natural bone marrow microenvironment they quickly cease to exist. Therefore in our cell line model we chose to mimic the effects of the local bone marrow microenvironment by examining the sensitivity of VDR cells to a number of therapies following their co-culture with HS-5 stromal cells. We furthermore explored the role of osteoblasts in multiple myeloma pathogenesis and drug resistance. Finally we examined the effect of interferon-gamma, a cytokine secreted by the bone marrow microenvironment, on the sensitivity of VDR to bortezomib. We found that PSMB8 was upregulated by interferon-gamma in VDR cell line, with reciprocal depression of PSMB5. Furthermore we established that PSMB8 is expressed in the CD138-positive cells in bone marrow biopsies of multiple myeloma patients, supporting the role for the use of PSMB8 inhibitors in the treatment of newly diagnosed and potentially bortezomib-refractory multiple myeloma.

4.5.2 VDR is subject to HS-5 stromal cell-induced drug resistance.

We examined the sensitivity of MM.1R and VDR to conventional and novel therapies in the presence versus absence of HS-5 stromal cells. We tested the sensitivity of each cell line to the proteasome inhibitors bortezomib and carfilzomib, the FDA-approved HDAC inhibitor vorinostat and the preclinical BET2-bromodomain inhibitor JQ1, in the presence and absence of HS-5 accessory cells.

We observed no change in the sensitivity of MM.1R to bortezomib when in co-culture with HS-5 stromal cells. VDR again retained the same degree of resistance to bortezomib following its co-culture with HS-5 cells (figure 3.5.2.1). Unusually MM.1R cells appeared to display reduced sensitivity to carfilzomib following their co-culture with HS-5 cells and the reason for this remains unclear. However VDR cells remained sensitive to carfilzomib despite their co-culture with HS-5 cells (figure 3.5.2.2).

VDR cells were found to be resistant to vorinostat and MLN4924 when co-cultured in the presence of HS-5 cells, (figure 3.5.3.1). In the *in vivo* setting vorinostat has proven activity in combination with bortezomib in phase 1 clinical trials of patients with relapsed and refractory myeloma.^[15] Therefore we combined vorinostat and bortezomib to determine if the duo could overcome HS-5 induced resistance in VDR. Combination of bortezomib with vorinostat was not sufficient to overcome the resistance induced by HS-5 cells. Similarly combination of MLN4924 with bortezomib did not overcome stromal cell-induced resistance (figure 3.5.3.2). These data emphasise the potent role of the bone marrow microenvironment in multiple myeloma pathogenesis, by adding an additional means of protection to an already drug resistant clone in supporting their survival.

4.5.3 Osteoblasts promote myeloma cell proliferation and contribute to drug resistance

We next investigated the effect of osteoblasts on the MM cell lines MM.1S, MM.1R and VDR to ascertain if the stromal-induced effects were specific to HS-5 cells alone. Historically osteoblasts have been thought play a protective role in the patient with multiple myeloma because osteoclasts, which act in direct opposition to osteoblasts, are highly supportive of myeloma cell growth and proliferation and survival, in addition to contributing to myelomatous bone disease. Osteoclasts result in bone breakdown and lytic lesions in myelomatous bone in comparison to osteoblasts which cause bone remodelling. Indeed an

inhibitor of activin A, a molecule which is secreted by myeloma cells to cause inhibition of osteoblasts, has been documented for its benefit in a preclinical model of myeloma by restoring osteoblast proliferation, improving bony disease and preventing myeloma cell growth in an *in vitro* model.^[84] However very recently the role of osteoblasts in contributing to myeloma cell growth and proliferation has emerged. Orlowski et al recently outlined how malignant plasma cells appear to reside in osteoblastic-rich niches in the bone marrow microenvironment. Furthermore they found that in these osteoblast alcoves the malignant plasma cells gain the ability to form stem-like cells and are exceptionally tumorigenic and display resistance to a number of therapies.^[192] We further studied the role of osteoblasts in myeloma cell lines by examining their effect on myeloma cell proliferation and alterations in drug sensitivity when these cell lines were in co-culture with an immortalized osteoblast-like cell line hFob.1.19.

We tested 8 myeloma cell lines for their proliferation rate when in co-culture with hFob cells including MM.1S, MM.1R, VDR, OPM2, KMS34, RPMI8226, OCImy5 and Dox40. Interestingly the bortezomib resistant cell line VDR displayed a marked increase in cell viability when co-cultured in the presence of hFob cell line compared to all other cell lines tested (figure 3.5.4.1). We examined the effect of osteoblasts on the drug sensitivity of MM.1S, MM.1R and VDR cell lines to a number of therapies. Interestingly MM.1S appeared to be the cell line that was most susceptible to changes in drug sensitivity when co-cultured with hFob cells, and this was observed in treatments with dexamethasone, doxorubicin and vorinostat. In addition resistance to doxorubicin was evident in MM.1R and VDR cells in co-culture with hFob (figure 3.5.4.2).

Since MM.1S appeared to be subject to hFob-induced drug resistance to a number of therapies, we further examined the potential mechanisms involved using MM.1S cell line. Transwell system was used to determine whether or not the observed resistance in MM.1S required direct cell-to-cell contact. We observed that direct cell-to-cell contact appeared to be necessary for osteoblast-

induced resistance to vorinostat in MM.1S, but was not necessary for osteoblast-induced resistance to doxorubicin in MM.1S, as resistance to doxorubicin was observed even when the cells were not in direct contact (figure 3.5.5.1). The reasoning for this difference has not been clarified but presumably is due to the fact that the osteoblast-induced resistance to doxorubicin is solely cytokine mediated, whereas osteoblast-induced resistance to vorinostat is likely by adhesion molecules between the two entities signalling resistance mechanisms.

Finally we hypothesized that perhaps the resistance observed that was induced by osteoblasts was due to a cell volume effect. The osteoblasts, which are much larger cells with a 5 times higher protein content we hypothesized might account for the resistance observed (figure 3.5.6.1). Therefore we co-cultured MM.1S cell with luciferase-negative MM cells or hFob cell in a 5:1 ratio respectively to determine whether or not the resistance observed was merely due to a mass effect. The resistance observed to doxorubicin or vorinostat in MM.1S-mcl in co-culture with hFob was not replicated when MM.1S-mcl cells were co-cultured with luciferase-negative cells, suggesting that this phenomenon is not a mass related effect secondary to the size of the hFob cells (figure 3.5.6.2).

It is however interesting to note that in MM.1S, MM.1R and VDR, no resistance to the novel therapies bortezomib, lenalidomide or preclinical agent JQ1 was observed. With regards to lenalidomide, this IMiD has recently been documented for its ability to down-regulate osteoblast activity in the *in vitro* setting, by inducing osteoblast inhibitors and suppressing promoters of osteoblast differentiation. This may explain why osteoblast-induced resistance is not observed with lenalidomide treatment.^[193] In contrast to this, bortezomib is known for its bone anabolic effects. Kaiser et al have shown that bortezomib stimulates differentiation of osteoblasts by inhibiting the breakdown of the vitamin D receptor and thus upregulating differentiation of osteoblasts.^[194] Therefore it is not clear why in our bortezomib treatments osteoblast-induced resistance is not observed. JQ1 has not yet been documented for its effects on osteoblasts.

These novel findings present somewhat of a clinical conundrum for future treatment of multiple myeloma. Lytic bone lesions contribute greatly to morbidity and mortality in patients with multiple myeloma by causing severe bone pain, pathological fractures, even paralysis when vertebral fractures occur. Recent efforts have heavily focused on upregulation of osteoblastogenesis in multiple myeloma in order to promote bone strength and prevent such bone lesions and reduce morbidity and mortality in multiple myeloma patients. The evidence to date for osteoblasts protective effect on malignant plasma cells reflects our findings in the *in vitro* setting only and further studies are needed to confirm our findings. However if osteoblastogenesis is be found to contribute to myeloma cell survival and/or drug resistance in the *in vivo* setting the role for inducers of osteoblastogenesis in multiple myeloma may need to be re-examined.

4.5.4 Role of the immunoproteasome and interferon-gamma in bortezomib resistance *in vitro*

For reasons outlined in results section 3.5.7 above, MM.1R and VDR cells were pre-treated with interferon-gamma for 48 hours and subsequently treated with bortezomib for 24 hours (0-80nM), and compared to a non-pre-treated control. No change in sensitivity of MM.1R to bortezomib was observed with interferon-gamma pre-treatment. However in VDR pre-treatment with interferon-gamma resulted in increased sensitivity to bortezomib at concentrations of 40nM (mean difference=18.24% relative cell viability vs. no interferon-gamma pre-treatment control; p=0.03) and 80nM (mean difference=12.19% relative cell viability vs. no interferon-gamma pre-treatment control; p=0.01), (figure 3.5.7.1). As we had hypothesized that interferon-gamma pre-treatment would up-regulate PSMB8 and down-regulate PSMB5 we next tested our hypothesis by examining to protein expression level of both proteasome subunits by western blot. Lysates from MM1R or VDR for the following conditions were examined for their expression levels of PSMB5, PSMB8 and poly-ubiquitinated proteins:

1. Control
2. Interferon-gamma alone
3. Bortezomib alone
4. Interferon-gamma pre-treatment and subsequent bortezomib treatment.

In both MM.1R and VDR, interferon-gamma-treated conditions (2/4 above) resulted in down-regulation of PSMB5 and up-regulation of PSMB8, as anticipated. In MM.1R, both bortezomib treatment alone (3) and interferon-gamma pre-treatment with subsequent bortezomib treatment resulted in marked accumulation of polyubiquitinated proteins. In VDR, interferon-gamma alone (2) or bortezomib alone (3) did not result in accumulation of polyubiquitinated proteins. However pre-treatment of VDR with interferon-gamma and subsequent bortezomib treatment (4) did result in an accumulation of polyubiquitinated proteins in VDR (figure 3.5.7.2). In summary, this data demonstrated that pre-treatment of VDR with interferon-gamma resulted in down-regulation of PSMB5, up-regulation of PSMB8, with resultant proteasome inhibition as suggested by accumulation of polyubiquitinated proteins.

Further review of the literature revealed 2 important studies relating to this research. Firstly, in 2005, Altun et al demonstrated that myeloma cell lines contain both constitutive and immunoproteasome subunits. At baseline, MM cell lines contain more constitutive than immunoproteasome subunits, however the latter is up-regulated by interferon-gamma. By 2-dimensional gel electrophoresis the active catalytic subunits for $\beta 5$, $\beta 1$ and $\beta 2$ subunits, or $\beta 5i$, $\beta 1i$ and $\beta 2i$ were examined following their treatment with bortezomib with and without interferon-gamma pre-treatment. They found that pre-treatment with interferon gamma up-regulated the $\beta 5i$ subunit (i.e. PSMB8), and that bortezomib had the ability to inhibit its catalytic activity. Therefore in VDR cell line, PSMB8 up-regulation by interferon-gamma may allow bortezomib to inhibit the proteasome via $\beta 5i$ inhibition and this may explain why we see accumulation of polyubiquitinated proteins in bortezomib-treated VDR when pre-treated with interferon-gamma.^[55]

Secondly, in 2008, another group have previously suggested a role for use of interferon-gamma to ameliorate the effects of bortezomib in preclinical models of B cell neoplasms including Burkitt's lymphoma, mantle cell lymphoma and myeloma. They found that pre-treatment of the B cell lymphoma cell line KARPAS422 and 5 out of 6 bortezomib-sensitive B cell lines tested (including RPMI8226 myeloma cell line) markedly increased the sensitivity of these cell lines to bortezomib. The plasmacytoma cell line U266 demonstrated the greatest increase in sensitivity to bortezomib when pre-treated with interferon-gamma. These findings may be mediated at least in part by increased immunoproteasome assembly as demonstrated by RT-PCR subunit expression levels following interferon-gamma pre-treatment.^[56] Interferon-gamma however is also known to alter transcription of a large number of genes including caspase-8 that promotes apoptosis,^[57] and Mitsiades et al have also demonstrated caspase-8 up-regulation by bortezomib.^[40] Therefore we cannot assume that the effects of interferon-gamma are solely mediated by immunoproteasome subunit up-regulation. However our data and the data of others both support a role for interferon-gamma treatment with bortezomib to augment its potency, and in particular our study supports a role for interferon-gamma pre-treatment in the setting of bortezomib-refractory myeloma.

4.5.5 Role of the immunoproteasome in the *in vivo* setting in bortezomib-refractory myeloma

We showed that PSMB5 was over-expressed in bortezomib-resistant VDR and by up-regulation of PSMB8 by interferon-gamma, we could increase the degree of accumulation of polyubiquitinated proteins in VDR and, to a certain degree, increase the sensitivity of VDR to bortezomib. However clinical samples of multiple myeloma patients have not been previously examined for their proteasome subunit expression levels, therefore we undertook immunohistochemistry on bone marrow trephines of patients with bortezomib-sensitive (diagnostic samples) and bortezomib-refractory (diagnostic and

relapsed samples) multiple myeloma to determine which proteasome subunits are expressed at diagnosis and at time of relapse.

The following samples were analysed by immunohistochemistry for their expression of PSMB5 and PSMB8:

1. Diagnostic bone marrow biopsies of 7 patients who achieved at least a very good partial response (VGPR) to a bortezomib-containing regimen (termed “diagnostic: responder”).
2. Diagnostic bone marrow biopsies of 6 patients who subsequently were found to relapse following a bortezomib-based regimen (termed “diagnostic: non-responder”).
3. Bone marrow biopsies of 7 patients at time of relapse to a bortezomib-containing regimen (of which 6 correlate to diagnostic samples in no. 2 above), (termed “relapsed: non-responder”).

We found that PSMB5 was strongly expressed in both bortezomib-responders and bortezomib non-responders at time of diagnosis in all samples tested. At time of relapse PSMB5 expression was positive in 5 out of 7 relapsed samples tested (table 3.5.8.1). PSMB8 was expressed in all 7 bortezomib-responders at time of diagnosis, although the expression appeared reduced compared to PSMB5 expression. This may be secondary to differences in the two antibodies used, however would fit with current knowledge that PSMB5 is highly expressed in myeloma cell lines, and PSMB8 is also expressed but to a lesser degree compared to PSMB5. Similarly PSMB8 was expressed in 5 out of 6 bortezomib-non-responders at time of diagnosis. Interestingly, at time of relapse, PSMB8 was expressed in only 2 out of 7 bortezomib-non-responders (table 3.5.8.2). Unusually, in “sample 5 non-responder”, PSMB8 was negative at time of diagnosis and positive at time of relapse following a bortezomib-containing regimen (table 3.5.8.2).

In summary, in bortezomib-responders, PSMB5 and PSMB8 were expressed in 100% of samples for both subunits. In bortezomib non-responders, PSMB5 and PSMB8 were expressed in 100% and 83% of samples respectively at time of

diagnosis. At time of relapse, PSMB5 and PSMB8 were expressed in 71% and 29% of samples respectively (table 4.5.5.1).

	Diagnosis: Responder	Diagnosis: Non-Responder	Relapse: Non-Responder
PSMB5	100% (7/7)	100% (6/6)	71% (5/7)
PSMB8	100% (7/7)	83% (5/6)	29% (2/7)

Table 4.5.5.1 PSMB5 and PSMB8 expression in patients with bortezomib sensitive (diagnostic samples) or bortezomib resistant (diagnostic and relapse samples) myeloma. Figures represent the percentage and number of samples (in brackets) of bone marrow biopsy samples tested in which PSMB5 or PSMB8 expression was found to be positive by immunohistochemistry.

A number of conclusions can be drawn from this study. Firstly our *in vitro* model VDR mirrors the *in vivo* setting of bortezomib refractory patients, in that PSMB5 is strongly expressed, this was demonstrated at time of diagnosis and at time of relapse in bortezomib-refractory patients. Similarly, PSMB8 levels are reduced in VDR and also reduced at time of relapse in bortezomib non-responders. In VDR we demonstrated over-expression of PSMB5 at the protein level, have outlined its potential role in bortezomib resistance *in vitro*, and the potential to overcome this resistance by up-regulation of PSMB8 using interferon-gamma. Niewerth et al have recently published their data on induction of the immunoproteasome subunit β -5i using interferon-gamma with subsequent resensitisation of a bortezomib-resistant leukaemia cell line to bortezomib, which mirrors our myeloma cell line model. Their data suggests inducing the immunoproteasome β -5i subunit using interferon-gamma and subsequently exposing the cells to a PSMB8 inhibitor, ONX0914 (PR-975), in order to overcome bortezomib resistance. Interferon-gamma pre-treatment also resensitised bortezomib-resistant cell lines to bortezomib, however resensitisation to the immunoproteasome inhibitor ONY0914 was more pronounced than that of bortezomib.^[195] Our *in vivo* study confirmed that PSMB5 is over-expressed at time of relapse and that PSMB8 is suppressed at time of relapse in known bortezomib-non-responders, therefore our *in vivo* data support the

aforementioned *in vitro* study, and further emphasises the need for examining the use of interferon-gamma in conjunction with bortezomib or ONX0914 in patients with relapsed and refractory multiple myeloma.

Finally, PSMB8 appears to be strongly expressed at diagnosis in both bortezomib-responders and bortezomib non-responders supporting the role for a PSMB8-specific inhibitor *in vivo*. Another PSMB8 inhibitor, PR-924, is now under investigation in the pre-clinical setting for use in multiple myeloma. PR-924 has been documented for its efficacy in multiple myeloma in the *in vitro* and *in vivo* setting in a SCID-hu mouse model of plasmacytoma xenografts.^[58] Our *in vivo* data support the suggestion by Singh et al to assess the efficacy of PSMB8 inhibitors in the *in vivo* setting for treatment of newly diagnosed multiple myeloma. Finally in two of the seven bortezomib-refractory samples examined at time of relapse, PSMB8 was positively expressed, also supporting a role for PSMB8 inhibitors in relapsed and refractory disease if patients are found to express PSMB8.

Chapter 5

Summary, Conclusion and Future Work

CHAPTER 5. SUMMARY, CONCLUSION AND FUTURE WORK

5.1 SUMMARY AND CONCLUSION

5.1.1 Characterisation of an isogenic cell line model of bortezomib resistance *in vitro* and *in vivo*.

- VDR demonstrated marked resistance to bortezomib in the *in vitro* setting compared to MM.1R, and VDR retains its resistance to dexamethasone similar to its parent cell line.
- Conventional compounds such as doxorubicin and vincristine have comparable toxicity in VDR and parental MM1R.
- Recently FDA-approved novel therapies such as vorinostat, lenalidomide, and pomalidomide are highly toxic to both MM.1R and VDR.
- The investigational reagent JQ1 displays marked anti-tumour activity in VDR as well as MM.1R.
- VDR cells are also resistant to MLN2238, a novel orally bioavailable compound that specifically targets the proteasome beta-5 subunit, which is the same active site targeted by bortezomib.
- While VDR cells are resistant to bortezomib and MLN2238, they are highly sensitive to the second generation, irreversible proteasome inhibitor carfilzomib.
- High-throughput screen of a database of compounds with FDA-approval for use in oncology demonstrated that VDR has marked sensitivity to the taxanes and topoisomerase-1 and -2 inhibitors.
- Bortezomib resistance in VDR does not appear to be PGP-mediated.
- An *in vivo* study examining the effect of bortezomib or carfilzomib in MM did not reveal a statistically significant reduction in tumour burden in VDR compared to vehicle mice.
- VDR-mice displayed a statistically significant improvement in overall survival in both bortezomib-treated and carfilzomib-treated mice compared to vehicle-mice.

5.1.2 Whole exome sequencing of MM.1R and VDR

- We performed whole exome sequencing analysis of the cell lines MM.1R and VDR to determine SNVs, insertions or deletions that were present in bortezomib resistant VDR but not bortezomib-sensitive MM.1R cell line.
- 28 non-synonymous single nucleotide variants (SNV) were detected in VDR that were not present in MM.1R
- SIFT and Polyphen predictions found 7 SNVs to be “damaging” by both algorithms and 6 SNVs were found to be “damaging” by either SIFT or Polyphen algorithms.
- A deletion in ABCA7 gene was found in VDR but not MM.1R.
- Reduced transcript levels of ABCA7 gene has been correlated with reduction of disease free interval in patients post-therapy for colorectal cancer.
- However neither ABCA7 gene down-regulation nor deletion have been implicated in haematological malignancy in the *in vivo* setting to date.
- No insertions were identified between the MM.1R and VDR comparisons.
- A missense mutation involving a single amino acid substitution in the PSMB5 gene was identified in VDR at chromosomal position g.23502844 involving a threonine to alanine substitution at position 80 of exon 2 in the uncleaved (propeptide) version of PSMB5 gene, with 100% allelic frequency of mutPSMB5 in VDR, and 100% wtPSMB5 frequency in MM.1R.
- Introduction of mutPSMB5 via lentiviral construct into bortezomib sensitive cell line KMS11 rendered these cells initially bortezomib-sensitive cells now resistant to bortezomib.
- Additionally, over-expression of wtPSMB5 reduced the sensitivity of KMS11 cells to bortezomib, however to a lesser degree than mutPSMB5.

5.1.3 Gene expression profiles of MM.1R and VDR

- 353 genes were over-expressed in VDR compared to MM.1R. In comparison only 84 genes were down-regulated in VDR compared to MM.1R. (whereby fold change >1.2 , $p < 0.01$).
- Pathway analysis revealed “cellular apoptosis” as a specific pathway in which 4 transcripts up-regulated in VDR play a role. These genes include CFLAR, CASP8, CASP10, and NFKBIA
- Transcripts that were down-regulated in VDR compared to MM.1R were noted to participate in a number of cellular processes mainly concerned with the immune system.
- An shRNA screen of 27 selected target genes was undertaken to determine if shRNA knockdown and subsequent bortezomib treatment resensitised VDR cell cells to bortezomib. 11 genes were found to cause $>40\%$ cell death of VDR cells compared to control hairpins following shRNA knockdown and subsequent treatment with bortezomib 50nM.
- PSMB5 shRNA knockdown resulted in resensitisation of VDR to bortezomib 50nM. We validated successful shRNA knockdown of PSMB5 in MM.1R and VDR by immunoblot. We furthermore demonstrated that shRNA knockdown of PSMB5 and subsequent treatment of VDR cells (used at even lower concentrations of bortezomib compared to initial screen: 50nM vs. 20-40nM), resulted in significant resensitisation of VDR to bortezomib.

5.1.4 Proteomic profiling of MM.1R and VDR by label-free mass spectrometry

- 238 proteins were differentially expressed in the MM.1R vs. VDR comparison, of which 106 were over-expressed and 132 down-regulated in VDR vs. MM.1R.
- CCL3 has known pathogenesis in myeloma and demonstrated a 22-fold higher expression level in VDR compared to MM.1R.
- DAVID functional annotation tool revealed a number of proteins over-expressed in VDR that are involved in apoptosis, regulation of cellular metabolic processes, cellular homeostasis, cell cycle process and proteasomal ubiquitin-dependent protein catabolic process.
- Three proteins that were found to be down-regulated in VDR compared to MM.1R were found to be involved in aminoacyl tRNA biosynthesis.
- We also analysed proteins differentially expressed in MM.1R and VDR following bortezomib treatment, of which the majority of proteins were down-regulated in bortezomib-treated MM.1R.
- By comparing bortezomib-treated MM.1R to bortezomib-treated VDR, 109 proteins out of a total 323 were downregulated in bortezomib-treated-VDR compared to bortezomib-treated-MM.1R.
- 5 proteins that were down-regulated in bortezomib-treated VDR compared to bortezomib-treated MM.1R are involved in the MAP-kinase signalling pathway, which when altered, is well documented for its role in carcinogenesis. These proteins include FLNA, HSP72/HSPA6, PPP3C, MEK2C and HSP27/HSPB1.
- 215 proteins were up-regulated in bortezomib-treated VDR compared to bortezomib-treated MM.1R. Two target proteins of interest included CCL3 and EIF5A.
- PSMB5 is over-expressed 3.85-fold in VDR compared to MM.1R at baseline. A 13-fold increase in PSMB5 expression is observed in bortezomib-treated VDR compared to bortezomib-treated MM.1R, supporting the role of PSMB5 dysregulation in VDR as a potential mechanism for bortezomib resistance in this cell line.

5.1.5 Functional studies and potential role of the bone marrow microenvironment in the pathogenesis of bortezomib resistance in VDR

- No change in the sensitivity of MM.1R or VDR to bortezomib was observed following their short term co-culture with HS-5 stromal cells
- MM.1R cells appeared to display reduced sensitivity to carfilzomib following their co-culture with HS-5 cells, however VDR cells retained their sensitivity to carfilzomib despite their co-culture with HS-5 cells.
- VDR cells displayed resistance to vorinostat and MLN4924 when co-cultured in the presence of HS-5 cells, and combination of bortezomib with either agent was not sufficient to overcome the resistance observed.
- VDR displayed a marked increase in cell viability when co-cultured in the presence of hFob cell line.
- MM.1S appeared to be the cell line that was most susceptible to changes in drug sensitivity when co-cultured with hFob cells. Resistance to doxorubicin was evident in MM.1R and VDR cells in co-culture with hFob.
- Direct cell-to-cell contact appeared to be necessary for osteoblast-induced resistance to vorinostat in MM.1S, but was not necessary for osteoblast-induced resistance to doxorubicin in MM.1S.
- By pre-treating VDR cells with interferon-gamma before bortezomib treatment, we observed an increase in sensitivity of VDR cells to bortezomib, and an increase in poly-ubiquitinated proteins and increased expression of PSMB8 as demonstrated by western blot.
- Immunohistochemistry on 7 bone marrow trephines of patients with bortezomib-sensitive and bortezomib-refractory multiple myeloma revealed the following:
 1. PSMB5 was expressed at diagnosis in all bortezomib responders and bortezomib non-responders tested.
 2. At time of relapse, PSMB5 was expressed in 5 out of 7 samples tested.
 3. PSMB8 was expressed at diagnosis in all bortezomib responders and in 5 out of 6 bortezomib non-responders.
 4. At time of relapse, PSMB8 was expressed in 2 out of 7 samples tested.

5.1.6 CONCLUSION

The main aim of this thesis was to examine the intrinsic and extrinsic mechanisms of bortezomib resistance in multiple myeloma based on our study of an isogenic cell line model of bortezomib resistance. VDR displayed stable resistance to bortezomib compared to parental bortezomib-sensitive cell line MM.1R. in a number of toxicological-based assays. VDR retained its resistance to dexamethasone similar to MM.1R. The toxicity profile of this cell line to other conventional, novel and investigational therapies was also comparable with MM.1R. Interestingly, VDR was also resistant to the orally bioactive alternative form of bortezomib, MLN2238, but was highly sensitive to the irreversible proteasome inhibitor carfilzomib. The resistance to bortezomib did not appear to be mediated by p-glycoprotein, and was secondary to a difference in proliferation rate between the two cell lines. An *in vivo* study examining the effect of bortezomib or carfilzomib in VDR did not reveal a statistically significant reduction in tumour burden in either cell lines compared to vehicle mice. In MM.1R-mice, a statistically significant improvement in overall survival was observed in bortezomib treated mice, compared to controls and compared to carfilzomib treated mice. VDR-mice displayed a statistically significant improvement in overall survival in both bortezomib-treated and carfilzomib-treated mice compared to vehicle-mice. The *in vivo* study emphasises the pertinent role of the bone marrow microenvironment in multiple myeloma pathogenesis, and the reasons for the findings of this *in vivo* study should be clarified.

Whole exome sequencing of MM.1R and VDR identified 28 non-synonymous single nucleotide variants found in VDR that were not present in MM.1R. A single amino acid substitution in the PSMB5 gene was identified in VDR involving a threonine to alanine substitution with 100% allelic frequency in VDR, and 100% wtPSMB5 frequency in MM.1R. This PSMB5 mutation was previously documented and has been shown by 3D *in silico* modelling to induce a conformational change in the bortezomib binding pocket. Introduction of mutPSMB5 via lentiviral construct into the bortezomib sensitive cell line KMS11 rendered these cells resistant to bortezomib. Over-expression of wtPSMB5

reduced the sensitivity of KMS11 cells to bortezomib, but to a lesser degree than mutPSMB5. In addition a deletion in ABCA7 gene was found in VDR but not MM.1R. Reduced transcript levels of ABCA7 gene has been correlated with reduction of disease free interval in patients post-therapy for colorectal cancer. However neither ABCA7 gene down-regulation nor deletion have been implicated in haematological malignancy in the *in vivo* setting to date.

Gene expression profiling revealed a number of genes differentially expressed in VDR compared to MM.1R. Pathway analysis revealed “cellular apoptosis” as a specific pathway in which 4 transcripts that are up-regulated in VDR play a role. These genes include CFLAR, CASP8, CASP10, and NFKBIA. Transcripts that were down-regulated in VDR compared to MM.1R were noted to participate in a number of cellular processes mainly concerned with the immune system. An shRNA screen of 27 selected target genes was undertaken to determine if shRNA knockdown and subsequent bortezomib treatment resensitised VDR cell cells to bortezomib. Here, 11 of 27 genes analysed were found to cause >40% cell death of VDR cells compared to control hairpins following shRNA knockdown and subsequent treatment with bortezomib 50nM. In particular, PSMB5 shRNA knockdown resulted in resensitisation of VDR to bortezomib 50nM. We validated successful shRNA knockdown of PSMB5 in MM.1R and VDR by immunoblot. We furthermore demonstrated that shRNA knockdown of PSMB5 and subsequent treatment of VDR cells (used at even lower concentrations of bortezomib compared to initial screen: 50nM vs. 20-40nM), resulted in significant resensitisation of VDR to bortezomib, suggesting PSMB5 as a major factor in bortezomib-induced resistance in VDR.

By label-free mass spectrometry 238 proteins were differentially expressed in the MM.1R vs. VDR comparison, including a number of interesting targets such as CCL3 which has known pathogenesis in myeloma. Three proteins that were found to be down-regulated in VDR compared to MM.1R are involved in aminoacyl tRNA biosynthesis. By comparing bortezomib-treated MM.1R to bortezomib-treated VDR, we demonstrated 5 proteins that were down-regulated in bortezomib-treated VDR compared to bortezomib-treated MM.1R that are involved in the MAP-kinase signalling pathway, known for its role in

carcinogenesis. Proteins up-regulated in bortezomib-treated VDR compared to bortezomib-treated MM.1R included PSMB7, PSMB6, CCL3, GSTP1 and EIF5A. In addition PSMB5 is over-expressed also at the protein level 3.85-fold in VDR compared to MM.1R at baseline. A 13-fold increase in PSMB5 expression is observed in bortezomib-treated VDR compared to bortezomib-treated MM.1R, supporting the role of PSMB5 dysregulation in VDR as a potential mechanism for bortezomib resistance in this cell line.

We examined a number of extrinsic factors that play a further role in bortezomib resistance in VDR. No change in the sensitivity of MM.1R or VDR to bortezomib was observed following their co-culture with HS-5 stromal cells. MM.1R cells appeared to display reduced sensitivity to carfilzomib following their co-culture with HS-5 cells and the mechanism for this observation remains unclear. However VDR cells retained their sensitivity to carfilzomib despite their co-culture with HS-5 cells. Examining other novel therapies, VDR cells displayed resistance to vorinostat and MLN4924 when co-cultured in the presence of HS-5 cells, and combination of bortezomib with either agent was not sufficient to overcome the resistance observed. We furthermore investigated the effect of osteoblasts on the isogenic cell line model. VDR displayed a marked increase in cell viability when co-cultured in the presence of hFob cell line. Again the mechanism for this finding needs to be clarified. MM.1S (rather than MM.1R or VDR) appeared to be the cell line that was most susceptible to changes in drug sensitivity when co-cultured with hFob cells, and was evident for dexamethasone, doxorubicin and vorinostat treatments. Resistance to doxorubicin only was evident in MM.1R and VDR cells in co-culture with hFob. Direct cell-to-cell contact appeared to be necessary for osteoblast-induced resistance to vorinostat in MM.1S, but was not necessary for osteoblast-induced resistance to doxorubicin in MM.1S. Finally by pre-treating VDR cells with interferon-gamma before bortezomib treatment, an increase in sensitivity of VDR cells to bortezomib, and an increase in poly-ubiquitinated proteins and increased expression of PSMB8 as demonstrated by western blot was observed. Immunohistochemistry on 7 bone marrow trephines of patients with bortezomib-refractory multiple myeloma revealed varied expression levels of

PSMB5 (100%) and PSMB8 (83%) in the bone marrow biopsies of these patients at diagnosis, whereas at time of relapse, 71% of samples were positive for PSMB5 but only 29% positive for PSMB8.

These final studies of extrinsic mechanisms of drug resistance have provided a number of interesting conclusions. Panproteasome inhibition through carfilzomib could be considered a more effective means of myeloma cell death in the setting of bortezomib resistance and its efficacy does not appear to be abrogated by the presence of accessory HS-5 stromal cells. Osteoblast-like cells hFob appear to support the growth of VDR cells, and in grand-parent cell line MM.1S, appears to induce resistance to a number of novel and conventional therapies, and the mechanisms for these latter findings should be further investigated. Finally PSMB8 over-expression by interferon-gamma stimulation appears to induce a degree of resensitisation of VDR to bortezomib. PSMB8 expression is lost in a number of bortezomib-refractory patients. Bortezomib resistance *in vivo* could potentially be overcome by upregulation of PSMB8 by pre-treatment of patients with interferon-gamma and subsequent treatment with bortezomib or a PSMB8 inhibitor. In addition, PSMB8 is expressed at diagnosis in bortezomib responders and non-responders supporting the proposal for clinical trials for use of PSMB8 inhibitors in patients with newly diagnosed multiple myeloma. If patients are found to over-express PSMB8 in bone marrow trephine samples at time of relapse, as was observed in a small number of our patients, a PSMB8 inhibitor may also be beneficial in patients with bortezomib-refractory disease.

5.2 FUTURE WORK

5.2.1 Characterisation of an isogenic cell line model of bortezomib resistance *in vitro* and *in vivo*.

- Generation of further models of resistance to novel therapies such as carfilzomib.
- Longer follow-up of *in vivo* study to determine if VDR displays greater resistance to bortezomib in the *in vivo* setting that mirrors the *in vitro* setting.
- Investigate reasoning for greater reduction in tumour burden in MM.1R-mice treated with bortezomib compared to carfilzomib.
- Generation of models of drug resistance in myeloma in the setting of the bone marrow microenvironment.

5.2.2 Whole exome sequencing of MM.1R and VDR

- Evaluate CD138-positive cells of bortezomib-refractory multiple myeloma patients for deletion in ABCA7 gene to determine if this finding in the *in vitro* models correlates in the *in vivo* setting
- Evaluate a greater number of bortezomib-refractory patients for mutPSMB5 identified in VDR by our group and others, later in their disease stage, following multiple lines of bortezomib-based regimens.

5.2.3 Gene expression profiles of MM.1R and VDR

- Validation of further targets identified by shRNA knockdown screen as markers that when eliminated, increase the sensitivity of VDR to bortezomib.

5.2.4 Proteomic profiling of MM.1R and VDR by label-free mass spectrometry

- *In vitro* assay to examine the efficacy of a specific CCL3 inhibitor in bortezomib-resistant cell line VDR

- Validation of further biomarkers upregulated in VDR as identified by label-free mass spectrometry in particular those of the MAP-kinase pathway, and clarify their role bortezomib resistance.

5.2.5 Role of the bone marrow microenvironment in the pathogenesis of bortezomib resistance in VDR

- Investigate the mechanism for the observed stromal induced carfilzomib-resistance in MM1.R by HS-5 cells that was not apparent in VDR.
- Although not directly implicated in bortezomib resistance, one should investigate the mechanisms of osteoblast-induced increase in proliferation rate in VDR, and osteoblast-induced drug-resistance in MM.1S.
- Analyse a greater number of bone marrow biopsies of patients with bortezomib-refractory myeloma at time of diagnosis and relapse to confirm the expression levels of PSMB5 and PSMB8 observed in our study
- An *in vivo* mouse model of bortezomib-refractory myeloma examining the tolerability of interferon-gamma with subsequent bortezomib or PSMB8 inhibitor in the *in vivo* setting, with a view to progressing to phase 1 clinical trials in patients with bortezomib-refractory myeloma.

6. SCIENTIFIC WORK PUBLISHED OR PRESENTED

Journal Publications:

New proteasome inhibitors in myeloma.

Lawasut P, Chauhan D, Laubach J, **Hayes C**, Fabre C, Maglio M, Mitsiades C, Hideshima T, Anderson KC, Richardson PG.
Curr Hematol Malig Rep. 2012 Dec;7(4):258-66.

Presentations to Learned Societies

Poster Presentations:

1. **Human Proteome Organization (HUPO). Geneva, Switzerland, September 2011. Hayes CA**, O' Gorman P, Ooi MG, Jakubikova J, Jacobs H, Delmore J, McMillin DW, Klippel S, Anderson KC, Richardson PG, Clynes M, Mitsiades CS, Dowling P. Osteoclasts in multiple myeloma: molecular characterization of the synergistic pathways involved.
2. **Haematology Association of Ireland Congress, Ireland, October 2011. Hayes CA**, Jakubikova J, Ooi MG, Jacobs H, Delmore J, McMillin DW, Anderson KC, Richardson PG, Clynes M, O' Gorman P, Mitsiades CS, Dowling P. Proteomic profile of the multiple myeloma cell line NCI-H929 following osteoclast co-culture.
3. **American Society of Haematology Annual Congress, San Diego, CA. December 2011. Hayes CA**, Dowling P, Negri J, Henry M, Buon L, Jakubikova J, Delmore J, McMillin DW, Klippel S, Jacobs HM, van de Donk N, Dhimolea E, Lawasut P, Richardson PG, Anderson KC, Clynes M, O' Gorman P, Mitsiades CS. Proteomic characterization of an isogenic multiple myeloma cell line model of bortezomib resistance.
4. **American Society of Haematology Annual Congress, Atlanta, Georgia, December 2012. Catriona A. Hayes**, Paul Dowling, Richard W.J. Groen, Douglas W. McMillin, Jake E. Delmore, Hannah M. Jacobs, Niels W.C.J. van de Donk, Eugen Dhimolea, Paul G. Richardson, Kenneth C. Anderson, Martin Clynes, Peter O'Gorman, Constantine S. Mitsiades. Cells of the Osteoblast Lineage Confer Myeloma Cell Resistance to Established and Investigational Therapeutic Agents.
5. **European School of Haematology International Conference on Multiple Myeloma, Dublin, October 2013. C Hayes**, P Dowling, M Henry, S Madden, J Meiller, E Dhimolea, MBariteau, J Negri, B. Aftab, A. Schinzel, N Kohl, M Clynes, C Mitsiades, P O'Gorman. Characterisation Of

An Isogenic Cell Line Model Of Bortezomib Resistance In Multiple Myeloma.

Oral Presentations:

6. **Haematology Association of Ireland Congress, Ireland, October 2011.**
CA Hayes, D McMillin, HM Jacobs, J Delmore, P Lawasut, E Dhimolea, M Clynes, P Dowling, PG Richardson, KC Anderson, P O' Gorman, CS Mitsiades. Pre-clinical investigation of an alternative pathophysiologic role for osteoblasts in multiple myeloma.
7. **Haematology Association of Ireland Congress, Ireland, October 2013.**
C Hayes, P Dowling, M Henry, S Madden, J Meiller, E Dhimolea, MBariteau, J Negri, B. Aftab, A. Schinzel, N Kohl, M Clynes, C Mitsiades, P O'Gorman. Characterisation Of An Isogenic Cell Line Model Of Bortezomib Resistance In Multiple Myeloma.

REFERENCES

1. Sant, M., et al., *Survival for haematological malignancies in Europe between 1997 and 2008 by region and age: results of EURO CARE-5, a population-based study*. *Lancet Oncol*, 2014. **15**(9): p. 931-42.
2. Richardson, P.G., et al., *Extended follow-up of a phase 3 trial in relapsed multiple myeloma: final time-to-event results of the APEX trial*. *Blood*, 2007. **110**(10): p. 3557-60.
3. Moreau, P., et al., *Proteasome inhibitors in multiple myeloma: 10 years later*. *Blood*, 2012. **120**(5): p. 947-59.
4. Kumar, S.K., et al., *Risk of progression and survival in multiple myeloma relapsing after therapy with IMiDs and bortezomib: a multicenter international myeloma working group study*. *Leukemia*, 2012. **26**(1): p. 149-57.
5. Kyle, R.A., et al., *Prevalence of monoclonal gammopathy of undetermined significance*. *N Engl J Med*, 2006. **354**(13): p. 1362-9.
6. Kyle, R.A. and S.V. Rajkumar, *Criteria for diagnosis, staging, risk stratification and response assessment of multiple myeloma*. *Leukemia*, 2009. **23**(1): p. 3-9.
7. Durie, B.G. and S.E. Salmon, *A clinical staging system for multiple myeloma. Correlation of measured myeloma cell mass with presenting clinical features, response to treatment, and survival*. *Cancer*, 1975. **36**(3): p. 842-54.
8. Greipp, P.R., et al., *International staging system for multiple myeloma*. *J Clin Oncol*, 2005. **23**(15): p. 3412-20.
9. Kleber, M., et al., *Validation of the Freiburg Comorbidity Index in 466 Multiple Myeloma Patients and Combination With the International Staging System Are Highly Predictive for Outcome*. *Clin Lymphoma Myeloma Leuk*, 2013.
10. Engelhardt, M., et al., *European Myeloma Network recommendations on the evaluation and treatment of newly diagnosed patients with multiple myeloma*. *Haematologica*, 2014. **99**(2): p. 232-42.
11. Richardson, P.G., et al., *Lenalidomide, bortezomib, and dexamethasone combination therapy in patients with newly diagnosed multiple myeloma*. *Blood*, 2010. **116**(5): p. 679-86.
12. Morgan, G.J., et al., *First-line treatment with zoledronic acid as compared with clodronic acid in multiple myeloma (MRC Myeloma IX): a randomised controlled trial*. *Lancet*, 2010. **376**(9757): p. 1989-99.
13. McCarthy, P.L., et al., *Lenalidomide after stem-cell transplantation for multiple myeloma*. *N Engl J Med*, 2012. **366**(19): p. 1770-81.
14. Richardson, P., et al., *Phase I trial of oral vorinostat (suberoylanilide hydroxamic acid, SAHA) in patients with advanced multiple myeloma*. *Leuk Lymphoma*, 2008. **49**(3): p. 502-7.

15. Weber, D.M., et al., *Phase I Trial of Vorinostat Combined With Bortezomib for the Treatment of Relapsing and/or Refractory Multiple Myeloma*. Clin Lymphoma Myeloma Leuk, 2012. **12**(5): p. 319-24.
16. Hideshima, T., P.G. Richardson, and K.C. Anderson, *Mechanism of action of proteasome inhibitors and deacetylase inhibitors and the biological basis of synergy in multiple myeloma*. Mol Cancer Ther, 2011. **10**(11): p. 2034-42.
17. DeAngelo, D.J., et al., *Phase Ia/II, two-arm, open-label, dose-escalation study of oral panobinostat administered via two dosing schedules in patients with advanced hematologic malignancies*. Leukemia, 2013. **27**(8): p. 1628-36.
18. Richardson, P.G., et al., *PANORAMA 2: panobinostat in combination with bortezomib and dexamethasone in patients with relapsed and bortezomib-refractory myeloma*. Blood, 2013. **122**(14): p. 2331-7.
19. San-Miguel, J.F., et al., *Phase Ib study of panobinostat and bortezomib in relapsed or relapsed and refractory multiple myeloma*. J Clin Oncol, 2013. **31**(29): p. 3696-703.
20. Siegel, D.S., et al., *A phase 2 study of single-agent carfilzomib (PX-171-003-A1) in patients with relapsed and refractory multiple myeloma*. Blood, 2012. **120**(14): p. 2817-25.
21. Brinchen, S., et al., *Carfilzomib, cyclophosphamide, and dexamethasone in patients with newly diagnosed multiple myeloma: a multicenter, phase 2 study*. Blood, 2014. **124**(1): p. 63-9.
22. Jagannath, S., et al., *An Open-Label Single-Arm Pilot Phase II Study (PX-171-003-A0) of Low-Dose, Single-Agent Carfilzomib in Patients With Relapsed and Refractory Multiple Myeloma*. Clin Lymphoma Myeloma Leuk, 2012. **12**(5): p. 310-8.
23. Lendvai, N., et al., *A phase 2 single-center study of carfilzomib 56 mg/m² with or without low-dose dexamethasone in relapsed multiple myeloma*. Blood, 2014. **124**(6): p. 899-906.
24. Siegel, D., et al., *Integrated safety profile of single-agent carfilzomib: experience from 526 patients enrolled in 4 phase II clinical studies*. Haematologica, 2013. **98**(11): p. 1753-61.
25. Chauhan, D., et al., *A novel orally active proteasome inhibitor induces apoptosis in multiple myeloma cells with mechanisms distinct from Bortezomib*. Cancer Cell, 2005. **8**(5): p. 407-19.
26. Richardson, P.G., et al., *Phase 1 study of twice-weekly ixazomib, an oral proteasome inhibitor, in relapsed/refractory multiple myeloma patients*. Blood, 2014. **124**(7): p. 1038-46.
27. Larocca, A., et al., *Pomalidomide, cyclophosphamide, and prednisone for relapsed/refractory multiple myeloma: a multicenter phase 1/2 open-label study*. Blood, 2013. **122**(16): p. 2799-806.
28. Leleu, X., et al., *Pomalidomide plus low-dose dexamethasone is active and well tolerated in bortezomib and lenalidomide-refractory multiple myeloma: Intergroupe Francophone du Myelome 2009-02*. Blood, 2013. **121**(11): p. 1968-75.
29. Richardson, P.G., et al., *Phase 1 study of pomalidomide MTD, safety, and efficacy in patients with refractory multiple myeloma who have received lenalidomide and bortezomib*. Blood, 2013. **121**(11): p. 1961-7.

30. Richardson, P.G., et al., *Pomalidomide alone or in combination with low-dose dexamethasone in relapsed and refractory multiple myeloma: a randomized phase 2 study*. Blood, 2014. **123**(12): p. 1826-32.
31. San Miguel, J., et al., *Pomalidomide plus low-dose dexamethasone versus high-dose dexamethasone alone for patients with relapsed and refractory multiple myeloma (MM-003): a randomised, open-label, phase 3 trial*. Lancet Oncol, 2013. **14**(11): p. 1055-66.
32. Richardson, P.G., et al., *Perifosine, an oral, anti-cancer agent and inhibitor of the Akt pathway: mechanistic actions, pharmacodynamics, pharmacokinetics, and clinical activity*. Expert Opin Drug Metab Toxicol, 2012. **8**(5): p. 623-33.
33. Jakubowiak, A.J., et al., *Perifosine plus lenalidomide and dexamethasone in relapsed and relapsed/refractory multiple myeloma: a Phase I Multiple Myeloma Research Consortium study*. Br J Haematol, 2012. **158**(4): p. 472-80.
34. McMillin, D.W., et al., *Molecular and cellular effects of NEDD8-activating enzyme inhibition in myeloma*. Mol Cancer Ther, 2012. **11**(4): p. 942-51.
35. McMillin, D.W., et al., *Antimyeloma activity of the orally bioavailable dual phosphatidylinositol 3-kinase/mammalian target of rapamycin inhibitor NVP-BEZ235*. Cancer Res, 2009. **69**(14): p. 5835-42.
36. Lonial, S., C.S. Mitsiades, and P.G. Richardson, *Treatment options for relapsed and refractory multiple myeloma*. Clin Cancer Res, 2011. **17**(6): p. 1264-77.
37. Jakubowiak, A.J., et al., *Phase I trial of anti-CS1 monoclonal antibody elotuzumab in combination with bortezomib in the treatment of relapsed/refractory multiple myeloma*. J Clin Oncol, 2012. **30**(16): p. 1960-5.
38. Groll, M., et al., *Structure of 20S proteasome from yeast at 2.4 Å resolution*. Nature, 1997. **386**(6624): p. 463-71.
39. Groll, M., et al., *Crystal structure of the boronic acid-based proteasome inhibitor bortezomib in complex with the yeast 20S proteasome*. Structure, 2006. **14**(3): p. 451-6.
40. Mitsiades, N., et al., *Molecular sequelae of proteasome inhibition in human multiple myeloma cells*. Proc Natl Acad Sci U S A, 2002. **99**(22): p. 14374-9.
41. Hideshima, T., et al., *NF-kappa B as a therapeutic target in multiple myeloma*. J Biol Chem, 2002. **277**(19): p. 16639-47.
42. Mitsiades, N., et al., *The proteasome inhibitor PS-341 potentiates sensitivity of multiple myeloma cells to conventional chemotherapeutic agents: therapeutic applications*. Blood, 2003. **101**(6): p. 2377-80.
43. Ooi, M.G., et al., *Interactions of the Hdm2/p53 and proteasome pathways may enhance the antitumor activity of bortezomib*. Clin Cancer Res, 2009. **15**(23): p. 7153-60.
44. Uyama, M., et al., *Regulation of osteoblastic differentiation by the proteasome inhibitor bortezomib*. Genes Cells, 2012. **17**(7): p. 548-58.
45. Pennisi, A., et al., *The proteasome inhibitor, bortezomib suppresses primary myeloma and stimulates bone formation in myelomatous and nonmyelomatous bones in vivo*. Am J Hematol, 2009. **84**(1): p. 6-14.
46. Zangari, M., et al., *A prospective evaluation of the biochemical, metabolic, hormonal and structural bone changes associated with bortezomib*

- response in multiple myeloma patients. Haematologica*, 2011. **96**(2): p. 333-6.
47. Parlati, F., et al., *Carfilzomib can induce tumor cell death through selective inhibition of the chymotrypsin-like activity of the proteasome. Blood*, 2009. **114**(16): p. 3439-47.
 48. Kuhn, D.J., et al., *Potent activity of carfilzomib, a novel, irreversible inhibitor of the ubiquitin-proteasome pathway, against preclinical models of multiple myeloma. Blood*, 2007. **110**(9): p. 3281-90.
 49. Martin, T.G., *Peripheral Neuropathy Experience in Patients With Relapsed and/or Refractory Multiple Myeloma Treated With Carfilzomib. Oncology (Williston Park)*, 2013. **27**(12 Suppl 3).
 50. Arastu-Kapur, S., et al., *Nonproteasomal targets of the proteasome inhibitors bortezomib and carfilzomib: a link to clinical adverse events. Clin Cancer Res*, 2011. **17**(9): p. 2734-43.
 51. Lawasut, P., et al., *New Proteasome Inhibitors in Myeloma. Curr Hematol Malig Rep*, 2012.
 52. Millward, M., et al., *Phase 1 clinical trial of the novel proteasome inhibitor marizomib with the histone deacetylase inhibitor vorinostat in patients with melanoma, pancreatic and lung cancer based on in vitro assessments of the combination. Invest New Drugs*, 2012. **30**(6): p. 2303-17.
 53. Ferrington, D.A. and D.S. Gregerson, *Immunoproteasomes: structure, function, and antigen presentation. Prog Mol Biol Transl Sci*, 2012. **109**: p. 75-112.
 54. Rock, K.L. and A.L. Goldberg, *Degradation of cell proteins and the generation of MHC class I-presented peptides. Annu Rev Immunol*, 1999. **17**: p. 739-79.
 55. Altun, M., et al., *Effects of PS-341 on the activity and composition of proteasomes in multiple myeloma cells. Cancer Res*, 2005. **65**(17): p. 7896-901.
 56. Busse, A., et al., *Sensitivity of tumor cells to proteasome inhibitors is associated with expression levels and composition of proteasome subunits. Cancer*, 2008. **112**(3): p. 659-70.
 57. Varela, N., et al., *Interferon-gamma sensitizes human myeloid leukemia cells to death receptor-mediated apoptosis by a pleiotropic mechanism. J Biol Chem*, 2001. **276**(21): p. 17779-87.
 58. Singh, A.V., et al., *PR-924, a selective inhibitor of the immunoproteasome subunit LMP-7, blocks multiple myeloma cell growth both in vitro and in vivo. Br J Haematol*, 2011. **152**(2): p. 155-63.
 59. Oerlemans, R., et al., *Molecular basis of bortezomib resistance: proteasome subunit beta5 (PSMB5) gene mutation and overexpression of PSMB5 protein. Blood*, 2008. **112**(6): p. 2489-99.
 60. Lu, S., et al., *Point mutation of the proteasome beta5 subunit gene is an important mechanism of bortezomib resistance in bortezomib-selected variants of Jurkat T cell lymphoblastic lymphoma/leukemia line. J Pharmacol Exp Ther*, 2008. **326**(2): p. 423-31.
 61. Ri, M., et al., *Bortezomib-resistant myeloma cell lines: a role for mutated PSMB5 in preventing the accumulation of unfolded proteins and fatal ER stress. Leukemia*, 2010. **24**(8): p. 1506-12.

62. Perez-Galan, P., et al., *Bortezomib resistance in mantle cell lymphoma is associated with plasmacytic differentiation*. Blood, 2011. **117**(2): p. 542-52.
63. Suzuki, E., et al., *Molecular mechanisms of bortezomib resistant adenocarcinoma cells*. PLoS One, 2011. **6**(12): p. e27996.
64. Franke, N.E., et al., *Impaired bortezomib binding to mutant beta5 subunit of the proteasome is the underlying basis for bortezomib resistance in leukemia cells*. Leukemia, 2012. **26**(4): p. 757-68.
65. Kuhn, D.J., et al., *Targeting the insulin-like growth factor-1 receptor to overcome bortezomib resistance in preclinical models of multiple myeloma*. Blood, 2012. **120**(16): p. 3260-70.
66. Sawyer, J.R., *The prognostic significance of cytogenetics and molecular profiling in multiple myeloma*. Cancer Genet, 2011. **204**(1): p. 3-12.
67. Chapman, M.A., et al., *Initial genome sequencing and analysis of multiple myeloma*. Nature, 2011. **471**(7339): p. 467-72.
68. Bollag, G., et al., *Vemurafenib: the first drug approved for BRAF-mutant cancer*. Nat Rev Drug Discov, 2012.
69. Lichter, D.I., et al., *Sequence analysis of beta-subunit genes of the 20S proteasome in patients with relapsed multiple myeloma treated with bortezomib or dexamethasone*. Blood, 2012. **120**(23): p. 4513-6.
70. Paget, S., *The distribution of secondary growths in cancer of the breast. 1889*. Cancer Metastasis Rev, 1989. **8**(2): p. 98-101.
71. Hideshima, T., et al., *Understanding multiple myeloma pathogenesis in the bone marrow to identify new therapeutic targets*. Nat Rev Cancer, 2007. **7**(8): p. 585-98.
72. Mitsiades, C.S., et al., *The role of the bone marrow microenvironment in the pathophysiology of myeloma and its significance in the development of more effective therapies*. Hematol Oncol Clin North Am, 2007. **21**(6): p. 1007-34, vii-viii.
73. Mitsiades, C.S., et al., *The role of the bone microenvironment in the pathophysiology and therapeutic management of multiple myeloma: interplay of growth factors, their receptors and stromal interactions*. Eur J Cancer, 2006. **42**(11): p. 1564-73.
74. Zhou, J., et al., *The role of the tumor microenvironment in hematological malignancies and implication for therapy*. Front Biosci, 2005. **10**: p. 1581-96.
75. Michigami, T., et al., *Cell-cell contact between marrow stromal cells and myeloma cells via VCAM-1 and alpha(4)beta(1)-integrin enhances production of osteoclast-stimulating activity*. Blood, 2000. **96**(5): p. 1953-60.
76. Pearce, R.N., et al., *Multiple myeloma disrupts the TRANCE/osteoprotegerin cytokine axis to trigger bone destruction and promote tumor progression*. Proc Natl Acad Sci U S A, 2001. **98**(20): p. 11581-6.
77. Yaccoby, S., et al., *Cancer and the microenvironment: myeloma-osteoclast interactions as a model*. Cancer Res, 2004. **64**(6): p. 2016-23.
78. Komori, T., *Regulation of bone development and maintenance by Runx2*. Front Biosci, 2008. **13**: p. 898-903.

79. Giuliani, N., et al., *Myeloma cells block RUNX2/CBFA1 activity in human bone marrow osteoblast progenitors and inhibit osteoblast formation and differentiation*. Blood, 2005. **106**(7): p. 2472-83.
80. Heider, U., et al., *Novel aspects of osteoclast activation and osteoblast inhibition in myeloma bone disease*. Biochem Biophys Res Commun, 2005. **338**(2): p. 687-93.
81. Tian, E., et al., *The role of the Wnt-signaling antagonist DKK1 in the development of osteolytic lesions in multiple myeloma*. N Engl J Med, 2003. **349**(26): p. 2483-94.
82. He, J., et al., *p38 MAPK in myeloma cells regulates osteoclast and osteoblast activity and induces bone destruction*. Cancer Res, 2012.
83. D'Souza, S., et al., *Gfi1 expressed in bone marrow stromal cells is a novel osteoblast suppressor in patients with multiple myeloma bone disease*. Blood, 2011. **118**(26): p. 6871-80.
84. Vallet, S., et al., *Activin A promotes multiple myeloma-induced osteolysis and is a promising target for myeloma bone disease*. Proc Natl Acad Sci U S A, 2010. **107**(11): p. 5124-9.
85. Vallet, S., et al., *A novel role for CCL3 (MIP-1alpha) in myeloma-induced bone disease via osteocalcin downregulation and inhibition of osteoblast function*. Leukemia, 2011. **25**(7): p. 1174-81.
86. Karadag, A., et al., *Human myeloma cells promote the production of interleukin 6 by primary human osteoblasts*. Br J Haematol, 2000. **108**(2): p. 383-90.
87. Fu, J., et al., *Myeloma cells inhibit osteogenic differentiation of mesenchymal stem cells and kill osteoblasts via TRAIL-induced apoptosis*. Arch Med Sci, 2010. **6**(4): p. 496-504.
88. Abdi, J., G. Chen, and H. Chang, *Drug resistance in multiple myeloma: latest findings and new concepts on molecular mechanisms*. Oncotarget, 2013. **4**(12): p. 2186-207.
89. Voorhees, P.M., et al., *Inhibition of interleukin-6 signaling with CNTO 328 enhances the activity of bortezomib in preclinical models of multiple myeloma*. Clin Cancer Res, 2007. **13**(21): p. 6469-78.
90. Markovina, S., et al., *Bone marrow stromal cells from multiple myeloma patients uniquely induce bortezomib resistant NF-kappaB activity in myeloma cells*. Mol Cancer, 2010. **9**: p. 176.
91. Noborio-Hatano, K., et al., *Bortezomib overcomes cell-adhesion-mediated drug resistance through downregulation of VLA-4 expression in multiple myeloma*. Oncogene, 2009. **28**(2): p. 231-42.
92. McMillin, D.W., et al., *Compartment-Specific Bioluminescence Imaging platform for the high-throughput evaluation of antitumor immune function*. Blood, 2012. **119**(15): p. e131-8.
93. McMillin, D.W., et al., *Tumor cell-specific bioluminescence platform to identify stroma-induced changes to anticancer drug activity*. Nat Med, 2010. **16**(4): p. 483-9.
94. Dowling, P., et al., *Recent advances in clinical proteomics using mass spectrometry*. Bioanalysis, 2010. **2**(9): p. 1609-15.
95. Dowling, P., et al., *Proteomic analysis of conditioned media from glucose responsive and glucose non-responsive phenotypes reveals a panel of*

- secreted proteins associated with beta cell dysfunction*. Electrophoresis, 2008. **29**(20): p. 4141-9.
96. Holland, A., et al., *Proteomic profiling of cardiomyopathic tissue from the aged mdx model of Duchenne muscular dystrophy reveals a drastic decrease in laminin, nidogen and annexin*. Proteomics, 2013. **13**(15): p. 2312-23.
 97. Holland, A., et al., *Intricate effects of primary motor neuronopathy on contractile proteins and metabolic muscle enzymes as revealed by label-free mass spectrometry*. Biosci Rep, 2014. **34**(4).
 98. O'Sullivan, D., et al., *7B7: a novel antibody directed against the Ku70/Ku80 heterodimer blocks invasion in pancreatic and lung cancer cells*. Tumour Biol, 2014. **35**(7): p. 6983-97.
 99. Buzzeeo, R., et al., *Characterization of a R115777-resistant human multiple myeloma cell line with cross-resistance to PS-341*. Clin Cancer Res, 2005. **11**(16): p. 6057-64.
 100. Lu, S., et al., *Different mutants of PSMB5 confer varying bortezomib resistance in T lymphoblastic lymphoma/leukemia cells derived from the Jurkat cell line*. Exp Hematol, 2009. **37**(7): p. 831-7.
 101. Stessman, H.A., et al., *Profiling bortezomib resistance identifies secondary therapies in a mouse myeloma model*. Mol Cancer Ther, 2013. **12**(6): p. 1140-50.
 102. Balsas, P., et al., *Bortezomib resistance in a myeloma cell line is associated to PSMbeta5 overexpression and polyploidy*. Leuk Res, 2012. **36**(2): p. 212-8.
 103. Politou, M., et al., *No evidence of mutations of the PSMB5 (beta-5 subunit of proteasome) in a case of myeloma with clinical resistance to Bortezomib*. Leuk Res, 2006. **30**(2): p. 240-1.
 104. O'Connor, R., et al., *The interaction of bortezomib with multidrug transporters: implications for therapeutic applications in advanced multiple myeloma and other neoplasias*. Cancer Chemother Pharmacol, 2013. **71**(5): p. 1357-68.
 105. Leich, E., et al., *Multiple myeloma is affected by multiple and heterogeneous somatic mutations in adhesion- and receptor tyrosine kinase signaling molecules*. Blood Cancer J, 2013. **3**: p. e102.
 106. Lopez-Corral, L., et al., *Heterogeneity of genomic evolution and mutational profiles in multiple myeloma*. Leukemia, 2014. **5**: p. 2997.
 107. Melchor, L., et al., *Single-cell genetic analysis reveals the composition of initiating clones and phylogenetic patterns of branching and parallel evolution in myeloma*. Leukemia, 2014.
 108. Walker, B.A., et al., *Intraclonal heterogeneity is a critical early event in the development of myeloma and precedes the development of clinical symptoms*. 2014. **28**(2): p. 384-90.
 109. Lohr, J.G., et al., *Widespread genetic heterogeneity in multiple myeloma: implications for targeted therapy*. Cancer Cell, 2014. **25**(1): p. 91-101.
 110. Sim, N.L., et al., *SIFT web server: predicting effects of amino acid substitutions on proteins*. Nucleic Acids Res, 2012. **40**(Web Server issue): p. W452-7.
 111. Adzhubei, I.A., et al., *A method and server for predicting damaging missense mutations*. Nat Methods, 2010. **7**(4): p. 248-9.

112. Kaminski, W.E., et al., *Identification of a novel human sterol-sensitive ATP-binding cassette transporter (ABCA7)*. Biochem Biophys Res Commun, 2000. **273**(2): p. 532-8.
113. Meurs, I., et al., *Effects of deletion of macrophage ABCA7 on lipid metabolism and the development of atherosclerosis in the presence and absence of ABCA1*. PLoS One, 2012. **7**(3): p. e30984.
114. Hlavata, I., et al., *The role of ABC transporters in progression and clinical outcome of colorectal cancer*. Mutagenesis, 2012. **27**(2): p. 187-96.
115. Agnelli, L., P. Tassone, and A. Neri, *Molecular profiling of multiple myeloma: from gene expression analysis to next-generation sequencing*. Expert Opin Biol Ther, 2013.
116. Terragna, C., et al., *Correlation between eight-gene expression profiling and response to therapy of newly diagnosed multiple myeloma patients treated with thalidomide-dexamethasone incorporated into double autologous transplantation*. Ann Hematol, 2013.
117. Rajpal, R., et al., *A novel panel of protein biomarkers for predicting response to thalidomide-based therapy in newly diagnosed multiple myeloma patients*. Proteomics, 2011. **11**(8): p. 1391-402.
118. Pulvino, M., et al., *Inhibition of proliferation and survival of diffuse large B-cell lymphoma cells by a small-molecule inhibitor of the ubiquitin-conjugating enzyme Ubc13-Uev1A*. Blood, 2012. **120**(8): p. 1668-77.
119. Berleth, E.S., et al., *Expression, tissue distribution, and cellular localization of the antiapoptotic TIP-B1 protein*. J Leukoc Biol, 2001. **69**(6): p. 995-1005.
120. Tsubaki, M., et al., *Macrophage inflammatory protein-1alpha induces osteoclast formation by activation of the MEK/ERK/c-Fos pathway and inhibition of the p38MAPK/IRF-3/IFN-beta pathway*. J Cell Biochem, 2010. **111**(6): p. 1661-72.
121. Dairaghi, D.J., et al., *CCR1 blockade reduces tumor burden and osteolysis in vivo in a mouse model of myeloma bone disease*. Blood, 2012. **120**(7): p. 1449-57.
122. Dimopoulos, M.A., et al., *Tanespimycin as antitumor therapy*. Clin Lymphoma Myeloma Leuk, 2011. **11**(1): p. 17-22.
123. Khong, T. and A. Spencer, *Targeting HSP 90 induces apoptosis and inhibits critical survival and proliferation pathways in multiple myeloma*. Mol Cancer Ther, 2011. **10**(10): p. 1909-17.
124. Reddy, N., et al., *Phase I Trial of the HSP90 Inhibitor PF-04929113 (SNX5422) in Adult Patients With Recurrent, Refractory Hematologic Malignancies*. Clin Lymphoma Myeloma Leuk, 2013. **13**(4): p. 385-91.
125. Richardson, P.G., et al., *Tanespimycin monotherapy in relapsed multiple myeloma: results of a phase 1 dose-escalation study*. Br J Haematol, 2010. **150**(4): p. 438-45.
126. Harries, L.W., et al., *Identification of genetic polymorphisms at the glutathione S-transferase Pi locus and association with susceptibility to bladder, testicular and prostate cancer*. Carcinogenesis, 1997. **18**(4): p. 641-4.
127. Wang, T., et al., *Glutathione S-transferase P1-1 (GSTP1-1) inhibits c-Jun N-terminal kinase (JNK1) signaling through interaction with the C terminus*. J Biol Chem, 2001. **276**(24): p. 20999-1003.

128. Advani, A.S., et al., *A Phase II trial of gemcitabine and mitoxantrone for patients with acute myeloid leukemia in first relapse*. Clin Lymphoma Myeloma Leuk, 2010. **10**(6): p. 473-6.
129. Stella, F., et al., *Glutathione S-transferase P1 mRNA expression in plasma cell disorders and its correlation with polymorphic variants and clinical outcome*. Cancer Epidemiol, 2013. **37**(5): p. 671-4.
130. Taylor, C.A., et al., *Modulation of eIF5A expression using SNS01 nanoparticles inhibits NF-kappaB activity and tumor growth in murine models of multiple myeloma*. Mol Ther, 2012. **20**(7): p. 1305-14.
131. Artero-Castro, A., et al., *Expression of the ribosomal proteins Rplp0, Rplp1, and Rplp2 in gynecologic tumors*. Hum Pathol, 2011. **42**(2): p. 194-203.
132. Artero-Castro, A., et al., *Rplp1 bypasses replicative senescence and contributes to transformation*. Exp Cell Res, 2009. **315**(8): p. 1372-83.
133. Mitsiades, C.S., et al., *Multiple myeloma: a prototypic disease model for the characterization and therapeutic targeting of interactions between tumor cells and their local microenvironment*. J Cell Biochem, 2007. **101**(4): p. 950-68.
134. Hideshima, T., et al., *Proteasome inhibitor PS-341 abrogates IL-6 triggered signaling cascades via caspase-dependent downregulation of gp130 in multiple myeloma*. Oncogene, 2003. **22**(52): p. 8386-93.
135. Bjorklund, C.C., et al., *Evidence of a role for CD44 and cell adhesion in mediating resistance to lenalidomide in multiple myeloma: therapeutic implications*. Leukemia, 2014. **28**(2): p. 373-83.
136. Mithraprabhu, S., T. Khong, and A. Spencer, *Overcoming inherent resistance to histone deacetylase inhibitors in multiple myeloma cells by targeting pathways integral to the actin cytoskeleton*. Cell Death Dis, 2014. **5**: p. e1134.
137. Zhu, Y.X., et al., *Identification of cereblon-binding proteins and relationship with response and survival after IMiDs in multiple myeloma*. Blood, 2014. **124**(4): p. 536-45.
138. Ao, L., et al., *Development of peptide-based reversing agents for p-glycoprotein-mediated resistance to carfilzomib*. Mol Pharm, 2012. **9**(8): p. 2197-205.
139. Kovacic, N., P.I. Croucher, and M.M. McDonald, *Signaling between tumor cells and the host bone marrow microenvironment*. Calcif Tissue Int, 2014. **94**(1): p. 125-39.
140. Olsen, O.E., et al., *Bone morphogenetic protein-9 suppresses growth of myeloma cells by signaling through ALK2 but is inhibited by endoglin*. Blood Cancer J, 2014. **4**: p. e196.
141. Romano, A., C. Conticello, and M. Cavalli, *Immunological Dysregulation in Multiple Myeloma Microenvironment*. 2014. **2014**: p. 198539.
142. Vacca, A., et al., *Angiogenesis in multiple myeloma*. Chem Immunol Allergy, 2014. **99**: p. 180-96.
143. Yuan, L., et al., *RANKL expression in myeloma cells is regulated by a network involving RANKL promoter methylation, DNMT1, microRNA and TNFalpha in the microenvironment*. Biochim Biophys Acta, 2014. **1843**(9): p. 1834-8.

144. Zhang, X., et al., *Up-regulation of connexin-43 expression in bone marrow mesenchymal stem cells plays a crucial role in adhesion and migration of multiple myeloma cells*. Leuk Lymphoma, 2014: p. 1-8.
145. Zi, F.M., et al., *Fibroblast activation protein protects bortezomib-induced apoptosis in multiple myeloma cells through beta-catenin signaling pathway*. Cancer Biol Ther, 2014. **15**(10).
146. Schuler, J., et al., *Preclinical models of multiple myeloma: a critical appraisal*. Expert Opin Biol Ther, 2013. **13 Suppl 1**: p. S111-23.
147. Sharma, S.V., D.A. Haber, and J. Settleman, *Cell line-based platforms to evaluate the therapeutic efficacy of candidate anticancer agents*. Nat Rev Cancer, 2010. **10**(4): p. 241-53.
148. Witt, O., et al., *HDAC family: What are the cancer relevant targets?* Cancer Lett, 2009. **277**(1): p. 8-21.
149. Jibodh, R.A., et al., *Taxanes: old drugs, new oral formulations*. Eur J Pharmacol, 2013. **717**(1-3): p. 40-6.
150. Horwitz, S.B., *Taxol (paclitaxel): mechanisms of action*. Ann Oncol, 1994. **5 Suppl 6**: p. S3-6.
151. Abidi, A., *Cabazitaxel: A novel taxane for metastatic castration-resistant prostate cancer-current implications and future prospects*. J Pharmacol Pharmacother, 2013. **4**(4): p. 230-7.
152. Mukai, H., et al., *Phase I dose-escalation and pharmacokinetic study (TED 11576) of cabazitaxel in Japanese patients with castration-resistant prostate cancer*. Cancer Chemother Pharmacol, 2014. **73**(4): p. 703-10.
153. Gazitt, Y., P. Shaughnessy, and M.L. Rothenberg, *A phase II trial with gemcitabine and paclitaxel for the treatment of refractory and relapsed multiple myeloma patients*. Oncol Rep, 2006. **16**(4): p. 877-84.
154. Pommier, Y., et al., *Mechanism of action of eukaryotic DNA topoisomerase I and drugs targeted to the enzyme*. Biochim Biophys Acta, 1998. **1400**(1-3): p. 83-105.
155. Burden, D.A. and N. Osheroff, *Mechanism of action of eukaryotic topoisomerase II and drugs targeted to the enzyme*. Biochim Biophys Acta, 1998. **1400**(1-3): p. 139-54.
156. Fox, E.J., *Mechanism of action of mitoxantrone*. Neurology, 2004. **63**(12 Suppl 6): p. S15-8.
157. Hajek, R., et al., *Design and rationale of FOCUS (PX-171-011): a randomized, open-label, phase 3 study of carfilzomib versus best supportive care regimen in patients with relapsed and refractory multiple myeloma (R/R MM)*. BMC Cancer, 2012. **12**: p. 415.
158. Jakubowiak, A.J., et al., *A phase 1/2 study of carfilzomib in combination with lenalidomide and low-dose dexamethasone as a frontline treatment for multiple myeloma*. Blood, 2012. **120**(9): p. 1801-9.
159. O'Connor, O.A., et al., *A phase 1 dose escalation study of the safety and pharmacokinetics of the novel proteasome inhibitor carfilzomib (PR-171) in patients with hematologic malignancies*. Clin Cancer Res, 2009. **15**(22): p. 7085-91.
160. Vij, R., et al., *An open-label, single-arm, phase 2 (PX-171-004) study of single-agent carfilzomib in bortezomib-naïve patients with relapsed and/or refractory multiple myeloma*. Blood, 2012. **119**(24): p. 5661-70.

161. Ombrello, M.J., K.A. Sikora, and D.L. Kastner, *Genetics, genomics, and their relevance to pathology and therapy*. Best Pract Res Clin Rheumatol, 2014. **28**(2): p. 175-189.
162. Armstrong, T., et al., *Type I collagen promotes the malignant phenotype of pancreatic ductal adenocarcinoma*. Clin Cancer Res, 2004. **10**(21): p. 7427-37.
163. Hall, C.L., et al., *Type I collagen receptor (alpha2beta1) signaling promotes prostate cancer invasion through RhoC GTPase*. Neoplasia, 2008. **10**(8): p. 797-803.
164. Hambrock, H.O., et al., *SC1/hevin. An extracellular calcium-modulated protein that binds collagen I*. J Biol Chem, 2003. **278**(13): p. 11351-8.
165. Yu, S.J., et al., *SPARCL1, Shp2, MSH2, E-cadherin, p53, ADCY-2 and MAPK are prognosis-related in colorectal cancer*. World J Gastroenterol, 2011. **17**(15): p. 2028-36.
166. Zhang, H., et al., *SPARCL1: a potential molecule associated with tumor diagnosis, progression and prognosis of colorectal cancer*. Tumour Biol, 2011. **32**(6): p. 1225-31.
167. Claeskens, A., et al., *Hevin is down-regulated in many cancers and is a negative regulator of cell growth and proliferation*. Br J Cancer, 2000. **82**(6): p. 1123-30.
168. Turtoi, A., et al., *Sparc-like protein 1 is a new marker of human glioma progression*. J Proteome Res, 2012. **11**(10): p. 5011-21.
169. Cao, F., et al., *Clinicopathological significance of reduced SPARCL1 expression in human breast cancer*. Asian Pac J Cancer Prev, 2013. **14**(1): p. 195-200.
170. Xiang, Y., et al., *SPARCL1 suppresses metastasis in prostate cancer*. Mol Oncol, 2013. **7**(6): p. 1019-30.
171. Fang, Z.Q., et al., *Gene expression profile and enrichment pathways in different stages of bladder cancer*. Genet Mol Res, 2013. **12**(2): p. 1479-89.
172. Khalifeh-Soltani, A., et al., *Mfge8 promotes obesity by mediating the uptake of dietary fats and serum fatty acids*. Nat Med, 2014. **20**(2): p. 175-83.
173. Tibaldi, L., et al., *New blocking antibodies impede adhesion, migration and survival of ovarian cancer cells, highlighting MFGE8 as a potential therapeutic target of human ovarian carcinoma*. PLoS One, 2013. **8**(8): p. e72708.
174. Abe, T., et al., *Regulation of Osteoclast Homeostasis and Inflammatory Bone Loss by MFG-E8*. J Immunol, 2014. **193**(3): p. 1383-91.
175. Tashiro, K., et al., *GAREM, a novel adaptor protein for growth factor receptor-bound protein 2, contributes to cellular transformation through the activation of extracellular signal-regulated kinase signaling*. J Biol Chem, 2009. **284**(30): p. 20206-14.
176. Girardot, M., et al., *Persistent STAT5 activation in myeloid neoplasms recruits p53 into gene regulation*. Oncogene, 2014. **0**.
177. Hideshima, T., et al., *The proteasome inhibitor PS-341 inhibits growth, induces apoptosis, and overcomes drug resistance in human multiple myeloma cells*. Cancer Res, 2001. **61**(7): p. 3071-6.
178. Tao, R.H., et al., *PMLRARalpha binds to Fas and suppresses Fas-mediated apoptosis through recruiting c-FLIP in vivo*. Blood, 2011. **118**(11): p. 3107-18.

179. Irmeler, M., et al., *Inhibition of death receptor signals by cellular FLIP*. Nature, 1997. **388**(6638): p. 190-5.
180. Micheau, O., et al., *The long form of FLIP is an activator of caspase-8 at the Fas death-inducing signaling complex*. J Biol Chem, 2002. **277**(47): p. 45162-71.
181. Stein, R., et al., *CD74: a new candidate target for the immunotherapy of B-cell neoplasms*. Clin Cancer Res, 2007. **13**(18 Pt 2): p. 5556s-5563s.
182. Kaufman, J.L., et al., *Phase I, multicentre, dose-escalation trial of monotherapy with milatuzumab (humanized anti-CD74 monoclonal antibody) in relapsed or refractory multiple myeloma*. Br J Haematol, 2013. **163**(4): p. 478-86.
183. Hofmann, C., et al., *PI3K-dependent multiple myeloma cell survival is mediated by the PIK3CA isoform*. Br J Haematol, 2014. **166**(4): p. 529-39.
184. Lopez-Corral, L., et al., *Transcriptome analysis reveals molecular profiles associated with evolving steps of monoclonal gammopathies*. Haematologica, 2014. **99**(8): p. 1365-72.
185. Bodet, L., et al., *ABT-737 is highly effective against molecular subgroups of multiple myeloma*. Blood, 2011. **118**(14): p. 3901-10.
186. Lin, J., et al., *Induction of apoptosis and antitumor effects of a small molecule inhibitor of Bcl-2 and Bcl-xl, gossypol acetate, in multiple myeloma in vitro and in vivo*. Oncol Rep, 2013. **30**(2): p. 731-8.
187. He, Y., et al., *Potentially functional polymorphisms in aminoacyl-tRNA synthetases genes are associated with breast cancer risk in a Chinese population*. Mol Carcinog, 2014.
188. Simpson, D. and G.M. Keating, *Sorafenib: in hepatocellular carcinoma*. Drugs, 2008. **68**(2): p. 251-8.
189. Escudier, B., et al., *Sorafenib in advanced clear-cell renal-cell carcinoma*. N Engl J Med, 2007. **356**(2): p. 125-34.
190. Schuler, A., et al., *The MADS transcription factor Mef2c is a pivotal modulator of myeloid cell fate*. Blood, 2008. **111**(9): p. 4532-41.
191. Wang, X., et al., *ERK5 pathway regulates transcription factors important for monocytic differentiation of human myeloid leukemia cells*. J Cell Physiol, 2014. **229**(7): p. 856-67.
192. Chen, Z., et al., *Osteoblastic niche supports the growth of quiescent multiple myeloma cells*. Blood, 2014. **123**(14): p. 2204-8.
193. Bolomsky, A., et al., *Immunomodulatory drugs thalidomide and lenalidomide affect osteoblast differentiation of human bone marrow stromal cells in vitro*. Exp Hematol, 2014. **42**(7): p. 516-25.
194. Kaiser, M.F., et al., *The proteasome inhibitor bortezomib stimulates osteoblastic differentiation of human osteoblast precursors via upregulation of vitamin D receptor signalling*. Eur J Haematol, 2013. **90**(4): p. 263-72.
195. Niewerth, D., et al., *Interferon-gamma-induced upregulation of immunoproteasome subunit assembly overcomes bortezomib resistance in human hematological cell lines*. J Hematol Oncol, 2014. **7**(1): p. 7.